2015

Microstructural and tectonic applications of texturally-controlled Sm/Nd garnet geochronology

BOSTON UNIVERSITY

GRADUATE SCHOOL OF ARTS AND SCIENCES

Thesis

MICROSTRUCTURAL AND TECTONIC APPLICATIONS OF TEXTURALLY-CONTROLLED Sm/Nd GARNET GEOCHRONOLOGY

by

EMILY MAVIS STEWART

B.S. Indiana University, 2013

Submitted in partial fulfillment of the

requirements for the degree of

Master of Arts

2015

Approved by

First Reader _____

Ethan Baxter, Ph.D.
Professor of Earth and Environment

Second Reader _____

Andrew Kurtz, Ph.D.
Associate Professor of Earth and Environment

Third Reader _____

Paul Hall, Ph.D.
Assistant Professor of Earth and Environment

ACKNOWLEDGMENTS

I would like to thank my committee members, Paul Hall and Andrew Kurtz, for all of their help in preparing and polishing this thesis. I would also like to thank all of my friends and lab mates, especially Jamie Kendall, Katie Eccles-Maneiro, Nora Sullivan, Besim Dragovic, Evan Ramos, and Darwin Janes who helped me throughout my MA work and made life as a graduate student worth living. Special thanks to my family: my mother and father (Susan and David) and brother and sister (Lillian and Paul) who have learned more about column chemistry than anyone should ever have to, and in the process have actually been the most wonderful and supportive family a person could ask for. Thanks to my collaborator, Domingo Aerden at UGR, and his family for hosting me during my work in Granada. Finally I would like to thank my advisor, Ethan Baxter, who opened my eyes to the world of isotope geochemistry and all that it allows us to explore.

MICROSTRUCTURAL AND TECTONIC APPLICATIONS OF TEXTURALLY-CONTROLLED Sm/Nd GARNET GEOCHRONOLOGY

EMILY MAVIS STEWART

Boston University Graduate School of Arts and Sciences, 2015

Major Professor: Ethan F. Baxter, Professor of Earth and Environment

ABSTRACT

High precision ^{147}Sm-^{143}Nd geochronology of garnet is performed in two localities to solve problems in tectonics. In Chapter 1, the age of the basal amphibolite unit of the Ballantrae Ophiolite complex in Scotland is dated at 477.6 ± 1.9 million years old. This age constrains the duration of Grampian orogenesis to 12.6 ± 3.1 million years and allows us to conclude that classic metamorphism by overthickening of continental crust cannot account for the very short-lived event in this region. In Chapter 2, we report ages from a Variscan relict (318 ± 130 Ma) to a range of Cenozoic ages from 35.5 ± 2.1 Ma to 9 ± 10 Ma in the Betic Cordillera of southern Spain. This alone indicates prolonged orogenesis in the region. These ages are linked directly to a microstructure known as a Foliation Intersection Axis (FIA). Results are inconclusive, but they generally indicate that there may be a relationship between broad scale plate motion and FIA orientations at a regional scale.

PREFACE

Samarium-Neodymium geochronology of garnet can be used to interrogate many parts of the Earth System. As with most types of geochronology, our field has advanced beyond asking simply "how old is this rock or this garnet?" Rather, we consider what processes were in motion when that garnet formed, and we try to decipher the record of those processes that is trapped within the rock. My thesis work focuses on the application of Sm-Nd garnet geochronology to mountain-building and tectonic processes.

Chapter 1 represents a fairly classical approach to geochronology. The basal units of the Ballantrae Ophiolite complex in Scotland are interpreted as recording the very beginning of collision and mountain-building in the Scottish Highlands. I use modern geochronologic methods to significantly improve our knowledge of the timing of this event by dating garnet in a basal garnet amphibolite. In some ways this work can be seen as dating a large scale structure – that is the obduction-related shear zone marked by ophiolite's metamorphic aureole.

In Chapter 2, I apply garnet geochronology to a microstructural problem. Garnets in the Betic Cordillera of southern Spain contain complex inclusion trails which may or may not record information about the direction of tectonic convergence at the time of garnet growth. Because I am considering a much smaller scale structure, more texturally precise sampling of garnet is necessary to resolve the relationship between different microstructures within a single rock or even a single crystal. This type of work pushes the boundaries of garnet micro-sampling and represents a brand-new way to pair high precision geochronology with very precise structural analysis.

Ultimately both chapters of this thesis use Sm-Nd garnet geochronology to answer questions about the nature of orogenesis on Earth. Both seek to better understand Plate Tectonics – perhaps the single most important process of our planet, which has allowed life as we know it to emerge and survive. Both chapters make suggestions for future work which will help to refine and build upon the discoveries reported in my thesis. As technology and methodology continue to improve, Sm-Nd geochronology will be able to elucidate more and more problems around the globe. These chapters represent just two applications of structurally-controlled garnet geochronology towards a better understanding of mountain building, metamorphism, and middle-crustal processes in the Earth system.

TABLE OF CONTENTS

LIST OF TABLES

LIST OF FIGURES

LIST OF ABBREVIATIONS

A	Ampere
abs	absolute
Al	aluminum
Al_2O_3	aluminum oxide
AR	aqua regia
Ar	argon
B.S.	Bachelor of Science
bio	biotite
BU	Boston University
BC	Boston College
C	carbon
°C	degrees Celsius
Ca	calcium
CaO	calcium oxide
chl	chlorite
cld	chloritoid
CHUR	chondritic uniform reservoir
cm	centimeter
CO	Claire Ostwald
CO_2	carbon dioxide

conc	concentration
DGA	Domingo Aerden
EAR	Division of Earth Sciences at NSF
EDS	Energy Dispersive Spectroscopy
EFB	Ethan F. Baxter
EMS	Emily M. Stewart
et al.	and others
EMP	electron microprobe
Fe	iron
FeO	iron oxide
FIA	Foliation Intersection Axis
g	gram
GPa	gigapascals
grt	garnet
gt	garnet
h	hour
H_2O	water
$HClO_4$	perchloric acid
HCl	hydrochloric acid
Hf	hafnium
HF	hydrofluoric acid
HNO_3	nitric acid

K	potassium
K_2O	potassium oxide
KAE	Katie A. Eccles
km	kilometer
kV	kilovolt
Lu	lutetium
M	molar
M.A.	Master of Arts
Ma	million years ago
mL	milliliter
MLA	methyl lactic acid (2-hydroxyisobutyric acid)
mg	milligram
Mg	magnesium
MgO	magnesium oxide
min	minute
mm	millimeter
Mn	manganese
MnO	manganese oxide
mol	mole
mol%	mole percent
MSWD	mean square weighted deviation
mtx	matrix

Myr	million years
n	number of items
1.5N	1.5 normal solution
nA	nanoamp
Na	sodium
Na_2O	sodium oxide
Nd	neodymium
^{142}Nd	isotope of neodymium with mass number 142
^{143}Nd	isotope of neodymium with mass number 143
^{144}Nd	isotope of neodymium with mass number 144
^{145}Nd	isotope of neodymium with mass number 145
^{146}Nd	isotope of neodymium with mass number 146
^{148}Nd	isotope of neodymium with mass number 148
^{150}Nd	isotope of neodymium with mass number 150
NdO^+	neodymium oxide ion
ng	nanogram
NSF	National Science Foundation
O	oxygen
OH	hydroxide
Os	osmium
P	pressure
Pb	lead

%	percent
pg	picogram
P_2O_5	phosphorus oxide
ppm	parts per million
pow	powder
Rb	rubidium
^{87}Rb	isotope of rubidium with mass number 87
Re	rhenium
REE	rare earth element
RSD	relative standard deviation
σ	sigma
s	second
SD	standard deviation
SE	standard error
SEM	Scanning Electron Microscope
Si	silicon
SIGECO	Sistema de consulta y difusión web de cartografía geológica continua
SiO_2	silicon oxide
Sm	samarium
^{144}Sm	isotope of samarium with mass number 144
^{147}Sm	isotope of samarium with mass number 147
^{148}Sm	isotope of samarium with mass number 148

^{149}Sm	isotope of samarium with mass number 149
^{150}Sm	isotope of samarium with mass number 150
^{152}Sm	isotope of samarium with mass number 152
^{154}Sm	isotope of samarium with mass number 154
Sr	strontium
SrO	strontium oxide
t	time
$t_{1/2}$	half-life
T	temperature
Ta	tantalum
Ta_2O_5	tantalum oxide
Th	thorium
Ti	titanium
TIMS	thermal ionization mass spectrometer
TiO_2	titanium dioxide
Tour	tourmaline
µL	microliter
µm	micrometer
UGR	Universidad de Granada
USA	United States of America
wt%	weight percent
Y	yttrium

yr	year
Zn	zinc
Zr	zirconium

CHAPTER ONE: Onset of Grampian Orogenesis Constrained by Sm/Nd Garnet Age of the Ballantrae Ophiolite

INTRODUCTION

The Grampian phase of the Caledonian Orogeny in Scotland is, perhaps, the longest-studied metamorphic event in history. From its initial characterization by Barrow in his seminal paper on regional metamorphism (Barrow, 1893) to the more recent work on timescales of Grampian orogenesis, (e.g. Viete *et al.* 2013; Vorhies and Ague 2011; Baxter *et al.* 2002; Oliver *et al.* 2000) this small stretch of the Caledonides has been home to a large number of metamorphic studies. The orogeny is characterized by relatively short-lived, high-temperature medium-pressure metamorphism initiated by the closure of a marginal ocean basin. The Ballantrae ophiolite complex represents the remnant of this marginal sea obducted onto continental crust, thus it is interpreted that the age of formation of this ophiolite's metamorphic sole gives the oldest age of orogenesis in the region (Oliver 2001; Bluck *et al.*1980; Oliver *et al.* 2000). Many studies have focused on the duration and intensity of peak metamorphic conditions, but the timing of this first collision remains poorly constrained. In fact, while it is suggested that the entire orogeny may have lasted only ~15 m.y. (Oliver *et al.* 2000), the best constraint of its onset is reported as 478 ±8 Ma based on a K-Ar age from the Ballantrae (Bluck *et al.* 1980). With this in mind, we report a new high-precision Sm-Nd garnet age of

metamorphism in the Ballantrae ophiolite complex. This age helps to constrain the timing of onset of the Grampian Orogeny and provides the basis for further study of the timescales of metamorphism in the region.

GEOLOGIC SETTING

The Ballantrae Igneous Complex was first recognized as an ophiolite sequence quite early by Anderson (1936) who compared it to similar terranes in the Alps. With the subsequent development of Plate Tectonic theory, it was proposed that the Ballantrae represents oceanic lithosphere from a marginal basin that has been thrust onto continental crust (Church and Gayer 1973; Spray and Williams 1980). (See Fig 1.1) The complex itself has experienced significant post-obduction deformation (Church and Gayer 1973; Spray and Williams 1980). This fact combined with poor field exposure makes it impossible to discern a true ophiolitic succession. However, each of the expected lithologies (e.g. pillow lavas, sheeted diabase, gabbro, ultramafic cumulates, serpentinite mélange including blocks of blueschist) is present in the terrane (Church and Gayer 1973). The ophiolite proper is surrounded by a metamorphic "aureole" of variably metamorphosed basaltic rocks. This metamorphic sole was studied in detail by Spray and Williams (1980). The metabasites are highly schistose and range from greenschist up to amphibolite-granulite facies. The entire sole is less than 50 m thick and exhibits an "inverted" metamorphic gradient (with higher grade rocks structurally above those of lower grade). The sequence can be broadly divided into a plagioclase amphibolite unit and a lower grade epidote schist. Spray and Williams (1980) further divide the

amphibolite into four subunits (an upper and lower garnet-bearing amphibolite and an upper and lower garnet-free amphibolite.) Thermobarometric estimates yield peak temperatures of at least ~850 °C for the garnet amphibolite. It is generally accepted that this metamorphic sole was formed by overthrusting of oceanic crust and that this aureole marks the fault zone associated with obduction (Spray and Williams 1980; Bluck 1980; Oliver 2001).

In the broader context of Caledonian orogenesis, it is often interpreted that the obduction of the Ballantrae Ophiolite marks the onset of the Grampian Orogeny in Britain (Oliver 2001; Oliver *et al* 2000; Viete *et al.* 2013). This obduction was synchronous with the docking of the Midland Valley Terrane which led to metamorphism and deformation of sediments in the Dalradian super group. Figure 1.2 (Taken directly from Oliver 2001) is a schematic representation of this collision.

Prior to this study, the best constraint for obduction comes from a K-Ar hornblende age of 478 ±8 Ma for the basal amphibolite unit (Bluck *et al* 1980). This is within error of estimates for obduction of the Bay of Islands Ophiolite in Newfoundland (475 ± 5 Ma $^{40}Ar/^{39}Ar$ from Dallmeyer and Williams 1975) and suggests that Ballantrae obduction was associated with the large scale closure of the Iapetus ocean basin in the Ordivician (Oliver 2001).

EXISTING GEOCHRONOLOGY

While there is significant modern geochronologic work being done in the Scottish Highlands associated with Grampian orogenesis (e.g. Viete *et al.*2013; Viete *et al.*2011; Baxter and Ague 2002; Oliver 2001; Oliver *et al*. 2000) there is a relative

dearth of chronology in the Ballantrae Complex. Table 1.1 summarizes existing geochronology for the terrane. Ages range from 575 ± 32 Ma (Hamilton *et al.* 1984) evidently a pre-orogenic age, to 470 ± 10 Ma **(**Sawaki *et al.* 2010) during collision and deformation. Most relevant to our study, the K-Ar hornblende cooling age of Bluck *et al.* (1980) dates the metamorphism of the amphibolite in the ophiolitic aureole to 478 ± 8 Ma. Also significant is the Sm-Nd garnet age for the aureole's metapyroxenite of 505 ± 11 Ma (Hamilton *et al.* 1984). As the unit reached peak temperatures of 900 ± 70 °C, (Treloar *et al.* 1980) Hamilton *et al.* interpret this as a cooling age. Interestingly, this age is resolvably younger than the age of the adjacent amphibolite unit from Bluck *et al.* (1980). Hamilton *et al.* suggest that the metapyroxenite records the earliest phase of shortening and thrusting prior to obduction of the Ballantrae complex.

SAMPLE DESCRIPTIONS

Several metabasic rocks were collected from the metamorphic sole of the Ballentrae ophiolite complex near Knocklaugh. In the field, sample 11ESC-18A exhibited the most abundant garnet and was therefore singled out for geochronology. Preliminary analyses of garnet chemistry indicated unusually high (1ppm) concentrations of Nd paired with high $^{147}Sm/^{144}Nd$ ratios, thus the sample is ideal for high-precision chronology and is the focus of this study.

11ESC-18A was collected from a primary outcrop of dark, foliated metamorphic rock located near Knocklaugh (N55° 11.158', W004° 52.765'). Garnets range in size from ~2 mm up to ~10 mm in diameter and rare epidote and quartz

veins cut through the matrix. In thin section the matrix minerals can be identified as brown pleochroic amphibole, heavily sericitized plagioclase, and clinopyroxene with minor chlorite and opaque minerals. The matrix is texturally homogeneous; there is little variation in grain size which averages about 1 to 2 mm. The garnet porphyroblasts are rimmed by chlorite and include grains of amphibole, clinopyroxene, plagioclase, and opaques. The inclusions range in size from ~0.1 to ~0.5 mm and occupy up to ~75% of the volume of each garnet porphyroblast. These observations indicate that our sample belongs to the "garnet amphibolite" unit of the Ballantrae complex described in detail by Spray and Williams (1980).

ANALYTICAL METHODS

A ~1000 cm^3 chunk of rock free from veins or other visible evidence of later alteration was chosen for analysis. The weathering rind was removed with a rock saw and the entire chunk was crushed in a tungsten carbide mortar and pestle. At this stage a representative portion was separated for whole-rock chemical analysis and powdered to <200-mesh in an agate ball mill. The remaining portion was the reservoir from which the garnet separate was created. This was accomplished through a combination of magnetic separation using a Frantz separator, further crushing, sieving, and hand-picking. When a visually "pure" garnet separate was achieved it was crushed to a grain size of 100 to 200 mesh. The fine material which passed through the 200 mesh sieve was retained and labeled "garnet powder."

The whole rock fraction and garnet powder were fully dissolved in a multi-step dissolution procure using concentrated HF, concentrated HNO_3, and 1.5N HCl.

The 100 to 200 mesh garnet separate was treated in a partial dissolution cleansing procedure modified after Pollington and Baxter (2011). The aim of this procedure is to cleanse the separate of inclusions that cannot be removed mechanically, thus increasing the purity of the garnet separate. Several variations of this procedure were performed to determine the optimum duration of each step. Ultimately the garnet was kept in a closed beaker of 1 mL concentrated HF and 1 mL 1.5N HCl at 120°C for 45 minutes. To remove secondary fluorides it was then treated with 2mL of concentrated $HClO_4$ at 150°C for 3 hours and finally left in 2mL of concentrated HNO_3 at 120°C for another 3 hours. At this stage the separate was considered as pure as possible and fully dissolved in the same manner as the whole rock and powder.

Following full dissolution each sample was spiked with a ^{147}Sm-^{150}Nd mixed spike described in Harvey and Baxter (2009) and Sm and Nd from each sample were separated for analysis via multistep column chromatography. This procedure involved a clean-up cation exchange column to remove major elements (in particular Fe), a Tru-spec column to separate out the rare earth elements, and finally a 2-methyl lactic acid column to isolate Sm and Nd.

Three-column blanks from this procedure ranged from 4.6 to 24.6 pg Nd and < 1 to 3pg Sm. With a minimum sample size of 5.2 ng Nd, this yields a sample to blank ratio of at least 211:1. In order to quantify the effect of the blank on our calculations we perform a blank correction calculation on this smallest (and therefore most contamination-susceptible) sample, garnet 3. The $^{143}Nd/^{144}Nd$ of the

blank was taken to be canonical at 0.513 ± 0.001 while the $^{147}Sm/^{144}Nd$ of the blank was measured as 0.048 ± 0.035. Using a 10,000-iteration Monte Carlo simulation, blank-subtracted isotopic values for garnet 3 were calculated. The result is visible in Figure 1.3. Though the isotopic values themselves are statistically different, the effect on any age calculation is negligible. The isotopic mixing between any garnet and blank reservoirs occurs along a line that is roughly parallel to our calculated isochron, thus minimizing any effect on the accuracy of our ages. In this example, the age calculated using the measured values for garnet 3 is 477.6 ± 3.6 Ma while the blank-subtracted age yields 477.6 ±2.9 Ma. Given this good agreement between the two ages, we have confidence that these procedural blanks do not affect the accuracy of calculated ages.

After separation, Sm and Nd were analyzed on a Thermo-Finnigan TRITON Thermal Ionization Mass Spectrometer at the Boston University TIMS facility. Nd was loaded onto Re filaments with 2μL of a Ta_2O_5 activator slurry described in Harvey and Baxter (2009). It was run as an oxide (NdO^+) in static mode with amplifier rotation. A 4ng UCB Ames NdO standard was run along with every barrel to quantify our external reproducibility. The average $^{143}Nd/^{144}Nd$ for the time over which samples were run is 0.5121206±0.0000089 (17.3 ppm, 2σ, n=17). Sm was loaded onto zone-refined Re filaments and was run as a metal, also in static mode with amplifier rotation. $^{147}Sm/^{144}Nd$ reproducibility is 0.023% based on repeat analysis of a gravimetrically calibrated mixed Sm/Nd solution.

DATA

Table 1.2 summarizes the isotope data collected from whole rock, garnets, and "powders" for sample 11ESC-18A. Nd concentrations in the garnet are fairly consistent, ranging from 0.854 to 1.196 ppm. The whole rock has a much higher concentration of ~9ppm Nd, and the powders are intermediate, ranging from 0.925 to 2.279 ppm Nd. The $^{143}Nd/^{144}Nd$ and $^{147}Sm/^{144}Nd$ uncertainties reported here are the precisions (2σ S.E.) used for all subsequent calculations. In cases where the limit of our external reproducibility exceeds the internal precision, we report the external (17.3 ppm or 0.023% respectively). Table 1.3 shows data for two samples which were excluded from further analyses due to an unacceptably high Sm interference on what should be pure Nd isotopic measurements. The high Sm indicates a failure in column chemistry that did not fully separate Sm from Nd. Best practices have established a cutoff of $^{152}Sm/^{144}Nd$ =0.01 which both rejected samples exceed.

DISCUSSION

Garnet Age

An 8-point Sm/Nd isochron age for all accepted data is initially calculated using the program Isoplot (Ludwig, 2003). Figure 1.4 shows the resultant isochron, which gives an age of 477.6 ±5.5 Ma. The precision of this age can be attributed to scatter in the data set -- with an MSWD of 5.4, these data do not fall on a statistically robust line.

However, one can tell simply by inspection that one of the powders (Pow 4) falls significantly off of the line defined by the other points. To quantify this observation, a second Sm/Nd isochron age can be calculated for the remaining

seven samples. This isochron, shown in Figure1.5, gives a significantly improved MSWD of 2.0 and a more precise age of 477.6 ±1.9 Ma. For a seven-point isochron, an MSWD less than 2.26 is consistent with a true isochron, i.e. data are not statistically discordant (Wendt and Carl 1991). Furthermore, the clumping of the whole rock and garnet analyses means our calculated isochron is better considered as a four-point isochron. In this case, Wendt and Carl (1991) suggest that an MSWD less than 3.0 is acceptable. Thus we have confidence in the reliability of this result, and suggest that omitting garnet powder 4 gives a better indication of the actual age of garnet crystallization.

First, the precision of the $^{143}Nd/^{144}Nd$ measurement for powder 4 is surprisingly poor at 112 ppm, and only 60 useable cycles were collected on the TIMS. This is not in itself troubling; however, given the mass of Nd which should have been loaded onto the filament (12 ng) we would expect the precision to be nearly an order of magnitude better. This is the first indication that our analysis of powder 4 may not be completely reliable. Perhaps a significant amount of Nd was lost during column chemistry or loading. Alternatively, it could be that its ionization was inhibited leading to small beam size and poor statistics. Whatever the reason, it is clear that the 12 ng of Nd which were present in powder 4 after full dissolution were not effectively collected and analyzed.

Furthermore, it is not uncommon for uncleansed garnet powders to fall off an isochron -- garnets may include inherited phases which did not isotopically equilibrate with the whole rock (Baxter and Scherer 2013; Dragovic *et al.* 2012).

While it is true the powder C and powder D fit the isochron well, it is not implausible that powder 4 is compositionally different. Perhaps this particular scoop of powder (which can never be perfectly homogenized) contained a grain of monazite or another mineral with very high (thousands of ppm) concentrations of Nd. This so-called "nugget effect" (Matheron, 1963) could effectively contaminate powder 4 and pull it off the isochron. With all of this in mind, we assert that 477.6 ± 1.9 Ma is the most reliable age indicated by our isotopic measurements.

Age Significance: Growth or Closure?

Given this garnet age, what process is actually being dated? That is, should we consider this the age of garnet crystallization, closure, or something else? In general, diffusional resetting of Sm and Nd isotopes may begin to occur above ~700 °C (Baxter and Scherer 2013; Carlson 2012). Thermobarometric estimates for the Ballantrae's garnet amphibolite unit indicate peak temperatures of at least ~850 °C and pressures of ~7 kbar (Spray and Williams l980), therefore we must consider the possibility that the garnet in our sample exchanged Sm and Nd with the whole rock reservoir after growth. Were this to be the case, our reported age would be *younger* than the age of garnet crystallization. There is scant work on the Pressure-Temperature-time history of this unit in particular, but there is some evidence that our sample did not spend a long period of time at such high temperatures. First, Spray and Williams (1980) report some preserved major element zonation in garnet porphyroblasts, most notably an increase in Mg concentration in garnet rims. Increased Mg content in garnet is qualitatively associated with increased

temperature (e.g. Colin and Graham 1984)., thus we can associate this pattern with an increase up to peak temperature (~850 °C) late in the garnet's growth history. Spray and Williams do not report the lengthscale of this zonation, thus it is impossible to do any robust modeling of Mg diffusion profiles in the garnets. However, we can say that if the garnet spent much more than ~1 m.y. at 850 °C, we would expect the Mg zonation to be completely smoothed out (Carlson 2006). Since the zonation is preserved, we propose that garnets probably did not see temperatures above ~700 °C for much more than 1 m.y., thus resetting of slower-diffusing rare earth elements like Sm and Nd would be minimal (Carlson 2012; Baxter and Scherer 2013).

Furthermore, our garnet age is within error of Bluck *et al.*'s K-Ar hornblende cooling age of 478 ± 8 Ma. Propogating uncertainties, the time between garnet crystallization at 850 °C and hornblende closure at 500 °C (Harrison 1982) was -0.4 ± 8.22 m.y. (2σ). This yields a maximum time interval of 7.82 million years between garnet growth and amphibole cooling within 2σ uncertainty.

Using these values, we can solve for an exponential heat diffusion equation of the form

$$T = T_o e^{-\lambda t}$$

Where T_o is the initial temperatures given in degrees Kelvin, λ is some constant describing heat diffusivity in the medium of interest, and t is time in millions of years. Taking boundary conditions of $T(t=0)=T_o$=850 °C= 1173 K and T(t=7.82 m.y.) = 500 °C = 773 K, we find λ= 0.0477596. With this model we then calculate that the

unit would have cooled below 700 °C after only 3.00 m.y. This amount of time above 700 °C would be insufficient to significantly affect the garnet age according to REE diffusivities of Carlson (2012) (see also Baxter and Scherer 2013). Note also that this is the *maximum* time above 700 °C within a 2σ uncertainty envelope. It is statistically more probable that cooling was even faster. With this in mind, we prefer the interpretation that the age of 477.6 ±.1.9 Ma represents garnet growth, not closure. However, this evidence is ultimately inconclusive. In order to better constrain the P-T-t history of the unity and provide quantitative restraints on the degree of Sm/Nd diffusion, future microchemical characterization of the garnet (either via Microprobe or SEM analysis) is suggested.

Tectonic Significance

This new result is in good agreement with previous geochronologic work on the metamorphic sole of the Ballantrae Ophiolite. Most notably, our age is statistically indistinguishable from the K-Ar hornblende age reported by Bluck *et al*. (1980). More significantly, with a four-fold improvement in age precision we can begin to draw conclusions about the style of Grampian orogenesis that were previously obscured by larger uncertainties.

First we can examine the duration of the episode. As discussed above, the metamorphic age of the sole of the Ballantrae Ophiolite is linked to the timing of obduction and onset of orogenesis. Our results indicate that the amphibolite unit at the base of the complex reached garnet grade no later than 477.6 ±1.9 Ma. We and others (Oliver 2001; Bluck *et al.*1980; Oliver *et al.* 2000) assert that this offers a

robust constraint on the timing of onset of collision in the region. On the other end of the Grampian episode, detrital metamorphic garnet in molassic conglomerates of age 465 ± 2.5 Ma (biostratigraphic age constraint of Tucker and McKerrow 1995) signifies the start of erosion post-orogenesis. With our new constraint on the timing of Ballantrae obduction, we can significantly refine our knowledge of the duration of the Grampian episode. Propagating the uncertainties of our measurement, we constrain the duration of Grampian orogenesis to 12.6 ±3.1 million years (2σ). This represents a significant improvement on the previous constraint of 13.0 ± 8.4 m.y. (using the K/Ar age of Bluck *et al.* 1980). Figure 1.6 shows this relationship. Note that the Sm-Nd age of 505 ± 11 Ma (Hamilton *et al.* 1980) is shown, but as it is interpreted as a pre-obduction age we do not consider it a constraint on onset of Grampian orogenesis.

In a region that has been the subject of multiple studies using "geospeedometry" (e.g Viete *et al.* 2011; Ague and Baxter 2007) a new constraint on the onset of deformation and metamorphism is very valuable. As an example, we calculate a minimum heating rate for Dalradian metasediments near Glen Clova, the type locality for Barrovian-style metamorphism. Note that these metasediments *are not* a part of the Ballantrae Ophiolite Complex. Instead, they represent continental sediments which were buried, metamorphosed, and deformed as a result of Grampian orogenesis.

Baxter *et al.*(2002) and Oliver *et al.*(2000) provide garnet ages for peak conditions in the unit. Assuming sediments were at surface conditions (25 °C) at the

beginning of collision at 477.6 ±1.9 Ma and reached a temperature of at least 500 °C by 472.9 ± 2.9 Ma (Baxter *et al.* 2002, consistent with Oliver *et al.* 2000), we calculate a time-averaged heating rate of 101 (+284, -43) °C per m.y. This represents incredibly fast heating, inconsistent with heating due solely to overthickening and thermal relaxation (England and Thompson 1984). There are a number of possible explanations for this. First, perhaps our starting assumptions are unreasonable. Indeed, it is plausible and even probable that that the Barrovian metasediment in question was already somewhat buried at the onset of Grampian collision (when the Ballantrae sole reached 850 °C). Additionally, it may be inappropriate to consider gradual monotonic heating over this time period. It has been repeatedly suggested that Barrovian micaschists were subject to rapid thermal pulses as the result of contact metamorphism or other short-lived processes (e.g. Ague and Baxter 2007; Viete *et al.* 2011; Viete *et al.*2013). If this is the case, a time-averaged heating rate does not truly apply. Rather, the time window of 4.7 ±3.5 between collision and garnet growth simply represents the period in which these brief temperature spikes may have occurred.

Figure 1.7 represents this visually as a temperature-time path for Glen Clova metasediments modified after Baxter *et al.* (2002). This new constraint on the onset of the Ballantrae's obduction provides a starting-point for the metamorphic history of these continental metasediments. Even allowing for starting temperatures around ~100 °C (assuming some burial and diagenesis), time-averaged heating rates are on the order of 100 ° C /m.y. While much remains open to interpretation,

our data are broadly consistent with very short-lived metamorphism and thermal activity and rule out the gradual heating rates (on the order of 5 °C/ m.y.) that are commonly associated with classic regional metamorphism.

CONCLUSIONS

We report a Sm/Nd garnet age of 477.6 ± 1.9 Ma for the garnet amphibolite unit in the metamorphic sole of the Ballantrae Ophiolite. While further thermobarometric and kinetic analysis is needed, we prefer the interpretation that this age records garnet crystallization. Most significantly, this new data reveals the timing of obduction of the Ballantrae ophiolite complex and the onset of Grampian orogenesis in Scotland. We use this constraint to calculate a total duration of 12.6 ±3.1 Ma for the entire Grampian episode. Given such a short event, our results are broadly consistent with the suggestion that Barrovian metamorphism in the region was characterized by rapid, short-lived heating and correspondingly fast exhumation.

Table 1.1 shows existing geochronologic data for the Ballantrae Ophiolite complex. All errors given are 2σ standard errors.

Table 1.2 lists isotopic data for all accepted samples from 11ESC-18A. All uncertainties are 2σ stand errors. Where the internal precision of a given measurement exceeds our external reproducibility, the external limit is reported.

Table 1.3 lists isotopic data for two rejected samples. All uncertainties are 2σ standard errors. Where the internal precision of a given measurement exceeds our external reproducibility, the external limit is reported. The $^{152}Sm/^{144}Nd$ ratio reported is the oxygen isotope interference subtracted ratio in a nominally pure Nd aliquot. These two samples have $^{152}Sm/^{144}Nd > 0.01$ and were therefore excluded from further analysis.

Figure 1.1 is a very general geologic map of the Scottish highlands and a more detailed map of the Ballantrae Ophiolite Complex. It is taken directly from Spray and Williams (1980) with no alteration. Black boxes indicate areas where the metamorphic sole of the ophiolite is visible in outcrop.

Figure 1.2 is a schematic cross-section of Grampian orogenesis takin directly from Oliver (2001).

Figure 1.3 shows the results of a blank correction calculation on garnet 3 (the smallest, and therefore most susceptible sample). Note that while the data points are statistically distinguishable, this shift along the isochron does not have a significant effect on age calculations.

Figure 1.4 is an 8 point Sm/Nd isochron calculated and plotted using the program isoplot (Ludwig 2003). All errors are given as 2σ standard errors. Notice that Powder 4 falls visibly off the linear trend defined by the other 7 points.

Figure 1.5 is an 8 point Sm/Nd isochron calculated and plotted using the program isoplot (Ludwig 2003). All errors are given as 2σ standard errors. The given age of 477.6 ± 1.9 Ma is our preferred age of obduction of Ballantrae Ophiolite.

Figure 1.6 shows the duration of Grampian Orogenesis as constrained by our new age (477.6 ± 1.9 Ma) and a detrital garnet deposition age of 465 ± 2.5 Ma (Tucker and McKerrow 1995). The best previous constraint on onset of collision (478 ± 8 Ma from Bluck *et al*. 1980) is included for reference.

Figure 1.7 is a temperature-time path for Dalradian metasediments near Glen Clova modified after Baxter *et al.*(2002). The black circle represents our new constraint on the obduction of the Ballantrae Ophiolite complex and onset of orogenesis. The large temperature error bars on this point are meant to signify a range of conditions achievable through sedimentation and burial prior to orogenic heating. Squares are from Baxter *et al.*(2002) and triangles are from Oliver *et al.*(2000). Each point is keyed to a different path indicating peak conditions reached by that unit. Garnet and sillimante and kyanite isograds included for reference are from Spear and Cheney (1989) and McLellan (1985) respectively.

Publication	Age ±2 S.E.	Method	Tectonic Context
Hamilton *et al.* (1984)	575 ± 32 Ma	Sm-Nd whole rock	Pre-orogenic 'eclogite'
Hamilton *et al.* (1984)	505 ± 11 Ma	Sm-Nd whole rock	Pre-obduction pyroxenite
Bluck *et al.* (1980)	484 ± 4 Ma	U-Pb zircon	Pre-obduction trondhjemite
Bluck *et al.* (1980)	478 ± 8 Ma	K-Ar hornblende	Synorogenic amphibolite
Sawaki *et al.* (2010)	470 ± 10 Ma	U-Pb zircon	Synorogenic tuff

Table 1.1
Existing Chronology of the Ballantrae Ophiolite

Sample	**Ng Nd loaded**	**Nd (ppm)**	**Sm (ppm)**	**$^{147}Sm/^{144}Nd$**	**±2 S.E.** (abs)	**$^{143}Nd/^{144}Nd$**	**± 2 S.E. (abs)**	**± 2 S.E ppm**
WR1	28	9.774	3.385	0.20948	0.00005	0.5130187	0.000009	17
WR2	21	8.940	3.064	0.20733	0.00005	0.5129966	0.000016	31
Gt 3	5.2	1.009	1.937	1.16184	0.00089	0.5159929	0.000025	48
Gt 5	6.1	0.854	1.649	1.16817	0.00043	0.5160252	0.000013	26
Gt 7	12	1.196	2.326	1.17678	0.00029	0.5160271	0.000015	29
Pow D	11	0.925	1.065	0.69621	0.00016	0.5145318	0.000024	48
Pow C	49	2.279	2.137	0.56717	0.00013	0.5141251	0.000016	31
Pow 4*	12	2.343	2.181	0.56323	0.00018	0.5139841	0.000057	112

Table 1.2
Isotope Data for 11ESC-18A

Sample	Ng Nd loaded	Nd (ppm)	Sm (ppm)	$^{147}Sm/^{144}Nd$	$^{143}Nd/^{144}Nd$	± 2 S.E. (abs)	$^{152}Sm/^{144}Nd$
Gt 4	3.9	1.470	2.762	1.13665	0.5157855	0.000057	0.0280
Gt 6	13	0.902	1.769	1.18587	0.5160309	0.000020	0.0139

Table 1.3
Isotope Data for excluded samples of 11ESC-18A

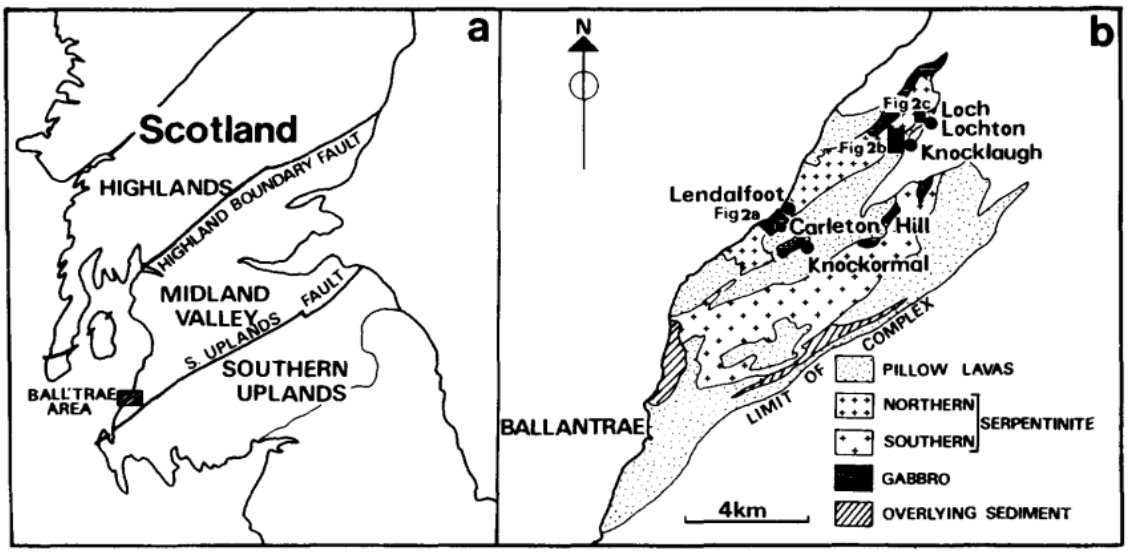

Figure 1.1
Geologic Map of the Ballantrae Ophiolite from Spray and Williams (1980)

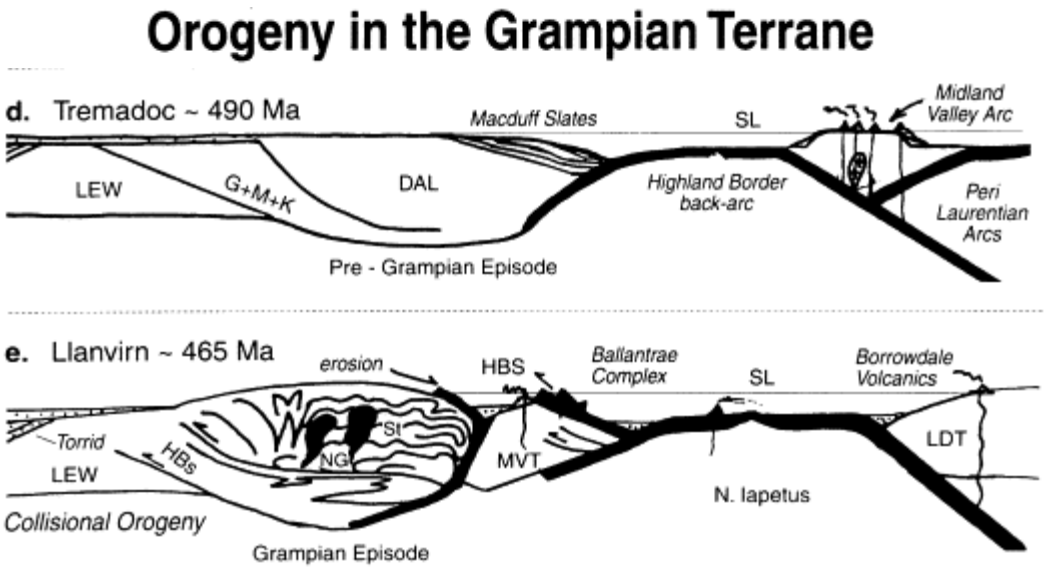

Figure 1.2
Schematic Representation of Grampian Collision From Oliver (2001)

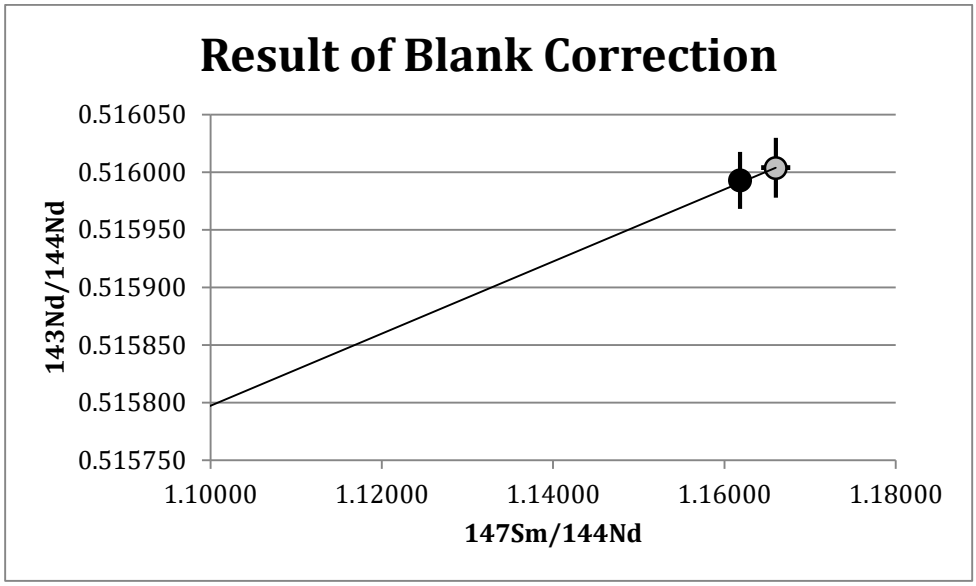

Figure 1.3
Blank Correction of Garnet 3

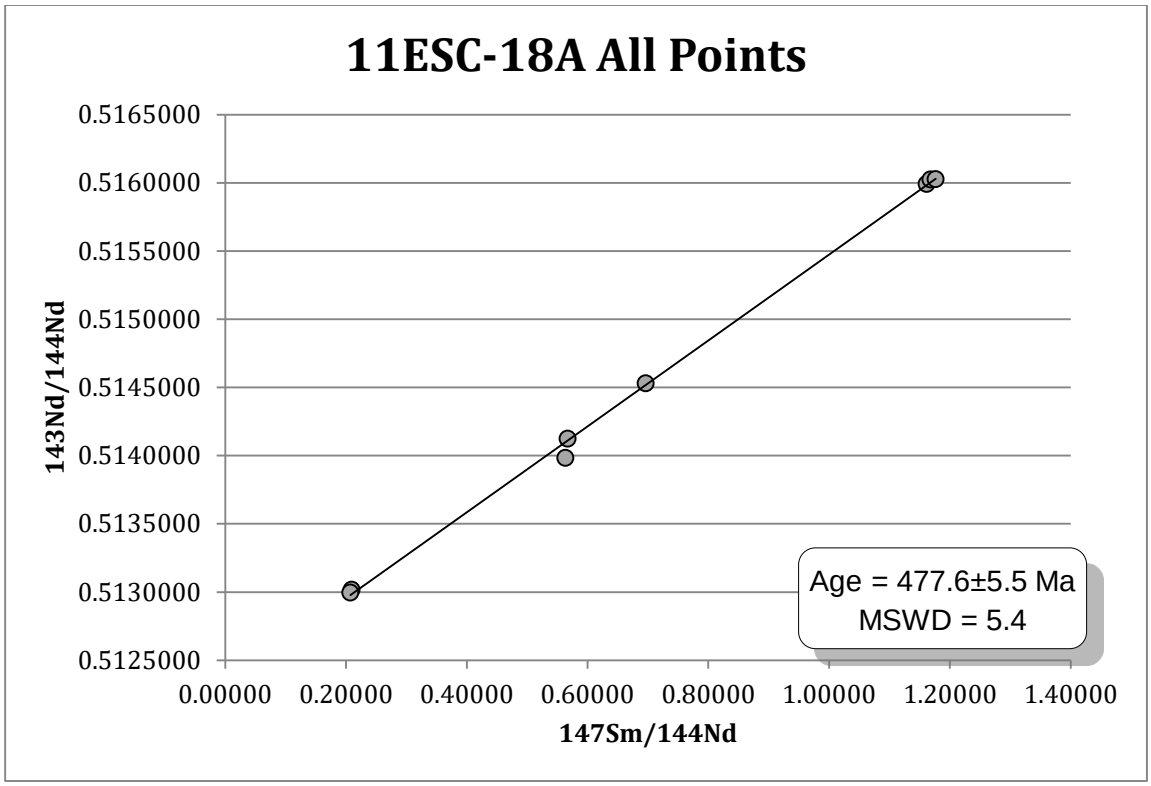

Figure 1.4
8 Point Isochron Including All Accepted Data

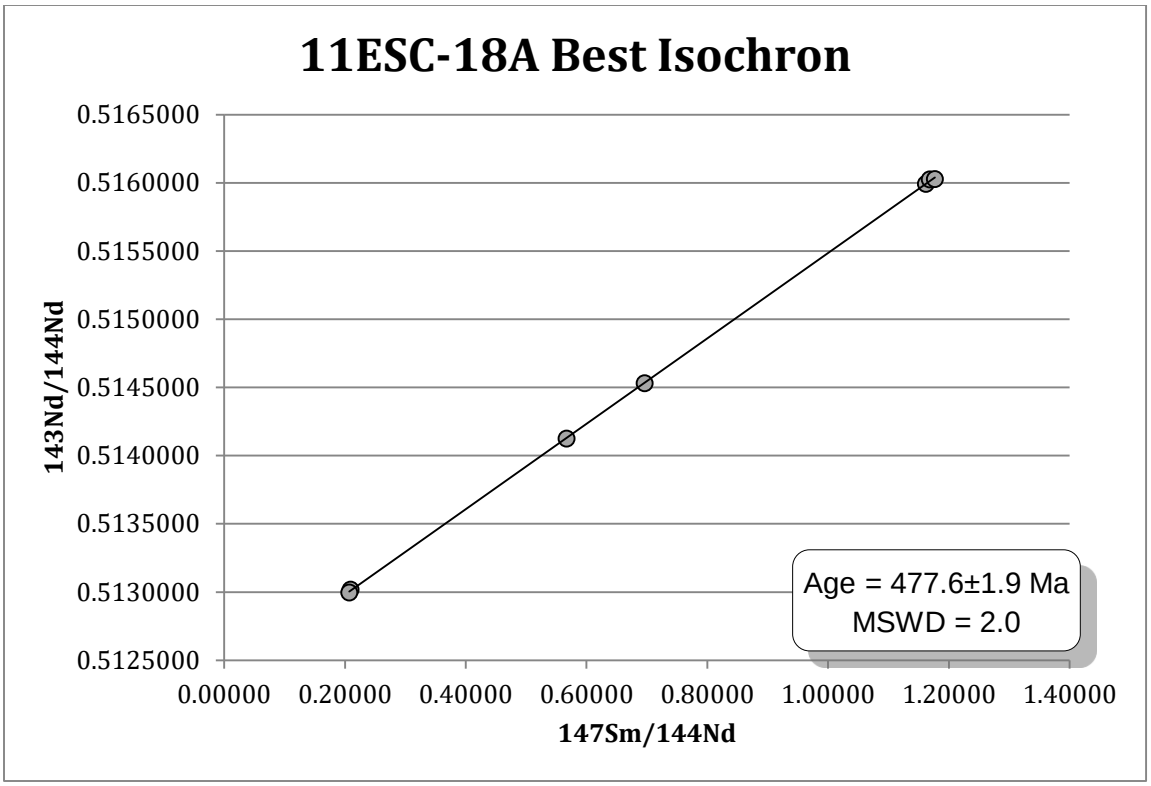

Figure 1.5
7 Point Isochron Representing Best Age of 11ESC-18A

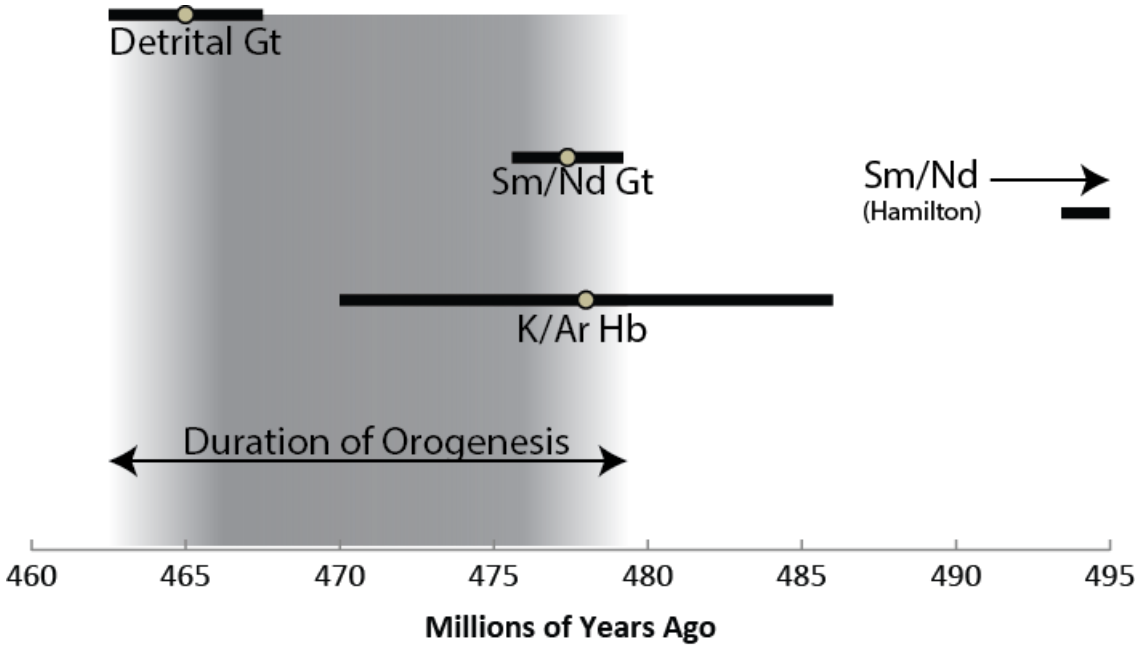

Figure 1.6
Duration of the Grampian Episode of the Caledonian Orogeny

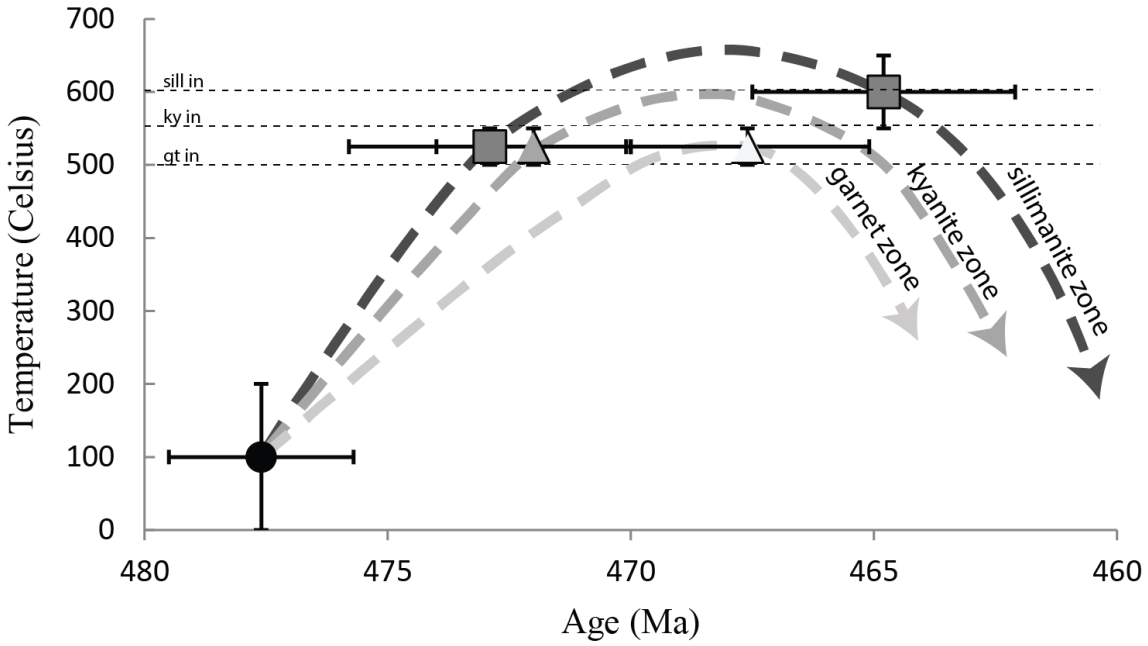

Figure 1.7
Temperature-Time Paths for Glen Clova Metasediments

CHAPTER TWO: Exploring the Tectonic Significance of Porphyroblast Inclusion Trails via Sm/Nd Garnet Geochronology in the Betic Cordillera, Spain

INTRODUCTION

Metamorphic microstructures are the lens through which we view ancient orogenesis and deformation. Over more than a century, a body of work has emerged to describe and interpret the textures that are present in metamorphic rocks (e.g. Cobbold and Gabais 1987; Hanmer and Passchier 1991; Goldstein 1988; Platt and Visser 1980). Mica fish, sigmoidal veins, and asymmetric boudinage are well-established indicators of shear-stress, but their interpretive utility is limited -- matrix structures often preserve only the last or strongest phase of deformation that a rock has endured. However, porphyroblastic minerals such as garnet may include textures that record the deformational setting at the time of their growth; these mineral "inclusion trails" offer a unique opportunity to tease out a more complete deformational history for a region.

Often, the inclusion trails within porphyroblasts are sigmoidal or spiral-shaped and exist at a high angle to the matrix fabric. Two competing hypotheses attempt to explain this relationship. One holds that porphyroblasts have rotated relative to a stationary matrix fabric as a result of shearing (e.g. Rosenfeld 1968, Passchier *et al.* 1992). Conversely, other researchers suggest that porphyroblasts do not rotate relative to geographic coordinates and any apparent rotational axis is interpreted as an intersection between subsequent foliations (e.g. Bell *et al.* 1989;

Hayward 1990). (Note that from here forward the term “foliation intersection axis” or FIA will be used to refer to this feature with no implications about formation intended.)

Whatever their formation mechanism, there is no doubt that porphyroblast inclusion trails preserve a great deal of information about deformation. In order to understand the *regional significance* of these microstructures, however, it is first necessary to understand how regionally-variable inclusion trail axes relate to one another both spatially and temporally. With this in mind, we report the results of Sm/Nd garnet geochronology of structurally characterized samples from the Betic Cordillera in southern Spain. Through this novel combination of microstructural and geochronologic data sets we aim to test the hypothesis that FIA orientations are regionally and temporally consistent, and may thus be interpreted as a proxy for broader tectonics/plate motion.

BACKGROUND

A foliation intersection axis (FIA) is defined as the axis of curvature of an inclusion trail within a porphyroblast. As mentioned above, there are multiple competing explanations for the formation of this feature. The more classic interpretation set forth by Rosenfeld (1968) is that FIA represent the axis of rotation of the including porphyroblast during shearing. This interpretation is appealing in its simplicity – one can easily visualize how porphyroblast growth synchronous with shearing would result in curving inclusion trails. However, this interpretation does have some limitations. First, while this model readily explains

smoothly curving inclusions, it fails to account for geometries defined by simultaneous truncation and deflection. Second, it cannot explain why two porphyroblasts in the same section would exhibit opposite shear senses, as is often observed (Bell and Hayward, 1992). Furthermore, a porphyroblast rotation model would predict a random distribution of foliation intersection axes, while in fact FIA tend to be subhorizontal or subvertical around the globe (Bell and Hayward, 1992). Finally, porphyroblast rotation is unlikely to occur as the result of coaxial deformation (i.e. simple shear) thus its application to many geologic settings is debatable (Fay et al., 2008).

An alternative interpretation of FIA is that they represent a curving foliation preserved within a stationary porphyroblast. In this case, the foliation intersection axis would represent the fold axis of a crenulation cleavage and/or the intersection lineation between two different foliations. FIA as intersection lineations are perhaps easier to visualize – a garnet or other porphyroblast overgrows a foliation Sn. A new foliation, Sn+1, develops as the porphyroblast continues to grow. The foliation in the core of the garnet, Sn, will be truncated by Sn+1, and the resultant intersection lineation is a FIA. Alternatively, as a foliation Sn is crenulated, the porphyroblast will overgrow that crenulation and the fold axis is a FIA. The power of this interpretation of FIA is that it allows one to look back in time at previous stress field orientations. With a detailed analysis of crosscutting relationships and FIA orientations, one could theoretically reconstruct the changing stress directions in a region at any time when porphyroblasts were crystallizing. There are some limitations to this method,

however. First, it is slightly more difficult to explain the existence of smoothly curving porphyroblast inclusion trails. While a fabric that anastomoses around porphyroblasts can account for sigmoidal inclusion trails (Bell and Hayward, 1992), critics suggest that porphyroblast rotation is a simpler, and therefore preferable, solution (e.g. Passchier *et al.* 1992). Second, it is not completely straightforward to identify FIA orientations. Two complementary methods exist: the asymmetry technique of Bell and Hayward (1992) (see also Hayward 1990) and Fitpitch program developed by Aerden (2003). With both of these techniques, however, the anastomosing nature of foliations means that the strike of a FIA can only be determined within ± 15°.

Despite these complexities, the relationship between FIA and stress direction is less hotly contested. With either a rotational or stationary porphyroblast model, the axis is expected to lie orthogonal to the major compressive stress. Figure 2.1 helps to demonstrate this relationship. What remains to be determined is whether synchronous FIA are similarly oriented at the regional scale. That is, is FIA orientation controlled by broad scale plate motions? Or do smaller scale processes (such as individual faults or shear zones) control their formation?

GEOLOGIC SETTING

In order to answer these questions, the Betic Cordillera in southern Spain provides an ideal location for this research. With 4 discrete FIA orientations measured in 93 garnetiferous rocks by Aerden *et al.* (2013) and multiple, consistent reconstructions of plate motion (Vissers and Meijer 2012; Handy *et al*. 2010;

Meijninger 2006) the addition of geochronology to this region has the potential to provide concrete answers to the above questions. Additionally, a detailed compilation of field data and macrostructural measurements is available in Aerden and Sayab (2008).

The Betic Cordillera on the southernmost coast of Spain is comprised of a fold and thrust belt in the North and a metamorphic hinterland to the South (De Galdeano, 1990). The fold and thrust belt, often termed the "external zone" is composed of late Triassic to middle Miocene sediments likely from the proposed Alkapeca microplate. The hinterland, "Alboran Domain", or "internal zone," is a stack of strongly metamorphosed thrust nappes. These are largely Paleozoic in age and of uncertain tectonic affinity, though ophiolite sequences from the closure of the westernmost Tethys, are interposed. (De Galdeano, 1990; Michard *et al.,* 2002; Puga *et al*., 2002; Aerden *et al*., 2013). The samples characterized in this study belong to the internal zone, specifically the Nevado-Filábride domain, so that is where we will focus this discussion.

The internal zone is classically divided into three major nappe complexes: the Nevado-Filábride, the Alpujárride, and the Maláguide from bottom to top. Based on its varying tectonic and lithologic characteristics, the Nevado-Filábride domain can be subdivided into two complexes: the Veleta Complex and the Mulhacén Complex (Puga et al., 2002). The Veleta Complex (VC) is the deepest unit of the internal zone and is dominated by graphitic schists with a history of a high pressure-low temperature metamorphism. The overlying Mulhacén Complex (MC)

is primarily continental crustal basement with an ophiolitic sequence tectonically intercalated. Due in large part to its structural similarity with Alpine sequences, it is suggested that the MC is composed of continental crust from the Adria and Alkapeca microplates separated by Tethyan oceanic crust. The age of metamorphism in the Nevado-Filábride domain remains uncertain with
suggested ages ranging from late Cretaceous through Miocene (Aerden *et al.* 2013; Puga *et al.* 2002; Augier *et al*. 2005). Figure 2.2 is a geologic map of the region taken directly from Puga *et al.* (2002).

A number of studies have attempted to reconstruct large scale plate movements in the Mediterranean using paleomagnetic data, oceanic magnetic isochrons, and structural analysis (e.g. Vissers and Meijer, 2012; Rosenbaum et al., 2002; Michard et al., 2002, Bakker et al., 1989; De Galdeano, 1990). There is general consensus that convergence between Africa and Europe began in the late Cretaceous with the northward subduction of the African plate beneath Eurasia. This convergence was the driving force for the Alpine Orogeny which reached its peak during the Paleocene to Eocene. In the Betic Cordillera, the collision of at least three microplates (Adria, Alkapeca, and Iberia) contributed to deformation and mountain building. The Iberian microplate underwent significant rotation and became coupled with Europe about ~30 Ma. This suture zone is marked by the Pyrenees mountain chain which is still under compression at present (Vissers and Meijer, 2012). The proposed Alkapeca microplate was destroyed by the closure of the Tethys and now forms the External Zones of the Betic Cordillera and The Rif

Cordillera in northern Africa (Michard et al., 2002). Paleomagnetic data suggests that the Adrian microplate (present day Italy) was coupled with Africa until ~39 Ma when it began to move west with respect to Iberia.

EXISTING STRUCTURAL WORK

Macroscopic structural studies have concluded that this zone was affected by four distinct phases of deformation (Bakker et al, 1989; Aerden and Sayab, 2008). Because of the difficulty of dating large scale structures, the timing of these deformational events remains largely unconstrained. The recent microstructural and petrological work of Aerden et al. (2013) attempts to link microstructure to macrostructure and, ultimately, plate motion. This study used the aforementioned Asymmetry Technique and the program Fitpitch to identify foliation intersection axes in garnet porphyroblasts of the Nevado-Filábride Domain. 83 samples from the Mulhacén Complex and 10 samples from the Veleta Complex were collected for petrologic and microstructural analysis. Both FIA identification techniques returned four sets of FIA in the samples. Based on crosscutting relationships, the FIA orientation trends from oldest to youngest are 1) NE-SW, 2) NW-SE, 3)W-E, and 4)NNW-SSE. In addition to linking these microstructures with macrostructure, Aerden *et al*. (2013) use major element zonation and thermobarometry to connect each of these FIA orientations to a region in Pressure-Temperature space. In essence, they have constrained the P-T-d evolution of the terrane.

Perhaps most importantly, Aerden *et al.* (2013) propose that the progression of these FIA can be linked to plate motion in the region (see Figure 2.3). Recall that

the trend of a given FIA (like a fold axis) should be perpendicular to the major compressive stress, in this case the direction of convergence. Aerden *et al*. (2013) note that the FIA they measure line up remarkably well with the tectonic reconstructions of the area. In fact, they estimate that the probability of this correlation occurring by chance is less than 0.1%. Despite the strength of this relationship, the absolute timing of these stress orientations remains speculative.

Prior to this study, the succession of these microstructural generations was constrained only by cross-cutting relationships. There was no absolutely chronology establishing the age of each FIA and its relationship to plate motion. Thus the primary contribution of our work is to offer an absolute constraint on the timing of formation of each FIA.

SAMPLE DESCRIPTIONS

Four previously characterized samples were selected for bulk garnet chronology. A detailed description of each sample can be found in Aerden *et al.* (2013), but their general characteristics as determined in that study are summarized here.

B13c

Sample B13c is a garnetiferous micaschist belonging to the Veleta Complex. Mineralogically, its matrix is composed of muscovite + biotite + quartz + chloritoid+ graphite + other opaques. Garnet porphyroblasts are regularly distributed throughout the matrix and are consistently ~1 to 2 mm in diameter. Their inclusion

population is dominated by quartz with minor chlorite and Fe-oxides and sparse zircons. Figure 2.4 is a layered EDS image of a typical garnet from this sample. B13c is described in great detail in Aerden *et al.* (2010).

Structurally, the garnets in B13c exhibit overwhelmingly consistent, linear inclusions oriented northeast. This is interpreted as FIA generation 1. The matrix forms an incipient crenulation cleavage at the boundary of porphyroblasts indicating that garnets crystallized early during FIA generation 2. Thus, though the garnets include FIA 1, they are predicted to have grown during FIA 2 between 39 and 33 Ma.

B2b

Sample B2b is another garnetiferous michaschist, this time from the Mulhacen Complex. Garnets are larger (several mm in diameter) and account for a smaller proportion of the whole rock. The inclusion population is also very different from B13c; quartz remains the dominant inclusion but is accompanied by significant quantities of epidote, tourmaline, and opaque minerals. Figure 2.5 is a photomicrograph of a representative garnet porphyroblast.

The inclusion trails in B2b are more structurally complex. A pervasive Southeast striking inclusion trail is visible in garnet rims. This is interpreted as belonging to FIA set 2. An additional truncation is oriented at ~N015E and its interpretation is more ambiguous. It could alternately be assigned to FIA set 1 or FIA set 4; it may be crosscut by FIA 2 in some places, thus the preferred interpretation of Aerden *et al.* (2013) was that this represents the oldest FIA

generation. However, more structural characterization is needed, and the predicted age of the garnets is more poorly constrained. The average age of garnet in this sample may lie between FIA 2 and 3 and thus ranges from 39 to 19 Ma.

B3b

Sample B3b is yet another garnet bearing schist, this one from the ophiolitic subunit of the Mulhacen Complex. Chloritoid and garnet porphyroblasts exist in a mica rich matrix along with small (less than 1 mm) staurolite grains. Garnets are several mm in diameter and inclusion populations are more diverse. Quartz is a less dominant inclusion here. Instead, ilmenite, tourmaline, and epidote dominate with minor small staurolite.

Inclusion trails are bimodally distributed with south-southeast orientations in rims and east-northeast strikes in garnet cores. These are interpreted as FIA 4 and FIA 3 respectively, thus B3b is predicted to give the youngest bulk age. Figure 2.6 is a layered EDS image of a representative garnet porphyroblast.

B17a

The final sample selected for bulk garnet chronology is sample B17a. It also belongs to the ophiolitic subunit of the Mulhacen. Chloritoid is abundant in the matrix along with mica minerals and quartz. Inclusion trails are dominated by Fe-Mg oxides, tourmaline, and quartz. Figure 2.7 is a layered EDS map of a garnet from sample B17a.

Structurally B17a is characterized by ~east-west and south-southeast striking inclusion trails. These are interpreted as FIA 3 and FIA 2 respectively. Therefore it is expected that garnet crystallized between 39 and 19 Ma.

Garnets Selected for Zoned Work

Sample 27.1.2 was collected in May 2014 by the author and Domingo Aerden. It is a quartz rich micaschist with large garnet porphyroblasts up to ~1 cm in diameter. After cutting several horizontal slabs, two garnets from this sample were selected for detailed zoned analysis.

Garnet C2-1

Garnet C2-1 is around 1 cm in diameter with spiraling inclusion trails. The inclusions are dominated by quartz crystals on the order of 1 mm across. Very small (< 0.1 mm) zircon and rutile grains are distributed throughout the garnet and large (>1 mm) kyanites are present in the rim zones.

The garnet has a small core where inclusions trend ~east to west. From there they curve into or are truncated by north-south trending trails which curve back to east-west and finally approximately north-south again. These microstructural relationships appear to span all structural generations, thus each of these four zones is expected to correspond to one of the four FIA. Note however, that each zone could offer only an absolute lower bound on the age of the included structure. Figure 2.8 is a back-scatter electron image of garnet C2-1.

Garnet B6

Garnet B6 is also approximately 1 cm in diameter. The inclusions in B6 are dominated by coarse grained quartz and very fine zircon, monazite, and rutile. The inclusion trails rotate from east-west in the core, north-south in the mantle, and back to ~east-west in the rim. Figure 2.9 is an electron back-scatter map of garnet B6. These three zones correspond to the three inner zones of garnet C2-1, thus B6 is expected to yield older ages on the whole.

ANALYTICAL METHODS

SEM Analysis

All analyses were performed in the SEM lab at Boston College on a Tescan Vega 3 LMU variable pressure (VP) scanning electron microscope equipped with a LaB6 source and a variety of analytical detectors. Thin or thick sections were polished with a diamond suspension and carbon coated prior to loading in the machine. Images were created using backscattered electrons (BSE) and chemical maps and point analyses were achieved via Energy Dispersive Spectroscopy (EDS) at a voltage of 20 kV.

Bulk Preparation

The four samples chosen for bulk analysis were all processed similarly. A visibly unaltered ~fist-sized chunk was chosen and any weathering rind was removed with a rock saw. After coarsely crushing this chunk in a tungsten carbide, a representative portion was set aside for whole-rock isotopic analysis. Care was taken to avoid any grain size or mineralogical fractionation in this portioning. The whole-rock fraction was completely powdered to <200 mesh in an agate ball mill.

The remaining coarse-crushed material was the reservoir from which garnet separates were created. This separation was achieved through a combination of frantz magnetic separation, hand-picking, sieving, further crushing, and paper-shaking. When the separate was deemed sufficiently pure it was crushed in a small tungsten carbide percussion mortar to one of three grain sizes: 100 to 200 mesh, 140 to 200 mesh, or 140 to 230 mesh. The grain size was chosen to maximize the size of garnet grains while minimizing the number of unexposed inclusions or aggregate grains. Whatever material passed through the finer mesh after crushing was retained and labeled garnet "powder". Note that in some cases two different fist-sized chunks of sample were processed. This is designated by a "-1" or "-2" in the sample name. For example, sample B13c includes whole rock, powder, and garnet analyses from chunk B13c-1 and B13c-2.

Micro-drilling

The garnets chosen for zoned analysis were processed somewhat differently. A preliminary chunk of sample 27.1.2 was treated with exactly the above procedure to determine ideal grain size and laboratory procedures. Then a ~1mm thick slab of each garnet was cut, polished, and glued onto a glass slide using Crystalbond™. This slab was then carbon coated and analyzed on the SEM at Boston College. After imaging, destructive analysis could begin.

Using the chemical data from the SEM, four zones from each garnet were selected for analysis. The wafer of rock was removed from the glass slide and glued onto a carbon block. These zones were then separated from one another by drilling

on the Micromill drilling system from New Wave. Figures 2.10 and 2.11 show the planned drill paths for garnet C2-1 and B6, respectively. Figure 2.12 shows the progressive drilling of garnet C2-1 as each zone was drilled out and removed. Figure 2.13 shows two paths drilled in garnet B6. Note that the outer two zones of garnet B6 have not yet been separated for analysis. The inner two zones of garnet B6 were subsequently lumped together for analysis due to their small mass.

After drilling, each garnet zone was plucked from the carbon block and ultrasonicated in acetone to remove any remaining crystalbond. Once clean, each zone was crushed in a small tungsten carbide mortar and pestle, sieved to 100 to 230-mesh, passed through the frantz magnetic separator, and hand-picked until visually pure. More detail on this process is available in Appendix A

Clean Lab Dissolution and Column Chromatography

Both bulk garnet separates and individual zones were treated with identical procedures in the clean lab. They underwent partial dissolution (modified after Pollington and Baxter 2011) in order to eliminate mineral inclusions that were not mechanically separable. Several iterations of this procedure were performed to determine the optimum duration of each step. Each sample was left in a closed beaker of concentrated HF and 1.5N HCl at 120°C for a period of time ranging from 30 to 120 minutes. The duration of this step was chosen to create a separate of maximum purity while minimizing sample loss. After HF, each sample was kept in 2 mL of concentrated $HClO_4$ at 150 °C for either 3 hours or overnight. Finally the separate was treated with 2 mL of concentrated HNO_3 for 3 hours at 120 °C. This

was the final stage of the partial dissolution procedure. If any visible non-garnet grains remained at this stage they were removed by hand picking.

After partial dissolution, garnets were fully dissolved in a three-step procedure using first concentrated HF, then concentrated HNO_3 and 1.5 N HCl to break down secondary fluorides. An identical procedure was used to fully dissolve whole rocks and garnet "powders" which did not undergo any partial dissolution.

Subsequent to dissolution, Nd and Sm were spiked with a ^{147}Sm-^{150}Nd mixed spike (Harvey and Baxter 2009) and separated for analysis with a three-column liquid chromatography procedure. First samples were passed through a clean-up column to remove excess Fe and other major elements. Samples were then passed through a Tru-Spec column to eliminate all but the rare earth elements. Finally a 2-methyllactic acid column was used to isolate Sm and Nd. 3-column blanks ranged from 4.6 up to 33.9 pg Nd. Their effect on small samples will be considered in detail in the appendices.

TIMS Analysis

Sm and Nd were analyzed at the Boston University TIMS facility on a Thermo-Finnigan TRITON Thermal Ionization Mass Spectrometer. Nd is run in static mode as an oxide (e.g. NdO^+) and a Ta_2O_5 activator slurry described in Harvey and Baxter (2009) is used to facilitate ionization. A 4ng UCB Ames NdO standard was run along with every barrel to track our external reproducibility. The average $^{143}Nd/^{144}Nd$ for the time over which samples were run is 0.5121204±0.0000092 (17.9ppm, 2σ, n=67). Sm was loaded onto zone-refined Re filaments and was run as

a metal, also in static mode with amplifier rotation. $^{147}Sm/^{144}Nd$ reproducibility is 0.023% based on repeat analysis of a gravimetrically calibrated mixed Sm/Nd solution.

DATA

SEM Data

The results of all SEM spot analyses are listed in table 2.1. All abundances are given as total weight percent. Inclusions are identified and named based primarily on their chemistry, but also considering habit and other visual observations. Additional layered EDS images of garnets and their inclusion populations are shown in Figures 2.14, 2.15, 2.16, 2.17, and 2.18 corresponding to samples B3b, B3b, B17a, garnet C2-1, and garnet B6. Figure 2.19 is a Ca map of garnet B6 that shows a distinct chemical zonation not visible in other elements.

Isotope Data

Table 2.2, Table 2.3, Table 2.4 , Table 2.5, Table 2.6, Table 2.7, and Table 2.8 summarize the isotope data available for samples B13c, B3b, B17a, B2b, preliminary analysis of 27.1.2, garnet C2-1, and garnet B6 respectively. Errors reported are 2σ standard errors. Where our external reproducibility is worse than the internal precision of a given measurement, the external limit is reported. All subsequent isochron calculations are performed with the program Isoplot (Ludwig, 2003).

DISCUSSION

Garnet Ages

B13c

Figure 2.20 is a 6-point isochron including all of the data available for sample B13c. The calculated age of 34.9 ± 5.9 Ma is made significantly less precise as a result of the scatter among whole rock and powder analyses (MSWD = 4.2). When garnet powders fall off of a given isochron, it is generally best practice to exclude them from age calculations—they may inherited inclusion phases that may not have equilibrated with the whole rock reservoir during garnet crystallization. It is similarly reasonable to exclude wr2. This whole rock was processed in a pressurized acid digestion vessel in order to digest the significant graphite component of the rock, whereas wr1 was dissolved at atmospheric pressure and the graphite was simply centrifuged out. It is our interpretation that wr1 is a better representation of the reservoir with which the garnet equilibrated during growth. Any highly refractory mineral (e.g. zircons, which SEM data indicate are indeed present in B13c) which was digested at pressure but not at atmosphere should represent the difference between wr1 and wr2. As zircon is often an inheirited or relict phase and is very difficult to reset isotopically, we prefer the whole rock which excludes these resistant phases. With this in mind, we recalculate a 3-point isochron including only the two garnet analyses and wr1. Figure 2.21 shows the result of this calculation which yields an age of 35.5 ± 2.1 Ma. Thermobarometric estimates of Aerden *et al.* (2013) indicate peak temperatures not to exceed 550°C for this sample, thus it is simple to conclude that this age represents primary crystallization and has not been reset by diffusion.

B2b

Sample B2b yields a 12-point isochron visible in Figure 2.22. The age of 18.6 ± 7.4 Ma is rendered less precise in part because of the small spread along the x-axis. There is visible scatter, but the MSWD of 1.9 indicates that the data may have a reasonable probability of fitting a single line. Wendt and Carl (1991) suggest a cutoff of MSWD=1.9 for a 12-point isochron. Using this constraint, the data for B2b are right on the edge of statistically linear. It is, perhaps, more meaningful to consider this a 7-point isochron since many of the data cluster near a single point. In this case, Wendt and Carl calculate a an acceptable MSWD is less than 2.26, and these data pass well below that cutoff.

Notice that the garnet analyses range from 0.215 up to 0.569 in their $^{147}Sm/^{144}Nd$ ratio. The Garnets with the higher ratios are considered "cleaner" garnets while those low $^{147}Sm/^{144}Nd$ ratios are "dirty" or more contaminated by inclusions. However, the fact that all of the garnets fit a single line indicates that this contamination does not compromise our accuracy. Mixing between garnet and its inclusion population lowers the $^{147}Sm/^{144}Nd$ spread and effectively reduces our precision, but it does not appear to be affecting the accuracy of our age calculation.

It is interesting to consider the source of the not-insignificant scatter in garnet analyses. As mentioned before, this sample is interpreted as including multiple structural (and therefore presumably age) populations of garnet. Perhaps this scatter, then, is an indication of this real spread in garnet ages variably sampled in each scoop of garnet separate. To quantify this speculation, we calculate two new isochrons: Figure 2.23 is the oldest possible age from this data set, calculated using

only garnet 8 and the whole rocks and powders. Figure 2.24 shows the youngest possible age which includes only garnet 6 and all whole rocks and powders. These two results, 25.6 ± 6.6 Ma and 10 ± 9 Ma show a considerable spread in possible ages. As the sample is calculated to have reached peak temperatures of only ~550° C (Aerden *et al.*), this spread cannot be accounted for by variable diffusional resetting of garnet. Thus we interpret that sample B2b has a garnet population averaging 18.6 ± 7.4 Ma as a result of mixing between multiple garnet age populations which are at least as old as 25.6 ± 6.6 Ma and at least as young as 10 ± 9 Ma.

27.1.2

In a preliminary analysis of sample 27.1.2 we processed two different garnet separates; separate 1 was visually pristine and was carefully hand-picked to maximum purity. Separate 2 was visibly contaminated representing a separate that could be achieved solely through frantzing and sieving. Each separate was split in three and underwent partial dissolutions varying the time in HF from 30 minutes to 60 or 90 minutes. Even after partial dissolution separate 2 was visibly un-pure. Under a picking scope the contaminants were bright blue bladed crystals. Combined with SEM evidence of an aluminosilcate in the sample, we interpret this contamination to be Kyanite.

Omitting the data from separate 2, we can calculate an isochron using only the whole rock and separate 1 garnets and powder. This is visible in Figure 2.25. The result is an age of 15.8 ± 3.5 Ma. All of the garnets and powder fall on the same line (MSWD = 1.5) which indicates that our accuracy is not compromised by

incomplete cleansing. While $^{147}Sm/^{144}Nd$ ratios peak at 0.650, the concentration of Nd remaining in the garnet separates (between 2 and 6 ppm) indicates that it should be possible to clean the garnet more aggressively and yield even higher $^{147}Sm/^{144}Nd$.

27.1.2 Garnet C2-1

Each zone of garnet C2-1 was analyzed separately and paired with two whole rocks and a matrix (whole rock minus garnet) for age analysis. The analysis of zone A was so poor (2 S.E. on $^{143}Nd/^{144}Nd$ = 2815 ppm) that it is excluded from further consideration. Zone B gives the most precise age of 17.6 ± 6.2 Ma and the highest $^{147}Sm/^{144}Nd$ of 2.5384 ± 0.00114 (Figure 2.26). Zone C gives a high $^{147}Sm/^{144}Nd$ of 2.0202 ± 0.00286 but with poor internal precision as a result of small sample size the age is imprecise at 21 ± 26 Ma (see figure 2.27). Zone D has good internal precision but with a very low $^{147}Sm/^{144}Nd$ of only 0.2145 ± 0.00005 the age is 36 ± 19 Ma (Figure 2.28).

27.1.2 Garnet B6

As mentioned above, garnet B6 yielded only one zone for chronology. Zone A and B were drilled apart but ultimately lumped back together for analysis. Zones C and D have not yet been drilled. Zone A+B is paired with a whole rock for isochron analysis. Figure 2.29 shows the result of this calculation. Garnet B6 is anomalously old with an age of 318 ± 130 Ma. There are a few alternatively explanations for this result. One is that our pairing zone A and B with the modern whole-rock is inaccurate. Perhaps the core of this garnet equilibrated with a very isotopically

different whole rock reservoir. However, the magnitude of this effect is probably not enough to account for skewing an Eocene age to all the way to the Paleozoic. This would require a whole rock with $^{143}Nd/^{144}Nd \approx 0.51300$, a change of nearly 2000 ppm from the modern whole rock. This potential whole-rock with $\varepsilon_{Nd} = +7.2$ is totally unreasonable for a crustal source, which should yield negative ε_{Nd} (Bouvier *et al.*2008; DePaolo and Wasserburg 1976). With this in mind, whole-rock garnet disequilibrium *cannot* be called upon to account for the anomalously old age.

Alternatively, it is possible that the garnet core contains inherited relict grains that are much older. Once again, though, the magnitude of such an effect is unlikely to result in such an old age. Our SEM imaging shows the garnet core dominated by quartz inclusions with very minor (less than 1%) zircon. Such a small amount of zircon simply doesn't have the leverage to change the age so dramatically, especially considering the reasonably high $^{147}Sm/^{144}Nd$ ratio measured (see Amelin 2004). This leaves us with the possibility that the age of 318 ± 130 Ma is accurate, if imprecise. Sample 27.1.2 comes from the Mulhacen complex which is known to have relicts of Variscan metamorphism (Aerden *et al.*2013). Perhaps this age represents a relict garnet core that served as a nucleation center for garnet growth in later Cenozoic orogenesis. It is our interpretation that 318 ± 130 Ma is the actual age of garnet crystallization for the core garnet B6.

Summary

We find ages ranging from possible Variscan relicts at 318 ± 130 Ma to Cenozoic ages from 35.5 ± 2.1 Ma to 10 ± 9 Ma. This alone indicates a prolonged

period of metamorphism and orogenesis in the Betic Cordillera from late Eocene through Miocene. Prior to this work, the oldest Alpine garnet age for the region was only 18.2 Ma from Platt *et al.* (2006). The confirmation of late Eocene metamorphism in the Betic Cordillera alone is a significant contribution of this work. Figure 2.30 summarizes these results. The core of garnet B6 is omitted for clarity.

Failed Geochronology

Two of the samples selected for this study did not yield precise or accurate ages. Samples B3b and B17a both belong to the Ophiolitic subunit of the Mulhacen Complex and did not yield useable age results. Figure 2.31 shows what should be an isochron for sample B3b. Even with five garnet analyses processed at various grain sizes with up to 120 minutes in HF, no garnet achieved a $^{147}Sm/^{144}Nd$ ratio above 0.22. In fact most garnet analyses were hardly distinguishable from the whole rock. With such a poor spread along the x-axis, precise or reliably accurate Sm/Nd geochronology is impossible.

Sample B17a exhibits an even stranger pattern of isotope measurements. As seen in figure 2.32, there is almost no spread along the $^{147}Sm/^{144}Nd$ axis. With progressive leaching $^{147}Sm/^{144}Nd$ ratios increase marginally, but there is a corresponding decrease in$^{143}Nd/^{144}Nd$. It is apparent that the partial dissolution technique normally used to clean garnets for chronology is instead functioning to concentrate some contaminant phase.

Petrography indicates that there are abundant tourmaline inclusions in garnet from both samples B3b and B17a. This is confirmed by extensive point analyses on the SEM. Tourmaline can contain up to tens of ppm Nd (e.g. Marks *et al.* 2013; Jiang *et al.* 2004) and in the abundances observed certainly has the leverage to significantly skew the isotopic composition of a garnet with ~0.1 ppm Nd. Furthermore, tourmaline is known as a highly refractory mineral, not readily dissolved in HF at atmospheric pressure (Ito, 1962). Other minerals present in these samples, including scant monazite and allanite, may also have the leverage to contaminate the garnet separate so dramatically. However, these minerals should be easily removed with a partial dissolution procedure (Pollington and Baxter, 2011) and they are not very abundant in the samples of interest. Thus we conclude that the abundant tourmaline inclusions in samples B3b and B17a are being concentrated by our partial dissolution procedure and rendering our normal approach to geochronology impossible. It may be possible to separate the tourmaline inclusions from garnet by relying on tourmaline's more refractory nature. Rather than trying to dissolve away inclusions and leave the garnet as a solid residue, one could attempt to dissolve the garnet and retain the liquid while discarding remaining solids. Our normal full dissolution procedure involves keeping the sample in HF for many hours, but a shorter "full" dissolution may leave tourmaline undissolved and render the garnet separate more pure. This method is suggested for any future work on tourmaline-included samples.

Structural Significance

The major thrust of this research is an attempt to pair Sm/Nd garnet geochronology performed in the TIMS lab at Boston University with the detailed structural work performed at Universidad de Granada (e.g. Aerden *et al.* 2013; Aerden *et al.* 2010). With this in mind, we consider the structural characteristics of each successfully dated in sample in light of new geochronologic results.

B13c

Sample B13c is extremely well structurally characterized in Aerden *et al.* (2010) and also Aerden *et al.* (2013). As described above, it was predicted to give an age corresponding precisely to FIA generation 2. Our age result of 35.5 ± 2.1 Ma agrees remarkably with the age prediction of 39 to 33 Ma. Recall that the relationship between predicted age and measured age should only agree if broad scale plate motions control FIA orientation. This good agreement supports the relationship proposed by Aerden *et al.* (2013).

B2b

Both the structural and geochronologic characterizations of sample B2b are less precisely constrained. Garnets in B2b include FIA 2 and either FIA 1 or FIA 4. This ambiguity in structural classification makes the sample non-ideal for testing the model of Aerden *et al.* (2013). However, in light of the geochronologic data, we propose that the garnets in B2b grew syn-FIA 2 and FIA 4. The oldest age calculated for B2b is 25.6 ± 6.6 Ma. Assuming that this age is made slightly younger by mixing with syn-FIA 4 garnets, this age could easily represent garnets growning in the 33-39 Ma window of FIA 2. The youngest B2b age of 10 ± 9 Ma fits well into the FIA 4

window of 19 to 10 Ma. We suggest that B2b represents two periods of garnet growth between 33-39 Ma and 19 to 10 Ma resulting in the average age of 18.6 ± 7.4 Ma. However, due to poor constraints on the predicted age, this is not necessarily robust evidence of a correlation between plate motion and FIA orientation. If the N015E trending microstructure is instead taken to represent FIA1, this same set of geochronologic data would be seen to refute the model of Aerden *et al.* (2013). More detailed microstructural work is needed and we do not place too much weight on the structural significance of these ages.

27.1.2 Gt C2-1

Zone B of garnet C2-1 gives an age of 17.6 ±6.2 Ma. Because zone B includes the structural generation of FIA 2, we expect the overgrowing garnet to offer a hard lower bound on the age of FIA 2 and most likely to have grown early syn-FIA 3. The age is slightly younger than the predicted age of ~33 Ma, but is ultimately within the longer growth window of FIA 3.

Similarly, Zone C offers a hard lower bound on the age of FIA 3 and may have grown as late as syn-FIA4. With such poor age precision at 21 ± 26 Ma, zone three could literally have grown any time during Alpine orogenesis in Spain. The best we can say is that the age of zone C is not inconsistent with the predicted relationship between plate motion and microstructural orientations.

Finally, zone D is expected to give the age of FIA 4. As with zone three, our precision is not sufficient to resolve this relationship, but the age of 36 ± 19 does not refute the model.

Garnet B6

The age yield by the core of garnet B6 is certainly old enough at 318 ±130 to fit into the FIA 1 window of > 39 Ma predicted by Aerden *et al.* (2013). However, if the core is indeed of Variscan age, we have to conclude that it does not, in fact, record anything to do with Cenozoic plate motion.

Summary

Figure 2.33 summarizes the relationship between geochronologic and structural data -- ultimately these results are inconclusive. Given the combination of poor age precision on many samples and microstructural ambiguities on others, it is impossible to say for certain whether or not the proposed model of Aerden *et al.* (2013) holds water. We can say with certainty, however, that the model has not been refuted. The excellent agreement between model and measurement for the best constrained sample, B13c, is certainly tantalizing. Because the power of a microstructural proxy for broad scale plate motion is potentially enormous, it is worth considering what future work can be done to confirm or refute Aerden *et al.*'s model.

Suggestions for Future Work

First, most frustratingly, and perhaps most significantly we have discovered the limits of the utility of the partial dissolution procedure developed in Pollington and Baxter (2011). Until a new procedure is developed that can effectively separate garnet from fine grain tourmaline inclusions, samples similar to B3b and B17a should be avoided for geochronologic work. Basic petrographic observations of a

garnet's inclusion population should be sufficient to identify tourmaline. As work proceeds on this project, it will be important to select samples for analysis that are absent such problematic inclusion populations.

The other major problem encountered in the work was the small sample size of each garnet zone drilled for zoned analysis. The sub-nanogram masses of Nd remaining after crushing, frantzing, picking, sieving, and partial dissolution were insufficient to provide the necessary precision needed to resolve our questions, especially for such young samples where $^{143}Nd/^{144}Nd$ precision is the most crucial for age precision (Baxter & Scherer 2013). There are a number of ways to increase the Nd available for analysis. First, a thicker wafer of any garnet to be drilled could be cut. Simply increasing the width from ~ 1mm to ~2mm would effectively double the available Nd. Second, an altered rough preparation procedure for drilled zones may be adopted. Especially for zones which are less than 10 mg immediately after drilling, frantzing and sieving may be more destructive than helpful. I suggest that such zones be treated similar to single grain garnets prior to partial dissolution. Katie Eccles (personal communication) crushes these grains, does not sieve them to any particular grain size, and transfers them directly to a Teflon beaker (forgoing any time in glass where significant sample is lost). Adopting a similar procedure for small zones will help to minimize sample loss. Third, a less aggressive partial dissolution should be sufficient to clean garnets. Zone B and C of garnet C2-1 spent only 30 and 45 minutes in HF, respectively. This amount of time was enough to

achieve $^{147}Sm/^{144}Nd$ ratios >2, thus I propose that subsequently processed zones should spend no more than 45 minutes in HF during partial dissolution.

With this in mind, I suggest that zones 3 and 4 of garnet B6 should be drilled and processed with the above modifications. One or two more cm-scale garnet wafers from sample 27.1.2 should also be cut and drilled. Despite the poor precision of drilled samples in this study, all our results indicate that these zones *can* yield clean garnet with high $^{147}Sm/^{144}Nd$ and thus both accurate and precise ages with the adoption of slightly modified sample processing procedures. The ages from a new micro-drilled garnet should help to determine the validity of the model of Aerden *et al.* (2013).

Finally, additional structural characterization of sample B2b will also be extremely valuable. Through additional serial thin sectioning and characterization with the asymmetry technique (Bell and Hayward 1992) and Fitpitch (Aerden 2003) it may be possible to better constrain the structural generations contained in each garnet. This alone, in conjunction with our chronologic data on B2b, may be able to support or refute a relationship between plate motion and FIA orientation.

CONCLUSIONS

We report the results of new Sm/Nd garnet geochronology of structurally characterized samples from the Betic Cordillera, southern Spain. Our results include one possible relict Variscan age of 318 ±130 Ma and seven Alpine garnet ages ranging from 35.5 ± 2.1 Ma to 10 ± 9 Ma. This alone indicates prolonged Cenozoic orogenesis in the Betic range which was previously unconfirmed via radiometric

chronometry. Our best structurally and chronologically constrained sample, B13c, agrees well with the model of Aerden *et al.* (2013) which predicts a correlation between broad scale plate motion and porphyroblast inclusion trail orientations. We can neither refute nor confirm the validity of this model with our dataset, but we make proposals for future work. Ultimately we set the stage for further consideration of the relationship between tectonic plate motion and microstructures both in the Betic Cordillera and around the globe.

Table 2.1 lists all SEM spot analyses acquired as part of this study. Concentrations are given as total weight percent. Mineral interpretations are not provided via any computer software, and instead represent the author's interpretation.

Table 2.2 lists all available isotopic data for sample B13c. Note that the designation B13c-1 or -2 indicates which of two different chunks the sample of interest was taken from. All errors are 2.S.E. and external precision is reported where internal measurements exceed our lab-wide reproducibility.

Table 2.3 lists all available isotopic data for sample B3b. All errors are 2.S.E. and external precision is reported where internal measurements exceed our lab-wide reproducibility.

Table 2.4 lists all available isotopic data for sample B17a. All errors are 2.S.E. and external precision is reported where internal measurements exceed our lab-wide reproducibility.

Table 2.5 lists all available isotopic data for sample B2b. Note that the designation B2b-1 or -2 indicates which of two different chunks the sample of interest was taken from. All errors are 2.S.E. and external precision is reported where internal measurements exceed our lab-wide reproducibility.

Table 2.6 lists all available isotopic data from the preliminary characterization of sample 27.1.2. Each garnet preparation is named for its separate number (1 or 2) and its time spent in HF as part of partial dissolution (30, 60 or 90 minutes). All errors are 2.S.E. and external precision is reported where internal measurements exceed our lab-wide reproducibility.

Table 2.7 lists all available isotopic data from the garnet C2-1 and its surrounding whole rock/ matrix. Zones are lettered from the inside out, thus zone A is the core, zone D is the rim, etc. All errors are 2.S.E. and external precision is reported where internal measurements exceed our lab-wide reproducibility.

Table 2.8 lists all available isotopic data from the garnet B6 and its surrounding whole rock. Zone A + B is a combination of two zones which were drilled apart and later recombined due to small sample mass. All errors are 2.S.E. and external precision is reported where internal measurements exceed our lab-wide reproducibility.

Figure 2.1 is a hay bale representing curved inclusion trails and their defining axis or FIA.

Figure 2.2 is a geologic map and cross section of the internal zone of the Betic Cordillera taken directly from Puga et al. (2002) with no alteration.

Figure 2.3 demonstrates the proposed relationship between FIA orientation and Plate Motion from Aerden et al. (2013). Each solid black line shows the convergence direction between Iberia and the plate of interest. Corresponding perpendicular FIA are shown. The age of each FIA is predicted solely on the basis of an assumed relationship with plate reconstructions.

Figure 2.4 is a layered EDS image of a garnet in B13c. The garnet is ~1.5 mm in diameter.

Figure 2.5 is a photomicrograph of a garnet in sample B2b.

Figure 2.6 is a layered EDS image of a garnet in sample B3b.

Figure 2.7 is a layered EDS image of a garnet in sample B17a.

Figure 2.8 is a BSE image of garnet C2-1 from sample. 27.1.2.

Figure 2.9 is a BSE image of garnet B6 from sample 27.1.2.

Figure 2.10 shows the drill trenches planned for garnet C2-1. Each drill trench is marked by a red line with a width of 600 μm.

Figure 2.11 shows the drill trenches planned for garnet B6. Each drill trench is marked a red line with a width of 600 μm. The Outermost planned drill trench is only partially shown as it exceeds the bounds of the image.

Figure 2.12 shows the progressive drilling of garnet C2-1 as each zone is drilled out and removed.

Figure 2.13 shows the two trenches drilled in garnet B6. The outer two trenches have not yet been drilled.

Figure 2.14 is a layered EDS image of a garnet in Sample B3b.

Figure 2.15 is a layered EDS image of a garnet in sample B3b**.**

Figure 2.16 is a layered EDS image of a garnet in sample B17a.

Figure 2.17 is a Layered EDS Image of Garnet C2-1 in sample 27.1.2.

Figure 2.18 is a layered EDS image of garnet B6 in sample 27.1.2.

Figure 2.19 is a Ca elemental map of garnet B6 in sample 27.1.2. The distinct truncation pattern visible on the northernmost edge of the garnet is not visibly in other measured major or minor element paters.

Figure 2.20 is a 6 point isochron for sample B13c.

Figure 2.21 is a 3 point isochron for sample B13c. We believe that this represents the most precise and accurate age of garnet growth in sample B13c.

Figure 2.22 is a 12-point isochron for sample B2b.

Figure 2.23 is a 7 point isochron (albeit with functionally two real anchor points) representing the oldest possible measured age of garnet in B2b.

Figure 2.24 is a 7 point isochron (albeit with functionally two real anchor points) representing the youngest possible measured age of garnet in B2b.

Figure 2.25 is a 5 point isochron for preliminary characterization of 27.1.2.

Figure 2.26 is a 4 point isochron for zone B of Garnet C2-1 in sample 27.1.2.

Figure 2.27 is a 4 point isochron for zone C of Garnet C2-1 in sample 27.1.2.

Figure 2.28 is a 5 point isochron for zone D of Garnet C2-1 in sample 27.1.2.

Figure 2.29 is a 2 point isochron for Zone A + B of Garnet B6 in sample 27.1.2.

Figure 2.30 Summarizes all of ages produced as a result of this study. The age of the core of garnet B6 is omitted for visual clarity.

Figure 2.31 is a plot of available isotope data for sample B3b.

Figure 2.32 is a plot of all available isotope data for Sample B17a.

Figure 2.33 shows all new structurally-constrained garnet ages and their relationship to FIA generations. Gray boxes represent the age of each FIA generation predicted by the model of Aerden *et al.* (2013). Open squares represent zoned garnet ages and closed circles represent bulk garnet analyses.

Sample	Point #	O	Na	Mg	Al	Si	P	K	Ca	Ti	Mn	Fe	Zr	Ce	Mineral ID
B17a	3	49.43	0	0	0.04	49.62	0	0	0.01	0	0	0.18	0.23	-	Quartz
B17a	4	27.69	0.09	0.04	0.07	0.04	0.02	0	0	11.95	0.15	59.85	0.09	-	Ilmenite
B17a	5	27.69	0.09	0.02	0	0.02	0	0.01	0	13.4	0.19	58.55	0.04	-	Ilmenite
B17a	6	27.33	0.09	0.01	0.1	0.08	0.01	0.03	0.06	11.86	0.13	60.29	0	-	Ilmenite
B17a	7	27.04	0.08	0	0.08	0.08	0.03	0.01	0.09	10.55	0.11	61.94	0	-	Ilmenite
B17a	8	27.07	0.05	0.03	0.11	0.05	0.04	0	0.09	11.24	0.11	61.2	0	-	Ilmenite
B17a	9	48.63	0	0.38	0.02	0.08	0.03	0.07	50.28	0.04	0.09	0.22	0.06	-	Calcite
B17a	10	48.37	0.07	0.24	0.02	0.07	0.01	0.02	50.78	0	0	0.27	0	-	Calcite
B17a	11	48.65	0.02	0.22	0.05	0.09	0.02	0.01	50.67	0	0	0.27	0	-	Calcite
B17a	12	43.99	0.69	1.35	16.31	23.91	0.03	9.38	0.02	0.31	0.01	3.93	0.04	-	Biotite
B17a	13	44.74	0.65	1.39	16.08	23.92	0	9.26	0.03	0.19	0	3.72	0	-	Biotite
B17a	14	47.03	0.03	0.25	0.04	0.05	0	0.05	52.15	0.01	0.1	0.2	0.11	-	Calcite
B17a	15	48.12	0	0.23	0.03	0.03	0	0	51.25	0	0.01	0.19	0.06	-	Calcite
B17a	16	35.35	0.19	0.34	0.97	3.6	0	0.07	1.24	0.01	0.15	56.01	0	-	Fe-oxide
B17a	17	35.3	0.13	0.38	1.11	3.65	0	0.04	0.92	0	0.15	56.1	0.19	-	Fe-oxide

B17a	18	34.74	0.23	0.33	1.15	3.74	0.02	0.05	0.74	0.01	0.21	156.56	0	-	Fe-oxide
B17a	19	35.11	0	0	13.24	18.68	0	0	19.33	0.07	0.55	12.62	0.12	-	Epidote
B17a	20	36.12	0.11	0.87	11.28	17.43	0	0.01	6.22	0.1	2.12	25.49	0.19	-	Garnet
B17a	21	39.8	0.09	0	13.03	18.18	0	0	17.53	0.03	0.33	10.7	0.17	-	Epidote
B17a	22	35.44	0.08	0.75	11.15	17.55	0	0	5.62	0.12	3	26.18	0	-	Garnet
B17a	23	35.71	0.06	0.69	10.95	17.36	0	0	5.66	0.13	3.4	25.89	0	-	Garnet
B17a	24	35.55	0.02	0.7	11.01	17.49	0.04	0	5.19	0.06	4.38	25.36	0.05	-	Garnet
B17a	25	37.61	0.01	0	0.05	0.04	0.05	0.02	0.12	61.07	0	1.03	0	-	Rutile
B17a	26	39.67	0	0.04	0.11	0.13	0	0	0.2	58.83	0	1.01	0	-	Rutile
B17a	27	35.87	0.03	0	0.01	0.02	0.02	0.01	0.17	62.53	0	1.27	0	-	Rutile
B17a	28	54.59	3.34	0.33	1.38	1.84	0.09	2.45	10.75	0	0.18	2.26	0.06	-	Ca-oxide?
B17a	29	45.97	0.87	0.51	3.04	4.36	0.12	2.71	30.8	0.07	0.5	4.93	0.01	-	Ca-oxide?
B17a	30	45.54	5.11	0.06	22.49	23.77	0	0.84	0.21	0.32	0	1.62	0.01	-	Tourmaline
B17a	31	39.02	3.42	0.62	17.17	20.09	0	0.34	2.97	0.24	0.58	15.43	0.1	-	Tourmaline
B17a	32	48.63	0.01	0.02	0	49.95	0	0.04	0.01	0.02	0	0.4	0.22	-	Quartz
B17a	33	48.21	0.01	0	0.07	50.01	0	0	0	0	0	0.38	0.22	-	Quartz
B17a	34	49.63	0.01	0.26	0.05	0.1	0	0.06	49.1	0.08	0.06	0.63	0	-	Calcite

B17a	35	47.08	0.01	0.06	0.07	0.16	0.01	0.03	2 51.85	0	0.04	0.56	0.05	-	Calcite
B17a	36	45.91	1.96	4.57	16.91	18.1	0	0.02	0.96	0.3	0.17	10.98	0.08	0	Tourmaline
B17a	37	45.73	1.96	4.09	17.99	19.01	0	0.07	0.12	0.21	0.12	9.48	1.11	0	Tourmaline
B17a	38	47.3	2.05	4.21	17.82	18.52	0	0.02	0.12	0.24	0.01	9.38	0.14	0	Tourmaline
B17a	39	47.49	1.89	4.32	17.87	18.63	0	0.01	0.37	0.27	0.06	9.09	0	0	Tourmaline
B17a	40	48.75	0.04	0.03	0.05	49.41	0	0	0.1	0	0.05	0.72	0.13	0	Quartz
B17a	41	46.49	2.1	4.45	17.23	18.43	0	0	0.38	0.34	0.06	10.18	0.22	0	Tourmaline
B17a	42	41.18	0.06	2.13	22.39	11.61	0	0.03	0.07	0	0.27	22.13	0.05	0	Chloritoid
B17a	43	41.96	0.1	2.05	22.11	11.72	0.07	0.03	0.03	0.03	0.31	21.6	0	0	Chloritoid
B17a	44	26.31	0.04	0.03	0.15	0.15	0	0.03	0.11	10.53	0.15	62.02	0.12	0	Ilmenite
B17a	45	28.16	0.1	0.09	0.71	0.95	0.11	0.05	0.42	9.47	0.28	59.4	0	0	Ilmenite
B17a	46	29.94	0.09	0.77	5.77	8.62	0	0.07	1.98	5.18	0.95	46.32	0.15	0	Ilmenite
B17a	47	35.21	0.16	1.09	11.12	17.71	0	0.05	4.9	0.03	1.79	27.65	0.11	0	Garnet
B17a	48	39.48	0.07	0	12.85	17.97	0	0.02	17.44	0.07	0.7	11.08	0.03	0	Epidote
B17a	49	39.65	0	0.07	12.72	17.77	0.01	0.08	17.12	0	0.47	11.3	0	0.58	Epidote
B17a	50	42.18	0.08	0	12.65	17.8	0.02	0.03	16.3	0	0.68	10.02	0.06	0	Epidote
B17a	51	37.09	0.03	0	13.3	18.5	0.07	0.06	18.7	0.02	0.5	11.3	0	0	Epidote

						6			4			6			
B17a	52	40	0	0.02	12.83	17.79	0.03	0.01	17.4	0	0.68	11.11	0	0	Epidote
B17a	53	46.69	1.62	3.47	15.97	15.45	0	0.01	0.1	4.47	0.25	11.86	0	0	Ilmenite
B17a	54	47.3	1.69	4.04	18.86	18.67	0	0.01	0.18	0.15	0.1	8.91	0.03	0	Tourmaline
B17a	55	47.04	1.95	3.89	18.15	18.67	0.01	0.03	0.2	0.19	0.22	9.26	0.16	0	Tourmaline
B17a	56	47.01	1.84	3.98	17.96	18.01	0	0.03	0.26	0.96	0.1	8.96	0.18	0	Tourmaline
B17a	57	41.88	0.01	0.05	12.61	17.97	0.04	0.04	15.97	0.02	0.74	10.29	0	0	Epidote
B17a	58	10.89	0.19	0.34	6.56	11.99	0.17	0.2	8.71	0.34	11.23	48.94	0	0	Fe-Mn Silicate?
B17a	59	35.99	0.04	0.69	10.92	17.38	0	0	5.47	0.08	5.51	23.8	0.03	0	Garnet
B13c	61	36.49	0.09	0.34	11.43	17.81	0	0.04	7.03	0	3.66	23.1	0.02	0	Garnet
B13c	62	36.74	0.04	0.37	11.33	17.89	0	0.01	7.3	0.13	3.24	22.63	0.05	0	Garnet
B13c	63	49.47	0	0.03	0.04	49.31	0	0.16	0	0.02	0	0.25	0.03	0	Quartz
B13c	64	50.07	0.05	0	0	49.18	0	0.02	0.06	0	0.03	0.13	0.12	0	Quartz
B13c	65	43.81	0.12	4.58	12.61	12.34	0.17	0.02	0.34	0.03	0	25.69	0	0	Chlorite
B13c	66	43.77	0.14	4.02	12.64	11.47	0.3	0.09	0.37	0.1	0.08	26.9	0	0	Chlorite
B13c	67	45.05	0.09	4.75	12.45	12.63	0.05	0.07	0.34	0.06	0.05	24.46	0	0	Chlorite
B13c	68	45.79	0.79	0.54	19.43	23.2	0	7.85	0.04	0.22	0	1.82	0.09	0.12	Biotite

B13c	69	45.4	0.88	0.37	20.3	22.81	0	8.03	0.07	0.26	0.01	1.32	0.2	0.07	Biotite
B13c	70	45.84	0.72	0.42	19.53	23.83	0	7.78	0	0.27	0	1.41	0	0.16	Biotite
B13c	71	39.51	0.15	0.38	5.93	1.53	2.14	0.02	1.18	0.12	0.03	48.89	0	0	Fe-oxide
B13c	72	40.58	0.08	0.4	6.81	3.84	1.92	0	1.08	0.1	0	44.63	0.24	0.02	Fe-oxide
B13c	73	40.81	0.13	0.42	6.29	1.51	1.74	0	0.75	0.2	0.28	47.82	0	0	Fe-oxide
B13c	74	43.85	0.19	0.48	5.14	2.08	2.1	0.04	0.8	0.1	0	45.03	0.05	0.07	Fe-oxide
B13c	75	51.31	0.05	0.45	21.97	22.26	0.01	0	0.1	0	0	3.61	0	0.15	Chlorite
B13c	76	47.24	1.42	1.45	19.83	17.84	0	0.01	0.16	0.31	0.2	11.29	0.17	0	Chlorite
B13c	77	47.32	1.51	1.29	19.88	17.86	0.02	0.11	0.2	0.45	0.16	11.09	0	0	Chlorite
B13c	78	45.53	0.89	0.46	20.09	22.91	0	8.09	0.09	0.19	0	1.37	0.2	0.14	Biotite
B13c	79	45.15	0.83	0.25	19.26	24.51	0	7.82	0.12	0.26	0.07	1.27	0.16	0.18	Biotite
B13c	80	47.61	0.93	0.3	20	22.26	0.03	7.52	0.07	0.24	0.04	1	0	0	Biotite
B13c	81	41.52	0.04	0	15.05	18.55	0.03	0	17.4	0.07	0.14	6.37	0	0.42	Chlorite
B13c	82	41.79	0.04	0	15.15	18.43	0	0	17.23	0.16	0.15	6.15	0.11	0.3	Chlorite
B13c	83	31.07	0.03	0.06	0.36	15.55	0.73	0	0.03	0.07	0.14	1.47	48.02	0	Zircon
B13c	84	29.91	0.17	0.02	3.23	3.29	11.89	0.61	1.59	0.15	0	1.08	0	24.99	Monazite
B13c	85	31.13	0.08	0.02	2.56	12.2	9.84	0.53	0.55	0.02	0	0.15	0	21.0	Monazite

						4								1	
B13c	86	42.44	0.05	1.02	22.71	11.67	0.01	0	0.1	0.06	0.39	21.45	0.03	0	Chlorite
B13c	87	42.99	0.01	1.11	22.66	11.53	0.03	0	0.02	0.06	0.45	21.14	0	0	Chlorite
B13c	88	37.48	0.03	0.07	1.27	1.08	0.07	0.1	0.12	57.33	0	1.45	0	0.23	Rutile
B13c	89	38.79	0.03	0	0.27	0.06	0.02	0.04	0.01	60.28	0	0.47	0	0	Rutile
B3b	90	30.12	0.02	0	0.05	16.08	0	0.01	0	0.06	0.06	0.78	51.04	0	Zircon
B3b	91	28.55	0.13	0.08	0.16	0.06	0	0.01	0.05	9.49	0.29	60.98	0	0	Ilmenite
B3b	92	28.56	0.04	0.04	0.22	0.06	0	0	0	9.67	0.28	61.12	0	0	Ilmenite
B3b	93	48.95	1.93	5.09	18.59	18.73	0	0.02	0.17	0.13	0.12	6.1	0	0	Tourmaline
B3b	94	37.79	0.13	0.43	11.19	16.5	0	0.04	10.51	0.04	0.39	9.22	0	6.78	Allanite
B3b	95	41.75	0.05	0.12	14	18.1	0	0.02	16.41	0.04	0.46	8.68	0	0.37	Epidote
B3b	96	36.68	0.74	1.44	12.68	17.62	0.25	0.41	11.96	0.03	1.07	16.66	0	0.31	Garnet
B3b	97	41.64	0.06	0.13	13.94	18.11	0	0.04	16.3	0	0.39	8.74	0	0.21	Epidote
B3b	98	37.85	0.07	2.92	11.58	18.25	0	0	3.39	0.01	4.02	21.72	0	0.13	Garnet
B3b	99	38.4	0.07	2.84	11.52	18.3	0	0.07	3.52	0.03	3.64	21.4	0	0.06	Garnet
B3b	100	38.39	0	2.78	11.48	18.17	0	0.03	3.74	0.1	3.81	21.31	0	0	Garnet
B3b	101	47.07	1.71	3.48	19.15	18.77	0	0.02	0.16	0.96	0.02	8.67	0	0	Tourmaline

B3b	102	41.44	0.03	0.17	14.03	18.36	0	0.08	16.29	0.02	0.36	8.38	0	0.46	Epidote
B3b	103	41.61	0.06	0.13	13.86	18.11	0	0	16.39	0	0.37	8.66	0	0.36	Epidote
B3b	104	35.71	0.23	0.66	12.19	17.15	0	0.21	12.23	0.1	0.71	11.75	0	4.62	Allanite
B3b	105	50.63	0.33	3.26	10.17	15.94	0	0.36	2.65	0.16	1.06	13.25	0	0.13	Tourmaline
B3b	106	47.69	1.84	5.64	17.57	17.7	0	0.05	0.24	0.14	0.2	4.69	0	0	Tourmaline
B3b	107	47.23	1.38	1.51	20.67	18.06	0	0.09	0.19	0.61	0.13	9.97	0	0.1	Tourmaline
B3b	108	43.9	1.12	4.59	15.13	18.6	0	0.01	1.93	0.13	0.95	13.55	0	0	Chlorite
B3b	109	52.28	3.41	9.15	4.91	17.33	0	1.55	3.49	0.21	0.7	4.39	0	0	Biotite
B3b	110	41.1	0	0.13	13.88	18.38	0	0.03	16.73	0	0.45	8.65	0	0.51	Epidote
B3b	111	40.97	0.04	0.2	13.64	18.1	0	0	15.78	0	0.45	8.58	0	0.43	Epidote
B3b	112	40.82	0.02	0.13	13.94	18.18	0	0.03	17.43	0.02	0.36	8.41	0	0.41	Epidote
B3b	113	42.06	0	0.15	13.9	18.18	0	0.04	16.33	0	0.19	8.57	0	0.21	Allanite
B3b	114	38.61	0.24	0.29	11.7	16.75	0	0.15	12.3	0.08	0.54	9.39	0	4.71	Allanite
B3b	115	27.73	0.12	0.04	0.09	0.08	0	0	0.03	9.22	0.11	62.22	0	0.1	Ilmenite
B3b	116	27.99	0.09	0	0.17	0.06	0	0	0	9.77	0.31	61.3	0	0	Ilmenite
B3b	117	27.35	0.02	0.07	0.15	0.09	0	0	0.05	9.51	0.3	62.35	0	0	Ilmenite
B3b	118	47.01	0.13	4.25	22.67	11.92	0	0.01	0.04	0.01	0.38	13.47	0	0.03	Tourmaline

B3b	119	46.13	0.16	4.26	22.53	12.24	0	0.03	0.11	0	0.34	14.09	0	0	Tourmaline
B3b	120	46.04	0.45	1.07	29.15	13.56	0	0.01	0	0.2	0.36	6.94	0	0	Tourmaline
B3b	121	46.27	0.44	0.77	29.28	13.57	0	0.01	0.09	0.18	0.48	6.22	0	0	Tourmaline
B3b	122	45.65	0.36	1.08	29.11	13.63	0	0.03	0	0.22	0.34	8.06	0	0	Tourmaline
B3b	123	46.47	0.28	1.16	29.05	13.56	0	0	0.04	0.23	0.3	7.69	0	0.02	Tourmaline
B3b	124	42.75	0.61	1	29.81	14.16	0	0.05	0.04	0.21	0.49	7.91	0	0	Tourmaline
B3b	125	45.62	0.35	1.41	28.84	13.69	0	0.05	0.03	0.2	0.21	7.24	0	0.02	Tourmaline
B3b	126	47.58	0.08	0	34.05	17.38	0	0.14	0.02	0	0	0.55	0	0.04	Tourmaline
B3b	127	47.84	0.09	0.01	33.97	17.31	0	0.03	0	0	0	0.69	0	0	Tourmaline
B3b	128	48.21	4.61	0.12	21.55	22.09	0	1.85	0.35	0.1	0	0.86	0	0.24	Tourmaline
B3b	129	48.45	4.7	0.08	21.55	22.03	0	1.71	0.39	0.02	0.02	0.86	0	0	Tourmaline
B3b	130	51.84	0	0.02	0.02	47.17	0	0.03	0.01	0	0.02	0.36	0	0	Quartz
B3b	131	51.95	0	0.02	0	47.12	0	0.01	0	0	0	0.24	0	0.06	Quartz
B3b	132	47.27	4.87	0.07	22.11	22.52	0	1.45	0.54	0.02	0.01	0.97	0	0	Tourmaline
B3b	133	31.31	0.15	0.28	0.18	0.26	0	0.1	0.03	8.99	0.35	58.35	0	0	Ilmenite
B3b	134	31.78	0.08	0	0.09	0.16	0	0	0.03	9.59	0.36	57.9	0	0	Ilmenite
B3b	135	32.77	0.01	0	0.2	0.06	0	0	0.08	8.14	0.43	58.31	0	0	Ilmenite

B3b	136	31.22	0.08	0	0.13	0.05	0	0	0.01	9.05	0.31	59.14	0	0	Ilmenite
B3b	137	35.61	0.1	0.03	0.16	0.14	0	0.03	0.08	0.78	0.19	62.81	0	0	Fe-oxide
B3b	138	28.86	0.12	0.08	0.27	0.24	0	0	0.12	9.91	0.05	60.36	0	0	Fe-oxide
B3b	139	30.83	0.08	0.07	0.2	0.13	0	0.02	0.09	9.74	0	58.76	0	0	Fe-oxide
B3b	140	51.13	0.02	0	0	47.8	0	0.01	0.04	0.01	0.05	0.29	0	0	Quartz
B3b	141	51.26	0.08	0	0.02	47.6	0	0.08	0.02	0	0.04	0.32	0	0	Quartz
B3b	142	52.66	0	0	0.04	46.26	0	0.1	0.02	0	0.01	0.29	0	0	Quartz
B3b	143	45.64	1.44	2.46	10.44	14.41	0.4	1.45	2.62	0.05	2.83	16.15	0	0	Biotite
B3b	144	46.02	0.22	1.61	28.97	13.63	0	0.02	0	0.23	0.09	7.72	0	0	Tourmaline
B3b	145	46.44	0.34	1.72	28.1	13.66	0	0.13	0.06	0.25	0.12	7.59	0.07	0	Tourmaline
B3b	146	43.69	0.07	0.15	13.76	17.63	0	0.05	15.24	0.08	0.36	8.05	0	0.64	Epidote
B3b	147	39.92	0.26	2.5	10.46	14.26	0.88	0.3	3.17	0.08	2.48	25.4	0	0	Garnet
B3b	148	43.37	0.01	0.13	14.03	18.23	0	0.11	15.66	0	0.33	7.38	0	0	Epidote
B3b	149	49.85	0.08	0.2	0.6	46.69	0	0.06	0.3	0.01	0.27	1.43	0	0.1	Quartz
B3b	150	50.06	1.95	5.43	18.46	18.43	0	0	0.27	0.14	0.04	5.16	0	0.05	Tourmaline
B3b	151	32.04	0	0.03	0.17	0.1	0	0.02	0.01	11.38	0.16	55.96	0	0	Ilmenite
B3b	152	13.88	0.25	0.36	1.24	1.58	0	0.06	0.3	8.93	0.8	72.16	0	0	Ilmenite
B3b	153	17.29	0.25	0.33	1.07	1.35	0	0.11	0.17	10.4	0.55	68.3	0	0	Ilmenite

											9		8		
B3b	154	29.16	0.18	0.54	1.17	1.19	0	0.11	0.22	8.44	0.57	58.37	0	0	Ilmenite
B3b	155	39.54	0.04	0.04	0.05	0.14	0	0.01	0.08	56.74	0.03	2.44	0	0	Rutile
B3b	156	39.65	0.05	0.05	0.05	0.11	0	0.05	0.01	57.94	0.01	1.1	0	0.08	Rutile
B3b	157	40.35	0.13	0.03	0.04	0.11	0	0.04	0	57.38	0.02	1.19	0	0	Rutile
B3b	158	30.63	0	0.05	0.08	0.15	0	0.05	0.03	9.49	0.33	58.72	0	0.15	Ilmenite
B3b	159	34.02	0.33	7.97	11.26	13.8	0.32	0.55	0.57	0.77	0.81	29.07	0	0.08	Chlorite
B3b	160	31.73	0.23	0.14	0.21	0.17	0	0.06	0.08	9.65	0.46	57.16	0	0	Ilmenite
B3b	161	40.48	0.33	0.43	11.17	18.55	0	0.03	10.09	0.04	0.62	8.34	0	4.84	Allanite
B3b	162	40.05	0.07	2.69	11.65	18.28	0	0.01	3.64	0.01	4.49	19.04	0	0	Garnet
B3b	163	40.25	0.01	2.69	11.63	18.26	0	0.04	3.41	0.01	4.73	18.61	0	0.02	Garnet
B3b	164	36.98	0.26	2.98	11.99	18.68	0	0.31	4.09	0.08	3.29	21.02	0	0.15	Garnet
B3b	165	75.43	0.78	0.34	0.41	2.21	0	0.27	1.02	0	0	2.1	0	0	error
B3b	166	49.62	1.49	4.16	19.13	18.24	0	0.02	0.63	0.26	0.16	6.16	0	0.1	Tourmaline
B3b	167	44.5	0.28	1.69	29.25	13.78	0	0.02	0.03	0.23	0.16	8.18	-	0	Tourmaline
B3b	168	44.97	0.33	1.66	29.03	13.5	0	0.06	0	0.29	0.25	8.12	-	0	Tourmaline
B3b	169	47.05	0.14	12.66	12.7	13.16	0	0.07	0.01	0.05	0.31	13.68	-	0.07	Chlorite
B3b	170	47	1.04	0.82	18.2	22.4	0	7.75	0.11	0.12	0.01	2.03	-	0.04	Biotite

					1	8									
					12.6	12.9						13.6			
B3b	171	47.78	0.17	12.48	3	7	0	0.02	0	0.02	0.15	8	-	0.06	Chlorite
						47.6									
B3b	172	51.59	0	0.01	0	5	0	0.07	0.08	0	0.03	0.06	-	0	Quartz
						42.4									
B3b	173	56.72	0.05	0.03	0.06	4	0	0.09	0.09	0.03	0.04	0.06	-	0	Quartz
					18.6	22.4									
B3b	174	46.91	1.23	0.67	2	2	0	7.73	0.05	0.14	0.06	2.01	-	0	Biotite
					17.6	20.9									
B3b	175	50.23	1.33	0.97	9	6	0	6.57	0.08	0.08	0	2.01	-	0	Biotite
					12.9	13.3						18.3			
B3b	176	43.31	0.15	11.08	7	6	0	0.07	0.1	0.01	0.34	5	-	0.17	Chlorite
					17.4	22.1									
B3b	177	48.16	0.95	0.82	1	6	0	7.41	0.09	0.13	0.06	2.65	-	0.05	Biotite
					13.6	18.2			15.3						
B3b	178	43.4	0.02	0.18	7	1	0	0.02	8	0	0.43	7.76	-	0.35	Epidote
					13.5	17.6			16.1						
B3b	179	41.8	0.61	0.23	7	4	0	0.58	3	0	0.42	8.02	-	0.26	Epidote
						46.5									
B3b	180	52.13	0.08	0.05	0.3	9	0	0.03	0.02	0.06	0	0.24	-	0.1	Quartz
												59.6			
B3b	181	30.23	0.05	0.02	0.17	0.1	0	0	0.06	9.39	0.27	8	-	0	Ilmenite
										10.1		71.8			
B3b	182	12.69	0.27	0.31	1.77	1.67	0.19	0.09	0.37	7	0.59	9	-	0	Ilmenite
												61.2			
B3b	183	30.01	0.01	0.02	0.04	0.11	0	0.04	0	8.06	0.39	8	-	0	Ilmenite
												58.3			
B3b	184	30.59	0.23	0.02	0.1	0.13	0	0.06	0.02	9.67	0.79	9	-	0	Ilmenite
					10.6	16.4									
B3b	185	39.71	0.09	0.34	4	9	0	0	9.08	0.02	0.5	9.58	-	6.69	Allanite
					11.9	18.3						19.5			
B3b	186	40.36	0.01	3.21	4	9	0	0.04	3.91	0.04	2.4	8	-	0	Garnet

B3b	187	40.88	0.03	3.45	11.87	18.32	0	0.06	3.62	0.09	1.81	19.88	-	0	Garnet
B3b	188	38.34	0.04	3.03	11.83	18.45	0	0.11	4.07	0.11	2.9	20.85	-	0.04	Garnet
B3b	189	43.79	0.02	0.36	13.96	18.19	0	0.05	14.41	0.02	0.37	8.65	-	0.11	Epidote
B3b	190	53.91	0.09	0	0.02	45	0	0.04	0.09	0	0	0.25	-	0	Quartz
B3b	191	30.91	0.36	0.34	0.58	62.21	0	0.99	1.76	0	0.26	0.6	-	0	Quartz
B3b	192	54.63	0.01	0	0.04	44.71	0	0	0.04	0	0.02	0.06	-	0.13	Quartz
B3b	193	53.1	0.09	0.03	0	46.08	0	0.11	0.04	0.04	0	0.11	-	0.08	Quartz
B3b	194	52.26	1.98	5.11	18.18	17.94	0	0.03	0.08	0.15	0	4.14	-	0.05	Tourmaline
B3b	195	53.23	0	0.05	0.15	45.16	0	0.02	0.08	0	0.03	0.77	-	0	Quartz
B3b	196	51.86	2.18	5.12	17.71	17.71	0	0.04	0.16	0.15	0.1	4.63	-	0.08	Tourmaline
B3b	197	51.97	1.97	5.33	18.17	17.85	0	0	0.19	0	0.04	4.42	-	0	Tourmaline
B3b	198	51.31	2.05	6	17.79	18.27	0	0.05	0.36	0.13	0	3.95	-	0.09	Tourmaline
B3b	199	48.52	2.31	1.21	15.94	18.74	0.56	2.73	0.56	0.08	0.28	8.75	-	0	Biotite
B3b	200	45.36	0.03	0.72	13.61	18.01	0	0.09	12.05	0.03	0.76	8.7	-	0.15	Epidote
B3b	201	47.95	0.73	0.31	12.54	16.34	0	0.55	13.02	0	0.32	6.69	-	0.38	Epidote
B3b	202	51.8	2.05	4.31	18.51	18	0	0.07	0.15	0.12	0.02	4.89	-	0.09	Tourmaline
B3b	203	45.08	0	0.21	13.98	18.21	0	0	13.87	0.01	0.6	7.87	-	0.05	Epidote

B3b	204	42.59	0.51	1.04	10.61	16.69	0	0.03	8.41	0	0.31	7.29	-	5.91	Allanite
B3b	205	34.45	0.09	0.09	0.63	0.48	0	0	0.15	9.05	0.4	54.35	-	0.14	Ilmenite
B3b	206	39.46	1.03	1.09	4.89	5.08	0	0.29	0.69	5.48	0.53	40.63	-	0.01	Ilmenite
B3b	207	34.47	0.15	0.09	0.68	0.16	0	0	0.1	9.17	0.28	54.89	-	0	Ilmenite
B3b	208	35.32	0.08	0.09	0.25	0.06	0	0	0.03	9.45	0.17	54.53	-	0	Ilmenite
B3b	209	42.48	0.17	3.01	11.79	18.41	0	0.06	3.24	0	3.23	17.53	-	0.06	Garnet
B3b	210	42.32	0.11	3	11.97	18.52	0	0.05	3.28	0.04	3.39	17.31	-	0	Garnet
B3b	211	40.68	0.16	2.82	12.02	18.87	0	0.06	3.5	0.05	3.31	18.38	-	0.05	Garnet
B3b	212	42.64	0	2.92	11.79	18.32	0	0.09	3.27	0	3.68	17.05	-	0	Garnet
B3b	213	26.9	0.46	0.24	0.38	0.5	0	0.22	0.16	11	0.05	60.08	-	0	Ilmenite
B3b	214	30.61	0.29	0.11	0.12	0.21	0	0.05	0.03	10.17	0.07	58.35	-	0	Ilmenite
B3b	215	47.24	0.53	1.47	28.23	13.36	0	0	0.02	0.31	0.21	6.3	-	0	Chlorite
B3b	216	47.07	0.64	1.57	28.21	13.2	0	0.03	0.07	0.21	0.22	6.33	-	0	Ch
B3b	217	43.31	0.23	3.14	11.64	18.29	0	0.3	2.99	0.08	2.8	16.89	-	0	Garnet
Gt B6	218	33.38	0.14	0.97	11.22	17.27	0.01	0.02	1.47	0.05	0.28	35.08	0.01	0.06	Garnet
Gt B6	219	29.94	0.1	0.95	10.94	17.13	0.01	0	2.33	0.03	0.79	37.69	0	0	Garnet
Gt B6	220	33.34	0.07	0.84	11.3	17.0	0.09	0	2.33	0.02	1	33.9	0	0	Garnet

					3	3						3			
					11.13	16.94						31.34			
Gt B6	221	33.93	0.13	0.63			0	0	3.3	0.1	2.34		0	0.1	Garnet
					11.09	17.42									
Gt B6	222	34.75	0.11	0.59			0.01	0	2.74	0.08	2.27	30.9	0	0	Garnet
					11.26	17.43						32.05			
Gt B6	223	34.57	0.12	0.84			0	0	2.17	0	1.55		0.01	0	Garnet
					11.35	16.36						31.27			
Gt B6	224	36.63	0.01	0.91			0.09	0.02	2.19	0.13	0.92		0	0	Garnet
					11.64	17.09						29.24			
Gt B6	225	38.78	0.14	1.14			0	0.05	1.2	0.04	0.58		0	0.02	Garnet
					11.24	17.17						34.47			
Gt B6	226	34.09	0.03	1.06			0	0	1.18	0.16	0.47		0	0.12	Garnet
					11.37	17.27						30.75			
Gt B6	227	35.12	0.07	0.76			0.11	0	2.42	0.07	2		0	0.03	Garnet
					11.78	14.96						26.36			
Gt B6	228	42.15	1.05	0.72			0.17	0.2	1.57	0.1	0.89		0	0	Garnet
					11.11	16.89						35.04			
Gt B6	229	33.68	0.13	1.09			0.04	0	1.49	0.06	0.36		0	0.1	Garnet
					11.18	17.01						34.19			
Gt C2-1	231	33.79	0.09	0.73			0	0	1.97	0.17	0.83		0	0	Garnet
					11.14	17.02						32.66			
Gt C2-1	232	34.01	0.05	0.64			0.01	0.01	2.59	0.09	1.74		0	0.02	Garnet
					11.47	17.48						30.71			
Gt C2-1	233	33.88	0.12	0.56			0.04	0	3.13	0.05	2.46		0.01	0.07	Garnet
					11.12	16.36						34.61			
Gt C2-1	234	32.07	0.1	0.53			0.16	0.01	2.68	0.01	2.31		0	0.04	Garnet
					11.37	17.16						31.69			
Gt C2-1	235	35.32	0.09	0.67			0.07	0	2.23	0.14	1.25		0	0	Garnet
						17.25						28.94			
Gt C2-1	236	38.65	0.07	0.81	11.45		0.07	0	1.95	0.02	0.69		0	0.03	Garnet
					10.53	15.52						38.15			
Gt C2-1	237	32.74	0.01	0.9			0.25	0	1.27	0.08	0.51		0	0.03	Garnet

Gt C2-1	238	37.05	0.08	0.69	11.26	17.39	0.01	0	2.26	0.08	1.54	29.42	0	0.02	Garnet
Gt C2-1	239	32.32	0.08	0.53	10.79	15.49	0.22	0.04	2.37	0.03	2	35.97	0	0	Garnet
Gt C2-1	240	26.55	0.1	0.65	10.32	16.11	0.08	0.06	2.7	0.11	1.53	41.53	0	0.12	Garnet
Gt C2-1	241	45.43	0	0	35.91	18.11	0.1	0.01	0	0.01	0	0.33	0	0.02	Kyanite
Gt C2-1	242	45.89	0	0.01	35.44	17.92	0.18	0	0.02	0	0	0.42	0	0	Kyanite
Gt C2-1	243	45.56	0.04	0.02	35.85	17.94	0	0	0.01	0.02	0.03	0.37	0	0.12	Kyanite
Gt C2-1	244	51.03	0.13	0.04	31.44	16.71	0.19	0	0.12	0	0.01	0.31	0	0	Kyanite
Gt C2-1	245	45.58	0.03	0	36.17	17.79	0.08	0	0	0	0	0.34	0	0	Kyanite
Gt C2-1	246	45.04	0.05	0.01	35.95	18.17	0.14	0.01	0.02	0	0	0.36	0	0.08	Kyanite
Gt C2-1	247	47.68	0.05	0	33.24	16.2	0.31	0.03	0.63	0.01	0.05	1.72	0	0.03	Kyanite
Gt B6	249	48.37	0.03	0.01	33.39	17.28	0.29	0	0	0	0.06	0.41	0	0.12	Kyanite
Gt B6	250	33.05	0.08	0	0.02	0.05	17.36	0.01	41.92	0.06	0.14	0.27	0.29	0.09	Apatite
Gt B6	251	29.67	0.09	0	0.13	16.01	0.71	0.02	0	0	0.08	0.92	50.11	0.3	Zircon
Gt B6	252	34.23	0.05	0	0.02	0.04	0	0	0.01	64.52	0.08	0.5	0.02	0.4	Rutile
Gt B6	253	26.48	0	0.31	4.3	5.76	9.22	0	0.92	0	0	10.84	0	18.84	Monazite
Gt B6	254	48.26	0.07	0.01	0.06	51.14	0.08	0.03	0.05	0	0.03	0.15	0	0.1	Quartz
Gt B6	255	44.92	0.06	0	35.9	18.0	0.06	0	0	0.02	0.07	0.68	0	0	Kyanite

						5	5								
Gt C2-1	256	29.65	0	0.04	0.08	16.33	1.41	0	0	0	0	0.77	49.98	0	Zircon
Gt C2-1	257	39.6	0.11	0.02	0.94	1.97	0.03	0	0.2	52.78	0.18	3.48	0	0.63	Rutile
Gt C2-1	258	31.6	0	0.06	0.12	15.92	1.14	0	0	0	0	0.63	49.41	0	Zircon
Gt C2-1	259	40.29	0.11	0.95	22.34	11.4	0	0	0.04	0.08	0.44	24.29	0	0	Chlorite
Gt C2-1	260	44.36	0.06	0.91	22.19	11.59	0.04	0	0.01	0.01	0.24	20.49	0	0.08	Chlorite
Gt C2-1	261	46.55	4.88	0.07	23.97	21.77	0.1	0.42	1.34	0.03	0.07	0.77	0	0	Kyanite

Table 2.1
All SEM Data

sample	Ng Nd loaded	Nd ppm	Sm ppm	$^{147}Sm/^{144}Nd$	±2 S.E.	$^{143}Nd/^{144}Nd$	± 2 S.E. (abs)	± 2 S.E ppm
B13c-1 gt1	1.85	0.12	0.52	2.68096	0.00062	0.512558	0.000035	67.3
B13c-2 gt1	3.13	0.17	0.39	1.42211	0.00060	0.512212	0.000086	168.
B13c-1 wr	66.8	27.4	5.35	0.11768	0.00004	0.511959	0.000009	17.4
B13c-1 wr2	59.1	27.5	5.34	0.11810	0.00003	0.511975	0.000009	17.4
B13c-1 gt pow	82.1	8.11	2.29	0.17056	0.00004	0.511994	0.000009	17.4
B13c-2 gt pow	26.3	13.1	3.06	0.14110	0.00016	0.511969	0.000015	29.5

Table 2.2
B13c Isotope Data

sample	Ng Nd loaded	Nd (ppm)	Sm (ppm)	$^{147}Sm/^{144}Nd$	±2 S.E.	$^{143}Nd/^{144}Nd$	± 2 S.E. (abs)	± 2 S.E ppm
gt2	132	3.99	0.83	0.12609	0.00003	0.511969	0.000010	19.6
gt3	0.47	0.23	0.09	0.21957	0.00171	0.512011	0.000050	98.6
gt5	2.20	0.44	0.13	0.17969	0.00018	0.512001	0.000041	79.2
wr1	60.4	33.4	6.64	0.12032	0.00003	0.511966	0.000009	18.0
wr2	45.2	34.1	6.77	0.12018	0.00006	0.511960	0.000008	16.1
pow1	134	27.5	5.40	0.11889	0.00003	0.511958	0.000009	18.0

Table 2.3
B3b isotope data

sample	Ng Nd loaded	Nd (ppm)	Sm (ppm)	$^{147}Sm/^{144}Nd$	±2 S.E.	$^{143}Nd/^{144}Nd$	± 2 S.E. (abs)	± 2 S.E ppm
wr	26.2	18.6	3.5	0.11388	0.00003	0.512106	0.000009	17.4
gt1	173	5.8	1.0	0.10644	0.00002	0.512081	0.000009	17.4
gt2	88.2	15.2	2.6	0.10176	0.00002	0.512095	0.000009	17.4
gt3	95.5	3.3	0.7	0.11816	0.00003	0.512069	0.000009	17.4
gt4	103	2.5	0.5	0.12324	0.00003	0.512067	0.000009	17.4
gt5	16.1	1.5	0.3	0.13169	0.00005	0.512078	0.000009	17.4
pow1	29.3	29.5	5.1	0.10538	0.00002	0.512105	0.000009	17.4
pow2	20.4	17.6	3.2	0.11090	0.00007	0.512071	0.000014	28.0

Table 2.4
All Isotope Data for Sample B17a

sample	Ng Nd	Nd (ppm)	Sm (ppm)	$^{147}Sm/^{144}Nd$	±2 S.E.	$^{143}Nd/^{144}Nd$	± 2 S.E (abs)	± 2 S.E ppm
B2b-1 wr1	40.6	21	4.0	0.113499	0.00011	0.5121120	0.000009	17.4
B2b-1 wr2	22.3	17	3.3	0.113973	0.00003	0.5121089	0.000018	35.6
B2b-2 wr1	65.2	24	4.8	0.119529	0.00003	0.5121009	0.000011	20.9
B2b-1 gt 2	30.4	1.7	0.7	0.231988	0.00005	0.5121219	0.000009	17.4
B2b-1 gt 3	22.1	2.9	1.0	0.215674	0.00005	0.5121284	0.000009	17.4
B2b-1 gt 4	10.7	0.8	0.4	0.310055	0.00008	0.5121191	0.000012	24.2
B2b-1 gt 5	7.4	1.3	0.8	0.36398	0.00032	0.5121306	0.000016	31.0
B2b-1 gt 6	2.6	0.5	0.5	0.569151	0.00044	0.5121342	0.000031	60.5
B2b-2 gt 8	10.5	1.0	0.8	0.49808	0.00011	0.5121708	0.000016	31.3
B2b-1 pow1	75.5	20	4.3	0.126823	0.00003	0.5121063	0.000009	17.4
B2b-1 pow2	266	27	5.4	0.120805	0.00003	0.5121069	0.000009	17.4
B2b-1 pow4	12.4	6.4	1.3	0.118195	0.00003	0.5121074	0.000013	24.7

Figure 2.5
Isotope Data for Sample B2b

sample	Ng Nd loaded	Nd (ppm)	Sm (ppm)	$^{147}Sm/^{144}Nd$	±2 S.E.	$^{143}Nd/^{144}Nd$	± 2 S.E. (abs)	± 2 S.E ppm
wr	89.2	30	5.6	0.11431	0.00023	0.511978	0.000009	18.3
sep1 pow	70.4	19	6.9	0.17638	0.00005	0.511981	0.000012	24.1
sep1-30	186	2.4	2.5	0.65000	0.00015	0.512037	0.000011	21.5
sep1-60	120	3.5	3.8	0.64724	0.00015	0.512024	0.000020	39.7
sep1-90	473	5.9	3.9	0.39660	0.00009	0.511998	0.000009	17.9
sep2 pow	286	97	16.5	0.131205	0.00003	0.511985	0.000009	17.9
sep2-30	338	10	4.7	0.271559	0.00006	0.511995	0.000009	17.9
sep2-60	220	12	5.1	0.258301	0.00006	0.512002	0.000009	17.9
sep2-90	330	17	6.3	0.225765	0.00005	0.512016	0.000009	17.9

Table 2.6
Isotope Data from Preliminary Bulk analysis of 27.1.2

sample	Ng Nd	Nd (ppm)	Sm (ppm)	$^{147}Sm/^{144}Nd$	±2 S.E.	$^{143}Nd/^{144}Nd$	± 2 S.E (abs)	± 2 S.E ppm
matrix 1	73.8	25.1	4.8	0.1167	0.00004	0.5119672	0.000009	18
wr2	181	31.1	6.1	0.1176	0.00003	0.5119748	0.000009	18
wr3	211	36.3	7.0	0.1163	0.00032	0.5119836	0.000009	18
Zone A	0.90	0.30	1.3	0.6446	0.00345	0.5113698	0.001439	2815
Zone B	0.90	0.30	1.3	2.5384	0.00114	0.5122522	0.000099	194
Zone C	0.38	0.38	1.3	2.0202	0.00286	0.5122331	0.000326	636
Zone D	13.3	2.65	4.7	0.2145	0.00005	0.5119981	0.000012	23
Zone D pow	42.4	42.4	10.9	0.1560	0.00004	0.5119759	0.000012	24

Table 2.7
Isotope Data for Garnet C2-1

sample	Ng Nd	Nd (ppm)	Sm (ppm)	$^{147}Sm/^{144}Nd$	±2 S.E.	$^{143}Nd/^{144}Nd$	± 2 S.E	± 2 S.E ppm
wr2	232	33.2	6.45	0.11735	0.00003	0.511988	0.000009	18
zone A+B	0.36	0.36	0.40	0.67253	0.00176	0.513145	0.000491	957

Table 2.8
Isotope Data for garnet B6

Figure 2.1
Hay bale representing curved inclusion trails and their axis

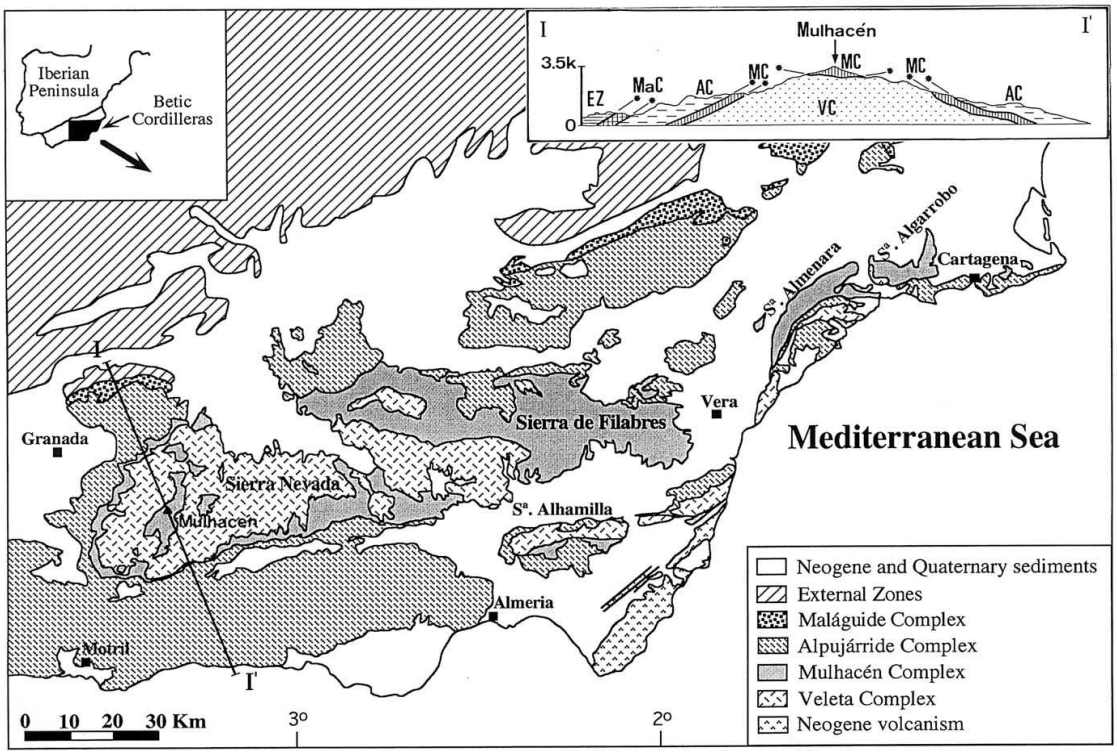

Figure 2.2
Geologic Map of the Betic Cordillera from Puga *et al.*2002

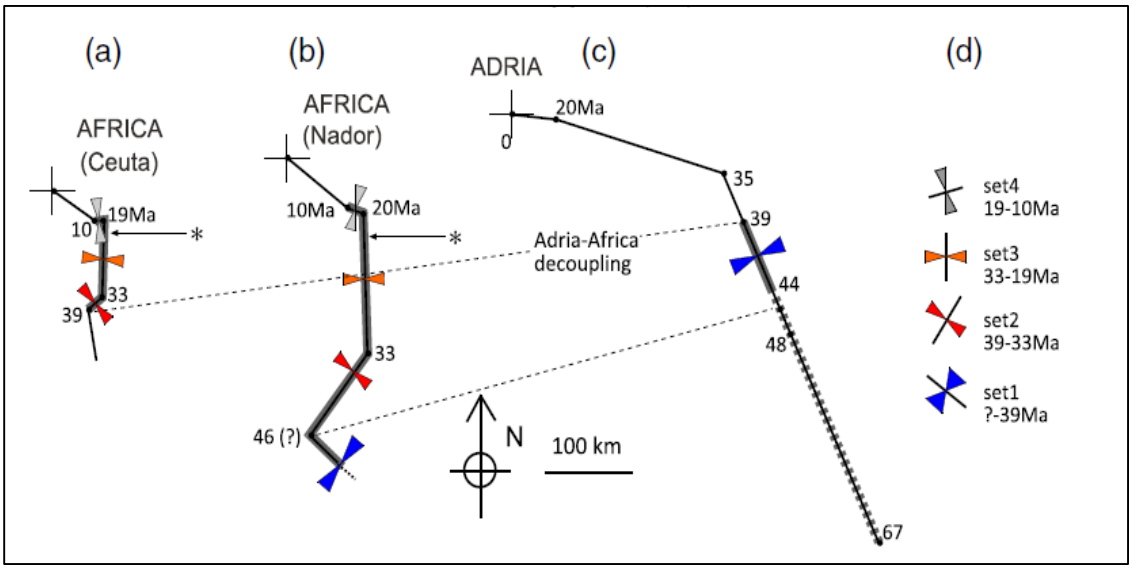

Figure 2.3
Relationship Between FIA orientation and Plate Motion from Aerden *et al.* 2013

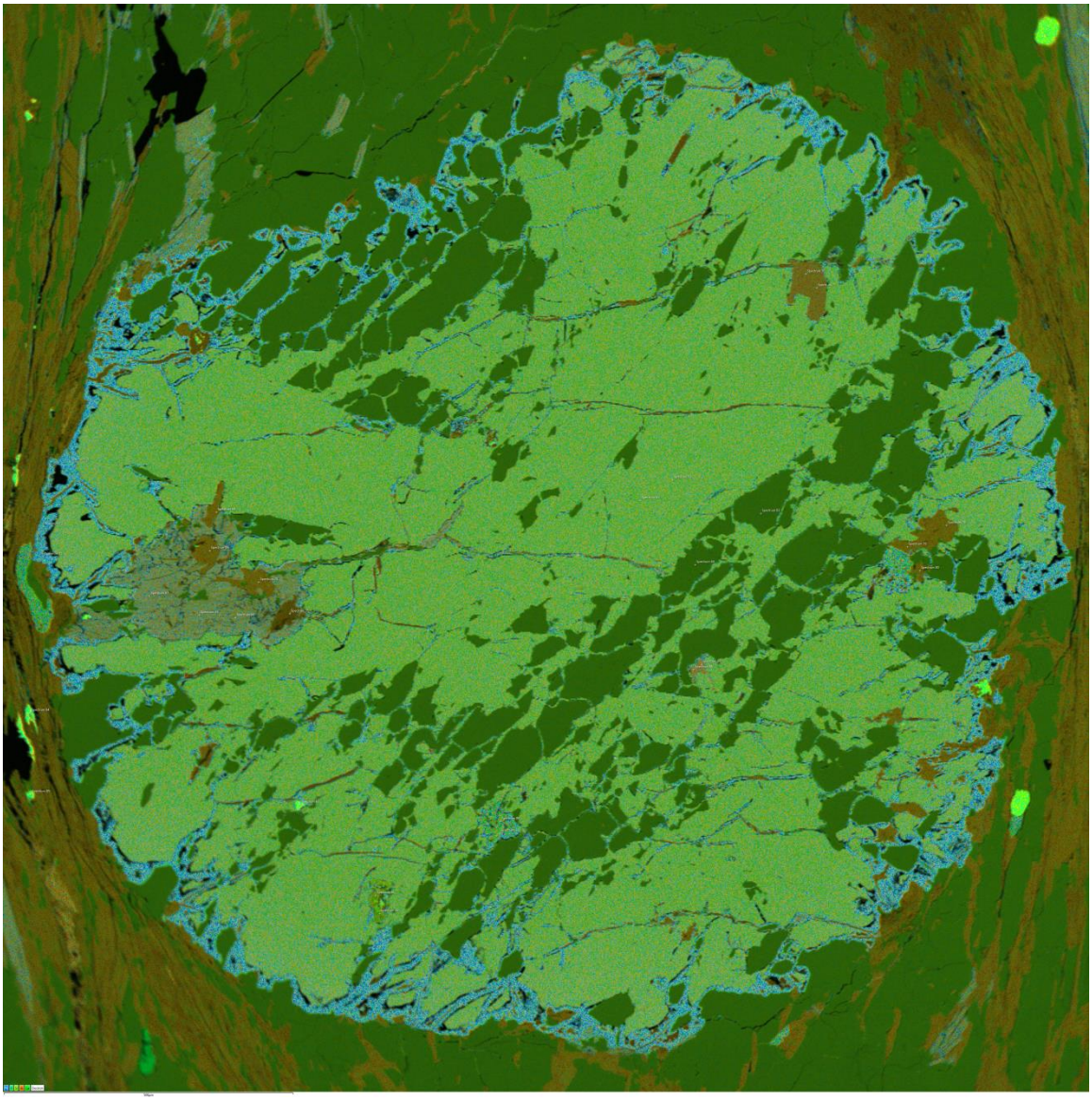

Figure 2.4
Layered EDS image of a garnet in B13c

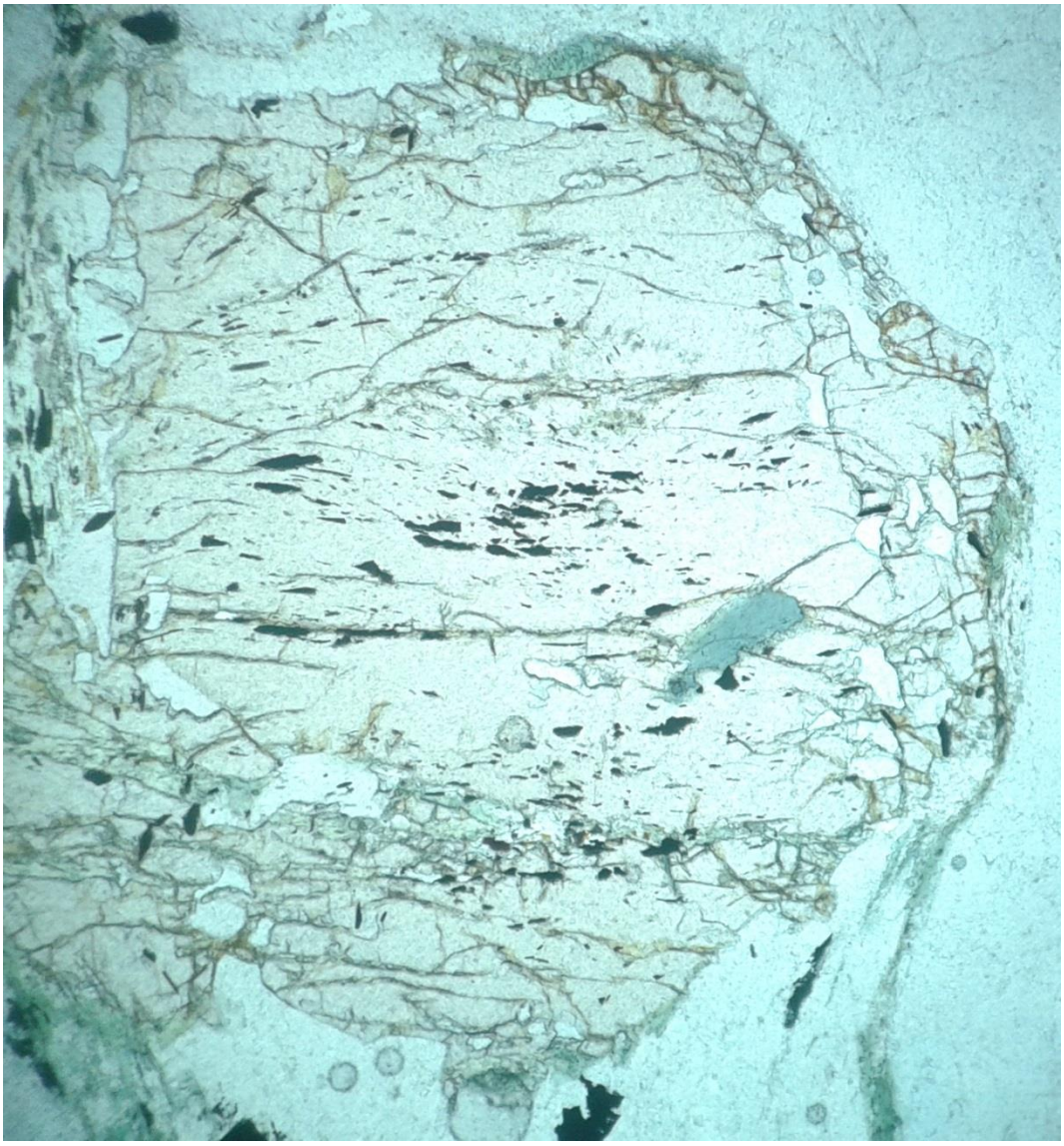

Figure 2.5
Photomicrograph of garnet in sample B2b

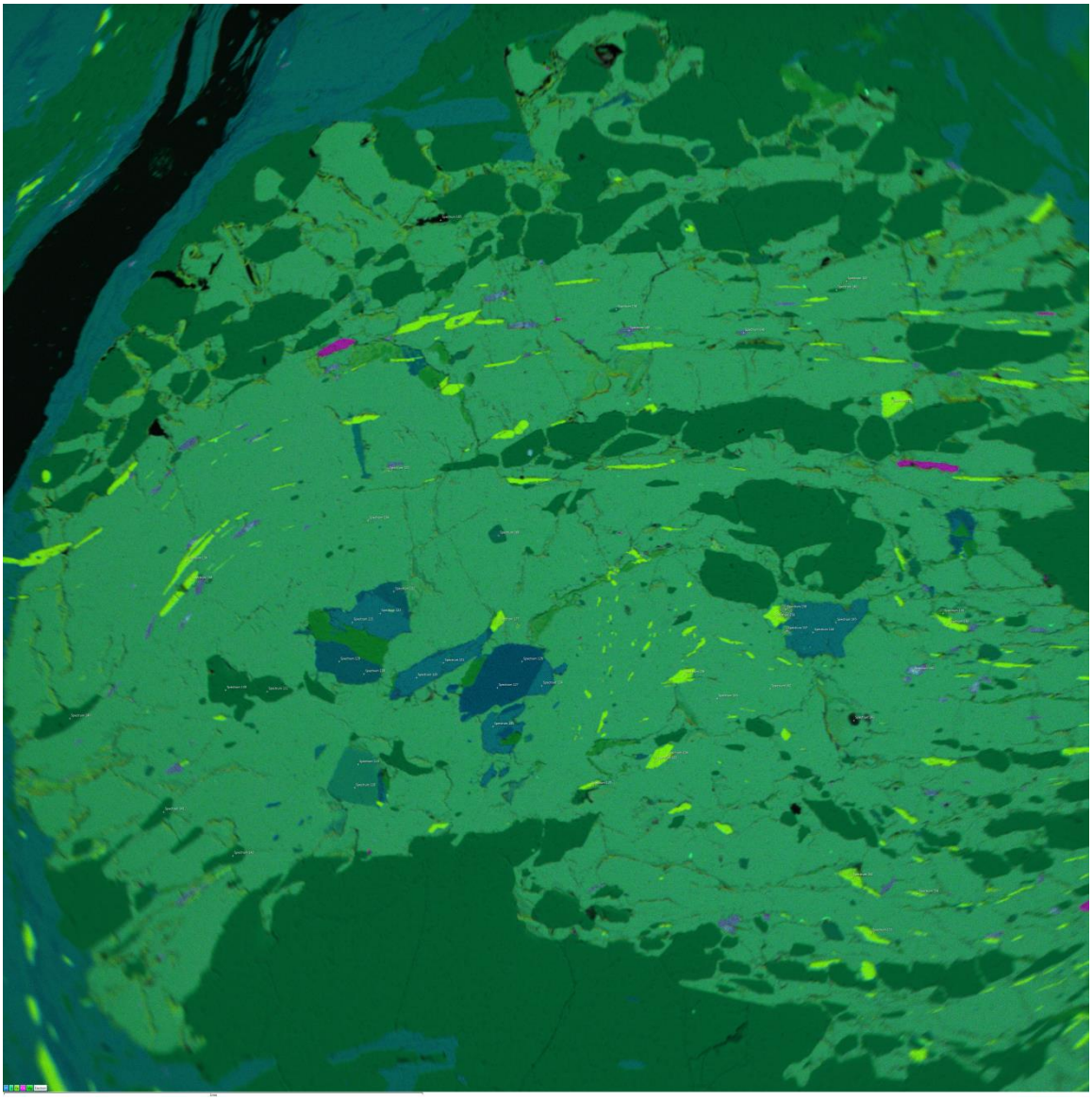

Figure 2.6
Layered EDS image of garnet in B3b

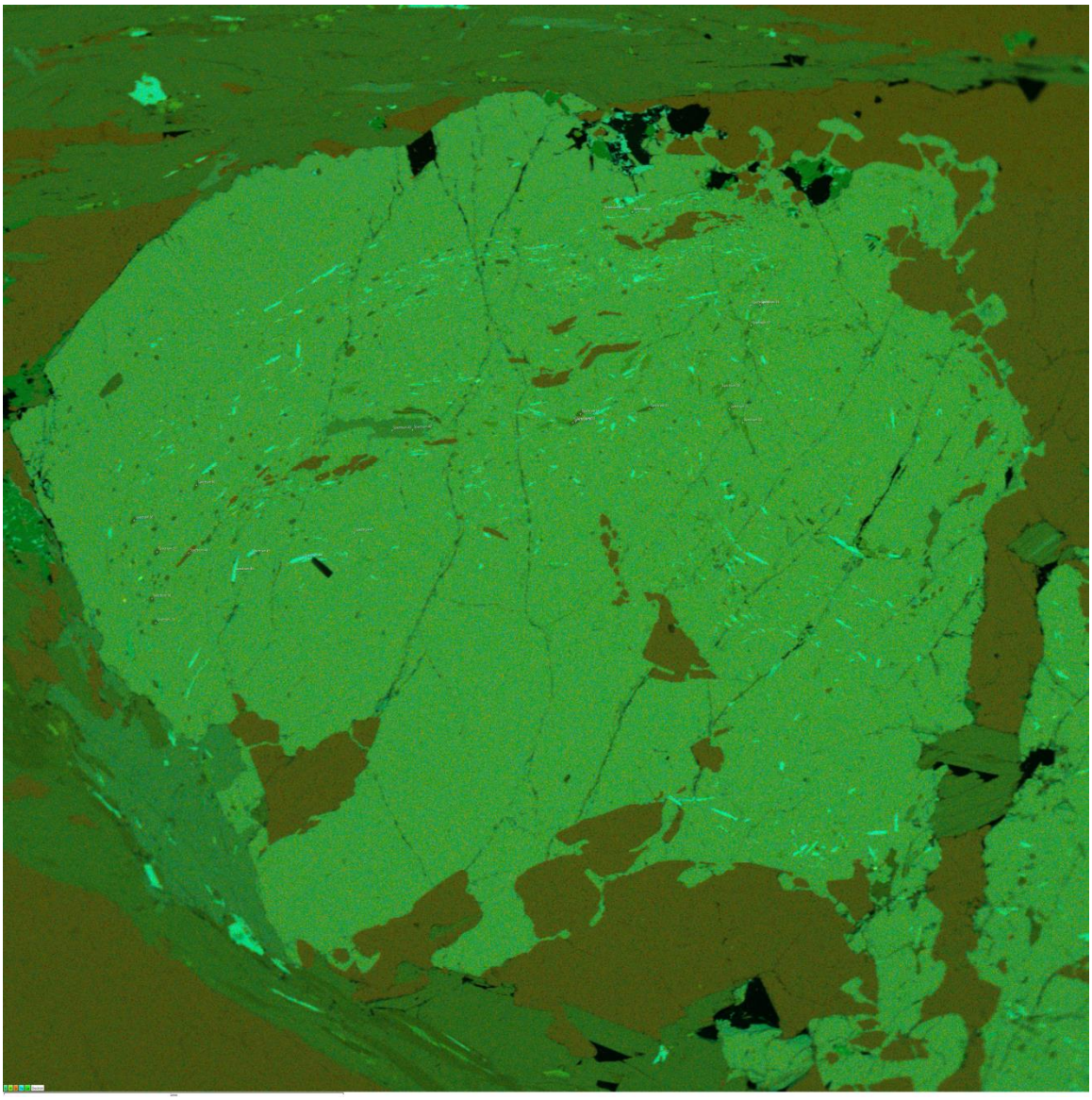

Figure 2.7
Layered EDS image of garnet in B17a

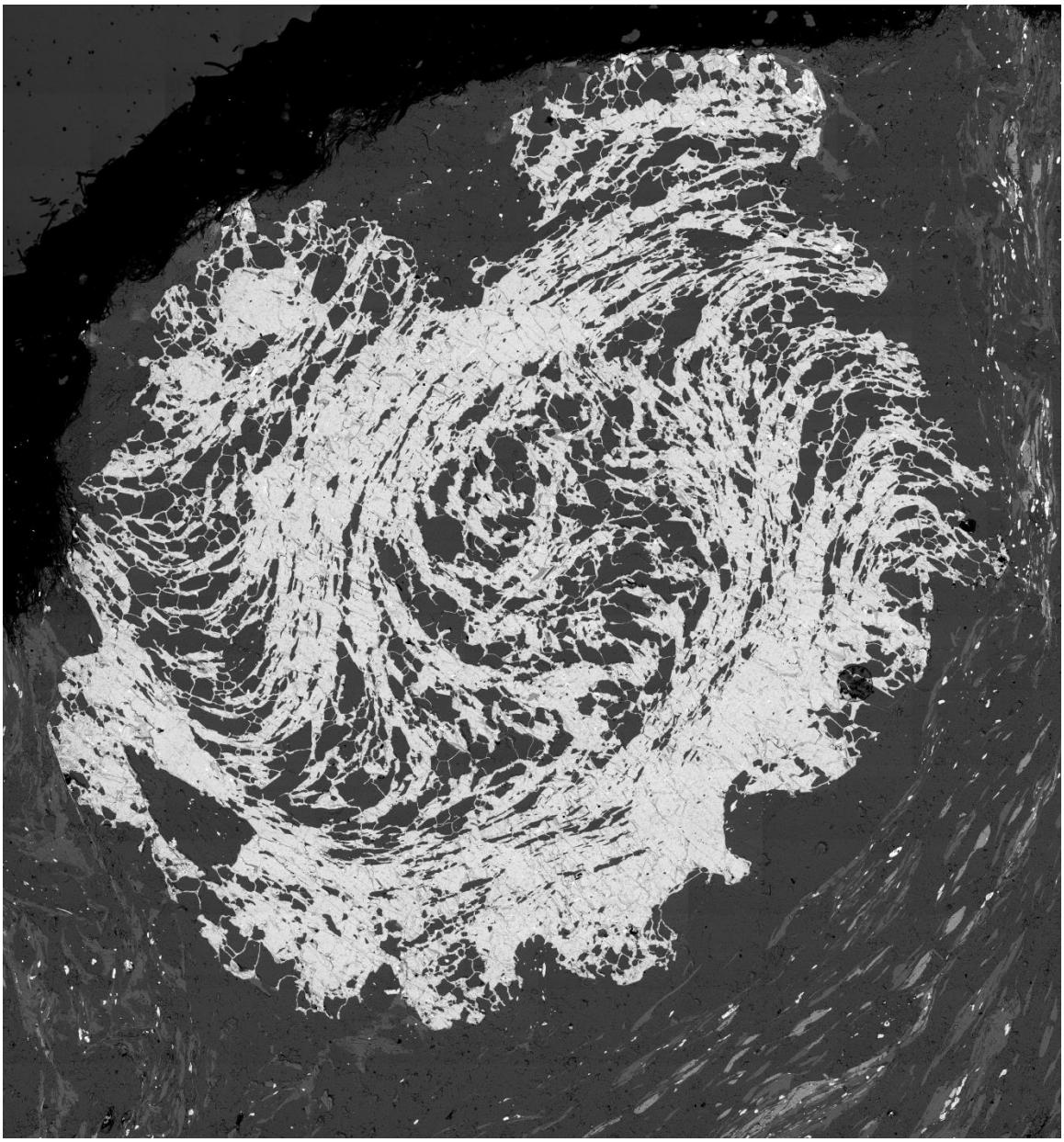

Figure 2.8
BSE image of garnet C2-1

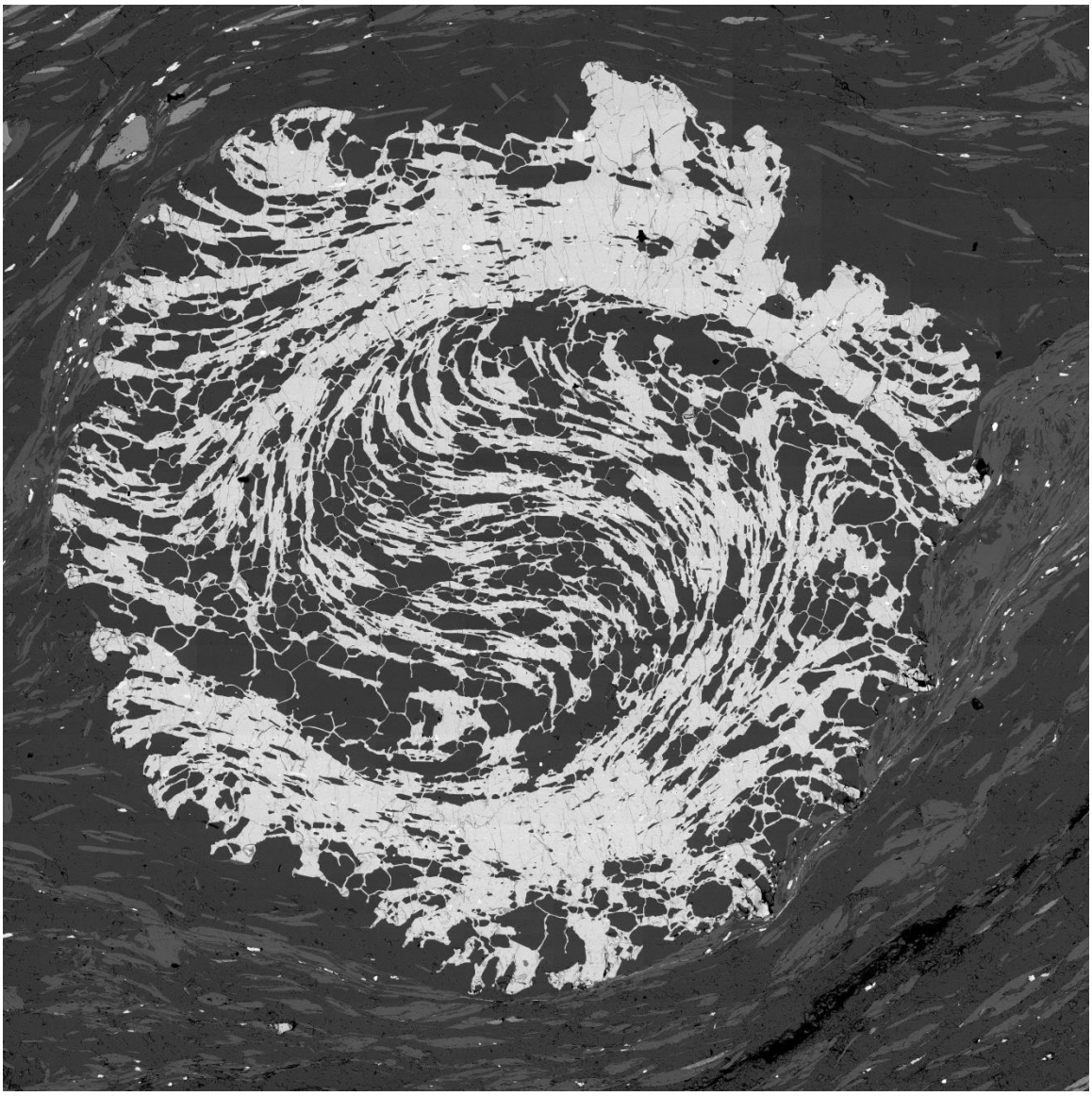

Figure 2.9
BSE image of garnet B6

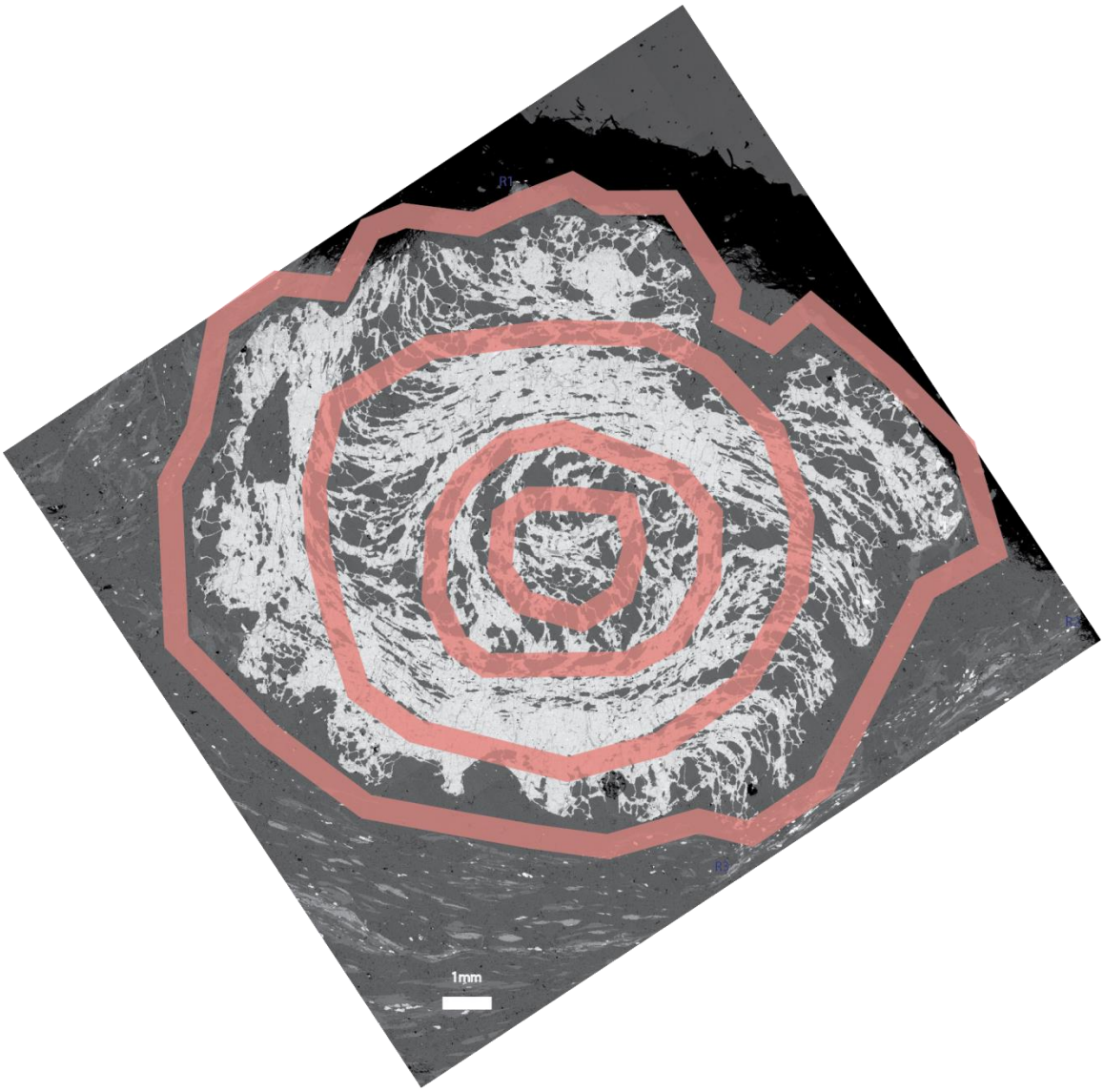

Figure 2.10
Drill trenches planned for garnet C2-1

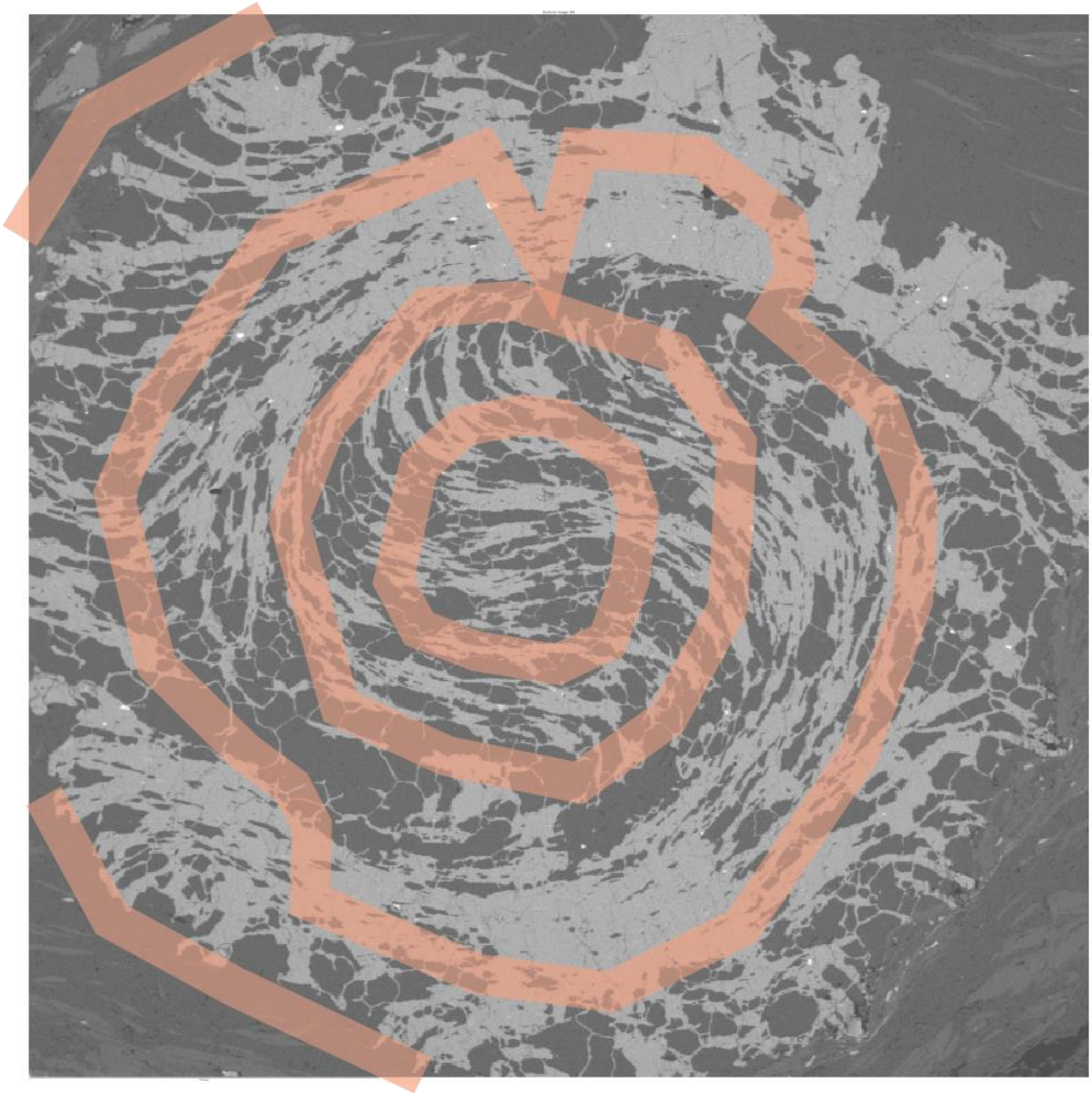

Figure 2.11
Drill trenches planned for garnet B6

Figure 2.12
Progressive drilling of garnet C2-1

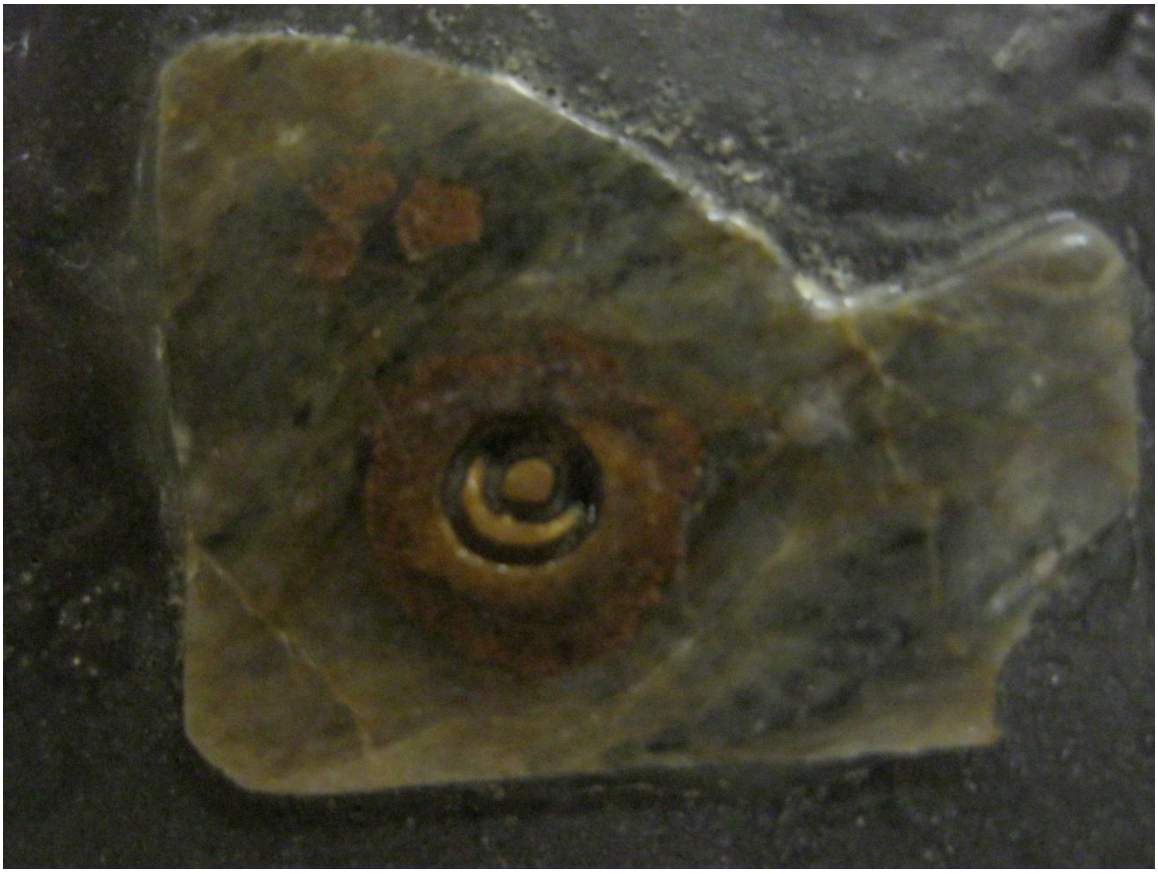

Figure 2.13
Garnet B6 drill trenches

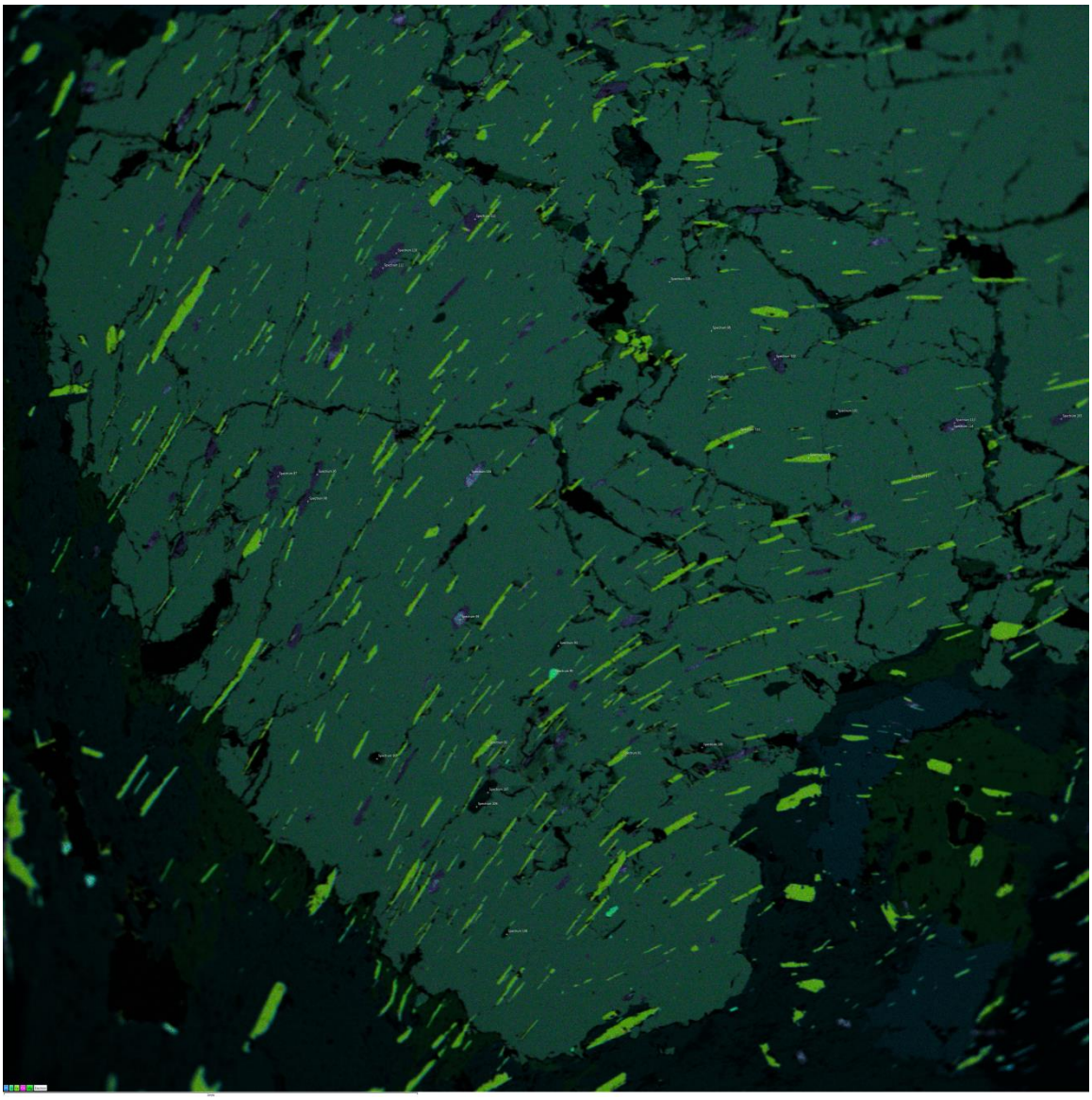

Figure 2.14
Layered EDS image of Sample B3b

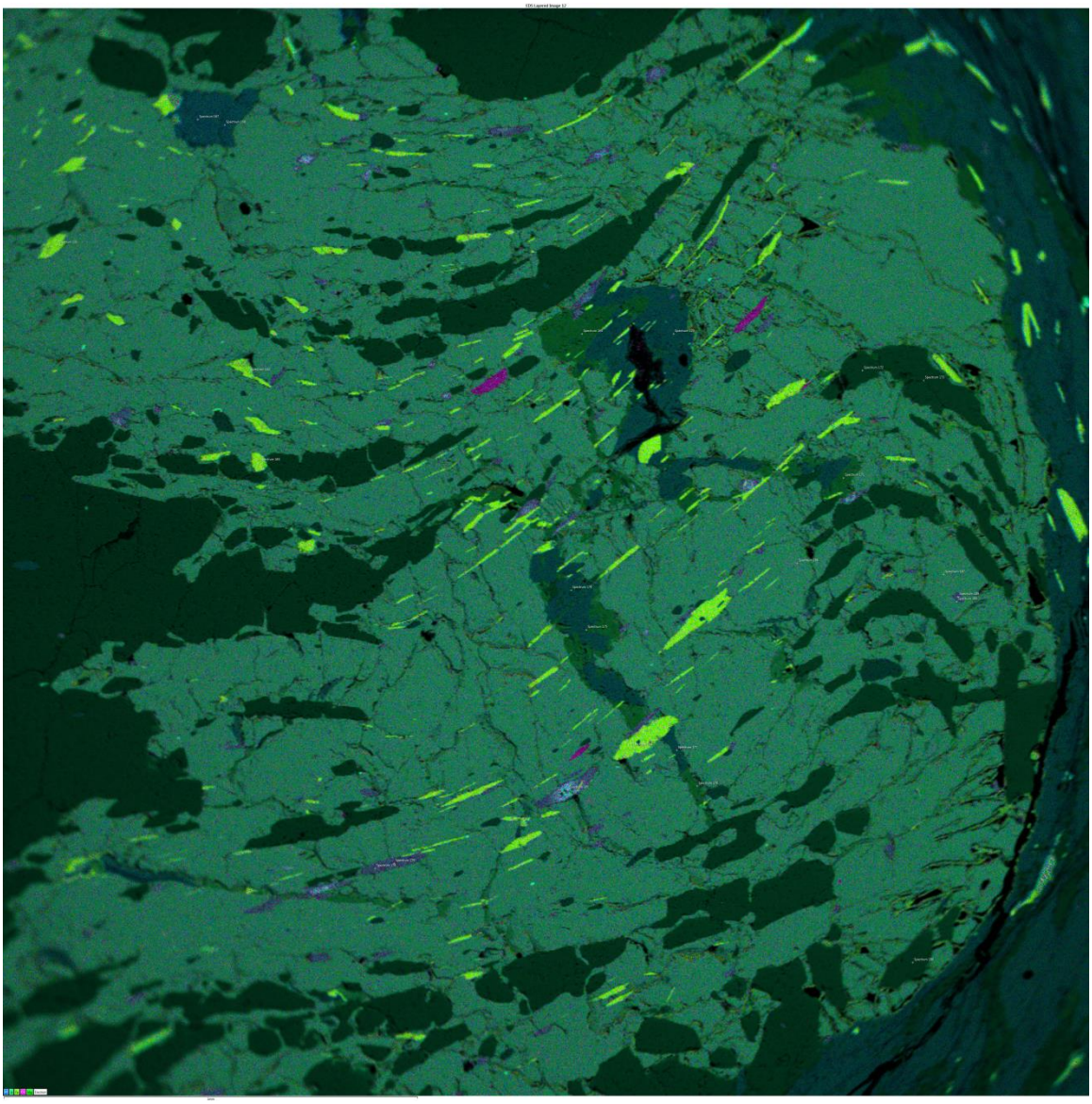

Figure 2.15
Layered EDS image of sample B3b

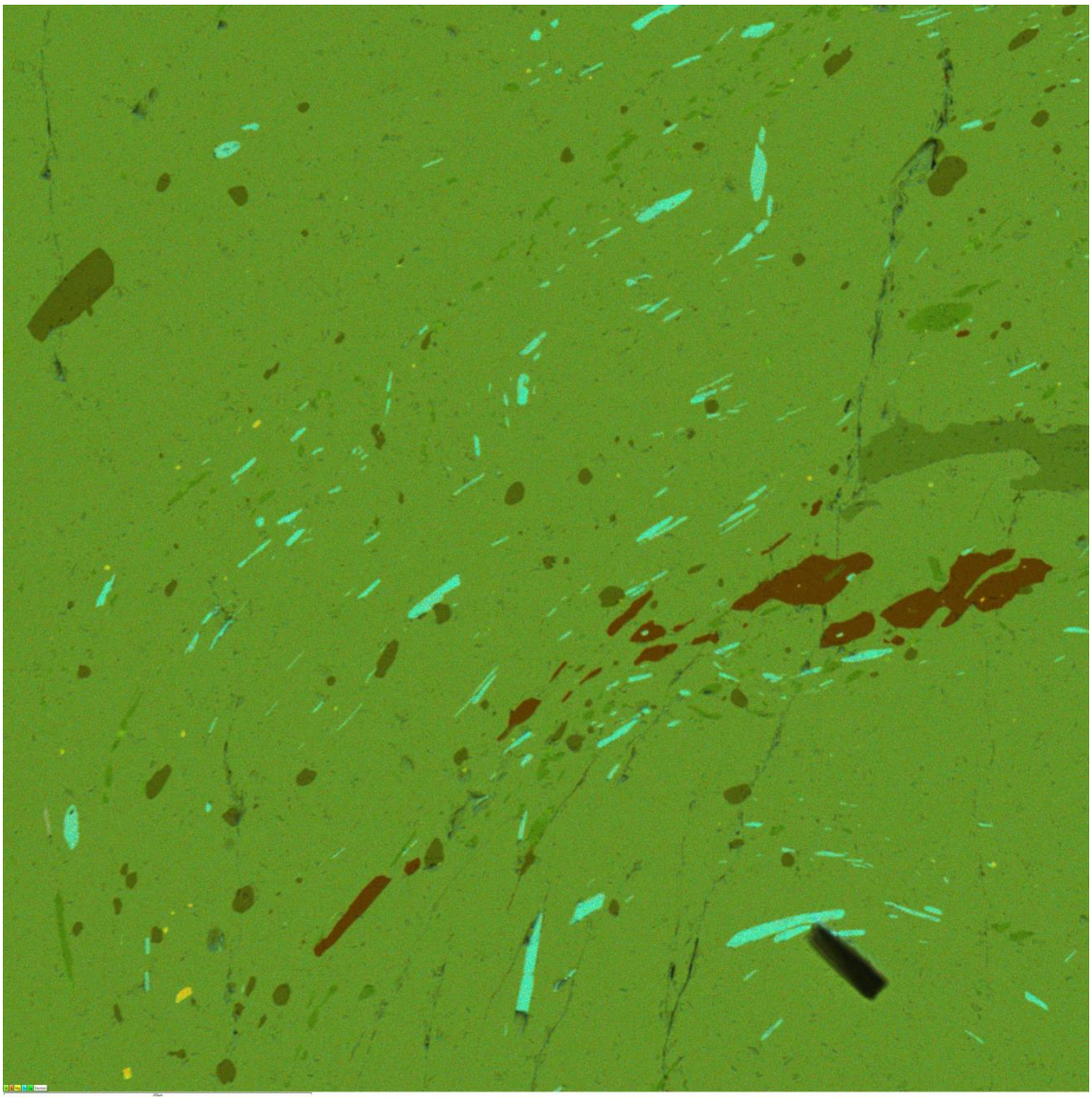

Figure 2.16
Layered EDS image of B17a

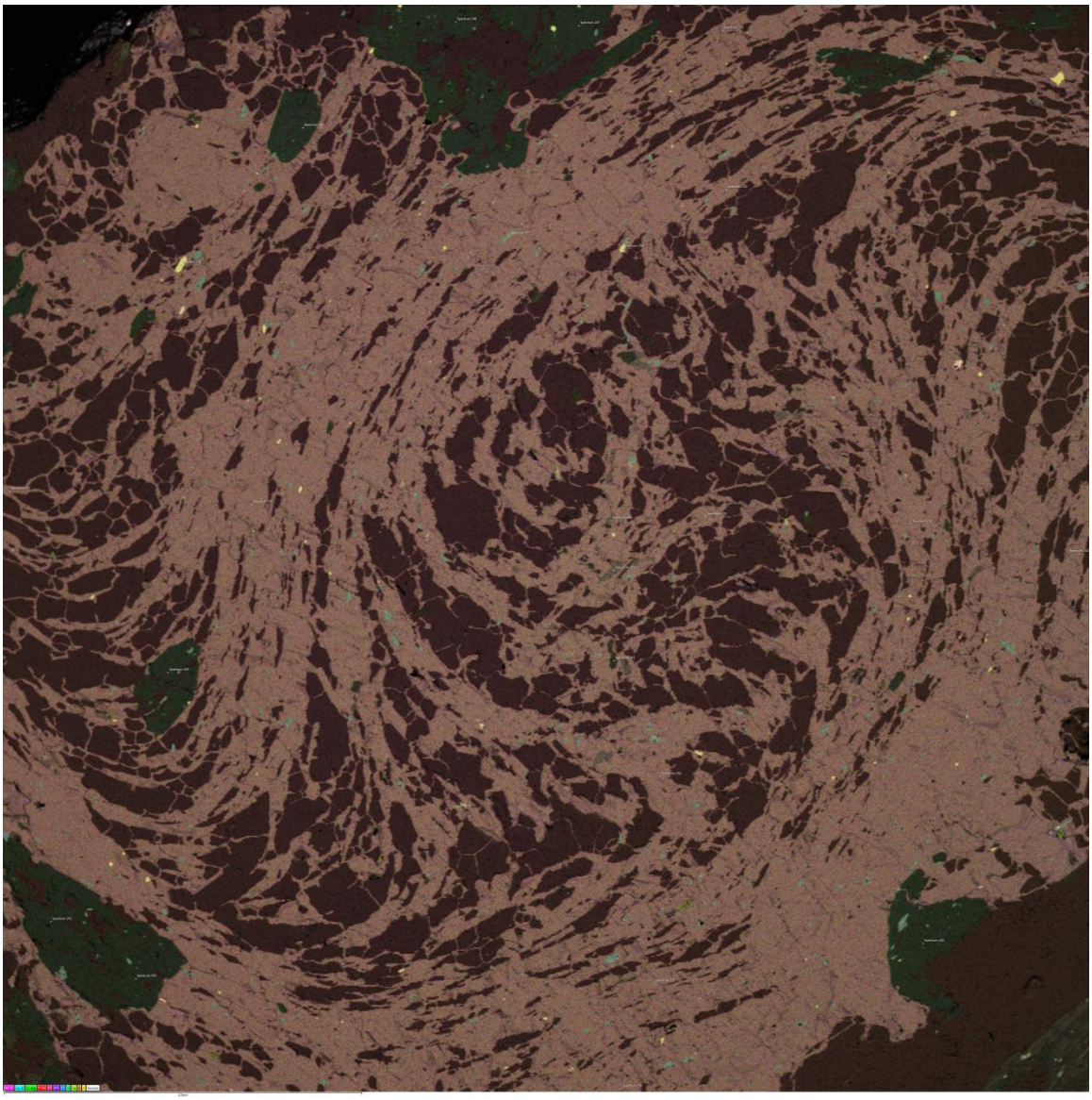

Figure 2.17
Layred EDS Image of Garnet C2-1

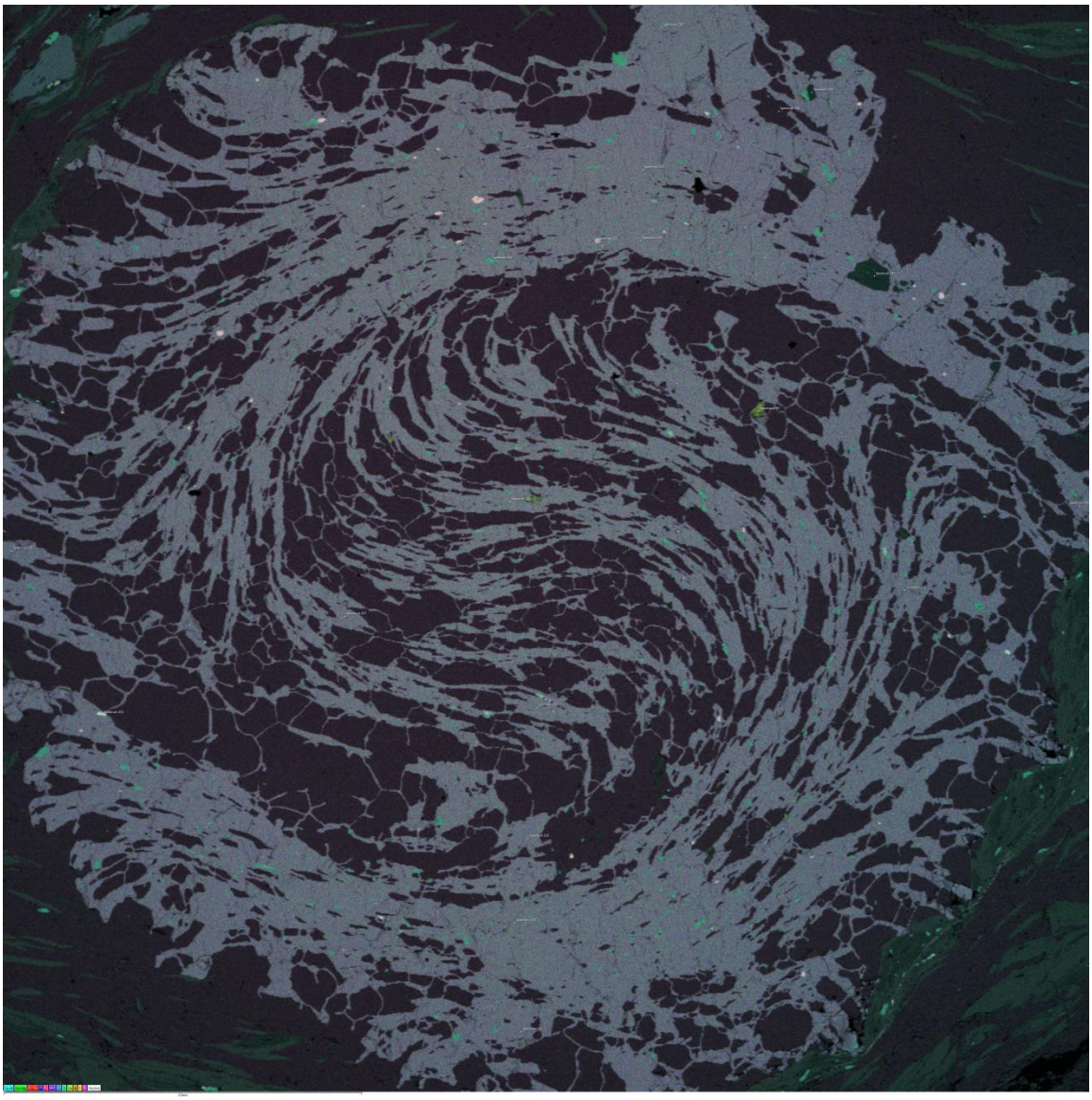

Figure 2.18
Layered EDS image of garnet B6

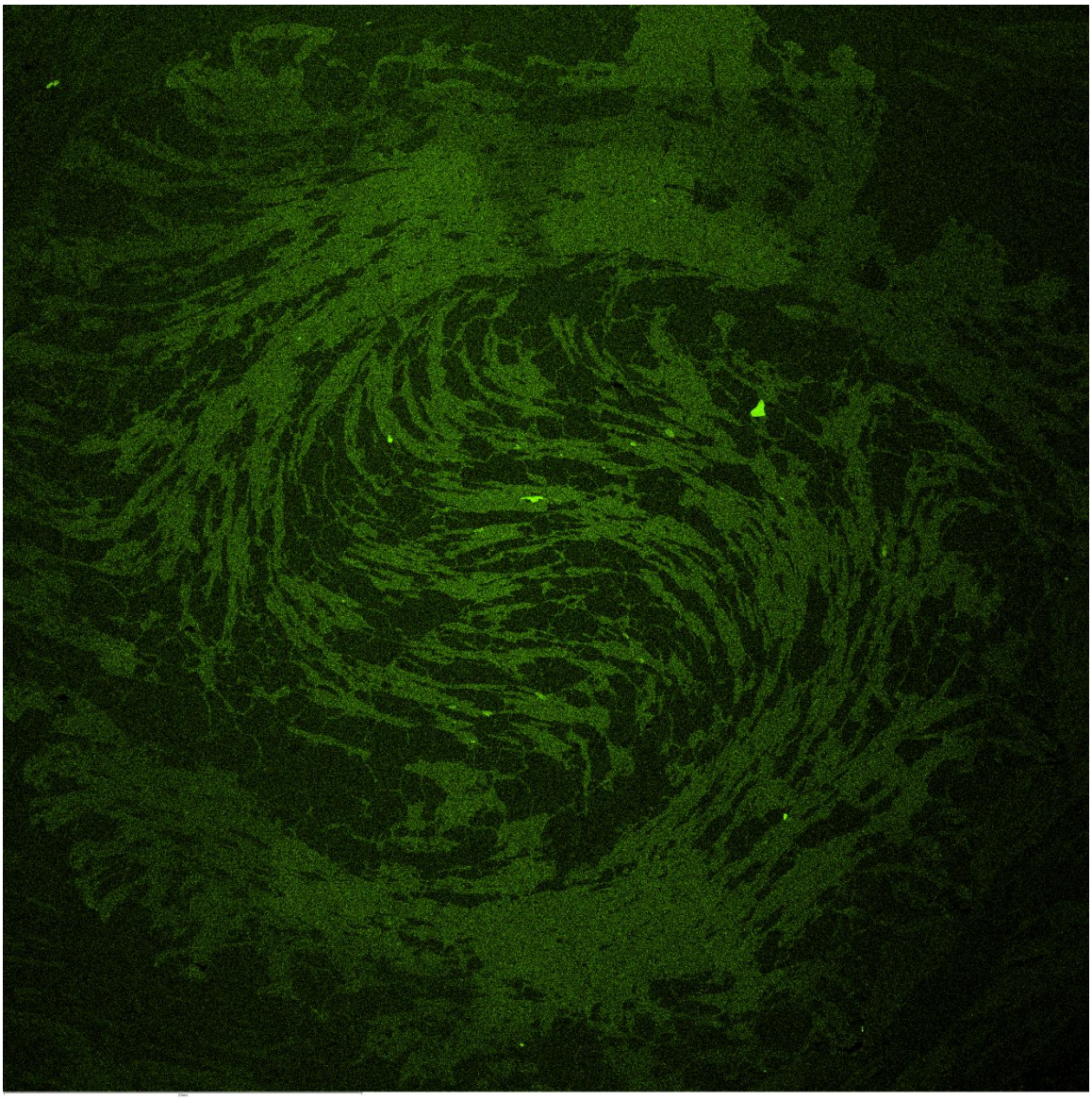

Figure 2.19
Ca EDS map of garnet B6

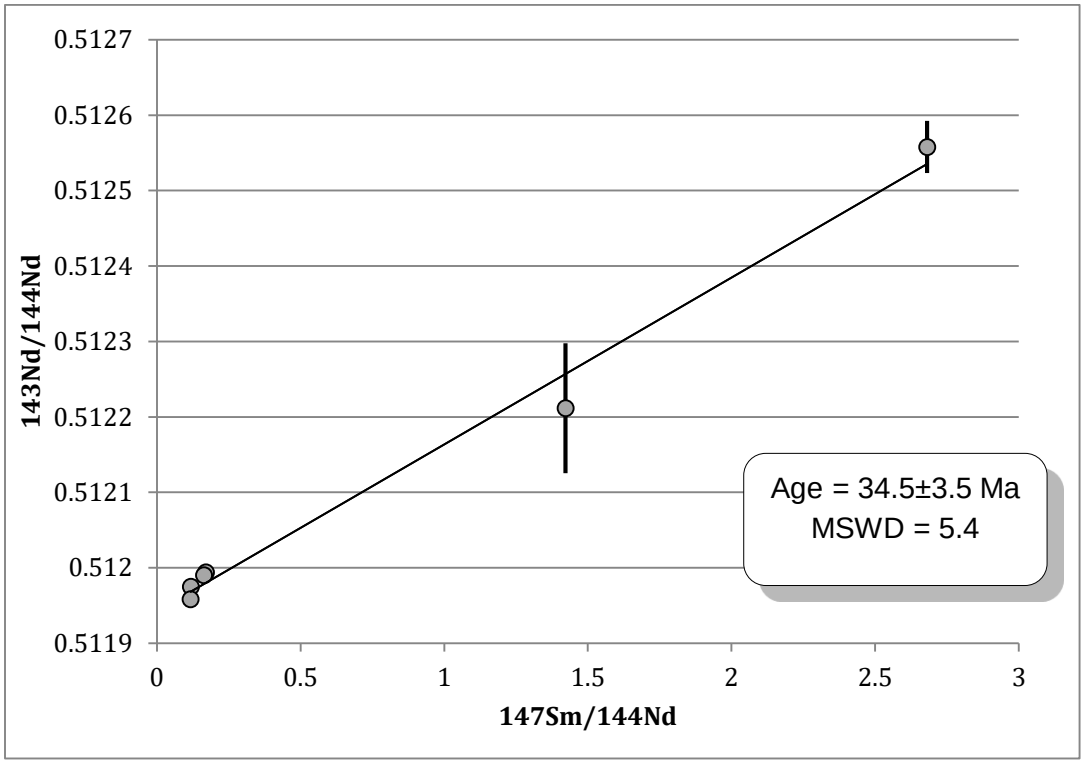

Figures 2.20
6 Point Isochron for B13c

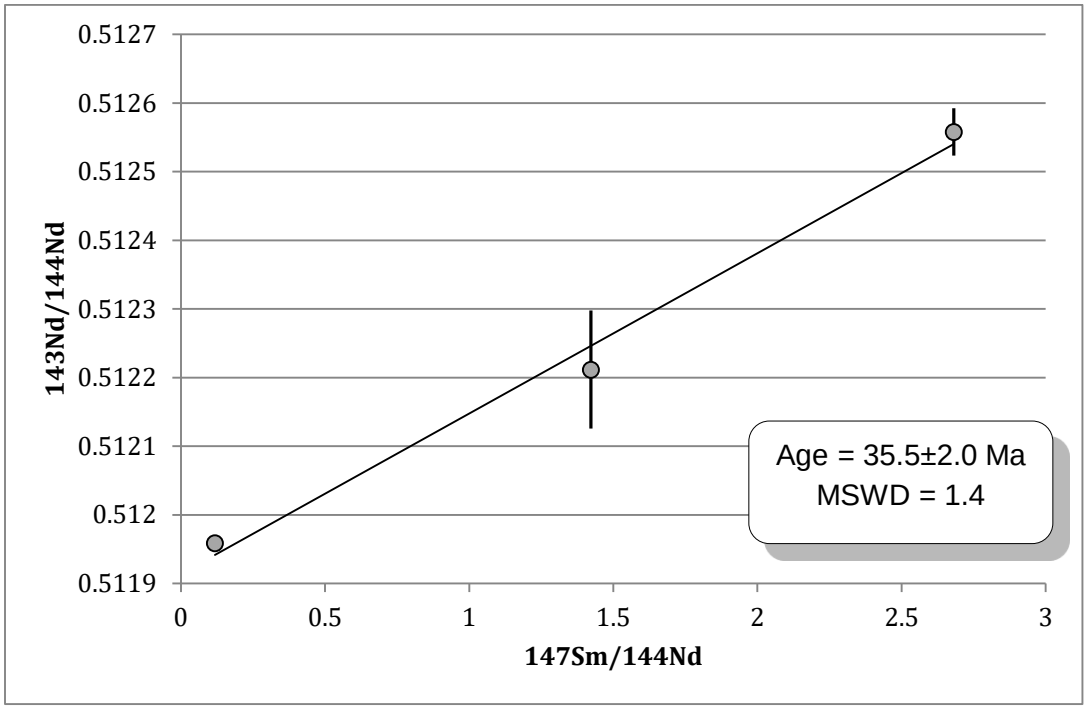

Figure 2.21
Three-point isochron for B13c

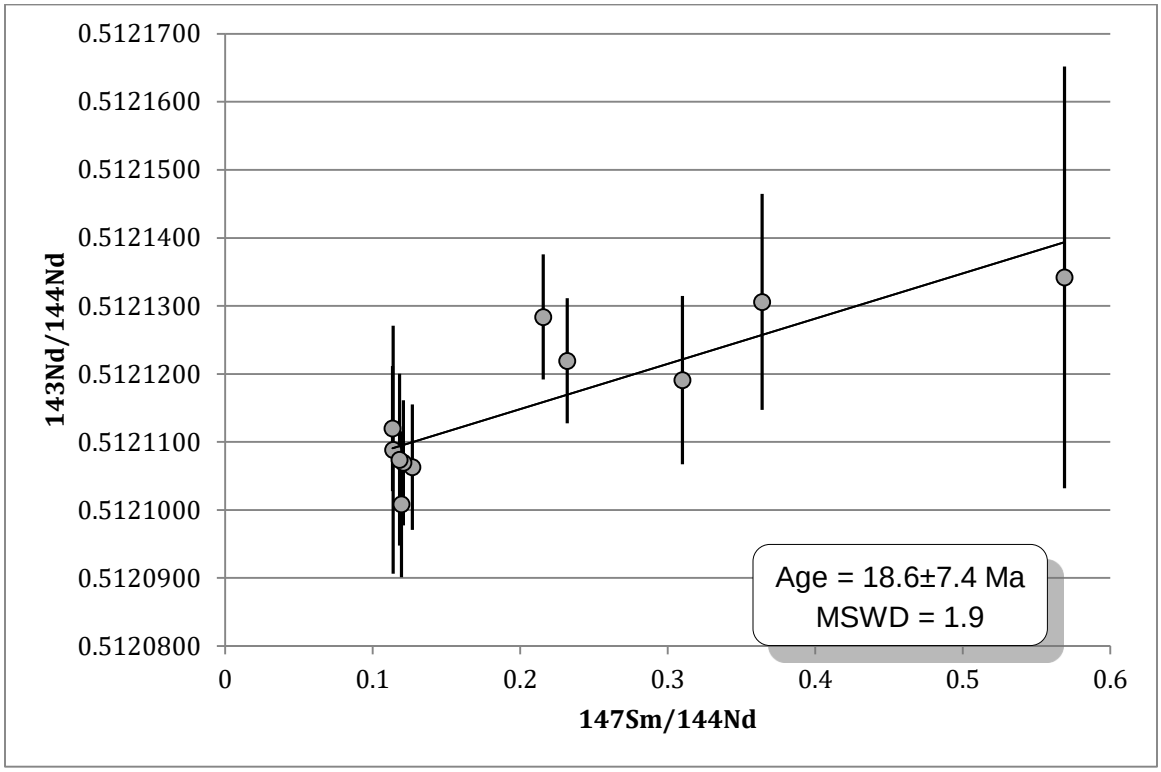

Figure 2.22
12-point isochron for sample B2b

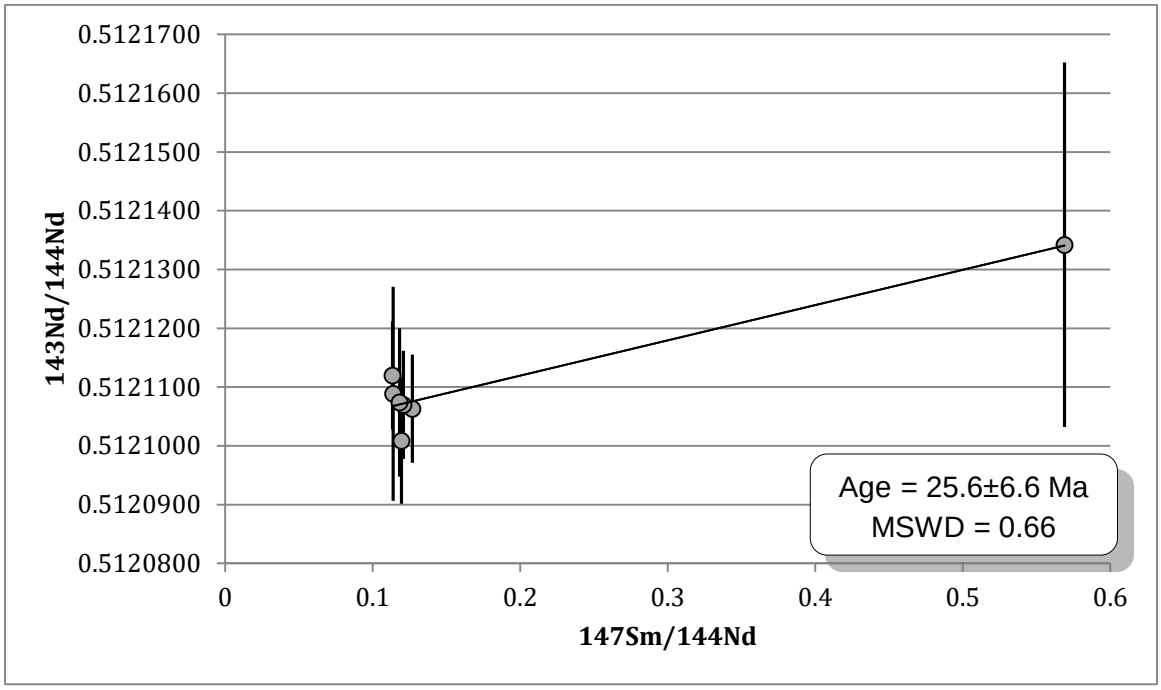

Figure 2.23
Oldest Isochron for B2b

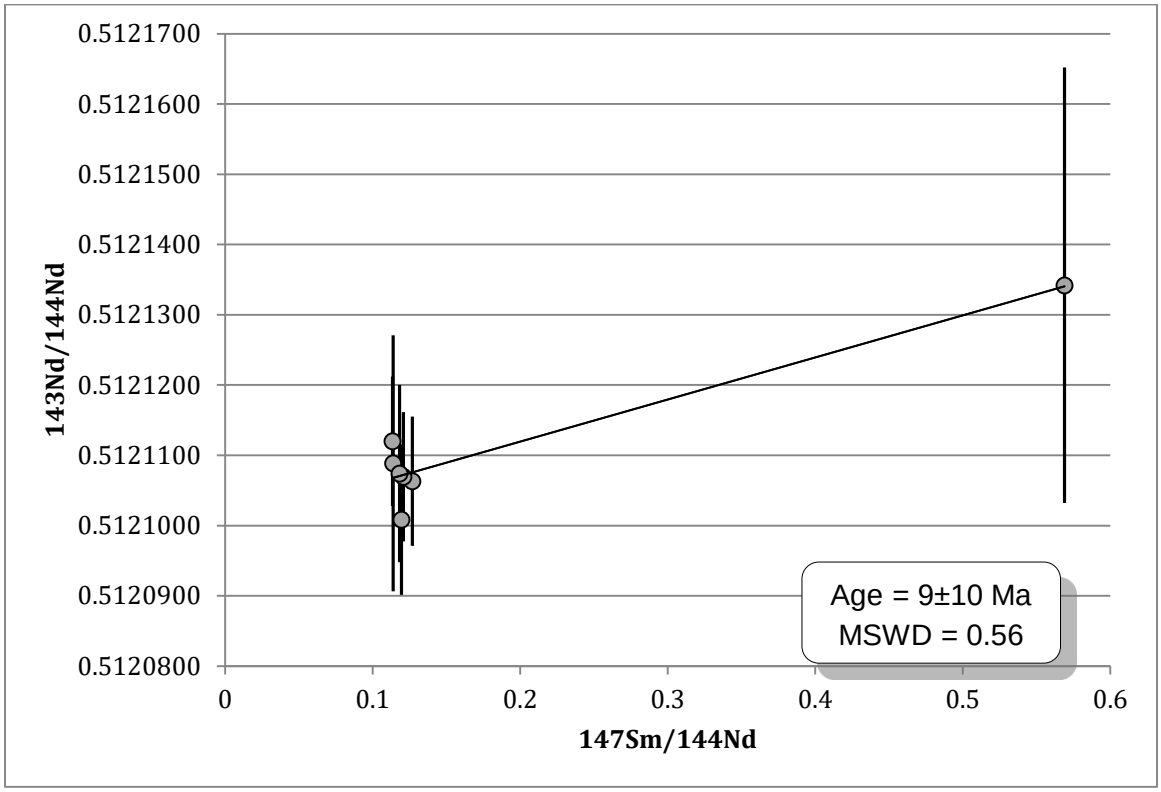

Figure 2.24
Youngest Isochron for sample B2b

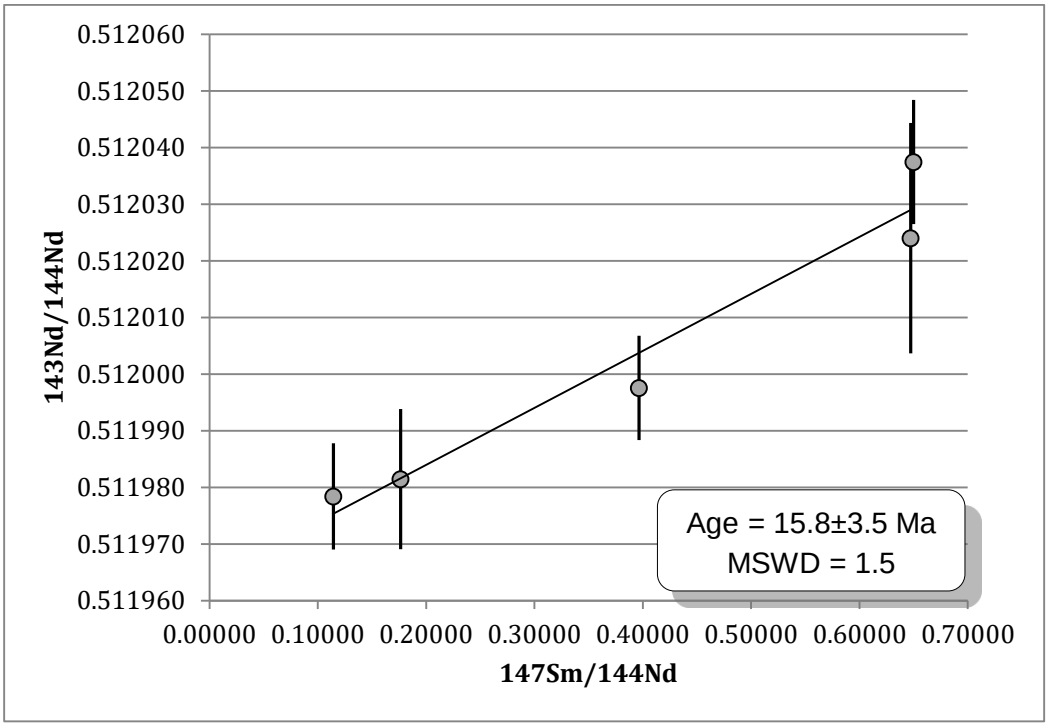

Figure 2.25
5-point isochron for Preliminary characterization of 27.1.2

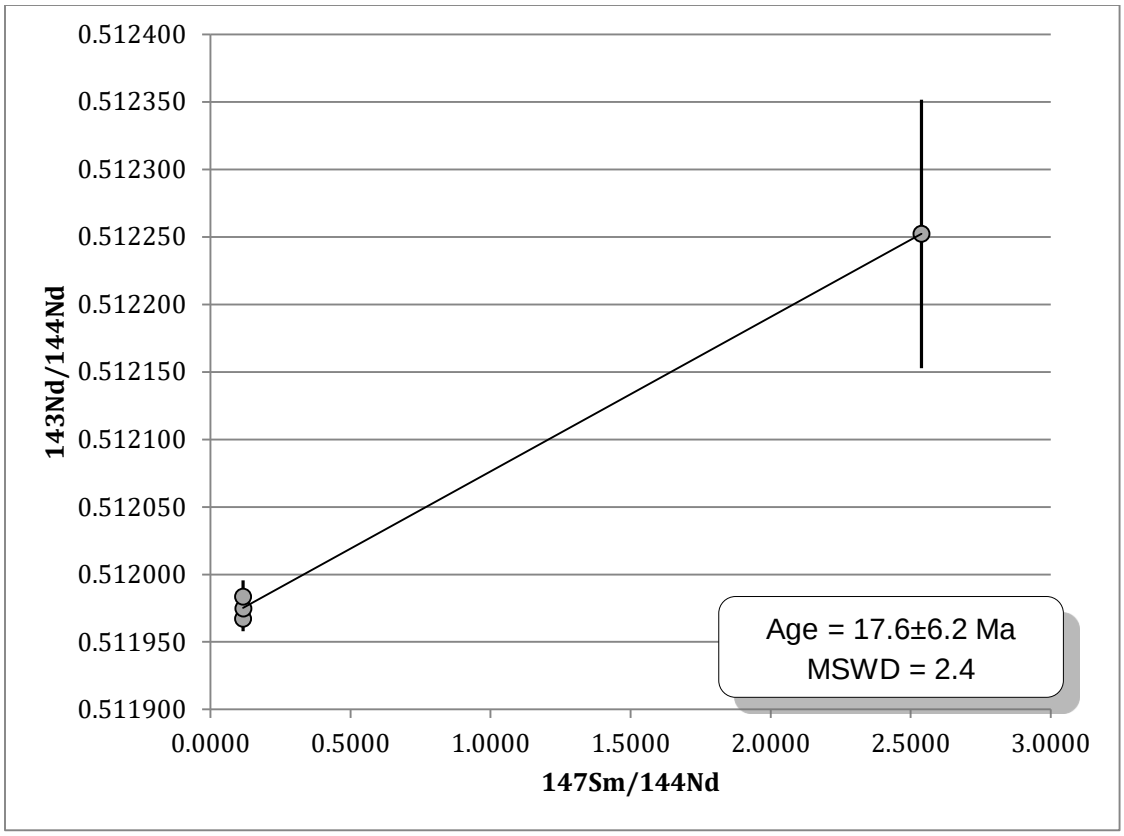

Figure 2.26
Garnet C2-1 zone B Isochron

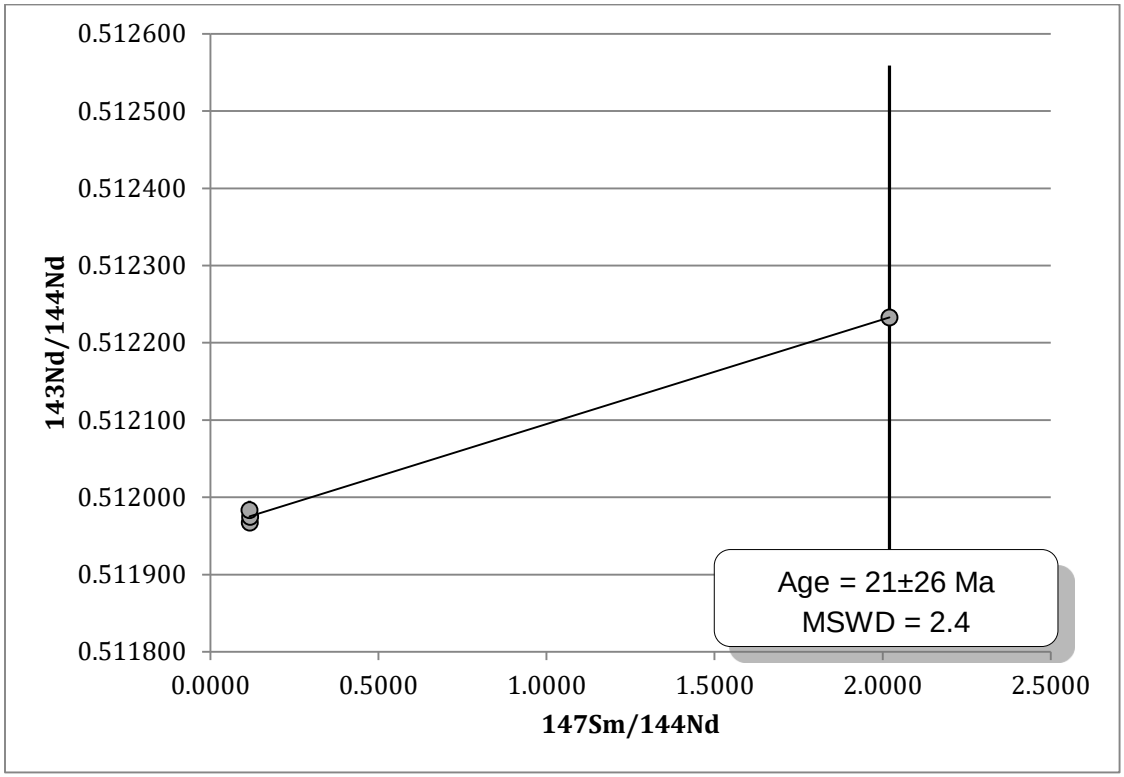

Figure 2.27
Garnet C2-1 Zone C Isochron

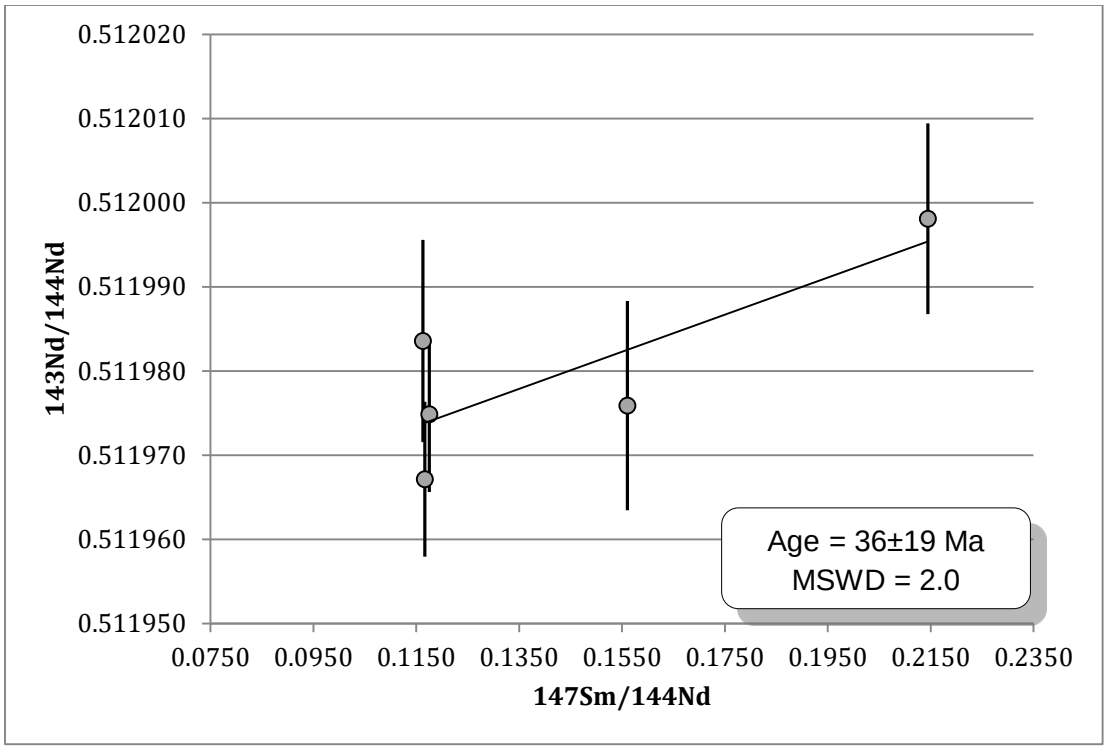

Figure 2.28
Garnet C2-1 Zone D Isochron

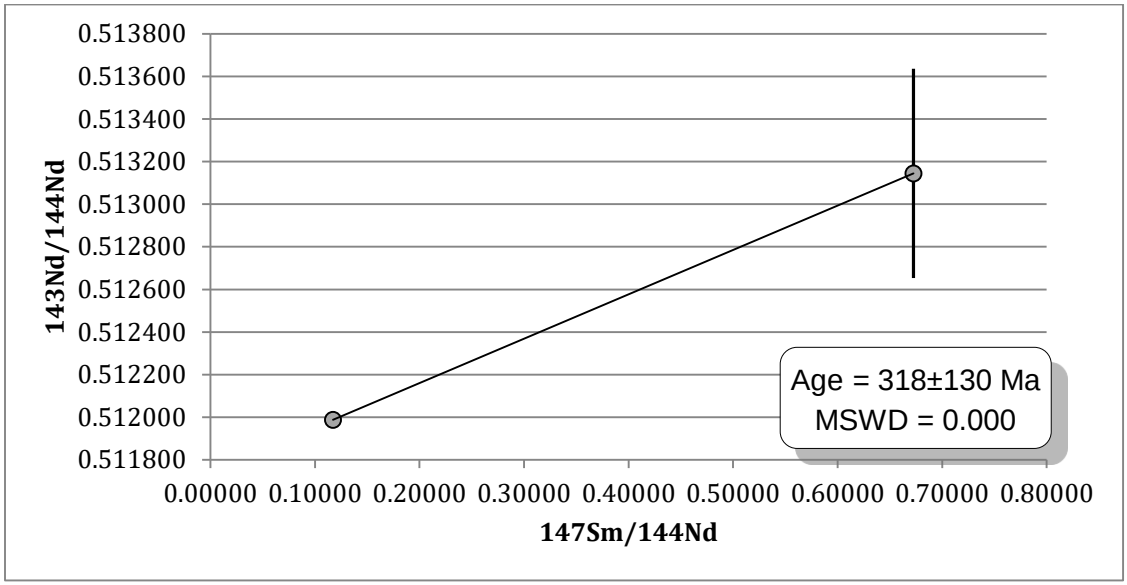

Figure 2.29
Garnet B6 zone 1 + 2 Isochron

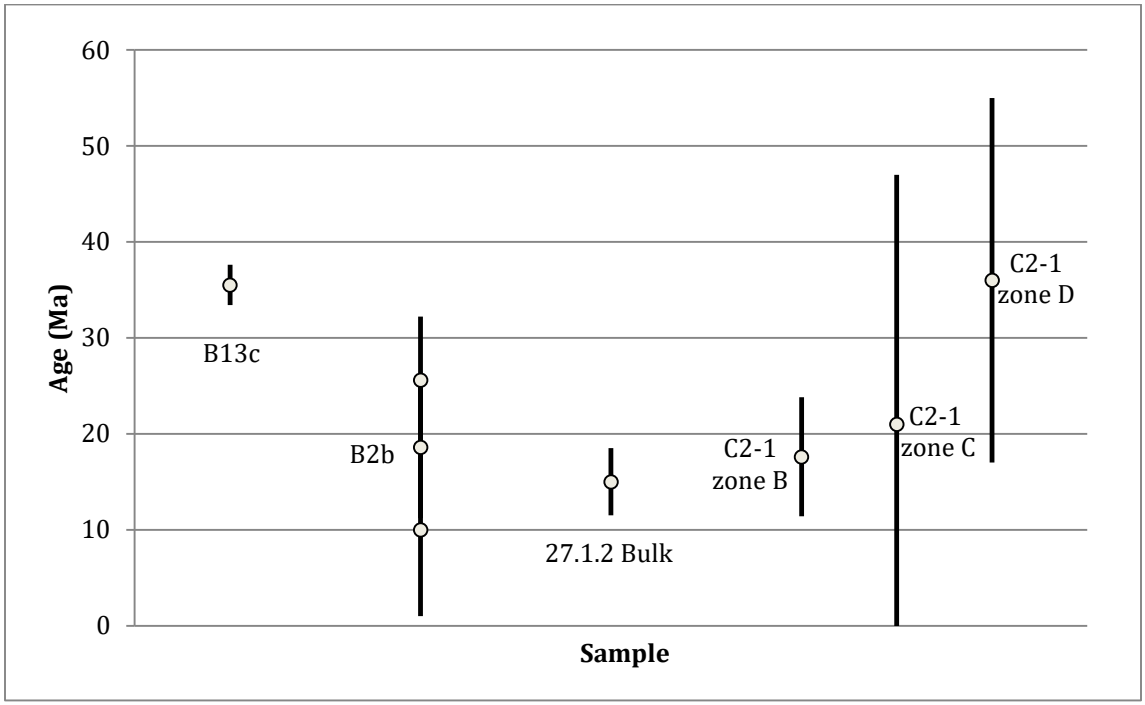

Figure 2.30
Summary of ages

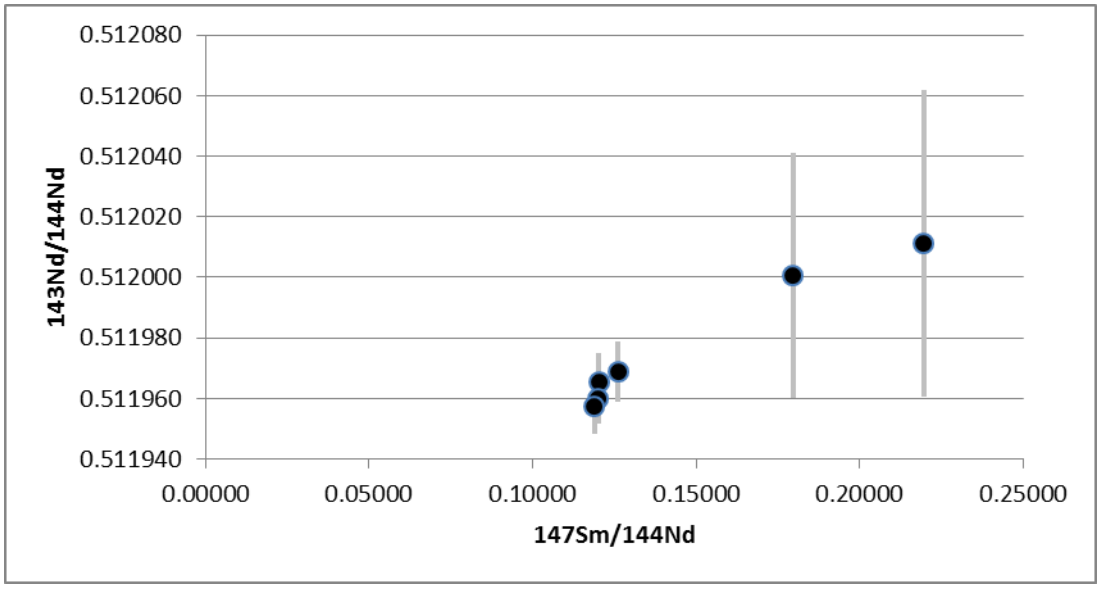

Figure 2.31
Isotope data for sample B3b

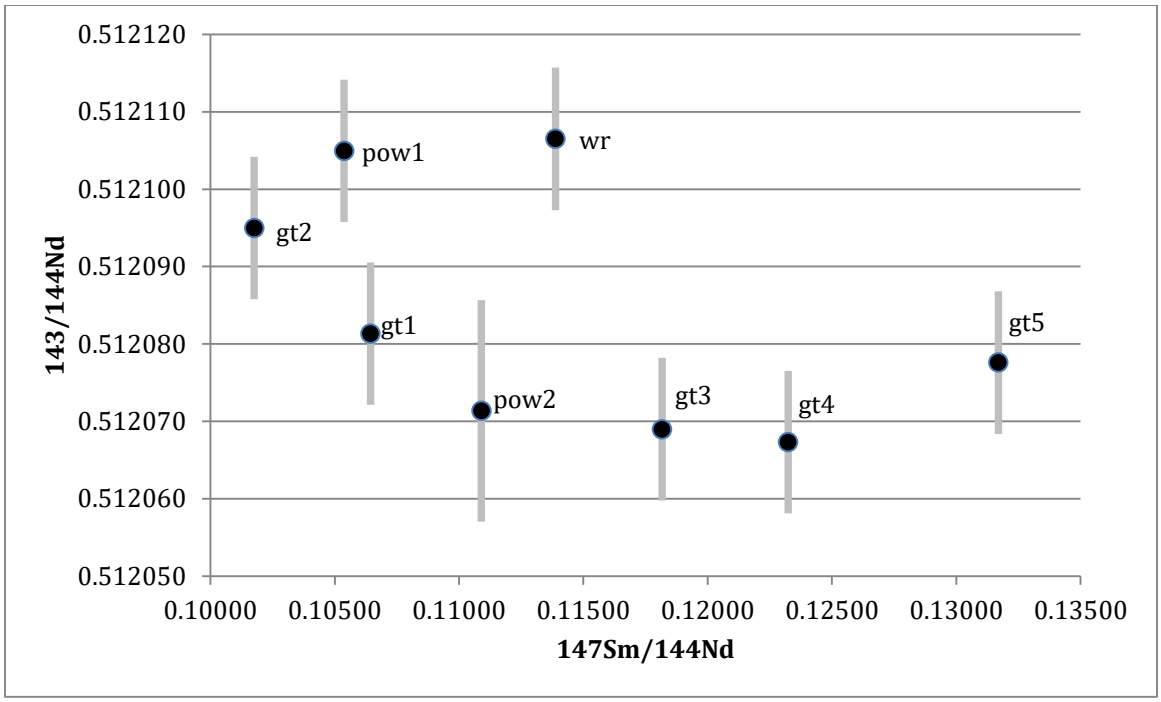

Figure 2.32
Isotope data for Sample B17a

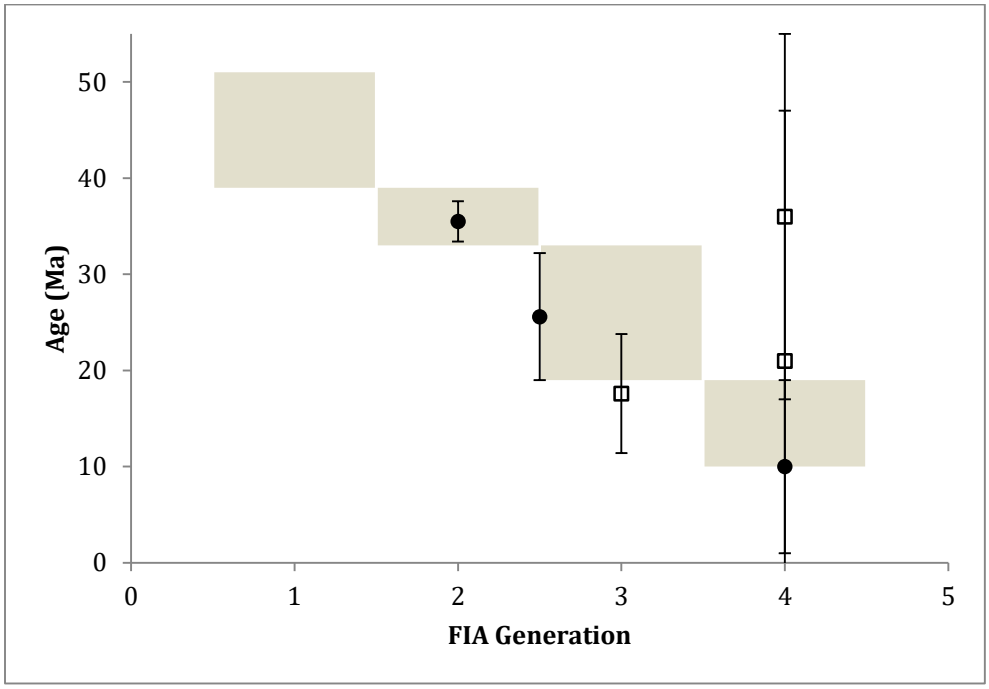

Figure 2.33
Garnet Ages and their relationship to FIA Generations

APPENDIX A: Sample Preparation and Mineral Separation

Preparation for bulk garnet chronology

An appropriate chunk of each hand sample was selected; care was taken to avoid macroscopically evident veins, secondary minerals, or other signs of alteration. This chunk was separated from the available hand sample with a large rock saw. Any ink or paint labels and markings were also sawed off at this stage. This chunk was then crushed by hand in a large tungsten carbide mortar and pestle. At this stage a portion of the sample was set aside for bulk rock chemical analysis. This portioning was achieved by pouring the crushed sample evenly over two sheets of paper and splitting it down the middle. Particular care was taken to avoid any preferential inclusion of different minerals or grain sizes.

The portion separated for bulk rock analysis was powdered in an agate ball mill until 100% of it passed through a 200-mesh sieve. At this point it was ready for dissolution and clean lab chemistry.

The remaining portion was the reservoir from which the garnet mineral separate was drawn. Mineral separation was achieved through a combination of hand picking, paper shaking (to remove mica minerals), sieving, and magnetic separation via the Frantz. The Frantz was always set with a side angle of 20° and a current varying from 0.4A up to 0.6A. The current was generally selected such that garnet was pulled to the

"high" (i.e. more magnetically susceptible) side. When the garnet separate was deemed sufficiently pure it was hand crushed in a small tungsten carbide mortar

and pestle to one of three grain sizes: first, passing through a 100-mesh sieve but catching in a 200-mesh; second, passing through a 140-mesh sieve but catching in a 200-mesh; third, passing through a 140-mesh sieve but catching in a 230-mesh. The grain size was chosen to maximize the size of garnet grains while minimizing the presence of aggregate grains or unexposed mineral inclusions in the separate. Any part of the garnet separate which passed through the finer mesh size (e.g. any garnet crushed smaller than 200 mesh in a 100 to 200-mesh grain size selection) was retained and labeled as garnet "powder".

Preparation for Zoned Garnet Chronology

The garnets chosen for zoned analysis were processed somewhat differently. A preliminary chunk of sample 27.1.2 was treated with exactly the above procedure to determine ideal grain size and laboratory procedures. Then a ~1mm thick slab of each garnet was cut, polished, and glued onto a glass slide using Crystalbond™. This slab was then carbon coated and analyzed on the SEM at Boston College. After imaging, destructive analysis could begin.

Using the chemical data from the SEM, four zones from each garnet were selected for analysis. The wafer of rock was removed from the glass slide and glued onto a carbon block. These zones were then separated from one another by drilling on the Micromill drilling system from New Wave. Figures 2.10 and 2.11 show the planned drill paths for garnet C2-1 and B6, respectively. Figure 2.12 shows the progressive drilling of garnet C2-1 as each zone was drilled out and removed. Figure 2.13 shows two paths drilled in garnet B6. Note that the outer two zones of garnet

B6 have not yet been separated for analysis. The inner two zones of garnet B6 were subsequently lumped together for analysis due to their small mass.

After drilling, each garnet zone was plucked from the carbon block and ultrasonicated in acetone to remove any remaining crystalbond. Once clean, each zone was crushed in a small tungsten carbide mortar and pestle, sieved to 100 to 230-mesh, passed through the frantz magnetic separator, and hand-picked until visually pure. Table A.1 shows the mass of garnet at each stage of this process.

Table A.1 lists the mass of each garnet zone at different stages in the mechanical preparation process.

Sample	After drilling (mg)	After frantz (mg)	after pick/crush (mg)
C2-1 zone A	4.4	n/a	1.2
C2-1 zone B	13.7	6.7	6.0
C2-1 zone C	59.0	37.2	32.0
C2-1 zone D	112.1	38.1	30.8
B6 zone A	-	n/a	1.5
B6 zone B	-	n/a	1.0

Table A.1
Masses of zones during mineral separation

APPENDIX B: Nd Data Reduction Sheets

This appendix contains Nd data reduction sheets for every sample mentioned in the above chapters. Each page corresponds to one analyzed sample and samples appear in the same order in which they appear in the text. Note that some sample names were changed in the text for clarity. “Zone A” in the text corresponds to “zone 1”, “zone B” is “zone 2”, etc. on these data reduction sheets.

Sample:	**11ESC-18A3_al1**		
Date:	11/23/2014	Position #:	9
Approx Nd load (ng):	-		

Rspike Values Nd {SmNd 0.15 A spike, 6-12-08 calib}

142/144	143/144	145/144	146/144	148/144	150/144	[Nd150]
0.830433	0.494001	0.436936	0.885201	0.740574	198.371260	0.125778
						nm/g

Wt Sample (g)=	0.00288	g
Wt Spike (g)=	0.23611	g

Mass Spectrometer Information:

Number of cycles measured:	720			
Number of cycles used:	520			
Amplifier rotation:	yes			
	start	average (from sheet)	ending	
Filament Current range: from	3700.0412	3903.827256	3974.938582	mAmps
Beam intensity range: from	0.25713561	0.91930889	0.359130339	volts 142Nd.16O
Temperature range: from	1463.44322	1554.192918	1609.98779	°C

Final Ratio Data:

Interference Values

Ce140-O16/Nd144-O16	NO Ce	Ce interference is NOT corrected in this sheet
Pr141-O16/Nd144-O16	3.75E-01	
Sm152-O16/Nd144-O16	2.33E-03	(Measured-Includes Nd150-O18)
Sm154-O16/Nd144-O16	4.39E-04	
Sm152-O16/Nd144-O16	*0.000538*	*(Oxygen isotope interference subtracted)*

for Ratios: Non-interference subtracted grand mean ratios (input RAW values w/o normalization)

	158/160	159/160	161/160	162/160	164/160	166/160
Ratios	1.14E+00	5.13E-01	0.348	7.23E-01	2.45E-01	8.74E-01
%StdErr	8.88E-04	7.28E-04	0	3.58E-14	1.32E-03	1.44E-03

for %StdErr: input %StdErr from online normalized values, or from offline PrSm correction sheet

for comparison only	142/144	143/144	145/144	146/144	148/144	150/144
DePaolo 88, p.14:	1.141854	na	0.348416	0.721882	0.241572	na

FINAL Interference subtracted grand mean ratios: 146/144 set to 0.7219

	142/144	143/144	145/144	146/144	148/144	150/144	150t/144s
Ratios	1.142302	0.513019	0.347000	0.721900	0.241578	0.236471	1.562812
2 S.E.	0.000020	0.000007	0.000000	0.000000	0.000006	0.000007	0.000045

Epsilon143=	7.43	using (143/144)chur=	0.512638
±	0.15	(Hamilton et al. 1983)	

linked from Sm sheet

[Sm147]=	3.375773	nm/g	[Nd144]=	16.11512	nm/g
±	0.000426		±	0.00046	
[Sm]=	3.384575	ppm	[Nd]=	9.77341	ppm
±	0.000428		±	0.00028	
TOT ng Sm=	9.74757462		TOT ng Nd=	28.14743382	
	Sm147/Nd144=	0.209479	Tot pg Nd=	**28147.43382**	
	±	0.000027	pg Nd/mL	9773414.521	

Sample:	**11ESC-18A4 wr al1 NOTE: MISLABELED ON BARREL!!!**
Date:	7/4/2015
Position #:	2
Approx Nd load (ng):	-

Rspike Values Nd {SmNd 0.15 A spike, 6-12-08 calib}

142/144	143/144	145/144	146/144	148/144	150/144	[Nd150]
0.830433	0.494001	0.436936	0.885201	0.740574	198.371260	0.125778
						nm/g

Wt Sample (g)=	0.002402	g
Wt Spike (g)=	0.5288	g

Mass Spectrometer Information:

Number of cycles measured:	275			
Number of cycles used:	252			
Amplifier rotation:	yes			
	start	average (from sheet)	ending	
Filament Current range: from	3724.94087	3742.052688	3749.965667	mAmps
Beam intensity range: from	0.45833521	0.42593471	0.286812739	volts 142Nd.16O
Temperature range: from	1453.06471	1511.729140	1579.68254	°C

Final Ratio Data:

Interference Values

Ce140-O16/Nd144-O16	NO Ce	Ce interference is NOT corrected in this sheet
Pr141-O16/Nd144-O16	9.29E-03	
Sm152-O16/Nd144-O16	4.54E-03	(Measured-Includes Nd150-O18)
Sm154-O16/Nd144-O16	1.58E-04	
Sm152-O16/Nd144-O16	*0.000248*	*(Oxygen isotope interference subtracted)*

for Ratios: Non-interference subtracted grand mean ratios (input RAW values w/o normalization)

	158/160	159/160	161/160	162/160	164/160	166/160
Ratios	1.14E+00	5.12E-01	0.348	7.24E-01	2.47E-01	2.09E+00
%StdErr	1.82E-03	1.54E-03	0	2.52E-14	2.69E-03	3.03E-03

for %StdErr: input %StdErr from online normalized values, or from offline PrSm correction sheet

for comparison only	142/144	143/144	145/144	146/144	148/144	150/144
DePaolo 88, p.14:	1.141854	na	0.348416	0.721882	0.241572	na

FINAL Interference subtracted grand mean ratios: 146/144 set to 0.7219

	142/144	143/144	145/144	146/144	148/144	150/144	150t/144s
Ratios	1.142307	0.512997	0.346575	0.721900	0.241575	0.236471	0.532378
2 S.E.	0.000042	0.000016	0.000000	0.000000	0.000013	0.000014	0.000032

Epsilon143= 7.00 using (143/144)chur= 0.512638
± 0.31 (Hamilton et al. 1983)

linked from Sm sheet

[Sm147]=	3.056309	nm/g	[Nd144]=	14.74157	nm/g
±	0.000588		±	0.00089	
[Sm]=	3.064278	ppm	[Nd]=	8.94039	ppm
±	0.000589		±	0.00054	
TOT ng Sm=	7.36039535		TOT ng Nd=	21.47481379	
		Sm147/Nd144= 0.207326	Tot pg Nd=	**21474.81379**	
		± 0.000042	pg Nd/mL	8940388.754	

Sample:	11ESC-18A gt 3	Position #:	4
Date:	6/14/2015		
Approx Nd load (ng):	-		

Rspike Values Nd {SmNd 1.0 A spike, 6-12-08 calib}

142/144	143/144	145/144	146/144	148/144	150/144	[Nd150]
0.830433	0.494001	0.436936	0.885201	0.740574	198.371260	0.049114 nm/g

Wt Sample (g)=	0.00513	g
Wt Spike (g)=	0.05004	g

Mass Spectrometer Information:

Number of cycles measured:	400			
Number of cycles used:	399			
Amplifier rotation:	yes			
	start	average (from sheet)	ending	
Filament Current range: from	3700.0412	3728.725323	3779.995422	mAmps
Beam intensity range: from	0.12548891	0.21544007	0.129316138	Volts 142Nd.16O
Temperature range: from	1529.45055	1563.926972	1591.721612	° C

Final Ratio Data:

Interference Values

Ce140-O16/Nd144-O16	NO Ce	Ce interference is NOT corrected in this sheet
Pr141-O16/Nd144-O16	1.54E-02	
Sm152-O16/Nd144-O16	6.16E-03	(Measured-Includes Nd150-O18)
Sm154-O16/Nd144-O16	4.34E-03	
Sm152-O16/Nd144-O16	*0.005088*	*(Oxygen isotope interference subtracted)*

for Ratios: Non-interference subtracted grand mean ratios (input RAW values w/o normalization)

	158/160	159/160	161/160	162/160	164/160	166/160
Ratios	1.14E+00	5.14E-01	0.348	7.23E-01	2.46E-01	5.27E-01
%StdErr	3.47E-03	2.40E-03	0	9.43E-16	9.05E-03	5.80E-03

for %StdErr: input %StdErr from online normalized values, or from offline PrSm correction sheet

for comparison only	**142/144**	**143/144**	**145/144**	**146/144**	**148/144**	**150/144**
DePaolo 88, p.14, ln. B':	1.141854	na	0.348416	0.721882	0.241572	na

FINAL Interference subtracted grand mean ratios: **146/144 set to 0.7219**

	142/144	**143/144**	**145/144**	**146/144**	**148/144**	**150/144**	**150t/144s**
Ratios	1.144306	0.515993	0.347195	0.721900	0.241614	0.236471	3.471730
2 S.E.	0.000079	0.000025	0.000000	0.000000	0.000044	0.000027	0.000403

Epsilon143= **65.44** **using (143/144)chur=** **0.512638**
± **0.48** **(Hamilton et al. 1983)**

linked from Sm sheet

[Sm147]=	1.932389	nm/g	**[Nd144]=**	**1.66322**	nm/g
±	0.001465		**±**	**0.00019**	
[Sm]=	1.937427	ppm	**[Nd]=**	**1.00870**	ppm
±	0.001469		**±**	**0.00012**	
TOT ng Sm=	9.93900137		**TOT ng Nd=**	**5.174636306**	

Sm147/Nd144= **1.161836**
± **0.000891**

Sample:	11ESC-18A gt5
Date:	6/14/2015
Approx Nd load (ng):	-

Position #: 7

Rspike Values Nd {SmNd 1.0 A spike, 6-12-08 calib}

142/144	143/144	145/144	146/144	148/144	150/144	[Nd150]
0.830433	0.494001	0.436936	0.885201	0.740574	198.371260	0.049114 nm/g

Wt Sample (g)=	0.0072	g
Wt Spike (g)=	0.04881	g

Mass Spectrometer Information:

Number of cycles measured:	175			
Number of cycles used:	96			
Amplifier rotation:	yes			
	start	average (from sheet)	ending	
Filament Current range: from	3599.94202	3599.942016	3599.942016	mAmps
Beam intensity range: from	0.81186008	1.09460224	1.101628505	Volts 142Nd.16O
Temperature range: from	1526.95971	1543.915598	1561.416361	° C

Final Ratio Data:

Interference Values

Ce140-O16/Nd144-O16	NO Ce	Ce interference is NOT corrected in this sheet
Pr141-O16/Nd144-O16	1.27E-02	
Sm152-O16/Nd144-O16	7.87E-03	(Measured-Includes Nd150-O18)
Sm154-O16/Nd144-O16	5.87E-03	
Sm152-O16/Nd144-O16	*0.006918*	*(Oxygen isotope interference subtracted)*

for Ratios: Non-interference subtracted grand mean ratios (input RAW values w/o normalization)

	158/160	159/160	161/160	162/160	164/160	166/160
Ratios	1.14E+00	5.14E-01	0.348	7.23E-01	2.46E-01	4.75E-01
%StdErr	3.62E-03	1.29E-03	0	2.66E-14	8.83E-03	4.98E-03

for %StdErr: input %StdErr from online normalized values, or from offline PrSm correction sheet

for comparison only	**142/144**	**143/144**	**145/144**	**146/144**	**148/144**	**150/144**
DePaolo 88, p.14, ln. B':	1.141854	na	0.348416	0.721882	0.241572	na

FINAL Interference subtracted grand mean ratios: **146/144 set to 0.7219**

	142/144	**143/144**	**145/144**	**146/144**	**148/144**	**150/144**	**150t/144s**
Ratios	1.142365	0.516025	0.347397	0.721900	0.241610	0.236471	4.229823
2 S.E.	0.000083	0.000013	0.000000	0.000000	0.000043	0.000024	0.000422

Epsilon143= 66.07 **using (143/144)chur= 0.512638**
± 0.26 **(Hamilton et al. 1983)**

linked from Sm sheet

[Sm147]=	1.645156	nm/g	**[Nd144]=**	**1.40832**	nm/g
±	0.000590		**±**	**0.00014**	
[Sm]=	1.649446	ppm	**[Nd]=**	**0.85411**	ppm
±	0.000592		**±**	**0.00009**	
TOT ng Sm=	11.8760096		**TOT ng Nd=**	**6.14961056**	
	Sm147/Nd144=	**1.168166**			
	±	**0.000435**			

Sample:	11ESC-18A
Date:	7/4/2015
Approx Nd load (ng):	-

Position #: 8

Rspike Values Nd {SmNd 1.0 A spike, 6-12-08 calib}

142/144	143/144	145/144	146/144	148/144	150/144	[Nd150]
0.830433	0.494001	0.436936	0.885201	0.740574	198.371260	0.049114
						nm/g

Wt Sample (g)=	0.01	g
Wt Spike (g)=	0.264	g

Mass Spectrometer Information:

Number of cycles measured:	800			
Number of cycles used:	800			
Amplifier rotation:	yes			
	start	average (from sheet)	ending	
Filament Current range: from	3700.0412	3758.0016	3950.038911	mAmps
Beam intensity range: from	0.164823	0.21033865	0.094627926	Volts 142Nd.16O
Temperature range: from	1483.7851	1521.477259	1589.230769	° C

Final Ratio Data:

Interference Values

Ce140-O16/Nd144-O16	NO Ce	Ce interference is NOT corrected in this sheet
Pr141-O16/Nd144-O16	6.47E-03	
Sm152-O16/Nd144-O16	3.37E-03	(Measured-Includes Nd150-O18)
Sm154-O16/Nd144-O16	1.31E-03	
Sm152-O16/Nd144-O16	*0.001541*	*(Oxygen isotope interference subtracted)*

for Ratios: Non-interference subtracted grand mean ratios (input RAW values w/o normalization)

	158/160	159/160	161/160	162/160	164/160	166/160
Ratios	1.14E+00	5.14E-01	0.348	7.24E-01	2.46E-01	8.96E-01
%StdErr	2.01E-03	1.47E-03	0	3.43E-14	3.09E-03	2.86E-03

for %StdErr: input %StdErr from online normalized values, or from offline PrSm correction sheet

for comparison only	**142/144**	**143/144**	**145/144**	**146/144**	**148/144**	**150/144**
DePaolo 88, p.14, ln. B':	1.141854	na	0.348416	0.721882	0.241572	na

FINAL Interference subtracted grand mean ratios: **146/144 set to 0.7219**

	142/144	**143/144**	**145/144**	**146/144**	**148/144**	**150/144**	**150t/144s**
Ratios	1.142763	0.516027	0.346794	0.721900	0.241615	0.236471	1.520411
2 S.E.	0.000046	0.000015	0.000000	0.000000	0.000015	0.000014	0.000087

Epsilon143= 66.11 **using (143/144)chur= 0.512638**
± 0.29 **(Hamilton et al. 1983)**

linked from Sm sheet

[Sm147]=	2.319881	nm/g	**[Nd144]=**	**1.97137**	nm/g
±	0.000554		**±**	**0.00011**	
[Sm]=	2.325930	ppm	**[Nd]=**	**1.19559**	ppm
±	0.000556		**±**	**0.00007**	
TOT ng Sm=	23.2593008		**TOT ng Nd=**	**11.95587988**	

Sm147/Nd144= 1.176784
± 0.000289

Sample:	**11ESC-18A gt powder d**		
Date:	6/14/2015	Position #:	3
Approx Nd load (ng):	-		

Rspike Values Nd {SmNd 0.15 A spike, 6-12-08 calib}

142/144	143/144	145/144	146/144	148/144	150/144	[Nd150]
0.830433	0.494001	0.436936	0.885201	0.740574	198.371260	0.125778

nm/g

Wt Sample (g)=	0.0122	g
Wt Spike (g)=	0.32145	g

Mass Spectrometer Information:

Number of cycles measured:	320			
Number of cycles used:	300			
Amplifier rotation:	yes			
	start	average (from sheet)	ending	
Filament Current range: from	3700.0412	3735.141395	3784.62501	mAmps
Beam intensity range: from	0.20691428	0.29494744	0.213659189	volts 142Nd.16O
Temperature range: from	1507.44811	1551.612129	1586.739927	° C

Final Ratio Data:

Interference Values

Ce140-O16/Nd144-O16	NO Ce	Ce interference is NOT corrected in this sheet
Pr141-O16/Nd144-O16	5.77E-03	
Sm152-O16/Nd144-O16	9.12E-03	(Measured-Includes Nd150-O18)
Sm154-O16/Nd144-O16	3.56E-03	
Sm152-O16/Nd144-O16	*0.004235*	*(Oxygen isotope interference subtracted)*

for Ratios: Non-interference subtracted grand mean ratios (input RAW values w/o normalization)

	158/160	159/160	161/160	162/160	164/160	166/160
Ratios	1.14E+00	5.13E-01	0.348	7.24E-01	2.50E-01	2.38E+00
%StdErr	3.06E-03	2.38E-03	0	2.40E-14	6.49E-03	4.50E-03

for %StdErr: input %StdErr from online normalized values, or from offline PrSm correction sheet

for comparison only	142/144	143/144	145/144	146/144	148/144	150/144
DePaolo 88, p.14:	1.141854	na	0.348416	0.721882	0.241572	na

FINAL Interference subtracted grand mean ratios: 146/144 set to 0.7219

	142/144	143/144	145/144	146/144	148/144	150/144	150t/144s
Ratios	1.143175	0.514532	0.346464	0.721900	0.241601	0.236471	0.460240
2 S.E.	0.000070	0.000024	0.000000	0.000000	0.000031	0.000021	0.000041

Epsilon143= 36.94 using (143/144)chur= 0.512638
± 0.48 (Hamilton et al. 1983)

linked from Sm sheet

[Sm147]=	1.061898	nm/g	[Nd144]=	1.52526	nm/g
±	0.000081		±	0.00014	
[Sm]=	1.064666	ppm	[Nd]=	0.92503	ppm
±	0.000081		±	0.00008	
TOT ng Sm=	12.9889287		TOT ng Nd=	11.28535631	
		Sm147/Nd144=	0.696209	Tot pg Nd=	**11285.35631**
		±	0.000082	pg Nd/mL	925029.2054

Sample:	**11ESC-18A_gt_pow_c**		
Date:	6/14/2015	Position #:	2
Approx Nd load (ng):	-		

Rspike Values Nd {SmNd 0.15 A spike, 6-12-08 calib}

142/144	143/144	145/144	146/144	148/144	150/144	[Nd150]
0.830433	0.494001	0.436936	0.885201	0.740574	198.371260	0.125778

nm/g

Wt Sample (g)=	0.0217	g
Wt Spike (g)=	1.04045	g

Mass Spectrometer Information:

Number of cycles measured:	140			
Number of cycles used:	100			
Amplifier rotation:	yess			
	start	average (from sheet)	ending	
Filament Current range: from	3599.94202	3600.394965	3612.829786	mAmps
Beam intensity range: from	0.78647709	0.96355255	0.599133606	volts 142Nd.16O
Temperature range: from	1525.71429	1560.947253	1589.64591	° C

Final Ratio Data:

Interference Values

Ce140-O16/Nd144-O16	NO Ce	Ce interference is NOT corrected in this sheet
Pr141-O16/Nd144-O16	2.24E-03	
Sm152-O16/Nd144-O16	9.24E-03	(Measured-Includes Nd150-O18)
Sm154-O16/Nd144-O16	4.60E-03	
Sm152-O16/Nd144-O16	*0.005501*	*(Oxygen isotope interference subtracted)*

for Ratios: Non-interference subtracted grand mean ratios (input RAW values w/o normalization)

	158/160	159/160	161/160	162/160	164/160	166/160
Ratios	1.13E+00	5.12E-01	0.348	7.24E-01	2.49E-01	1.83E+00
%StdErr	1.79E-03	1.56E-03	0	2.78E-14	3.18E-03	2.90E-03

for %StdErr: input %StdErr from online normalized values, or from offline PrSm correction sheet

for comparison only	142/144	143/144	145/144	146/144	148/144	150/144
DePaolo 88, p.14:	1.141854	na	0.348416	0.721882	0.241572	na

FINAL Interference subtracted grand mean ratios: 146/144 set to 0.7219

	142/144	143/144	145/144	146/144	148/144	150/144	150t/144s
Ratios	1.142339	0.514125	0.346676	0.721900	0.241582	0.236471	0.623073
2 S.E.	0.000041	0.000016	0.000000	0.000000	0.000015	0.000014	0.000036

Epsilon143= 29.01 using (143/144)chur= 0.512638
± 0.31 (Hamilton et al. 1983)

linked from Sm sheet

[Sm147]=	2.131181	nm/g	[Nd144]=	3.75755	nm/g
±	0.000012		±	0.00022	
[Sm]=	2.136738	ppm	[Nd]=	2.27886	ppm
±	0.000012		±	0.00013	
TOT ng Sm=	46.3672094		TOT ng Nd=	49.45126857	
		Sm147/Nd144=	0.567173	Tot pg Nd=	**49451.26857**
		±	0.000033	pg Nd/mL	2278860.303

Sample:	**11ESC-18A gt pow 4**		
Date:	7/4/2015	Position #:	4
Approx Nd load (ng):	-		

Rspike Values Nd {SmNd 0.15 A spike, 6-12-08 calib}

142/144	143/144	145/144	146/144	148/144	150/144	[Nd150]
0.830433	0.494001	0.436936	0.885201	0.740574	198.371260	0.125778

nm/g

Wt Sample (g)=	0.0052398	g
Wt Spike (g)=	0.31012	g

Mass Spectrometer Information:

Number of cycles measured:	95			
Number of cycles used:	80			
Amplifier rotation:	yes			
	start	average (from sheet)	ending	
Filament Current range: from	3749.96567	3749.965667	3749.965667	mAmps
Beam intensity range: from	0.15968896	0.16986911	0.125625176	volts 142Nd.16O
Temperature range: from	1495.40904	1527.091168	1560.17094	°C

Final Ratio Data:

Interference Values

Ce140-O16/Nd144-O16	NO Ce	Ce interference is NOT corrected in this sheet
Pr141-O16/Nd144-O16	8.77E-03	
Sm152-O16/Nd144-O16	1.04E-02	(Measured-Includes Nd150-O18)
Sm154-O16/Nd144-O16	4.93E-03	
Sm152-O16/Nd144-O16	*0.005983*	*(Oxygen isotope interference subtracted)*

for Ratios: Non-interference subtracted grand mean ratios (input RAW values w/o normalization)

	158/160	159/160	161/160	162/160	164/160	166/160
Ratios	1.13E+00	5.12E-01	0.348	7.25E-01	2.51E-01	2.15E+00
%StdErr	6.76E-03	5.59E-03	0	1.80E-14	1.43E-02	1.25E-02

for %StdErr: input %StdErr from online normalized values, or from offline PrSm correction sheet

for comparison only	142/144	143/144	145/144	146/144	148/144	150/144
DePaolo 88, p.14:	1.141854	na	0.348416	0.721882	0.241572	na

FINAL Interference subtracted grand mean ratios: 146/144 set to 0.7219

	142/144	143/144	145/144	146/144	148/144	150/144	150t/144s
Ratios	1.143272	0.513984	0.346402	0.721900	0.241579	0.236471	0.518858
2 S.E.	0.000154	0.000057	0.000000	0.000000	0.000069	0.000059	0.000130

Epsilon143= 26.26 using (143/144)chur= 0.512638
± 1.12 (Hamilton et al. 1983)

linked from Sm sheet

[Sm147]=	2.175490	nm/g	[Nd144]=	3.86250	nm/g
±	0.000433		±	0.00097	
[Sm]=	2.181162	ppm	[Nd]=	2.34251	ppm
±	0.000434		±	0.00059	
TOT ng Sm=	11.4288546		TOT ng Nd=	12.27427377	
	Sm147/Nd144=	0.563234	Tot pg Nd=	**12274.27377**	
	±	0.000180	pg Nd/mL	2342508.068	

Sample:	11ESC-18A
Date:	6/14/2015
Approx Nd load (ng):	-

Position #: 5

Rspike Values Nd {SmNd 1.0 A spike, 6-12-08 calib}

142/144	143/144	145/144	146/144	148/144	150/144	[Nd150]
0.830433	0.494001	0.436936	0.885201	0.740574	198.371260	0.049114 nm/g

Wt Sample (g)=	0.00266	g
Wt Spike (g)=	0.02447	g

Mass Spectrometer Information:

Number of cycles measured:	80			
Number of cycles used:	70			
Amplifier rotation:	yes			
	start	average (from sheet)	ending	
Filament Current range: from	3749.96567	3757.902102	3774.990463	mAmps
Beam intensity range: from	0.26385655	0.21701017	0.061382028	Volts 142Nd.16O
Temperature range: from	1541.07448	1569.950462	1603.345543	° C

Final Ratio Data:

Interference Values

Ce140-O16/Nd144-O16	NO Ce	Ce interference is NOT corrected in this sheet
Pr141-O16/Nd144-O16	2.48E-02	
Sm152-O16/Nd144-O16	2.89E-02	(Measured-Includes Nd150-O18)
Sm154-O16/Nd144-O16	2.38E-02	
Sm152-O16/Nd144-O16	*0.028042*	*(Oxygen isotope interference subtracted)*

for Ratios: Non-interference subtracted grand mean ratios (input RAW values w/o normalization)

	158/160	159/160	161/160	162/160	164/160	166/160
Ratios	1.13E+00	5.13E-01	0.348	7.22E-01	2.55E-01	4.32E-01
%StdErr	1.40E-02	5.54E-03	0	2.18E-14	9.35E-02	4.76E-02

for %StdErr: input %StdErr from online normalized values, or from offline PrSm correction sheet

for comparison only	**142/144**	**143/144**	**145/144**	**146/144**	**148/144**	**150/144**
DePaolo 88, p.14, ln. B':	1.141854	na	0.348416	0.721882	0.241572	na

FINAL Interference subtracted grand mean ratios: **146/144 set to 0.7219**

	142/144	**143/144**	**145/144**	**146/144**	**148/144**	**150/144**	**150t/144s**
Ratios	1.143637	0.515786	0.347961	0.721900	0.241664	0.236471	5.364540
2 S.E.	0.000319	0.000057	0.000000	0.000000	0.000452	0.000225	0.005106

Epsilon143= 61.40 **using (143/144)chur= 0.512638**
± 1.11 **(Hamilton et al. 1983)**

linked from Sm sheet

[Sm147]=	2.754955	nm/g	**[Nd144]=**	**2.42376**	nm/g
±	0.001274		**±**	**0.00231**	
[Sm]=	2.762138	ppm	**[Nd]=**	**1.46995**	ppm
±	0.001277		**±**	**0.00140**	
TOT ng Sm=	7.34728682		**TOT ng Nd=**	**3.910057356**	
		Sm147/Nd144=	**1.136647**		
		±	**0.001203**		

Sample:	11ESC-18A gt6		
Date:	7/4/2015	Position #:	7
Approx Nd load (ng):	-		

Rspike Values Nd {SmNd 1.0 A spike, 6-12-08 calib}

142/144	143/144	145/144	146/144	148/144	150/144	[Nd150]
0.830433	0.494001	0.436936	0.885201	0.740574	198.371260	0.049114 nm/g

Wt Sample (g)=	0.01451	g
Wt Spike (g)=	0.37743	g

Mass Spectrometer Information:

Number of cycles measured:	720			
Number of cycles used:	480			
Amplifier rotation:	yes			
	start	average (from sheet)	ending	
Filament Current range: from	3700.0412	3720.790926	3724.940871	mAmps
Beam intensity range: from	0.1895594	0.22586632	0.433027864	Volts 142Nd.16O
Temperature range: from	1494.16361	1538.611315	1555.189255	° C

Final Ratio Data:

Interference Values

Ce140-O16/Nd144-O16	NO Ce	Ce interference is NOT corrected in this sheet
Pr141-O16/Nd144-O16	1.27E-02	
Sm152-O16/Nd144-O16	1.61E-02	(Measured-Includes Nd150-O18)
Sm154-O16/Nd144-O16	1.18E-02	
Sm152-O16/Nd144-O16	*0.013874*	*(Oxygen isotope interference subtracted)*

for Ratios: Non-interference subtracted grand mean ratios (input RAW values w/o normalization)

	158/160	159/160	161/160	162/160	164/160	166/160
Ratios	1.14E+00	5.14E-01	0.348	7.22E-01	2.51E-01	1.09E+00
%StdErr	2.91E-03	1.91E-03	0	2.71E-14	1.11E-02	4.67E-03

for %StdErr: input %StdErr from online normalized values, or from offline PrSm correction sheet

for comparison only	**142/144**	**143/144**	**145/144**	**146/144**	**148/144**	**150/144**
DePaolo 88, p.14, ln. B':	1.141854	na	0.348416	0.721882	0.241572	na

FINAL Interference subtracted grand mean ratios: **146/144 set to 0.7219**

	142/144	**143/144**	**145/144**	**146/144**	**148/144**	**150/144**	**150t/144s**
Ratios	1.143693	0.516031	0.347452	0.721900	0.241693	0.236471	1.164457
2 S.E.	0.000067	0.000020	0.000000	0.000000	0.000054	0.000022	0.000109

Epsilon143= 66.19 **using (143/144)chur= 0.512638**
± 0.38 **(Hamilton et al. 1983)**

linked from Sm sheet

[Sm147]=	1.764138	nm/g	**[Nd144]=**	**1.48764**	nm/g
±	0.000192		**±**	**0.00014**	
[Sm]=	1.768738	ppm	**[Nd]=**	**0.90221**	ppm
±	0.000193		**±**	**0.00008**	
TOT ng Sm=	25.6643823		**TOT ng Nd=**	**13.0911162**	

Sm147/Nd144= 1.185867
± 0.000170

Sample: B13c-1_gt_Nd
Date: 8/17/2014
Approx Nd load (ng):
Position #: 7

Rspike Values Nd {SmNd 1.0 A spike, 6-12-08 calib}

142/144	143/144	145/144	146/144	148/144	150/144	[Nd150]
0.830433	0.494001	0.436936	0.885201	0.740574	198.371260	0.049114
						nm/g

Wt Sample (g)= 0.0158 g
Wt Spike (g)= 0.04884 g

Mass Spectrometer Information:

Number of cycles measured: 118
Number of cycles used: 100
Amplifier rotation: yes

	start	average (from sheet)	ending	
Filament Current range: from	3800.01526	3800.01526	3800.015259	mAmps
Beam intensity range: from	0.22466431	0.25530785	0.065498168	Volts 142Nd.16O
Temperature range: from	1522.8083	1565.39756	1602.515263	° C

Final Ratio Data:

Interference Values

Ce140-O16/Nd144-O16	NO Ce	Ce interference is NOT corrected in this sheet
Pr141-O16/Nd144-O16	4.04E-02	
Sm152-O16/Nd144-O16	8.74E-03	(Measured-Includes Nd150-O18)
Sm154-O16/Nd144-O16	5.70E-03	
Sm152-O16/Nd144-O16	*0.006655*	*(Oxygen isotope interference subtracted)*

for Ratios: Non-interference subtracted grand mean ratios (input RAW values w/o normalization)

	158/160	159/160	161/160	162/160	164/160	166/160
Ratios	1.14E+00	5.11E-01	0.348	7.24E-01	2.48E-01	1.02E+00
%StdErr	8.09E-03	3.37E-03	0	2.81E-14	2.06E-02	9.39E-03

for %StdErr: input %StdErr from online normalized values, or from offline PrSm correction sheet

for comparison only	**142/144**	**143/144**	**145/144**	**146/144**	**148/144**	**150/144**
DePaolo 88, p.14, ln. B':	1.141854	na	0.348416	0.721882	0.241572	na

FINAL Interference subtracted grand mean ratios: **146/144 set to 0.7219**

	142/144	**143/144**	**145/144**	**146/144**	**148/144**	**150/144**	**150t/144s**
Ratios	1.145484	0.512558	0.346940	0.721900	0.241614	0.236471	1.272973
2 S.E.	0.000185	0.000035	0.000000	0.000000	0.000099	0.000044	0.000239

Epsilon143= -1.56 using (143/144)chur= 0.512638
± 0.67 (Hamilton et al. 1983)
2sigma ppm 67.3161159

linked from Sm sheet

[Sm147]= 0.518132 nm/g **[Nd144]=** **0.19326** nm/g
± 0.000040 **±** **0.00004**
[Sm]= 0.519483 ppm **[Nd]=** **0.11721** ppm
± 0.000040 **±** **0.00002**
TOT ng Sm= 8.20783621 **TOT ng Nd=** **1.851873836**

Sm147/Nd144= **2.681014**
± **0.000545**

Sample:	14_08_17_pos03_B13c-1_al1_Nd
Date:	8/17/2014
Position #:	3
Approx Nd load (ng):	

Rspike Values Nd {SmNd 0.15 A spike, 6-12-08 calib}

142/144	143/144	145/144	146/144	148/144	150/144	[Nd150]
0.830433	0.494001	0.436936	0.885201	0.740574	198.371260	0.125778
						nm/g

Wt Sample (g)=	0.00244	g
Wt Spike (g)=	0.25195	g

Mass Spectrometer Information:

Number of cycles measured:	1040			
Number of cycles used:	800			
Amplifier rotation:	yes			
	start	average (from sheet)	ending	
Filament Current range: from	3499.96796	3656.01007	3830.045014	mAmps
Beam intensity range: from	0.30971276	0.53334111	0.72759109	volts 142Nd.16O
Temperature range: from	1479.21856	1506.76313	1536.507937	°C

Final Ratio Data:

Interference Values

Ce140-O16/Nd144-O16	NO Ce	Ce interference is NOT corrected in this sheet
Pr141-O16/Nd144-O16	6.11E-01	
Sm152-O16/Nd144-O16	1.11E-03	(Measured-Includes Nd150-O18)
Sm154-O16/Nd144-O16	4.85E-05	
Sm152-O16/Nd144-O16	*0.000040*	*(Oxygen isotope interference subtracted)*

for Ratios: Non-interference subtracted grand mean ratios (input RAW values w/o normalization)

	158/160	159/160	161/160	162/160	164/160	166/160
Ratios	1.14E+00	5.12E-01	0.348	7.22E-01	2.43E-01	5.22E-01
%StdErr	9.46E-04	8.04E-04	0	2.99E-14	1.38E-03	1.69E-03

for %StdErr: input %StdErr from online normalized values, or from offline PrSm correction sheet

for comparison only	142/144	143/144	145/144	146/144	148/144	150/144
DePaolo 88, p.14:	1.141854	na	0.348416	0.721882	0.241572	na

FINAL Interference subtracted grand mean ratios: 146/144 set to 0.7219

	142/144	143/144	145/144	146/144	148/144	150/144	150t/144s
Ratios	1.142056	0.511975	0.347389	0.721900	0.241597	0.236471	3.477933
2 S.E.	0.000022	0.000008	0.000000	0.000000	0.000007	0.000008	0.000118

Epsilon143= -12.93 using (143/144)chur= 0.512638
± 0.16 (Hamilton et al. 1983)

2 sigma ppm 16.0819448

linked from Sm sheet

[Sm147]=	5.334732	nm/g	[Nd144]=	45.17006	nm/g
±	0.000203		±	0.00153	
[Sm]=	5.348641	ppm	[Nd]=	27.39450	ppm
±	0.000203		±	0.00093	
TOT ng Sm=	13.0506845		TOT ng Nd=	66.84257546	
		Sm147/Nd144=	0.118103	Tot pg Nd=	**66842.57546**
		±	0.000006	pg Nd/mL	27394498.14

Sample:	B13c-1b al1		
Date:	11/23/2014	Position #:	10
Approx Nd load (ng):	-		

Rspike Values Nd {SmNd 0.15 A spike, 6-12-08 calib}

142/144	143/144	145/144	146/144	148/144	150/144	[Nd150]
0.830433	0.494001	0.436936	0.885201	0.740574	198.371260	0.125778
						nm/g

Wt Sample (g)=	0.0021524	g
Wt Spike (g)=	0.3091	g

Mass Spectrometer Information:

Number of cycles measured:	800			
Number of cycles used:	600			
Amplifier rotation:	yes			
	start	average (from sheet)	ending	
Filament Current range: from	0.48601184	3829.773078	3874.964523	mAmps
Beam intensity range: from	3800.01526	0.65722095	0.517793514	volts 142Nd.16O
Temperature range: from	1528.62027	1554.693162	1589.230769	° C

Final Ratio Data:

Interference Values

Ce140-O16/Nd144-O16	NO Ce	Ce interference is NOT corrected in this sheet
Pr141-O16/Nd144-O16	2.60E-01	
Sm152-O16/Nd144-O16	2.21E-03	(Measured-Includes Nd150-O18)
Sm154-O16/Nd144-O16	7.42E-04	
Sm152-O16/Nd144-O16	*0.000913*	*(Oxygen isotope interference subtracted)*

for Ratios: Non-interference subtracted grand mean ratios (input RAW values w/o normalization)

	158/160	159/160	161/160	162/160	164/160	166/160
Ratios	1.14E+00	5.11E-01	0.348	7.23E-01	2.44E-01	6.34E-01
%StdErr	1.10E-03	8.37E-04	0	4.79E-14	1.39E-03	1.61E-03

for %StdErr: input %StdErr from online normalized values, or from offline PrSm correction sheet

for comparison only	142/144	143/144	145/144	146/144	148/144	150/144
DePaolo 88, p.14:	1.141854	na	0.348416	0.721882	0.241572	na

FINAL Interference subtracted grand mean ratios: 146/144 set to 0.7219

	142/144	143/144	145/144	146/144	148/144	150/144	150t/144s
Ratios	1.142084	0.511959	0.347207	0.721900	0.241593	0.236471	2.506552
2 S.E.	0.000025	0.000009	0.000000	0.000000	0.000007	0.000008	0.000080

Epsilon143= -13.25 using (143/144)chur= 0.512638

± 0.17 (Hamilton et al. 1983)

linked from Sm sheet

[Sm147]=	5.327924	nm/g	[Nd144]=	45.27495	nm/g
±	0.001613		±	0.00145	
[Sm]=	5.341816	ppm	[Nd]=	27.45811	ppm
±	0.001618		±	0.00088	
TOT ng Sm=	11.4977144		TOT ng Nd=	59.10077984	
		Sm147/Nd144=	0.117679	Tot pg Nd=	**59100.77984**
		±	0.000036	pg Nd/mL	27458109.44

Sample:	B13c-1b gt powder al1		
Date:	11/23/2014	Position #:	12
Approx Nd load (ng):	-		

Rspike Values Nd {SmNd 0.15 A spike, 6-12-08 calib}

142/144	143/144	145/144	146/144	148/144	150/144	[Nd150]
0.830433	0.494001	0.436936	0.885201	0.740574	198.371260	0.125778
						nm/g

Wt Sample (g)=	0.0101223	g
Wt Spike (g)=	0.51207	g

Mass Spectrometer Information:

Number of cycles measured:	720			
Number of cycles used:	720			
Amplifier rotation:	yes			
	start	average (from sheet)	ending	
Filament Current range: from	3599.94202	3716.588672	3749.965667	mAmps
Beam intensity range: from	0.25976943	0.76837139	0.755429733	volts 142Nd.16O
Temperature range: from	1466.34921	1514.569495	1543.150183	°C

Final Ratio Data:

Interference Values

Ce140-O16/Nd144-O16	NO Ce	Ce interference is NOT corrected in this sheet
Pr141-O16/Nd144-O16	5.34E-01	
Sm152-O16/Nd144-O16	2.12E-03	(Measured-Includes Nd150-O18)
Sm154-O16/Nd144-O16	5.51E-04	
Sm152-O16/Nd144-O16	*0.000672*	*(Oxygen isotope interference subtracted)*

for Ratios: Non-interference subtracted grand mean ratios (input RAW values w/o normalization)

	158/160	159/160	161/160	162/160	164/160	166/160
Ratios	1.14E+00	5.12E-01	0.348	7.22E-01	2.44E-01	7.09E-01
%StdErr	1.50E-03	7.42E-04	0	5.79E-14	1.27E-03	1.47E-03

for %StdErr: input %StdErr from online normalized values, or from offline PrSm correction sheet

for comparison only	142/144	143/144	145/144	146/144	148/144	150/144
DePaolo 88, p.14:	1.141854	na	0.348416	0.721882	0.241572	na

FINAL Interference subtracted grand mean ratios: 146/144 set to 0.7219

	142/144	143/144	145/144	146/144	148/144	150/144	150t/144s
Ratios	1.142234	0.511994	0.347279	0.721900	0.241598	0.236471	2.101829
2 S.E.	0.000034	0.000008	0.000000	0.000000	0.000006	0.000007	0.000062

Epsilon143= -12.56 using (143/144)chur= 0.512638
± 0.15 (Hamilton et al. 1983)

linked from Sm sheet

[Sm147]=	2.281007	nm/g	[Nd144]=	13.37373	nm/g
±	0.000114		±	0.00039	
[Sm]=	2.286955	ppm	[Nd]=	8.11083	ppm
±	0.000114		±	0.00024	
TOT ng Sm=	23.1492431		TOT ng Nd=	82.10022205	
		Sm147/Nd144=	0.170559	Tot pg Nd=	**82100.22205**
		±	0.000010	pg Nd/mL	8110826.793

Sample:	**B13c-2 gt powder al1**		
Date:	11/23/2014	Position #:	13
Approx Nd load (ng):			

Rspike Values Nd {SmNd 0.15 A spike, 6-12-08 calib}

142/144	143/144	145/144	146/144	148/144	150/144	[Nd150]
0.830433	0.494001	0.436936	0.885201	0.740574	198.371260	0.125778
						nm/g

Wt Sample (g)=	0.007622	g
Wt Spike (g)=	0.40805	g

Mass Spectrometer Information:

Number of cycles measured:	640			
Number of cycles used:	640			
Amplifier rotation:	yes			
	start	average (from sheet)	ending	
Filament Current range: from	3700.0412	3918.294761	4149.98703	mAmps
Beam intensity range: from	0.44447845	0.78628792	0.897498543	volts 142Nd.16O
Temperature range: from	1471.74603	1529.044490	1611.648352	°C

Final Ratio Data:

Interference Values

Ce140-O16/Nd144-O16	NO Ce	Ce interference is NOT corrected in this sheet
Pr141-O16/Nd144-O16	1.93E-01	
Sm152-O16/Nd144-O16	1.96E-03	(Measured-Includes Nd150-O18)
Sm154-O16/Nd144-O16	3.81E-04	
Sm152-O16/Nd144-O16	*0.000463*	*(Oxygen isotope interference subtracted)*

for Ratios: Non-interference subtracted grand mean ratios (input RAW values w/o normalization)

	158/160	159/160	161/160	162/160	164/160	166/160
Ratios	1.14E+00	5.11E-01	0.348	7.24E-01	2.45E-01	7.30E-01
%StdErr	1.34E-03	7.50E-04	0	5.66E-14	1.76E-03	1.47E-03

for %StdErr: input %StdErr from online normalized values, or from offline PrSm correction sheet

for comparison only	142/144	143/144	145/144	146/144	148/144	150/144
DePaolo 88, p.14:	1.141854	na	0.348416	0.721882	0.241572	na

FINAL Interference subtracted grand mean ratios: 146/144 set to 0.7219

	142/144	143/144	145/144	146/144	148/144	150/144	150t/144s
Ratios	1.142168	0.511990	0.346819	0.721900	0.241579	0.236471	2.033853
2 S.E.	0.000031	0.000008	0.000000	0.000000	0.000008	0.000007	0.000060

Epsilon143= -12.63 using (143/144)chur= 0.512638
± 0.15 (Hamilton et al. 1983)

linked from Sm sheet

[Sm147]=	2.252661	nm/g	[Nd144]=	13.69521	nm/g
±	0.000140		±	0.00040	
[Sm]=	2.258534	ppm	[Nd]=	8.30580	ppm
±	0.000140		±	0.00024	
TOT ng Sm=	17.2145478		TOT ng Nd=	63.3068136	
		Sm147/Nd144=	0.164485	Tot pg Nd=	**63306.8136**
		±	0.000011	pg Nd/mL	8305800.787

Sample: _25_pos03_B3b-1_gt2
Date: 3/25/2015
Approx Nd load (ng): -
Position #: 3

Rspike Values Nd {SmNd 1.0 A spike, 6-12-08 calib}

142/144	143/144	145/144	146/144	148/144	150/144	[Nd150]
0.830433	0.494001	0.436936	0.885201	0.740574	198.371260	0.049114
						nm/g

Wt Sample (g)= 0.0331 g
Wt Spike (g)= 0.40948 g

Mass Spectrometer Information:

Number of cycles measured: 560
Number of cycles used: 560
Amplifier rotation: yes

	start	average (from sheet)	ending	
Filament Current range: from		3647.513929		mAmps
Beam intensity range: from		0.53735637		Volts 142Nd.16O
Temperature range: from		1511.622493		° C

Final Ratio Data:

Interference Values

Ce140-O16/Nd144-O16	NO Ce	Ce interference is NOT corrected in this sheet
Pr141-O16/Nd144-O16	8.38E-03	
Sm152-O16/Nd144-O16	1.23E-03	(Measured-Includes Nd150-O18)
Sm154-O16/Nd144-O16	4.72E-04	
Sm152-O16/Nd144-O16	*0.000559*	*(Oxygen isotope interference subtracted)*

for Ratios: Non-interference subtracted grand mean ratios (input RAW values w/o normalization)

	158/160	159/160	161/160	162/160	164/160	166/160
Ratios	1.14E+00	5.11E-01	0.348	7.22E-01	2.43E-01	3.29E-01
%StdErr	1.11E-03	9.80E-04	0	4.75E-14	1.56E-03	1.98E-03

for %StdErr: input %StdErr from online normalized values, or from offline PrSm correction sheet

for comparison only	**142/144**	**143/144**	**145/144**	**146/144**	**148/144**	**150/144**
DePaolo 88, p.14, ln. B':	1.141854	na	0.348416	0.721882	0.241572	na

FINAL Interference subtracted grand mean ratios: **146/144 set to 0.7219**

	142/144	**143/144**	**145/144**	**146/144**	**148/144**	**150/144**	**150t/144s**
Ratios	1.141868	0.511969	0.347385	0.721900	0.241596	0.236471	10.814704
2 S.E.	0.000025	0.000010	0.000000	0.000000	0.000008	0.000009	0.000428

Epsilon143= **-13.05** **using (143/144)chur=** **0.512638**
± **0.20** **(Hamilton et al. 1983)**

linked from Sm sheet

[Sm147]= 0.828521 nm/g **[Nd144]=** **6.57088** nm/g
± 0.000054 **±** **0.00026**
[Sm]= 0.830681 ppm **[Nd]=** **3.98507** ppm
± 0.000054 **±** **0.00016**
TOT ng Sm= 27.495555 **TOT ng Nd=** **131.9058302**

Sm147/Nd144= **0.126090**
± **0.000010**

Sample: 18_Pos08_B3b-1_gt3_Nd
Date: 4/18/2015 Position #: 8
Approx Nd load (ng): -

Rspike Values Nd {SmNd 1.0 A spike, 6-12-08 calib}

142/144	143/144	145/144	146/144	148/144	150/144	[Nd150]
0.830433	0.494001	0.436936	0.885201	0.740574	198.371260	0.049114 nm/g

Wt Sample (g)= 0.002 g
Wt Spike (g)= 0.01402 g

Mass Spectrometer Information:

Number of cycles measured:
Number of cycles used:
Amplifier rotation: yes

	start	average (from sheet)	ending	
Filament Current range: from		3627.308194		mAmps
Beam intensity range: from		0.13597389		Volts 142Nd.16O
Temperature range: from		1554.174756		° C

Final Ratio Data:

Interference Values

Ce140-O16/Nd144-O16	NO Ce	Ce interference is NOT corrected in this sheet
Pr141-O16/Nd144-O16	1.31E-01	
Sm152-O16/Nd144-O16	6.45E-03	(Measured-Includes Nd150-O18)
Sm154-O16/Nd144-O16	3.65E-03	
Sm152-O16/Nd144-O16	*0.004153*	*(Oxygen isotope interference subtracted)*

for Ratios: Non-interference subtracted grand mean ratios (input RAW values w/o normalization)

	158/160	159/160	161/160	162/160	164/160	166/160
Ratios	1.14E+00	5.11E-01	0.348	7.24E-01	2.47E-01	1.13E+00
%StdErr	3.27E-02	4.93E-03	0	2.80E-14	1.67E-02	1.02E-02

for %StdErr: input %StdErr from online normalized values, or from offline PrSm correction sheet

for comparison only	**142/144**	**143/144**	**145/144**	**146/144**	**148/144**	**150/144**
DePaolo 88, p.14, ln. B':	1.141854	na	0.348416	0.721882	0.241572	na

FINAL Interference subtracted grand mean ratios: 146/144 set to 0.7219

	142/144	**143/144**	**145/144**	**146/144**	**148/144**	**150/144**	**150t/144s**
Ratios	1.147923	0.512011	0.346912	0.721900	0.241657	0.236471	1.121656
2 S.E.	0.000751	0.000050	0.000000	0.000000	0.000081	0.000048	0.000229

Epsilon143= -12.23 using (143/144)chur= 0.512638
± 0.99 (Hamilton et al. 1983)

linked from Sm sheet

[Sm147]= 0.084792 nm/g **[Nd144]=** **0.38617** nm/g
± 0.000661 **±** **0.00008**
[Sm]= 0.085013 ppm **[Nd]=** **0.23420** ppm
± 0.000662 **±** **0.00005**
TOT ng Sm= 0.17002624 **TOT ng Nd=** **0.468407885**

Sm147/Nd144= **0.219570**
± **0.001712**

Sample:	B3b-1 gt5
Date:	4/18/2015
Approx Nd load (ng):	-

Position #: 6

Rspike Values Nd {SmNd 1.0 A spike, 6-12-08 calib}

142/144	143/144	145/144	146/144	148/144	150/144	[Nd150]
0.830433	0.494001	0.436936	0.885201	0.740574	198.371260	0.049114 nm/g

Wt Sample (g)=	0.005	g
Wt Spike (g)=	0.03474	g

Mass Spectrometer Information:

Number of cycles measured:	220			
Number of cycles used:	220			
Amplifier rotation:	yes			
	start	average (from sheet)	ending	
Filament Current range: from	3749.96567	3751.098039	3790.005341	mAmps
Beam intensity range: from	0.07494868	0.13961758	0.065464028	Volts 142Nd.16O
Temperature range: from	1499.1453	1532.432012	1570.964591	° C

Final Ratio Data:

Interference Values

Ce140-O16/Nd144-O16	NO Ce	Ce interference is NOT corrected in this sheet
Pr141-O16/Nd144-O16	4.43E-02	
Sm152-O16/Nd144-O16	2.98E-03	(Measured-Includes Nd150-O18)
Sm154-O16/Nd144-O16	1.31E-03	
Sm152-O16/Nd144-O16	*0.001531*	*(Oxygen isotope interference subtracted)*

for Ratios: Non-interference subtracted grand mean ratios (input RAW values w/o normalization)

	158/160	159/160	161/160	162/160	164/160	166/160
Ratios	1.14E+00	5.11E-01	0.348	7.24E-01	2.45E-01	7.07E-01
%StdErr	1.01E-02	3.96E-03	0	1.77E-14	8.29E-03	7.67E-03

for %StdErr: input %StdErr from online normalized values, or from offline PrSm correction sheet

for comparison only	**142/144**	**143/144**	**145/144**	**146/144**	**148/144**	**150/144**
DePaolo 88, p.14, ln. B':	1.141854	na	0.348416	0.721882	0.241572	na

FINAL Interference subtracted grand mean ratios: **146/144 set to 0.7219**

	142/144	**143/144**	**145/144**	**146/144**	**148/144**	**150/144**	**150t/144s**
Ratios	1.143839	0.512001	0.346968	0.721900	0.241617	0.236471	2.130364
2 S.E.	0.000232	0.000041	0.000000	0.000000	0.000040	0.000036	0.000327

Epsilon143= -12.43 using (143/144)chur= 0.512638
± 0.79 (Hamilton et al. 1983)

linked from Sm sheet

[Sm147]=	0.130632	nm/g	**[Nd144]=**	**0.72697**	nm/g
±	0.000132		**±**	**0.00011**	
[Sm]=	0.130973	ppm	**[Nd]=**	**0.44089**	ppm
±	0.000132		**±**	**0.00007**	
TOT ng Sm=	0.65486543		**TOT ng Nd=**	**2.204450201**	
	Sm147/Nd144=	**0.179694**			
	±	**0.000184**			

Sample:	15_03_09_pos02_B3b-1_al1_NdO
Date:	3/9/2015
Position #:	2
Approx Nd load (ng):	-

Rspike Values Nd {SmNd 0.15 A spike, 6-12-08 calib}

142/144	143/144	145/144	146/144	148/144	150/144	[Nd150]
0.830433	0.494001	0.436936	0.885201	0.740574	198.371260	0.125778
						nm/g

Wt Sample (g)=	0.001807	g
Wt Spike (g)=	0.41075	g

Mass Spectrometer Information:

Number of cycles measured:	560			
Number of cycles used:	560			
Amplifier rotation:	yes			
	start	average (from sheet)	ending	
Filament Current range: from	3700.0412	3712.854342	3759.975586	mAmps
Beam intensity range: from	0.40791169	0.85604987	0.669370353	volts 142Nd.16O
Temperature range: from	1467.59463	1512.886447	1575.531136	° C

Final Ratio Data:

Interference Values

Ce140-O16/Nd144-O16	NO Ce	Ce interference is NOT corrected in this sheet
Pr141-O16/Nd144-O16	5.50E-03	
Sm152-O16/Nd144-O16	2.27E-03	(Measured-Includes Nd150-O18)
Sm154-O16/Nd144-O16	5.93E-04	
Sm152-O16/Nd144-O16	*0.000727*	*(Oxygen isotope interference subtracted)*

for Ratios: Non-interference subtracted grand mean ratios (input RAW values w/o normalization)

	158/160	159/160	161/160	162/160	164/160	166/160
Ratios	1.14E+00	5.11E-01	0.348	7.23E-01	2.44E-01	7.53E-01
%StdErr	8.09E-04	6.89E-04	0	4.75E-14	1.15E-03	1.40E-03

for %StdErr: input %StdErr from online normalized values, or from offline PrSm correction sheet

for comparison only	142/144	143/144	145/144	146/144	148/144	150/144
DePaolo 88, p.14:	1.141854	na	0.348416	0.721882	0.241572	na

FINAL Interference subtracted grand mean ratios: 146/144 set to 0.7219

	142/144	143/144	145/144	146/144	148/144	150/144	150t/144s
Ratios	1.141870	0.511966	0.347175	0.721900	0.241590	0.236471	1.926473
2 S.E.	0.000018	0.000007	0.000000	0.000000	0.000006	0.000007	0.000054

Epsilon143= -13.12 ± 0.14 using (143/144)chur= 0.512638 (Hamilton et al. 1983)

linked from Sm sheet

[Sm147]=	6.627360	nm/g	[Nd144]=	55.07915	nm/g
±	0.000368		±	0.00155	
[Sm]=	6.644640	ppm	[Nd]=	33.40411	ppm
±	0.000368		±	0.00094	
TOT ng Sm=	12.0068652		TOT ng Nd=	60.36122262	
Sm147/Nd144=	0.120324		Tot pg Nd=	**60361.22262**	
±	0.000007		pg Nd/mL	33404107.71	

Sample:	15_03_25_pos02_B3b-1b_wr_al1_Nd
Date:	3/25/2015
Position #:	2
Approx Nd load (ng):	-

Rspike Values Nd {SmNd 0.15 A spike, 6-12-08 calib}

142/144	143/144	145/144	146/144	148/144	150/144	[Nd150]
0.830433	0.494001	0.436936	0.885201	0.740574	198.371260	0.125778
						nm/g

Wt Sample (g)=	0.00132801	g
Wt Spike (g)=	0.35538	g

Mass Spectrometer Information:

Number of cycles measured:	520			
Number of cycles used:	440			
Amplifier rotation:	yes			
	start	average (from sheet)	ending	
Filament Current range: from	3898.73808	3910.037059	3970.058747	mAmps
Beam intensity range: from	0.50035384	0.88813993	0.74037399	volts 142Nd.16O
Temperature range: from	1455.55556	1507.307526		°C

Final Ratio Data:

Interference Values

Ce140-O16/Nd144-O16	NO Ce	Ce interference is NOT corrected in this sheet
Pr141-O16/Nd144-O16	1.70E-02	
Sm152-O16/Nd144-O16	1.91E-03	(Measured-Includes Nd150-O18)
Sm154-O16/Nd144-O16	1.58E-04	
Sm152-O16/Nd144-O16	*0.000211*	*(Oxygen isotope interference subtracted)*

for Ratios: Non-interference subtracted grand mean ratios (input RAW values w/o normalization)

	158/160	159/160	161/160	162/160	164/160	166/160
Ratios	1.14E+00	5.11E-01	0.348	7.23E-01	2.44E-01	8.31E-01
%StdErr	9.27E-04	8.06E-04	0	1.62E-14	1.29E-03	1.56E-03

for %StdErr: input %StdErr from online normalized values, or from offline PrSm correction sheet

for comparison only	142/144	143/144	145/144	146/144	148/144	150/144
DePaolo 88, p.14:	1.141854	na	0.348416	0.721882	0.241572	na

FINAL Interference subtracted grand mean ratios: 146/144 set to 0.7219

	142/144	143/144	145/144	146/144	148/144	150/144	150t/144s
Ratios	1.141854	0.511960	0.347206	0.721900	0.241593	0.236471	1.669127
2 S.E.	0.000021	0.000008	0.000000	0.000000	0.000006	0.000007	0.000052

Epsilon143= -13.23 using (143/144)chur= 0.512638
± 0.16 (Hamilton et al. 1983)

linked from Sm sheet

[Sm147]=	6.751941	nm/g		[Nd144]=	56.18052	nm/g
±	0.003343			±	0.00175	
[Sm]=	6.769546	ppm		[Nd]=	34.07206	ppm
±	0.003352			±	0.00106	
TOT ng Sm=	8.99002467			TOT ng Nd=	45.24804278	
		Sm147/Nd144=	0.120183	Tot pg Nd=	**45248.04278**	
		±	0.000060	pg Nd/mL	34072064.8	

Sample:	**B3b-1 gt powder**
Date:	Position #:
Approx Nd load (ng):	

Rspike Values Nd {SmNd 0.15 A spike, 6-12-08 calib}

142/144	143/144	145/144	146/144	148/144	150/144	[Nd150]
0.830433	0.494001	0.436936	0.885201	0.740574	198.371260	0.125778

nm/g

Wt Sample (g)=	0.004882	g
Wt Spike (g)=	0.51441	g

Mass Spectrometer Information:

Number of cycles measured:	480			
Number of cycles used:	400			
Amplifier rotation:	yes			
	start	average (from sheet)	ending	
Filament Current range: from	3649.99161	3649.991608	3649.991608	mAmps
Beam intensity range: from	1.01942684	2.24060295	1.964576759	volts 142Nd.16O
Temperature range: from	1509.52381	1542.472466	1590.891331	°C

Final Ratio Data:

Interference Values

Ce140-O16/Nd144-O16	NO Ce	Ce interference is NOT corrected in this sheet
Pr141-O16/Nd144-O16	6.49E-03	
Sm152-O16/Nd144-O16	1.36E-03	(Measured-Includes Nd150-O18)
Sm154-O16/Nd144-O16	2.18E-04	
Sm152-O16/Nd144-O16	*0.000280*	*(Oxygen isotope interference subtracted)*

for Ratios: Non-interference subtracted grand mean ratios (input RAW values w/o normalization)

	158/160	159/160	161/160	162/160	164/160	166/160
Ratios	1.14E+00	5.11E-01	0.348	7.22E-01	2.43E-01	5.26E-01
%StdErr	5.74E-04	4.94E-04	0	3.16E-15	8.06E-04	9.96E-04

for %StdErr: input %StdErr from online normalized values, or from offline PrSm correction sheet

for comparison only	142/144	143/144	145/144	146/144	148/144	150/144
DePaolo 88, p.14:	1.141854	na	0.348416	0.721882	0.241572	na

FINAL Interference subtracted grand mean ratios: 146/144 set to 0.7219

	142/144	143/144	145/144	146/144	148/144	150/144	150t/144s
Ratios	1.141910	0.511958	0.347435	0.721900	0.241594	0.236471	3.418319
2 S.E.	0.000013	0.000005	0.000000	0.000000	0.000004	0.000005	0.000068

Epsilon143= -13.27 using (143/144)chur= 0.512638

± 0.10 (Hamilton et al. 1983)

linked from Sm sheet

[Sm147]=	5.386097	nm/g	[Nd144]=	45.30323	nm/g
±	0.000426		±	0.00090	
[Sm]=	5.400140	ppm	[Nd]=	27.47526	ppm
±	0.000427		±	0.00055	
TOT ng Sm=	26.3634848		TOT ng Nd=	134.1342157	
	Sm147/Nd144=	0.118890	Tot pg Nd=	**134134.2157**	
	±	0.000010	pg Nd/mL	27475259.25	

Sample:	15_01_26_pos02_B17a-1_al1		
Date:	1/26/2015	Position #:	2
Approx Nd load (ng):	-		

Rspike Values Nd {SmNd 0.15 A spike, 6-12-08 calib}

142/144	143/144	145/144	146/144	148/144	150/144	[Nd150]
0.830433	0.494001	0.436936	0.885201	0.740574	198.371260	0.125778
						nm/g

Wt Sample (g)=	0.0014007	g
Wt Spike (g)=	0.2885	g

Mass Spectrometer Information:

Number of cycles measured:	800			
Number of cycles used:	800			
Amplifier rotation:	yes			
	start	average (from sheet)	ending	
Filament Current range: from	3700.0412	3805.483177	3849.939727	mAmps
Beam intensity range: from	0.46414382	0.48796406	0.450015932	volts 142Nd.16O
Temperature range: from	1505.37241	1543.965415	1559.7558	°C

Final Ratio Data:

Interference Values

Ce140-O16/Nd144-O16	NO Ce	Ce interference is NOT corrected in this sheet
Pr141-O16/Nd144-O16	6.68E-02	
Sm152-O16/Nd144-O16	2.43E-03	(Measured-Includes Nd150-O18)
Sm154-O16/Nd144-O16	2.02E-04	
Sm152-O16/Nd144-O16	*0.000239*	*(Oxygen isotope interference subtracted)*

for Ratios: Non-interference subtracted grand mean ratios (input RAW values w/o normalization)

	158/160	159/160	161/160	162/160	164/160	166/160
Ratios	1.14E+00	5.11E-01	0.348	7.23E-01	2.45E-01	1.07E+00
%StdErr	9.69E-04	8.37E-04	0	3.43E-14	1.44E-03	1.61E-03

for %StdErr: input %StdErr from online normalized values, or from offline PrSm correction sheet

for comparison only	142/144	143/144	145/144	146/144	148/144	150/144
DePaolo 88, p.14:	1.141854	na	0.348416	0.721882	0.241572	na

FINAL Interference subtracted grand mean ratios: 146/144 set to 0.7219

	142/144	143/144	145/144	146/144	148/144	150/144	150t/144s
Ratios	1.142040	0.512106	0.347071	0.721900	0.241578	0.236471	1.189986
2 S.E.	0.000022	0.000009	0.000000	0.000000	0.000007	0.000008	0.000038

Epsilon143= -10.37 using (143/144)chur= 0.512638
± 0.17 (Hamilton et al. 1983)

linked from Sm sheet

[Sm147]=	3.510633	nm/g	[Nd144]=	30.82816	nm/g
±	0.000218		±	0.00099	
[Sm]=	3.519786	ppm	[Nd]=	18.69650	ppm
±	0.000219		±	0.00060	
TOT ng Sm=	4.93016467		TOT ng Nd=	26.18818069	
		Sm147/Nd144= 0.113877	Tot pg Nd=	**26188.18069**	
		± 0.000008	pg Nd/mL	18696495.1	

Sample:	B17a-1_gt1_Nd
Date:	1/31/2015
Approx Nd load (ng):	-

Position #: 6

Rspike Values Nd {SmNd 1.0 A spike, 6-12-08 calib}

142/144	143/144	145/144	146/144	148/144	150/144	[Nd150]
0.830433	0.494001	0.436936	0.885201	0.740574	198.371260	0.049114 nm/g

Wt Sample (g)=	0.0299	g
Wt Spike (g)=	0.07552	g

Mass Spectrometer Information:

Number of cycles measured:	480			
Number of cycles used:	425			
Amplifier rotation:	yes			
	start	average (from sheet)	ending	
Filament Current range: from	3649.99161	3667.070000	3701.167315	mAmps
Beam intensity range: from	0.99515073	1.66612922	1.418304962	Volts 142Nd.16O
Temperature range: from	1431.47741	1476.519658	1536.507937	° C

Final Ratio Data:

Interference Values

Ce140-O16/Nd144-O16	NO Ce	Ce interference is NOT corrected in this sheet
Pr141-O16/Nd144-O16	1.61E-01	
Sm152-O16/Nd144-O16	7.20E-04	(Measured-Includes Nd150-O18)
Sm154-O16/Nd144-O16	1.66E-04	
Sm152-O16/Nd144-O16	*0.000209*	*(Oxygen isotope interference subtracted)*

for Ratios: Non-interference subtracted grand mean ratios (input RAW values w/o normalization)

	158/160	159/160	161/160	162/160	164/160	166/160
Ratios	1.14E+00	5.11E-01	0.348	7.23E-01	2.43E-01	2.50E-01
%StdErr	7.00E-04	5.69E-04	0	1.08E-14	1.03E-03	1.20E-03

for %StdErr: input %StdErr from online normalized values, or from offline PrSm correction sheet

for comparison only	**142/144**	**143/144**	**145/144**	**146/144**	**148/144**	**150/144**
DePaolo 88, p.14, ln. B':	1.141854	na	0.348416	0.721882	0.241572	na

FINAL Interference subtracted grand mean ratios: **146/144 set to 0.7219**

	142/144	**143/144**	**145/144**	**146/144**	**148/144**	**150/144**	**150t/144s**
Ratios	1.141811	0.512081	0.347316	0.721900	0.241594	0.236471	76.995709
2 S.E.	0.000016	0.000006	0.000000	0.000000	0.000005	0.000006	0.001848

Epsilon143= -10.86 using (143/144)chur= 0.512638
± 0.11 (Hamilton et al. 1983)

linked from Sm sheet

[Sm147]=	1.016650	nm/g	**[Nd144]=**	**9.55127**	nm/g
±	0.000203		**±**	**0.00023**	
[Sm]=	1.019301	ppm	**[Nd]=**	**5.79261**	ppm
±	0.000203		**±**	**0.00014**	
TOT ng Sm=	30.4770887		**TOT ng Nd=**	**173.198907**	
	Sm147/Nd144=	**0.106441**			
	±	**0.000021**			

Sample:	B17a-1_gt2
Date:	1/31/2015
Approx Nd load (ng):	-

Position #: 7

Rspike Values Nd {SmNd 1.0 A spike, 6-12-08 calib}

142/144	143/144	145/144	146/144	148/144	150/144	[Nd150]
0.830433	0.494001	0.436936	0.885201	0.740574	198.371260	0.049114
						nm/g

Wt Sample (g)=	0.0058	g
Wt Spike (g)=	0.02534	g

Mass Spectrometer Information:

Number of cycles measured:	615			
Number of cycles used:	516			
Amplifier rotation:	yes			
	start	average (from sheet)	ending	
Filament Current range: from		3650.779937		mAmps
Beam intensity range: from		0.98615787		Volts 142Nd.16O
Temperature range: from		1500.299003		° C

Final Ratio Data:

Interference Values

Ce140-O16/Nd144-O16	NO Ce	Ce interference is NOT corrected in this sheet
Pr141-O16/Nd144-O16	4.81E-01	
Sm152-O16/Nd144-O16	6.61E-04	(Measured-Includes Nd150-O18)
Sm154-O16/Nd144-O16	1.27E-04	
Sm152-O16/Nd144-O16	*0.000159*	*(Oxygen isotope interference subtracted)*

for Ratios: Non-interference subtracted grand mean ratios (input RAW values w/o normalization)

	158/160	159/160	161/160	162/160	164/160	166/160
Ratios	1.14E+00	5.12E-01	0.348	7.22E-01	2.43E-01	2.45E-01
%StdErr	8.80E-04	6.99E-04	0	3.48E-14	1.18E-03	1.56E-03

for %StdErr: input %StdErr from online normalized values, or from offline PrSm correction sheet

for comparison only	**142/144**	**143/144**	**145/144**	**146/144**	**148/144**	**150/144**
DePaolo 88, p.14, ln. B':	1.141854	na	0.348416	0.721882	0.241572	na

FINAL Interference subtracted grand mean ratios: **146/144 set to 0.7219**

	142/144	**143/144**	**145/144**	**146/144**	**148/144**	**150/144**	**150t/144s**
Ratios	1.141833	0.512095	0.347396	0.721900	0.241605	0.236471	116.831751
2 S.E.	0.000020	0.000007	0.000000	0.000000	0.000006	0.000007	0.003654

Epsilon143= -10.59 using (143/144)chur= 0.512638
± 0.14 (Hamilton et al. 1983)

linked from Sm sheet

[Sm147]=	2.551035	nm/g	**[Nd144]=**	**25.06937**	nm/g
±	0.000605		**±**	**0.00078**	
[Sm]=	2.557687	ppm	**[Nd]=**	**15.20394**	ppm
±	0.000607		**±**	**0.00048**	
TOT ng Sm=	14.8345842		**TOT ng Nd=**	**88.18285117**	
	Sm147/Nd144=	**0.101759**			
	±	**0.000024**			

Sample: 9_pos05_B17a-1_gt3_NdO
Date: 3/9/2015
Approx Nd load (ng): -
Position #: 5

Rspike Values Nd {SmNd 1.0 A spike, 6-12-08 calib}

142/144	143/144	145/144	146/144	148/144	150/144	[Nd150]
0.830433	0.494001	0.436936	0.885201	0.740574	198.371260	0.049114 nm/g

Wt Sample (g)= 0.0286 g
Wt Spike (g)= 0.07572 g

Mass Spectrometer Information:

Number of cycles measured: 625
Number of cycles used: 560
Amplifier rotation: yes

	start	average (from sheet)	ending	
Filament Current range: from	3700.0412	3700.041199	3700.041199	mAmps
Beam intensity range: from	0.4892067	0.87165153	0.681857286	Volts 142Nd.16O
Temperature range: from	1456.80098	1507.528170	1555.604396	° C

Final Ratio Data:

Interference Values

Ce140-O16/Nd144-O16	NO Ce	Ce interference is NOT corrected in this sheet
Pr141-O16/Nd144-O16	4.53E-03	
Sm152-O16/Nd144-O16	1.06E-03	(Measured-Includes Nd150-O18)
Sm154-O16/Nd144-O16	4.36E-04	
Sm152-O16/Nd144-O16	*0.000528*	*(Oxygen isotope interference subtracted)*

for Ratios: Non-interference subtracted grand mean ratios (input RAW values w/o normalization)

	158/160	159/160	161/160	162/160	164/160	166/160
Ratios	1.14E+00	5.11E-01	0.348	7.22E-01	2.43E-01	2.60E-01
%StdErr	7.81E-04	7.15E-04	0	4.29E-14	1.10E-03	1.48E-03

for %StdErr: input %StdErr from online normalized values, or from offline PrSm correction sheet

for comparison only	**142/144**	**143/144**	**145/144**	**146/144**	**148/144**	**150/144**
DePaolo 88, p.14, ln. B':	1.141854	na	0.348416	0.721882	0.241572	na

FINAL Interference subtracted grand mean ratios: **146/144 set to 0.7219**

	142/144	**143/144**	**145/144**	**146/144**	**148/144**	**150/144**	**150t/144s**
Ratios	1.141823	0.512069	0.347454	0.721900	0.241605	0.236471	42.347413
2 S.E.	0.000018	0.000007	0.000000	0.000000	0.000005	0.000007	0.001254

Epsilon143= -11.11 using (143/144)chur= 0.512638
± 0.14 (Hamilton et al. 1983)

linked from Sm sheet

[Sm147]= 0.650664 nm/g **[Nd144]=** **5.50650** nm/g
± 0.000074 **±** **0.00016**
[Sm]= 0.652361 ppm **[Nd]=** **3.33955** ppm
± 0.000074 **±** **0.00010**
TOT ng Sm= 18.6575124 **TOT ng Nd=** **95.51116273**

Sm147/Nd144= **0.118163**
± **0.000014**

Sample:	B17a-1 gt4
Date:	3/9/2015
Approx Nd load (ng):	-

Position #: 6

Rspike Values Nd {SmNd 1.0 A spike, 6-12-08 calib}

142/144	143/144	145/144	146/144	148/144	150/144	[Nd150]
0.830433	0.494001	0.436936	0.885201	0.740574	198.371260	0.049114 nm/g

Wt Sample (g)=	0.0416	g
Wt Spike (g)=	0.15268	g

Mass Spectrometer Information:

Number of cycles measured:	960			
Number of cycles used:	800			
Amplifier rotation:	yes			
	start	average (from sheet)	ending	
Filament Current range: from	3800.01526	3800.015259	3800.015259	mAmps
Beam intensity range: from	0.81953929	2.03097299	0.891517562	Volts 142Nd.16O
Temperature range: from	1451.40415	1536.714988	1589.64591	° C

Final Ratio Data:

Interference Values

Ce140-O16/Nd144-O16	NO Ce	Ce interference is NOT corrected in this sheet
Pr141-O16/Nd144-O16	2.35E-02	
Sm152-O16/Nd144-O16	1.01E-03	(Measured-Includes Nd150-O18)
Sm154-O16/Nd144-O16	3.55E-04	
Sm152-O16/Nd144-O16	*0.000433*	*(Oxygen isotope interference subtracted)*

for Ratios: Non-interference subtracted grand mean ratios (input RAW values w/o normalization)

	158/160	159/160	161/160	162/160	164/160	166/160
Ratios	1.14E+00	5.11E-01	0.348	7.22E-01	2.42E-01	2.80E-01
%StdErr	4.57E-04	4.09E-04	0	3.02E-14	6.55E-04	8.16E-04

for %StdErr: input %StdErr from online normalized values, or from offline PrSm correction sheet

for comparison only	**142/144**	**143/144**	**145/144**	**146/144**	**148/144**	**150/144**
DePaolo 88, p.14, ln. B':	1.141854	na	0.348416	0.721882	0.241572	na

FINAL Interference subtracted grand mean ratios: **146/144 set to 0.7219**

	142/144	**143/144**	**145/144**	**146/144**	**148/144**	**150/144**	**150t/144s**
Ratios	1.141832	0.512067	0.347605	0.721900	0.241597	0.236471	22.650437
2 S.E.	0.000010	0.000004	0.000000	0.000000	0.000003	0.000004	0.000370

Epsilon143= **-11.13** **using (143/144)chur=** **0.512638**
± **0.08** **(Hamilton et al. 1983)**

linked from Sm sheet

[Sm147]=	0.503159	nm/g	**[Nd144]=**	**4.08291**	nm/g
±	0.000073		**±**	**0.00007**	
[Sm]=	0.504471	ppm	**[Nd]=**	**2.47618**	ppm
±	0.000073		**±**	**0.00004**	
TOT ng Sm=	20.9859848		**TOT ng Nd=**	**103.0090492**	

Sm147/Nd144= **0.123235**
± **0.000018**

Sample: 5_pos04_B17a-1_gt5_Nd
Date: 3/25/2015 Position #: 4
Approx Nd load (ng): -

Rspike Values Nd {SmNd 1.0 A spike, 6-12-08 calib}

142/144	143/144	145/144	146/144	148/144	150/144	[Nd150]
0.830433	0.494001	0.436936	0.885201	0.740574	198.371260	0.049114 nm/g

Wt Sample (g)= 0.0109 g
Wt Spike (g)= 0.10296 g

Mass Spectrometer Information:

Number of cycles measured: 560
Number of cycles used: 560
Amplifier rotation: yes

	start	average (from sheet)	ending	
Filament Current range: from		3731.718346		mAmps
Beam intensity range: from		1.41658838		Volts 142Nd.16O
Temperature range: from		1536.827446		° C

Final Ratio Data:

Interference Values

Ce140-O16/Nd144-O16	NO Ce	Ce interference is NOT corrected in this sheet
Pr141-O16/Nd144-O16	4.01E-03	
Sm152-O16/Nd144-O16	1.78E-03	(Measured-Includes Nd150-O18)
Sm154-O16/Nd144-O16	7.67E-04	
Sm152-O16/Nd144-O16	*0.000908*	*(Oxygen isotope interference subtracted)*

for Ratios: Non-interference subtracted grand mean ratios (input RAW values w/o normalization)

	158/160	159/160	161/160	162/160	164/160	166/160
Ratios	1.14E+00	5.11E-01	0.348	7.23E-01	2.44E-01	4.27E-01
%StdErr	6.63E-04	5.38E-04	0	4.75E-14	1.01E-03	1.08E-03

for %StdErr: input %StdErr from online normalized values, or from offline PrSm correction sheet

for comparison only	**142/144**	**143/144**	**145/144**	**146/144**	**148/144**	**150/144**
DePaolo 88, p.14, ln. B':	1.141854	na	0.348416	0.721882	0.241572	na

FINAL Interference subtracted grand mean ratios: **146/144 set to 0.7219**

	142/144	**143/144**	**145/144**	**146/144**	**148/144**	**150/144**	**150t/144s**
Ratios	1.142009	0.512078	0.347191	0.721900	0.241599	0.236471	5.259588
2 S.E.	0.000015	0.000006	0.000000	0.000000	0.000005	0.000005	0.000114

Epsilon143= -10.93 using (143/144)chur= 0.512638
± 0.11 (Hamilton et al. 1983)

linked from Sm sheet

[Sm147]= 0.321333 nm/g **[Nd144]=** **2.44004** nm/g
± 0.000115 **±** **0.00005**
[Sm]= 0.322171 ppm **[Nd]=** **1.47983** ppm
± 0.000115 **±** **0.00003**
TOT ng Sm= 3.51166742 **TOT ng Nd=** **16.13009479**
Sm147/Nd144= **0.131692**
± **0.000047**

Sample:	15_01_26_pos04_B17a-1_gt_powd_1_Nd
Date:	1/26/2015
Position #:	4
Approx Nd load (ng):	1

Rspike Values Nd {SmNd 0.15 A spike, 6-12-08 calib}

142/144	143/144	145/144	146/144	148/144	150/144	[Nd150]
0.830433	0.494001	0.436936	0.885201	0.740574	198.371260	0.125778

nm/g

Wt Sample (g)=	0.00099397	g
Wt Spike (g)=	0.20512	g

Mass Spectrometer Information:

Number of cycles measured:	272			
Number of cycles used:	272			
Amplifier rotation:	yes			
	start	average (from sheet)	ending	
Filament Current range: from	3899.98932	3899.989319	3899.989319	mAmps
Beam intensity range: from	0.72573886	2.44881193	1.458656525	volts 142Nd.16O
Temperature range: from	1447.66789	1504.004884	1613.724054	°C

Final Ratio Data:

Interference Values

Ce140-O16/Nd144-O16	NO Ce	Ce interference is NOT corrected in this sheet
Pr141-O16/Nd144-O16	5.01E-01	
Sm152-O16/Nd144-O16	1.71E-03	(Measured-Includes Nd150-O18)
Sm154-O16/Nd144-O16	1.04E-04	
Sm152-O16/Nd144-O16	*0.000147*	*(Oxygen isotope interference subtracted)*

for Ratios: Non-interference subtracted grand mean ratios (input RAW values w/o normalization)

	158/160	159/160	161/160	162/160	164/160	166/160
Ratios	1.14E+00	5.12E-01	0.348	7.22E-01	2.43E-01	7.64E-01
%StdErr	9.77E-04	6.74E-04	0	1.68E-14	1.16E-03	1.40E-03

for %StdErr: input %StdErr from online normalized values, or from offline PrSm correction sheet

for comparison only	142/144	143/144	145/144	146/144	148/144	150/144
DePaolo 88, p.14:	1.141854	na	0.348416	0.721882	0.241572	na

FINAL Interference subtracted grand mean ratios: 146/144 set to 0.7219

	142/144	143/144	145/144	146/144	148/144	150/144	150t/144s
Ratios	1.141879	0.512105	0.347394	0.721900	0.241588	0.236471	1.874160
2 S.E.	0.000022	0.000007	0.000000	0.000000	0.000006	0.000007	0.000053

Epsilon143= -10.40 using (143/144)chur= 0.512638
± 0.13 (Hamilton et al. 1983)

linked from Sm sheet

[Sm147]=	5.126227	nm/g		[Nd144]=	48.64590	nm/g
±	0.000368			±	0.00136	
[Sm]=	5.139593	ppm		[Nd]=	29.50251	ppm
±	0.000369			±	0.00083	
TOT ng Sm=	5.1086011			TOT ng Nd=	29.32460869	
		Sm147/Nd144=	0.105378	Tot pg Nd=	**29324.60869**	
		±	0.000008	pg Nd/mL	29502508.82	

Sample:	15_03_09_pos03_B17a-1_gtpowd_2_NdO
Date:	3/9/2015
Position #:	3
Approx Nd load (ng):	-

Rspike Values Nd {SmNd 0.15 A spike, 6-12-08 calib}

142/144	143/144	145/144	146/144	148/144	150/144	[Nd150]
0.830433	0.494001	0.436936	0.885201	0.740574	198.371260	0.125778
						nm/g

Wt Sample (g)=	0.00115438	g
Wt Spike (g)=	0.15207	g

Mass Spectrometer Information:

Number of cycles measured:	85			
Number of cycles used:	80			
Amplifier rotation:	yes			
	start	average (from sheet)	ending	
Filament Current range: from	4100.06256	4100.062562	4100.062562	mAmps
Beam intensity range: from	1.35567225	2.34653526	1.403143987	volts 142Nd.16O
Temperature range: from	1537.75336	1592.183455	1649.010989	°C

Final Ratio Data:

Interference Values

Ce140-O16/Nd144-O16	NO Ce	Ce interference is NOT corrected in this sheet
Pr141-O16/Nd144-O16	2.96E-02	
Sm152-O16/Nd144-O16	2.08E-03	(Measured-Includes Nd150-O18)
Sm154-O16/Nd144-O16	3.33E-04	
Sm152-O16/Nd144-O16	*0.000433*	*(Oxygen isotope interference subtracted)*

for Ratios: Non-interference subtracted grand mean ratios (input RAW values w/o normalization)

	158/160	159/160	161/160	162/160	164/160	166/160
Ratios	1.14E+00	5.11E-01	0.348	7.23E-01	2.44E-01	8.05E-01
%StdErr	1.61E-03	1.40E-03	0	2.41E-14	2.34E-03	3.51E-03

for %StdErr: input %StdErr from online normalized values, or from offline PrSm correction sheet

for comparison only	142/144	143/144	145/144	146/144	148/144	150/144
DePaolo 88, p.14:	1.141854	na	0.348416	0.721882	0.241572	na

FINAL Interference subtracted grand mean ratios: 146/144 set to 0.7219

	142/144	143/144	145/144	146/144	148/144	150/144	150t/144s
Ratios	1.141920	0.512071	0.347055	0.721900	0.241592	0.236471	1.754649
2 S.E.	0.000037	0.000014	0.000000	0.000000	0.000011	0.000017	0.000123

Epsilon143= -11.05 using (143/144)chur= 0.512638
± 0.28 (Hamilton et al. 1983)

linked from Sm sheet

[Sm147]=	3.224172	nm/g	[Nd144]=	29.07301	nm/g
±	0.002027		±	0.00204	
[Sm]=	3.232578	ppm	[Nd]=	17.63204	ppm
±	0.002032		±	0.00124	
TOT ng Sm=	3.73162378		TOT ng Nd=	20.35407953	
		Sm147/Nd144= 0.110899	Tot pg Nd=	**20354.07953**	
		± 0.000070	pg Nd/mL	17632044.5	

Sample:	14_12_04_pos14_B2b-1_al1_Nd
Date:	12/4/2014
Position #:	14
Approx Nd load (ng):	-

Rspike Values Nd {SmNd 0.15 A spike, 6-12-08 calib}

142/144	143/144	145/144	146/144	148/144	150/144	[Nd150]
0.830433	0.494001	0.436936	0.885201	0.740574	198.371260	0.125778

nm/g

Wt Sample (g)=	0.0019058	g
Wt Spike (g)=	0.41303	g

Mass Spectrometer Information:

Number of cycles measured:	880			
Number of cycles used:	700			
Amplifier rotation:	yes			
	start	average (from sheet)	ending	
Filament Current range: from	3629.97177	3716.652798	3749.965667	mAmps
Beam intensity range: from	0.22539265	0.57404547	0.627880136	volts 142Nd.16O
Temperature range: from	1460.1221	1512.477649	1551.452991	°C

Final Ratio Data:

Interference Values

Ce140-O16/Nd144-O16	NO Ce	Ce interference is NOT corrected in this sheet
Pr141-O16/Nd144-O16	1.23E-01	
Sm152-O16/Nd144-O16	3.31E-03	(Measured-Includes Nd150-O18)
Sm154-O16/Nd144-O16	1.02E-03	
Sm152-O16/Nd144-O16	*0.001247*	*(Oxygen isotope interference subtracted)*

for Ratios: Non-interference subtracted grand mean ratios (input RAW values w/o normalization)

	158/160	159/160	161/160	162/160	164/160	166/160
Ratios	1.14E+00	5.11E-01	0.348	7.23E-01	2.45E-01	1.01E+00
%StdErr	1.33E-03	8.78E-04	0	5.37E-14	1.40E-03	1.71E-03

for %StdErr: input %StdErr from online normalized values, or from offline PrSm correction sheet

for comparison only	142/144	143/144	145/144	146/144	148/144	150/144
DePaolo 88, p.14:	1.141854	na	0.348416	0.721882	0.241572	na

FINAL Interference subtracted grand mean ratios: 146/144 set to 0.7219

	142/144	143/144	145/144	146/144	148/144	150/144	150t/144s
Ratios	1.142179	0.512112	0.347171	0.721900	0.241597	0.236471	1.288469
2 S.E.	0.000030	0.000009	0.000000	0.000000	0.000007	0.000008	0.000044

Epsilon143= -10.26 using (143/144)chur= 0.512638
± 0.18 (Hamilton et al. 1983)

linked from Sm sheet

[Sm147]=	3.986349	nm/g	[Nd144]=	35.12230	nm/g
±	0.003864		±	0.00120	
[Sm]=	3.996743	ppm	[Nd]=	21.30079	ppm
±	0.003874		±	0.00073	
TOT ng Sm=	7.616992		TOT ng Nd=	40.59504179	
		Sm147/Nd144=	0.113499	Tot pg Nd=	**40595.04179**
		±	0.000110	pg Nd/mL	21300788.01

Sample:	**B2b-1b al1**		
Date:	1/26/2015	Position #:	3
Approx Nd load (ng):	-		

Rspike Values Nd {SmNd 0.15 A spike, 6-12-08 calib}

142/144	143/144	145/144	146/144	148/144	150/144	[Nd150]
0.830433	0.494001	0.436936	0.885201	0.740574	198.371260	0.125778

nm/g

Wt Sample (g)=	0.0012908	g
Wt Spike (g)=	0.26811	g

Mass Spectrometer Information:

Number of cycles measured:	1440			
Number of cycles used:	1440			
Amplifier rotation:	yes			
	start	average (from sheet)	ending	
Filament Current range: from	3499.96796	3803.805473	3930.019074	mAmps
Beam intensity range: from	0.1420496	0.11519349	0.116730803	volts 142Nd.16O
Temperature range: from	1504.95726	1570.319394	1594.212454	° C

Final Ratio Data:

Interference Values

Ce140-O16/Nd144-O16	NO Ce	Ce interference is NOT corrected in this sheet
Pr141-O16/Nd144-O16	1.96E-01	
Sm152-O16/Nd144-O16	2.51E-03	(Measured-Includes Nd150-O18)
Sm154-O16/Nd144-O16	1.60E-04	
Sm152-O16/Nd144-O16	*0.000160*	*(Oxygen isotope interference subtracted)*

for Ratios: Non-interference subtracted grand mean ratios (input RAW values w/o normalization)

	158/160	159/160	161/160	162/160	164/160	166/160
Ratios	1.14E+00	5.12E-01	0.348	7.23E-01	2.45E-01	1.15E+00
%StdErr	1.87E-03	1.78E-03	0	3.57E-14	3.13E-03	3.30E-03

for %StdErr: input %StdErr from online normalized values, or from offline PrSm correction sheet

for comparison only	142/144	143/144	145/144	146/144	148/144	150/144
DePaolo 88, p.14:	1.141854	na	0.348416	0.721882	0.241572	na

FINAL Interference subtracted grand mean ratios: 146/144 set to 0.7219

	142/144	143/144	145/144	146/144	148/144	150/144	150t/144s
Ratios	1.141961	0.512109	0.347061	0.721900	0.241623	0.236471	1.089110
2 S.E.	0.000043	0.000018	0.000000	0.000000	0.000015	0.000016	0.000072

Epsilon143= -10.32 using (143/144)chur= 0.512638
± 0.36 (Hamilton et al. 1983)

linked from Sm sheet

[Sm147]=	3.242893	nm/g		[Nd144]=	28.45317	nm/g
±	0.000249			±	0.00188	
[Sm]=	3.251348	ppm		[Nd]=	17.25613	ppm
±	0.000249			±	0.00114	
TOT ng Sm=	4.19683996			TOT ng Nd=	22.27421056	
		Sm147/Nd144=	0.113973	Tot pg Nd=	**22274.21056**	
		±	0.000012	pg Nd/mL	17256128.41	

Sample: **B2b-2 wr**
Date: Position #:
Approx Nd load (ng):

Rspike Values Nd {SmNd 0.15 A spike, 6-12-08 calib}

142/144	143/144	145/144	146/144	148/144	150/144	[Nd150]
0.830433	0.494001	0.436936	0.885201	0.740574	198.371260	0.125778

nm/g

Wt Sample (g)= 0.0027 g
Wt Spike (g)= 0.62711 g

Mass Spectrometer Information:

Number of cycles measured:
Number of cycles used:
Amplifier rotation:

	start	average (from sheet)	ending	
Filament Current range: from		3500.606570		mAmps
Beam intensity range: from		1.17944973		volts 142Nd.16O
Temperature range: from		1501.676059		°C

Final Ratio Data:

Interference Values

Ce140-O16/Nd144-O16	NO Ce	Ce interference is NOT corrected in this sheet
Pr141-O16/Nd144-O16	4.41E-03	
Sm152-O16/Nd144-O16	3.37E-03	(Measured-Includes Nd150-O18)
Sm154-O16/Nd144-O16	1.14E-03	
Sm152-O16/Nd144-O16	*0.001389*	*(Oxygen isotope interference subtracted)*

for Ratios: Non-interference subtracted grand mean ratios (input RAW values w/o normalization)

	158/160	159/160	161/160	162/160	164/160	166/160
Ratios	1.14E+00	5.11E-01	0.348	7.23E-01	2.45E-01	9.68E-01
%StdErr	1.36E-03	1.05E-03	0	2.48E-14	1.92E-03	1.85E-03

for %StdErr: input %StdErr from online normalized values, or from offline PrSm correction sheet

for comparison only	142/144	143/144	145/144	146/144	148/144	150/144
DePaolo 88, p.14:	1.141854	na	0.348416	0.721882	0.241572	na

FINAL Interference subtracted grand mean ratios: 146/144 set to 0.7219

	142/144	143/144	145/144	146/144	148/144	150/144	150t/144s
Ratios	1.141976	0.512101	0.346991	0.721900	0.241598	0.236471	1.362386
2 S.E.	0.000031	0.000011	0.000000	0.000000	0.000009	0.000009	0.000050

Epsilon143= -10.48 using (143/144)chur= 0.512638
± 0.21 (Hamilton et al. 1983)

linked from Sm sheet

[Sm147]= 4.757264 nm/g [Nd144]= 39.80019 nm/g
± 0.000825 ± 0.00147
[Sm]= 4.769668 ppm [Nd]= 24.13781 ppm
± 0.000827 ± 0.00089
TOT ng Sm= 12.8781026 TOT ng Nd= 65.17208294
Sm147/Nd144= 0.119529 Tot pg Nd= **65172.08294**
± 0.000021 pg Nd/mL 24137808.5

Sample:	B2b-1 gt2
Date:	12/20/2014
Approx Nd load (ng):	-

Position #: 5

Rspike Values Nd {SmNd 1.0 A spike, 6-12-08 calib}

142/144	143/144	145/144	146/144	148/144	150/144	[Nd150]
0.830433	0.494001	0.436936	0.885201	0.740574	198.371260	0.049114 nm/g

Wt Sample (g)=	0.01754	g
Wt Spike (g)=	0.04593	g

ometer Information:

Number of cycles measured:	777			
Number of cycles used:	777			
Amplifier rotation:	yes			
	start	average (from sheet)	ending	
Filament Current range: from		3675.602884		mAmps
Beam intensity range: from		0.9916281		Volts 142Nd.16O
Temperature range: from		1543.835804		° C

)ata:

Interference Values

Ce140-O16/Nd144-O16	NO Ce	Ce interference is NOT corrected in this sheet
Pr141-O16/Nd144-O16	1.78E-02	
Sm152-O16/Nd144-O16	8.13E-04	(Measured-Includes Nd150-O18)
Sm154-O16/Nd144-O16	1.89E-04	
Sm152-O16/Nd144-O16	*0.000237*	*(Oxygen isotope interference subtracted)*

for Ratios: Non-interference subtracted grand mean ratios (input RAW values w/o normalization)

	158/160	159/160	161/160	162/160	164/160	166/160
Ratios	1.14E+00	5.11E-01	0.348	7.22E-01	2.43E-01	2.81E-01
%StdErr	7.84E-04	6.55E-04	0	4.99E-14	1.15E-03	1.45E-03

for %StdErr: input %StdErr from online normalized values, or from offline PrSm correction sheet

on only	**142/144**	**143/144**	**145/144**	**146/144**	**148/144**	**150/144**
o 88, p.14, ln. B':	1.141854	na	0.348416	0.721882	0.241572	na

FINAL Interference subtracted grand mean ratios: **146/144 set to 0.7219**

	142/144	**143/144**	**145/144**	**146/144**	**148/144**	**150/144**	**150t/144s**
Ratios	1.142191	0.512122	0.347395	0.721900	0.241587	0.236471	22.227021
2 S.E.	0.000018	0.000007	0.000000	0.000000	0.000006	0.000007	0.000644

Epsilon143= -10.07 **using (143/144)chur= 0.512638**
± 0.13 **(Hamilton et al. 1983)**

linked from Sm sheet

[Sm147]=	0.663158	nm/g	**[Nd144]=**	**2.85859**	nm/g
±	0.000069		**±**	**0.00008**	
[Sm]=	0.664887	ppm	**[Nd]=**	**1.73366**	ppm
±	0.000069		**±**	**0.00005**	
TOT ng Sm=	11.6621191		**TOT ng Nd=**	**30.40845433**	
	Sm147/Nd144=	**0.231988**			
	±	**0.000025**			

Sample:	B2b-1 gt3
Date:	1/31/2015
Approx Nd load (ng):	-

Position #: 8

Rspike Values Nd {SmNd 1.0 A spike, 6-12-08 calib}

142/144	143/144	145/144	146/144	148/144	150/144	[Nd150]
0.830433	0.494001	0.436936	0.885201	0.740574	198.371260	0.049114
						nm/g

Wt Sample (g)=	0.0076	g
Wt Spike (g)=	0.03521	g

Mass Spectrometer Information:

Number of cycles measured:	560			
Number of cycles used:	560			
Amplifier rotation:	yes			
	start	average (from sheet)	ending	
Filament Current range: from	3675.0164	3797.808832	3909.999237	mAmps
Beam intensity range: from	0.52271496	0.64747464	0.397828592	Volts 142Nd.16O
Temperature range: from	1445.59219	1523.151535	1606.666667	° C

Final Ratio Data:

Interference Values

Ce140-O16/Nd144-O16	NO Ce	Ce interference is NOT corrected in this sheet
Pr141-O16/Nd144-O16	2.08E-01	
Sm152-O16/Nd144-O16	1.24E-03	(Measured-Includes Nd150-O18)
Sm154-O16/Nd144-O16	5.48E-04	
Sm152-O16/Nd144-O16	*0.000655*	*(Oxygen isotope interference subtracted)*

for Ratios: Non-interference subtracted grand mean ratios (input RAW values w/o normalization)

	158/160	159/160	161/160	162/160	164/160	166/160
Ratios	1.14E+00	5.11E-01	0.348	7.23E-01	2.43E-01	2.85E-01
%StdErr	9.77E-04	8.27E-04	0	4.75E-14	1.56E-03	1.85E-03

for %StdErr: input %StdErr from online normalized values, or from offline PrSm correction sheet

for comparison only	**142/144**	**143/144**	**145/144**	**146/144**	**148/144**	**150/144**
DePaolo 88, p.14, ln. B':	1.141854	na	0.348416	0.721882	0.241572	na

FINAL Interference subtracted grand mean ratios: **146/144 set to 0.7219**

	142/144	**143/144**	**145/144**	**146/144**	**148/144**	**150/144**	**150t/144s**
Ratios	1.141832	0.512128	0.347205	0.721900	0.241595	0.236471	21.101120
2 S.E.	0.000022	0.000008	0.000000	0.000000	0.000008	0.000009	0.000779

Epsilon143= -9.94 using (143/144)chur= 0.512638
± 0.17 (Hamilton et al. 1983)

linked from Sm sheet

[Sm147]=	1.035521	nm/g	**[Nd144]=**	**4.80133**	nm/g
±	0.000137		**±**	**0.00018**	
[Sm]=	1.038221	ppm	**[Nd]=**	**2.91189**	ppm
±	0.000138		**±**	**0.00011**	
TOT ng Sm=	7.89047754		**TOT ng Nd=**	**22.13034497**	
	Sm147/Nd144=	**0.215674**			
	±	**0.000030**			

Sample: _09_pos07_B12b-1_gt4
Date: 3/9/2015
Approx Nd load (ng): -
Position #: 7

Rspike Values Nd {SmNd 1.0 A spike, 6-12-08 calib}

142/144	143/144	145/144	146/144	148/144	150/144	[Nd150]
0.830433	0.494001	0.436936	0.885201	0.740574	198.371260	0.049114 nm/g

Wt Sample (g)= 0.013 g
Wt Spike (g)= 0.05082 g

Mass Spectrometer Information:

Number of cycles measured:
Number of cycles used: 320
Amplifier rotation: yes

	start	average (from sheet)	ending	
Filament Current range: from	3800.01526	3800.015259	3800.015259	mAmps
Beam intensity range: from	0.15818763	0.60127532	0.627050528	Volts 142Nd.16O
Temperature range: from	1431.47741	1458.334402	1488.766789	° C

Final Ratio Data:

Interference Values

Ce140-O16/Nd144-O16	NO Ce	Ce interference is NOT corrected in this sheet
Pr141-O16/Nd144-O16	1.00E-02	
Sm152-O16/Nd144-O16	2.02E-03	(Measured-Includes Nd150-O18)
Sm154-O16/Nd144-O16	1.03E-03	
Sm152-O16/Nd144-O16	*0.001246*	*(Oxygen isotope interference subtracted)*

for Ratios: Non-interference subtracted grand mean ratios (input RAW values w/o normalization)

	158/160	159/160	161/160	162/160	164/160	166/160
Ratios	1.14E+00	5.11E-01	0.348	7.22E-01	2.43E-01	3.78E-01
%StdErr	1.70E-03	1.21E-03	0	2.28E-14	2.89E-03	2.61E-03

for %StdErr: input %StdErr from online normalized values, or from offline PrSm correction sheet

for comparison only	**142/144**	**143/144**	**145/144**	**146/144**	**148/144**	**150/144**
DePaolo 88, p.14, ln. B':	1.141854	na	0.348416	0.721882	0.241572	na

FINAL Interference subtracted grand mean ratios: **146/144 set to 0.7219**

	142/144	**143/144**	**145/144**	**146/144**	**148/144**	**150/144**	**150t/144s**
Ratios	1.141882	0.512119	0.347377	0.721900	0.241607	0.236471	7.084475
2 S.E.	0.000039	0.000012	0.000000	0.000000	0.000014	0.000012	0.000370

Epsilon143= **-10.12** **using (143/144)chur=** **0.512638**
± **0.24** **(Hamilton et al. 1983)**

linked from Sm sheet

[Sm147]= 0.421738 nm/g **[Nd144]=** **1.36020** nm/g
± 0.000103 **±** **0.00007**
[Sm]= 0.422837 ppm **[Nd]=** **0.82493** ppm
± 0.000103 **±** **0.00004**
TOT ng Sm= 5.49688337 **TOT ng Nd=** **10.72405309**

Sm147/Nd144= **0.310055**
± **0.000077**

Sample: _09_pos08_B2b-1_gt5
Date: 3/9/2015
Approx Nd load (ng): -
Position #: 8

Rspike Values Nd {SmNd 1.0 A spike, 6-12-08 calib}

142/144	143/144	145/144	146/144	148/144	150/144	[Nd150]
0.830433	0.494001	0.436936	0.885201	0.740574	198.371260	0.049114 nm/g

Wt Sample (g)= 0.0058 g
Wt Spike (g)= 0.02534 g

Mass Spectrometer Information:

Number of cycles measured: 317
Number of cycles used: 318
Amplifier rotation: yes

	start	average (from sheet)	ending	
Filament Current range: from	3800.01526	3863.788228	4126.08835	mAmps
Beam intensity range: from	0.25868101	0.40296334	0.049651606	Volts 142Nd.16O
Temperature range: from	1419.85348	1466.169792	1616.214896	° C

Final Ratio Data:

Interference Values

Ce140-O16/Nd144-O16	NO Ce	Ce interference is NOT corrected in this sheet
Pr141-O16/Nd144-O16	1.45E-02	
Sm152-O16/Nd144-O16	1.58E-03	(Measured-Includes Nd150-O18)
Sm154-O16/Nd144-O16	7.86E-04	
Sm152-O16/Nd144-O16	*0.000890*	*(Oxygen isotope interference subtracted)*

for Ratios: Non-interference subtracted grand mean ratios (input RAW values w/o normalization)

	158/160	159/160	161/160	162/160	164/160	166/160
Ratios	1.14E+00	5.11E-01	0.348	7.24E-01	2.44E-01	3.40E-01
%StdErr	1.76E-03	1.55E-03	0	2.29E-14	4.83E-03	3.79E-03

for %StdErr: input %StdErr from online normalized values, or from offline PrSm correction sheet

for comparison only	**142/144**	**143/144**	**145/144**	**146/144**	**148/144**	**150/144**
DePaolo 88, p.14, ln. B':	1.141854	na	0.348416	0.721882	0.241572	na

FINAL Interference subtracted grand mean ratios: **146/144 set to 0.7219**

	142/144	**143/144**	**145/144**	**146/144**	**148/144**	**150/144**	**150t/144s**
Ratios	1.141823	0.512131	0.347086	0.721900	0.241616	0.236471	9.836088
2 S.E.	0.000040	0.000016	0.000000	0.000000	0.000023	0.000018	0.000745

Epsilon143= -9.90 using (143/144)chur= 0.512638
± 0.31 (Hamilton et al. 1983)

linked from Sm sheet

[Sm147]= 0.768235 nm/g **[Nd144]=** **2.11060** nm/g
± 0.000673 **±** **0.00016**
[Sm]= 0.770238 ppm **[Nd]=** **1.28002** ppm
± 0.000674 **±** **0.00010**
TOT ng Sm= 4.46738183 **TOT ng Nd=** **7.42413163**

Sm147/Nd144= **0.363990**
± **0.000320**

Sample: _18_Pos05_B2b-1_gt6
Date: 4/18/2015 Position #: 5
Approx Nd load (ng): -

Rspike Values Nd {SmNd 1.0 A spike, 6-12-08 calib}

142/144	143/144	145/144	146/144	148/144	150/144	[Nd150]
0.830433	0.494001	0.436936	0.885201	0.740574	198.371260	0.049114 nm/g

Wt Sample (g)= 0.005 g
Wt Spike (g)= 0.02841 g

Mass Spectrometer Information:

Number of cycles measured: 465
Number of cycles used: 344
Amplifier rotation: yes

	start	average (from sheet)	ending	
Filament Current range: from	3499.96796	3532.493582	3599.942016	mAmps
Beam intensity range: from	0.07810857	0.16381025	0.105781174	Volts 142Nd.16O
Temperature range: from	1472.99145	1500.368794	1533.601954	° C

Final Ratio Data:

Interference Values

Ce140-O16/Nd144-O16	NO Ce	Ce interference is NOT corrected in this sheet
Pr141-O16/Nd144-O16	1.77E-02	
Sm152-O16/Nd144-O16	7.00E-03	(Measured-Includes Nd150-O18)
Sm154-O16/Nd144-O16	4.95E-03	
Sm152-O16/Nd144-O16	*0.005863*	*(Oxygen isotope interference subtracted)*

for Ratios: Non-interference subtracted grand mean ratios (input RAW values w/o normalization)

	158/160	159/160	161/160	162/160	164/160	166/160
Ratios	1.14E+00	5.10E-01	0.348	7.23E-01	2.47E-01	5.62E-01
%StdErr	4.81E-03	2.99E-03	0	2.44E-14	1.03E-02	6.96E-03

for %StdErr: input %StdErr from online normalized values, or from offline PrSm correction sheet

for comparison only	**142/144**	**143/144**	**145/144**	**146/144**	**148/144**	**150/144**
DePaolo 88, p.14, ln. B':	1.141854	na	0.348416	0.721882	0.241572	na

FINAL Interference subtracted grand mean ratios: 146/144 set to 0.7219

	142/144	**143/144**	**145/144**	**146/144**	**148/144**	**150/144**	**150t/144s**
Ratios	1.142410	0.512134	0.347188	0.721900	0.241627	0.236471	3.099074
2 S.E.	0.000110	0.000031	0.000000	0.000000	0.000050	0.000033	0.000432

Epsilon143= -9.83 using (143/144)chur= 0.512638
± 0.60 (Hamilton et al. 1983)

linked from Sm sheet

[Sm147]= 0.492227 nm/g **[Nd144]=** **0.86484** nm/g
± 0.000055 **±** **0.00012**
[Sm]= 0.493510 ppm **[Nd]=** **0.52451** ppm
± 0.000055 **±** **0.00007**
TOT ng Sm= 2.46754996 **TOT ng Nd=** **2.622526336**

Sm147/Nd144= **0.569151**
± **0.000102**

Sample: _20_pos04_B2b-2_gt8
Date: 5/20/2015
Approx Nd load (ng): -
Position #: 4

Rspike Values Nd {SmNd 1.0 A spike, 6-12-08 calib}

142/144	143/144	145/144	146/144	148/144	150/144	[Nd150]
0.830433	0.494001	0.436936	0.885201	0.740574	198.371260	0.049114
						nm/g

Wt Sample (g)= 0.0106 g
Wt Spike (g)= 0.05019 g

Mass Spectrometer Information:

Number of cycles measured: 243
Number of cycles used:
Amplifier rotation: yes

	start	average (from sheet)	ending	
Filament Current range: from		3500.009426		mAmps
Beam intensity range: from		0.53108524		Volts 142Nd.16O
Temperature range: from		1513.566091		° C

Final Ratio Data:

Interference Values

Ce140-O16/Nd144-O16	NO Ce	Ce interference is NOT corrected in this sheet
Pr141-O16/Nd144-O16	1.28E-02	
Sm152-O16/Nd144-O16	3.36E-03	(Measured-Includes Nd150-O18)
Sm154-O16/Nd144-O16	2.18E-03	
Sm152-O16/Nd144-O16	*0.002584*	*(Oxygen isotope interference subtracted)*

for Ratios: Non-interference subtracted grand mean ratios (input RAW values w/o normalization)

	158/160	159/160	161/160	162/160	164/160	166/160
Ratios	1.14E+00	5.11E-01	0.348	7.23E-01	2.44E-01	3.80E-01
%StdErr	2.14E-03	1.56E-03	0	2.80E-14	3.20E-03	3.58E-03

for %StdErr: input %StdErr from online normalized values, or from offline PrSm correction sheet

for comparison only	**142/144**	**143/144**	**145/144**	**146/144**	**148/144**	**150/144**
DePaolo 88, p.14, ln. B':	1.141854	na	0.348416	0.721882	0.241572	na

FINAL Interference subtracted grand mean ratios: **146/144 set to 0.7219**

	142/144	**143/144**	**145/144**	**146/144**	**148/144**	**150/144**	**150t/144s**
Ratios	1.142530	0.512171	0.347306	0.721900	0.241617	0.236471	6.993374
2 S.E.	0.000049	0.000016	0.000000	0.000000	0.000015	0.000017	0.000501

Epsilon143= -9.11 using (143/144)chur= 0.512638
± 0.31 (Hamilton et al. 1983)

linked from Sm sheet

[Sm147]= 0.810030 nm/g **[Nd144]=** **1.62631** nm/g
± 0.000133 **±** **0.00012**
[Sm]= 0.812142 ppm **[Nd]=** **0.98631** ppm
± 0.000134 **±** **0.00007**
TOT ng Sm= 8.60871047 **TOT ng Nd=** **10.45491757**
Sm147/Nd144= **0.498080**
± **0.000089**

Sample:	**B2b-1 gt powder 1**		
Date:	12/4/2014	Position #:	15
Approx Nd load (ng):	-		

Rspike Values Nd {SmNd 0.15 A spike, 6-12-08 calib}

142/144	143/144	145/144	146/144	148/144	150/144	[Nd150]
0.830433	0.494001	0.436936	0.885201	0.740574	198.371260	0.125778

nm/g

Wt Sample (g)=	0.0037	g
Wt Spike (g)=	0.41288	g

Mass Spectrometer Information:

Number of cycles measured:	~1200			
Number of cycles used:	940			
Amplifier rotation:	yes			
	start	average (from sheet)	ending	
Filament Current range: from		3772.860693		mAmps
Beam intensity range: from		1.21433257		volts 142Nd.16O
Temperature range: from		1507.681734		°C

Final Ratio Data:

Interference Values

Ce140-O16/Nd144-O16	NO Ce	Ce interference is NOT corrected in this sheet
Pr141-O16/Nd144-O16	1.40E-01	
Sm152-O16/Nd144-O16	2.33E-03	(Measured-Includes Nd150-O18)
Sm154-O16/Nd144-O16	8.29E-04	
Sm152-O16/Nd144-O16	*0.000998*	*(Oxygen isotope interference subtracted)*

for Ratios: Non-interference subtracted grand mean ratios (input RAW values w/o normalization)

	158/160	159/160	161/160	162/160	164/160	166/160
Ratios	1.14E+00	5.12E-01	0.348	7.22E-01	2.44E-01	6.50E-01
%StdErr	8.11E-04	5.01E-04	0	2.39E-15	8.47E-04	9.92E-04

for %StdErr: input %StdErr from online normalized values, or from offline PrSm correction sheet

for comparison only	142/144	143/144	145/144	146/144	148/144	150/144
DePaolo 88, p.14:	1.141854	na	0.348416	0.721882	0.241572	na

FINAL Interference subtracted grand mean ratios: 146/144 set to 0.7219

	142/144	143/144	145/144	146/144	148/144	150/144	150t/144s
Ratios	1.142028	0.512106	0.347373	0.721900	0.241591	0.236471	2.397143
2 S.E.	0.000019	0.000005	0.000000	0.000000	0.000004	0.000005	0.000048

Epsilon143= -10.37 using (143/144)chur= 0.512638

± 0.10 (Hamilton et al. 1983)

linked from Sm sheet

[Sm147]=	4.266974	nm/g	[Nd144]=	33.64503	nm/g
±	0.000416		±	0.00067	
[Sm]=	4.278099	ppm	[Nd]=	20.40486	ppm
±	0.000417		±	0.00040	
TOT ng Sm=	15.8289669		TOT ng Nd=	75.49797227	
		Sm147/Nd144=	0.126823	Tot pg Nd=	**75497.97227**
		±	0.000013	pg Nd/mL	20404857.37

Sample:	**B2b-1 gt powder 2**
Date:	12/20/2014
Position #:	3
Approx Nd load (ng):	

Rspike Values Nd {SmNd 0.15 A spike, 6-12-08 calib}

142/144	143/144	145/144	146/144	148/144	150/144	[Nd150]
0.830433	0.494001	0.436936	0.885201	0.740574	198.371260	0.125778

nm/g

Wt Sample (g)=	0.00975	g
Wt Spike (g)=	0.80828	g

Mass Spectrometer Information:

Number of cycles measured:	880			
Number of cycles used:	800			
Amplifier rotation:	yes			
	start	average (from sheet)	ending	
Filament Current range: from		3529.972686		mAmps
Beam intensity range: from		1.07796705		volts 142Nd.16O
Temperature range: from		1536.385989		°C

Final Ratio Data:

Interference Values

Ce140-O16/Nd144-O16	NO Ce	Ce interference is NOT corrected in this sheet
Pr141-O16/Nd144-O16	6.97E-02	
Sm152-O16/Nd144-O16	1.19E-03	(Measured-Includes Nd150-O18)
Sm154-O16/Nd144-O16	1.85E-04	
Sm152-O16/Nd144-O16	*0.000235*	*(Oxygen isotope interference subtracted)*

for Ratios: Non-interference subtracted grand mean ratios (input RAW values w/o normalization)

	158/160	159/160	161/160	162/160	164/160	166/160
Ratios	1.14E+00	5.12E-01	0.348	7.22E-01	2.43E-01	4.66E-01
%StdErr	6.66E-04	5.68E-04	0	3.00E-14	8.67E-04	1.11E-03

for %StdErr: input %StdErr from online normalized values, or from offline PrSm correction sheet

for comparison only	142/144	143/144	145/144	146/144	148/144	150/144
DePaolo 88, p.14:	1.141854	na	0.348416	0.721882	0.241572	na

FINAL Interference subtracted grand mean ratios: 146/144 set to 0.7219

	142/144	143/144	145/144	146/144	148/144	150/144	150t/144s
Ratios	1.141883	0.512107	0.347530	0.721900	0.241589	0.236471	4.315249
2 S.E.	0.000015	0.000006	0.000000	0.000000	0.000004	0.000005	0.000096

Epsilon143= -10.36 using (143/144)chur= 0.512638

± 0.11 (Hamilton et al. 1983)

linked from Sm sheet

[Sm147]=	5.435675	nm/g	[Nd144]=	44.99538	nm/g
±	0.000163		±	0.00100	
[Sm]=	5.449848	ppm	[Nd]=	27.28856	ppm
±	0.000163		±	0.00061	
TOT ng Sm=	53.1360176		TOT ng Nd=	266.0634381	
	Sm147/Nd144=	0.120805	Tot pg Nd=	**266063.4381**	
	±	0.000005	pg Nd/mL	27288557.75	

Sample:	**15_03_09_pos04_B2b-1_gtpowd_4_NdO**
Date:	3/9/2015
Position #:	4
Approx Nd load (ng):	-

Rspike Values Nd {SmNd 0.15 A spike, 6-12-08 calib}

142/144	143/144	145/144	146/144	148/144	150/144	[Nd150]
0.830433	0.494001	0.436936	0.885201	0.740574	198.371260	0.125778
						nm/g

Wt Sample (g)=	0.001924	g
Wt Spike (g)=	0.20369	g

Mass Spectrometer Information:

Number of cycles measured:	251			
Number of cycles used:	160			
Amplifier rotation:	yes			
	start	average (from sheet)	ending	
Filament Current range: from	3800.01526	3800.408618	3820.78584	mAmps
Beam intensity range: from	0.50646264	0.97122599	0.708032711	volts 142Nd.16O
Temperature range: from	1485.03053	1509.580891	1538.998779	°C

Final Ratio Data:

Interference Values

Ce140-O16/Nd144-O16	NO Ce	Ce interference is NOT corrected in this sheet
Pr141-O16/Nd144-O16	9.10E-03	
Sm152-O16/Nd144-O16	3.74E-03	(Measured-Includes Nd150-O18)
Sm154-O16/Nd144-O16	5.41E-04	
Sm152-O16/Nd144-O16	*0.000701*	*(Oxygen isotope interference subtracted)*

for Ratios: Non-interference subtracted grand mean ratios (input RAW values w/o normalization)

	158/160	159/160	161/160	162/160	164/160	166/160
Ratios	1.14E+00	5.11E-01	0.348	7.24E-01	2.46E-01	1.48E+00
%StdErr	1.37E-03	1.23E-03	0	2.80E-14	1.88E-03	2.40E-03

for %StdErr: input %StdErr from online normalized values, or from offline PrSm correction sheet

for comparison only	142/144	143/144	145/144	146/144	148/144	150/144
DePaolo 88, p.14:	1.141854	na	0.348416	0.721882	0.241572	na

FINAL Interference subtracted grand mean ratios: 146/144 set to 0.7219

	142/144	143/144	145/144	146/144	148/144	150/144	150t/144s
Ratios	1.141924	0.512107	0.346766	0.721900	0.241571	0.236471	0.797638
2 S.E.	0.000031	0.000013	0.000000	0.000000	0.000009	0.000011	0.000038

Epsilon143= -10.35 using (143/144)chur= 0.512638
± 0.25 (Hamilton et al. 1983)

linked from Sm sheet

[Sm147]=	1.255380	nm/g	[Nd144]=	10.62124	nm/g
±	0.000315		±	0.00051	
[Sm]=	1.258653	ppm	[Nd]=	6.44151	ppm
±	0.000316		±	0.00031	
TOT ng Sm=	2.42164885		TOT ng Nd=	12.39347264	
	Sm147/Nd144=	0.118195	Tot pg Nd=	**12393.47264**	
	±	0.000030	pg Nd/mL	6441513.846	

Sample:	**27.1.2 wr al1 MISLABED ON BARREL!**		
Date:	7/4/2015	Position #:	2
Approx Nd load (ng):	-		

Rspike Values Nd {SmNd 0.15 A spike, 6-12-08 calib}

142/144	143/144	145/144	146/144	148/144	150/144	[Nd150]
0.830433	0.494001	0.436936	0.885201	0.740574	198.371260	0.125778

nm/g

Wt Sample (g)=	0.0030185	g
Wt Spike (g)=	0.41376	g

Mass Spectrometer Information:

Number of cycles measured:	520			
Number of cycles used:	480			
Amplifier rotation:	yes			
	start	average (from sheet)	ending	
Filament Current range: from	3700.0412	3703.117164	3724.940871	mAmps
Beam intensity range: from	0.50809919	0.7034288	0.427295775	volts 142Nd.16O
Temperature range: from	1465.51893	1516.454925	1567.228327	°C

Final Ratio Data:

Interference Values

Ce140-O16/Nd144-O16	NO Ce	Ce interference is NOT corrected in this sheet
Pr141-O16/Nd144-O16	7.12E-03	
Sm152-O16/Nd144-O16	1.50E-03	(Measured-Includes Nd150-O18)
Sm154-O16/Nd144-O16	2.26E-04	
Sm152-O16/Nd144-O16	*0.000291*	*(Oxygen isotope interference subtracted)*

for Ratios: Non-interference subtracted grand mean ratios (input RAW values w/o normalization)

	158/160	159/160	161/160	162/160	164/160	166/160
Ratios	1.14E+00	5.11E-01	0.348	7.23E-01	2.44E-01	5.89E-01
%StdErr	1.15E-03	9.17E-04	0	2.68E-14	1.45E-03	1.70E-03

for %StdErr: input %StdErr from online normalized values, or from offline PrSm correction sheet

for comparison only	142/144	143/144	145/144	146/144	148/144	150/144
DePaolo 88, p.14:	1.141854	na	0.348416	0.721882	0.241572	na

FINAL Interference subtracted grand mean ratios: 146/144 set to 0.7219

	142/144	143/144	145/144	146/144	148/144	150/144	150t/144s
Ratios	1.142089	0.511978	0.347258	0.721900	0.241593	0.236471	2.825528
2 S.E.	0.000026	0.000009	0.000000	0.000000	0.000007	0.000008	0.000096

Epsilon143= -12.87 using (143/144)chur= 0.512638
± 0.18 (Hamilton et al. 1983)

linked from Sm sheet

[Sm147]=	5.568508	nm/g		[Nd144]=	48.71489	nm/g
±	0.011035			±	0.00165	
[Sm]=	5.583027	ppm		[Nd]=	29.54435	ppm
±	0.011064			±	0.00100	
TOT ng Sm=	16.8523666			TOT ng Nd=	89.17961583	
		Sm147/Nd144=	0.114308	Tot pg Nd=	**89179.61583**	
		±	0.000227	pg Nd/mL	29544348.46	

Sample:	**27.1.2 gtsep1 pow**		
Date:	7/4/2015	Position #:	6
Approx Nd load (ng):	-		

Rspike Values Nd {SmNd 0.15 A spike, 6-12-08 calib}

142/144	143/144	145/144	146/144	148/144	150/144	[Nd150]
0.830433	0.494001	0.436936	0.885201	0.740574	198.371260	0.125778

nm/g

Wt Sample (g)=	0.00377	g
Wt Spike (g)=	0.20811	g

Mass Spectrometer Information:

Number of cycles measured:	120			
Number of cycles used:	119			
Amplifier rotation:	yes			
	start	average (from sheet)	ending	
Filament Current range: from	3550.01755	3550.017548	3550.017548	mAmps
Beam intensity range: from	3.94181504	2.10953211	0.336570588	volts 142Nd.16O
Temperature range: from	1539.82906	1565.721263	1579.68254	°C

Final Ratio Data:

Interference Values

Ce140-O16/Nd144-O16	NO Ce	Ce interference is NOT corrected in this sheet
Pr141-O16/Nd144-O16	5.35E-03	
Sm152-O16/Nd144-O16	1.21E-03	(Measured-Includes Nd150-O18)
Sm154-O16/Nd144-O16	1.90E-04	
Sm152-O16/Nd144-O16	*0.000258*	*(Oxygen isotope interference subtracted)*

for Ratios: Non-interference subtracted grand mean ratios (input RAW values w/o normalization)

	158/160	159/160	161/160	162/160	164/160	166/160
Ratios	1.14E+00	5.11E-01	0.348	7.24E-01	2.44E-01	4.64E-01
%StdErr	1.50E-03	1.21E-03	0	2.83E-14	1.93E-03	2.04E-03

for %StdErr: input %StdErr from online normalized values, or from offline PrSm correction sheet

for comparison only	142/144	143/144	145/144	146/144	148/144	150/144
DePaolo 88, p.14:	1.141854	na	0.348416	0.721882	0.241572	na

FINAL Interference subtracted grand mean ratios: 146/144 set to 0.7219

	142/144	143/144	145/144	146/144	148/144	150/144	150t/144s
Ratios	1.142021	0.511981	0.346977	0.721900	0.241598	0.236471	4.434463
2 S.E.	0.000034	0.000012	0.000000	0.000000	0.000009	0.000010	0.000181

Epsilon143= -12.81 using (143/144)chur= 0.512638

± 0.24 (Hamilton et al. 1983)

linked from Sm sheet

[Sm147]=	6.870138	nm/g	[Nd144]=	30.78914	nm/g
±	0.001923		±	0.00126	
[Sm]=	6.888051	ppm	[Nd]=	18.67283	ppm
±	0.001928		±	0.00076	
TOT ng Sm=	25.9679531		TOT ng Nd=	70.39657112	
		Sm147/Nd144= 0.223135	Tot pg Nd=	**70396.57112**	
		± 0.000063	pg Nd/mL	18672830.54	

Sample: 27.1.2 gtsep1-30
Date: 6/27/2015
Approx Nd load (ng): -

Position #: 5

Rspike Values Nd {SmNd 1.0 A spike, 6-12-08 calib}

142/144	143/144	145/144	146/144	148/144	150/144	[Nd150]
0.830433	0.494001	0.436936	0.885201	0.740574	198.371260	0.049114
						nm/g

Wt Sample (g)= 0.07903 g
Wt Spike (g)= 0.20615 g

Mass Spectrometer Information:

Number of cycles measured: 800
Number of cycles used: 750
Amplifier rotation: yes

	start	average (from sheet)	ending	
Filament Current range: from		3531.873904		mAmps
Beam intensity range: from		0.36090718		Volts 142Nd.16O
Temperature range: from		1520.128710		° C

Final Ratio Data:

Interference Values

Ce140-O16/Nd144-O16	NO Ce	Ce interference is NOT corrected in this sheet
Pr141-O16/Nd144-O16	3.21E-03	
Sm152-O16/Nd144-O16	1.94E-03	(Measured-Includes Nd150-O18)
Sm154-O16/Nd144-O16	1.19E-03	
Sm152-O16/Nd144-O16	*0.001390*	*(Oxygen isotope interference subtracted)*

for Ratios: Non-interference subtracted grand mean ratios (input RAW values w/o normalization)

	158/160	159/160	161/160	162/160	164/160	166/160
Ratios	1.14E+00	5.11E-01	0.348	7.23E-01	2.44E-01	2.71E-01
%StdErr	1.18E-03	1.07E-03	0	4.35E-14	2.44E-03	2.53E-03

for %StdErr: input %StdErr from online normalized values, or from offline PrSm correction sheet

for comparison only	**142/144**	**143/144**	**145/144**	**146/144**	**148/144**	**150/144**
DePaolo 88, p.14, ln. B':	1.141854	na	0.348416	0.721882	0.241572	na

FINAL Interference subtracted grand mean ratios: **146/144 set to 0.7219**

	142/144	**143/144**	**145/144**	**146/144**	**148/144**	**150/144**	**150t/144s**
Ratios	1.141821	0.512037	0.347280	0.721900	0.241591	0.236471	30.258821
2 S.E.	0.000027	0.000011	0.000000	0.000000	0.000012	0.000012	0.001529

Epsilon143= -11.71 **using (143/144)chur= 0.512638**
± 0.21 **(Hamilton et al. 1983)**

linked from Sm sheet

[Sm147]= 2.519786 nm/g **[Nd144]=** **3.87657** nm/g
± 0.000222 **±** **0.00020**
[Sm]= 2.526356 ppm **[Nd]=** **2.35104** ppm
± 0.000222 **±** **0.00012**
TOT ng Sm= 199.657951 **TOT ng Nd=** **185.8026825**

Sm147/Nd144= **0.650005**
± **0.000066**

Sample:	27.1.2 gt1-60
Date:	7/4/2015
Approx Nd load (ng):	-

Position #: 9

Rspike Values Nd {SmNd 1.0 A spike, 6-12-08 calib}

142/144	143/144	145/144	146/144	148/144	150/144	[Nd150]
0.830433	0.494001	0.436936	0.885201	0.740574	198.371260	0.049114 nm/g

Wt Sample (g)=	0.03402	g
Wt Spike (g)=	0.39261	g

Mass Spectrometer Information:

Number of cycles measured:	95			
Number of cycles used:	80			
Amplifier rotation:	yes			
	start	average (from sheet)	ending	
Filament Current range: from	3700.0412	3727.982948	3752.593271	mAmps
Beam intensity range: from	2.19859103	1.16475588	0.286209205	Volts 142Nd.16O
Temperature range: from	1538.99878	1569.174298	1596.288156	° C

Final Ratio Data:

Interference Values

Ce140-O16/Nd144-O16	NO Ce	Ce interference is NOT corrected in this sheet
Pr141-O16/Nd144-O16	1.34E-03	
Sm152-O16/Nd144-O16	8.81E-03	(Measured-Includes Nd150-O18)
Sm154-O16/Nd144-O16	6.89E-03	
Sm152-O16/Nd144-O16	*0.008133*	*(Oxygen isotope interference subtracted)*

for Ratios: Non-interference subtracted grand mean ratios (input RAW values w/o normalization)

	158/160	159/160	161/160	162/160	164/160	166/160
Ratios	1.13E+00	5.10E-01	0.348	7.24E-01	2.47E-01	3.38E-01
%StdErr	2.75E-03	1.99E-03	0	2.42E-14	8.05E-03	6.19E-03

for %StdErr: input %StdErr from online normalized values, or from offline PrSm correction sheet

for comparison only	**142/144**	**143/144**	**145/144**	**146/144**	**148/144**	**150/144**
DePaolo 88, p.14, ln. B':	1.141854	na	0.348416	0.721882	0.241572	na

FINAL Interference subtracted grand mean ratios: **146/144 set to 0.7219**

	142/144	**143/144**	**145/144**	**146/144**	**148/144**	**150/144**	**150t/144s**
Ratios	1.141966	0.512024	0.347231	0.721900	0.241637	0.236471	10.233581
2 S.E.	0.000063	0.000020	0.000000	0.000000	0.000039	0.000029	0.001267

Epsilon143= -11.98 using (143/144)chur= 0.512638
± 0.40 (Hamilton et al. 1983)

linked from Sm sheet

[Sm147]=	3.754268	nm/g	**[Nd144]=**	**5.80041**	nm/g
±	0.000559		**±**	**0.00072**	
[Sm]=	3.764057	ppm	**[Nd]=**	**3.51780**	ppm
±	0.000560		**±**	**0.00044**	
TOT ng Sm=	128.053216		**TOT ng Nd=**	**119.6755999**	
		Sm147/Nd144=	**0.647242**		
		±	**0.000125**		

Sample:	27.1.2 gt1-90		
Date:	7/5/2015	Position #:	10
Approx Nd load (ng):	-		

Rspike Values Nd {SmNd 1.0 A spike, 6-12-08 calib}

142/144	143/144	145/144	146/144	148/144	150/144	[Nd150]
0.830433	0.494001	0.436936	0.885201	0.740574	198.371260	0.049114 nm/g

Wt Sample (g)=	0.07994	g
Wt Spike (g)=	0.52096	g

Mass Spectrometer Information:

Number of cycles measured:	140			
Number of cycles used:	140			
Amplifier rotation:	yes			
	start	average (from sheet)	ending	
Filament Current range: from	3749.96567	3749.965667	3749.965667	mAmps
Beam intensity range: from	1.89480304	11.2578663	6.04808668	Volts 142Nd.16O
Temperature range: from	1452.23443	1543.420024	1612.063492	° C

Final Ratio Data:

Interference Values

Ce140-O16/Nd144-O16	NO Ce	Ce interference is NOT corrected in this sheet
Pr141-O16/Nd144-O16	6.76E-03	
Sm152-O16/Nd144-O16	1.44E-03	(Measured-Includes Nd150-O18)
Sm154-O16/Nd144-O16	7.39E-04	
Sm152-O16/Nd144-O16	*0.000886*	*(Oxygen isotope interference subtracted)*

for Ratios: Non-interference subtracted grand mean ratios (input RAW values w/o normalization)

	158/160	159/160	161/160	162/160	164/160	166/160
Ratios	1.14E+00	5.11E-01	0.348	7.23E-01	2.43E-01	2.70E-01
%StdErr	7.43E-04	5.44E-04	0	1.82E-14	1.88E-03	1.37E-03

for %StdErr: input %StdErr from online normalized values, or from offline PrSm correction sheet

for comparison only	**142/144**	**143/144**	**145/144**	**146/144**	**148/144**	**150/144**
DePaolo 88, p.14, ln. B':	1.141854	na	0.348416	0.721882	0.241572	na

FINAL Interference subtracted grand mean ratios: **146/144 set to 0.7219**

	142/144	**143/144**	**145/144**	**146/144**	**148/144**	**150/144**	**150t/144s**
Ratios	1.141870	0.511998	0.347307	0.721900	0.241609	0.236471	30.494197
2 S.E.	0.000017	0.000006	0.000000	0.000000	0.000009	0.000006	0.000833

Epsilon143= -12.49 using (143/144)chur= 0.512638
± 0.11 (Hamilton et al. 1983)

linked from Sm sheet

[Sm147]=	3.870930	nm/g	**[Nd144]=**	**9.76026**	nm/g
±	0.000612		**±**	**0.00027**	
[Sm]=	3.881023	ppm	**[Nd]=**	**5.91935**	ppm
±	0.000614		**±**	**0.00016**	
TOT ng Sm=	310.249014		**TOT ng Nd=**	**473.1929082**	
	Sm147/Nd144=	**0.396601**			
	±	**0.000064**			

Sample:	15_07_04_pos05_27_1_2_gtsep2_pow		
Date:	7/4/2015	Position #:	5
Approx Nd load (ng):	-		

Rspike Values Nd {SmNd 0.15 A spike, 6-12-08 calib}

142/144	143/144	145/144	146/144	148/144	150/144	[Nd150]
0.830433	0.494001	0.436936	0.885201	0.740574	198.371260	0.125778

nm/g

Wt Sample (g)=	0.00296	g
Wt Spike (g)=	0.20671	g

Mass Spectrometer Information:

Number of cycles measured:	760			
Number of cycles used:	760			
Amplifier rotation:	yes			
	start	average (from sheet)	ending	
Filament Current range: from	3599.94202	3645.811808	3649.991608	mAmps
Beam intensity range: from	1.13995269	1.2815786	1.824780843	volts 142Nd.16O
Temperature range: from	1453.06471	1502.805090	1535.677656	°C

Final Ratio Data:

Interference Values

Ce140-O16/Nd144-O16	NO Ce	Ce interference is NOT corrected in this sheet
Pr141-O16/Nd144-O16	3.86E-03	
Sm152-O16/Nd144-O16	7.77E-04	(Measured-Includes Nd150-O18)
Sm154-O16/Nd144-O16	1.46E-04	
Sm152-O16/Nd144-O16	*0.000182*	*(Oxygen isotope interference subtracted)*

for Ratios: Non-interference subtracted grand mean ratios (input RAW values w/o normalization)

	158/160	159/160	161/160	162/160	164/160	166/160
Ratios	1.14E+00	5.11E-01	0.348	7.22E-01	2.42E-01	2.91E-01
%StdErr	5.77E-04	4.91E-04	0	4.52E-14	7.54E-04	1.02E-03

for %StdErr: input %StdErr from online normalized values, or from offline PrSm correction sheet

for comparison only	142/144	143/144	145/144	146/144	148/144	150/144
DePaolo 88, p.14:	1.141854	na	0.348416	0.721882	0.241572	na

FINAL Interference subtracted grand mean ratios: 146/144 set to 0.7219

	142/144	143/144	145/144	146/144	148/144	150/144	150t/144s
Ratios	1.141949	0.511985	0.347545	0.721900	0.241597	0.236471	18.129654
2 S.E.	0.000013	0.000005	0.000000	0.000000	0.000004	0.000005	0.000370

Epsilon143= -12.74 using (143/144)chur= 0.512638
± 0.10 (Hamilton et al. 1983)

linked from Sm sheet

[Sm147]=	16.436306	nm/g	[Nd144]=	159.24440	nm/g
±	0.001985		±	0.00325	
[Sm]=	16.479162	ppm	[Nd]=	96.57770	ppm
±	0.001990		±	0.00197	
TOT ng Sm=	48.7783184		TOT ng Nd=	285.8699843	
	Sm147/Nd144=	0.103214	Tot pg Nd=	**285869.9843**	
	±	0.000013	pg Nd/mL	96577697.41	

Sample: 27.1.2 gtsep2-30
Date: 6/27/2015
Approx Nd load (ng): -

Position #: 2

Rspike Values Nd {SmNd 1.0 A spike, 6-12-08 calib}

142/144	143/144	145/144	146/144	148/144	150/144	[Nd150]
0.830433	0.494001	0.436936	0.885201	0.740574	198.371260	0.049114
						nm/g

Wt Sample (g)= 0.03216 g
Wt Spike (g)= 0.15533 g

Mass Spectrometer Information:

Number of cycles measured:
Number of cycles used:
Amplifier rotation: yes

	start	average (from sheet)	ending	
Filament Current range: from		3607.049840		mAmps
Beam intensity range: from		1.88213373		Volts 142Nd.16O
Temperature range: from		1556.141484		° C

Final Ratio Data:

Interference Values

Ce140-O16/Nd144-O16	NO Ce	Ce interference is NOT corrected in this sheet
Pr141-O16/Nd144-O16	2.72E-02	
Sm152-O16/Nd144-O16	7.26E-04	(Measured-Includes Nd150-O18)
Sm154-O16/Nd144-O16	1.77E-04	
Sm152-O16/Nd144-O16	*0.000215*	*(Oxygen isotope interference subtracted)*

for Ratios: Non-interference subtracted grand mean ratios (input RAW values w/o normalization)

	158/160	159/160	161/160	162/160	164/160	166/160
Ratios	1.14E+00	5.11E-01	0.348	7.22E-01	2.42E-01	2.50E-01
%StdErr	5.71E-04	4.92E-04	0	3.23E-14	7.93E-04	1.00E-03

for %StdErr: input %StdErr from online normalized values, or from offline PrSm correction sheet

for comparison only	**142/144**	**143/144**	**145/144**	**146/144**	**148/144**	**150/144**
DePaolo 88, p.14, ln. B':	1.141854	na	0.348416	0.721882	0.241572	na

FINAL Interference subtracted grand mean ratios: **146/144 set to 0.7219**

	142/144	**143/144**	**145/144**	**146/144**	**148/144**	**150/144**	**150t/144s**
Ratios	1.141896	0.511995	0.347555	0.721900	0.241595	0.236471	72.976742
2 S.E.	0.000013	0.000005	0.000000	0.000000	0.000004	0.000005	0.001461

Epsilon143= -12.53 using (143/144)chur= 0.512638
± 0.10 (Hamilton et al. 1983)

linked from Sm sheet

[Sm147]= 4.701019 nm/g **[Nd144]=** **17.31122** nm/g
± 0.000443 **±** **0.00035**
[Sm]= 4.713276 ppm **[Nd]=** **10.49882** ppm
± 0.000444 **±** **0.00021**
TOT ng Sm= 151.578972 **TOT ng Nd=** **337.6419933**

Sm147/Nd144= **0.271559**
± **0.000026**

Sample: 27.1.2 gtsep2-60
Date: 6/27/2015
Approx Nd load (ng): -

Position #: 3

Rspike Values Nd {SmNd 1.0 A spike, 6-12-08 calib}

142/144	143/144	145/144	146/144	148/144	150/144	[Nd150]
0.830433	0.494001	0.436936	0.885201	0.740574	198.371260	0.049114 nm/g

Wt Sample (g)= 0.01827 g
Wt Spike (g)= 0.15586 g

Mass Spectrometer Information:

Number of cycles measured: 460
Number of cycles used: 460
Amplifier rotation: yes

	start	average (from sheet)	ending	
Filament Current range: from		3607.049840		mAmps
Beam intensity range: from		1.79923797		Volts 142Nd.16O
Temperature range: from		1556.141484		° C

Final Ratio Data:

Interference Values

Ce140-O16/Nd144-O16	NO Ce	Ce interference is NOT corrected in this sheet
Pr141-O16/Nd144-O16	6.54E-03	
Sm152-O16/Nd144-O16	1.34E-03	(Measured-Includes Nd150-O18)
Sm154-O16/Nd144-O16	6.86E-04	
Sm152-O16/Nd144-O16	*0.000816*	*(Oxygen isotope interference subtracted)*

for Ratios: Non-interference subtracted grand mean ratios (input RAW values w/o normalization)

	158/160	159/160	161/160	162/160	164/160	166/160
Ratios	1.14E+00	5.11E-01	0.348	7.22E-01	2.42E-01	2.57E-01
%StdErr	6.21E-04	4.91E-04	0	2.73E-14	8.39E-04	1.15E-03

for %StdErr: input %StdErr from online normalized values, or from offline PrSm correction sheet

for comparison only	**142/144**	**143/144**	**145/144**	**146/144**	**148/144**	**150/144**
DePaolo 88, p.14, ln. B':	1.141854	na	0.348416	0.721882	0.241572	na

FINAL Interference subtracted grand mean ratios: **146/144 set to 0.7219**

	142/144	**143/144**	**145/144**	**146/144**	**148/144**	**150/144**	**150t/144s**
Ratios	1.141940	0.512002	0.347591	0.721900	0.241593	0.236471	47.392129
2 S.E.	0.000014	0.000005	0.000000	0.000000	0.000004	0.000005	0.001086

Epsilon143= -12.41 using (143/144)chur= 0.512638
± 0.10 (Hamilton et al. 1983)

linked from Sm sheet

[Sm147]= 5.128989 nm/g
± 0.000239
[Sm]= 5.142362 ppm
± 0.000240
TOT ng Sm= 93.9509612

[Nd144]= 19.85667 nm/g
± 0.00045
[Nd]= 12.04256 ppm
± 0.00028
TOT ng Nd= 220.0176572

Sm147/Nd144= 0.258301
± 0.000013

Sample: 27.1.2 gt sep2-90
Date: 6/27/2015
Approx Nd load (ng): -
Position #: 4

Rspike Values Nd {SmNd 1.0 A spike, 6-12-08 calib}

142/144	143/144	145/144	146/144	148/144	150/144	[Nd150]
0.830433	0.494001	0.436936	0.885201	0.740574	198.371260	0.049114
						nm/g

Wt Sample (g)= 0.01962 g
Wt Spike (g)= 0.15542 g

Mass Spectrometer Information:

Number of cycles measured: 780
Number of cycles used: 780
Amplifier rotation: yes

	start	average (from sheet)	ending	
Filament Current range: from		3607.049840		mAmps
Beam intensity range: from		1.03162018		Volts 142Nd.16O
Temperature range: from		1556.141484		° C

Final Ratio Data:

Interference Values

Ce140-O16/Nd144-O16	NO Ce	Ce interference is NOT corrected in this sheet
Pr141-O16/Nd144-O16	1.15E-02	
Sm152-O16/Nd144-O16	7.69E-04	(Measured-Includes Nd150-O18)
Sm154-O16/Nd144-O16	2.22E-04	
Sm152-O16/Nd144-O16	*0.000258*	*(Oxygen isotope interference subtracted)*

for Ratios: Non-interference subtracted grand mean ratios (input RAW values w/o normalization)

	158/160	159/160	161/160	162/160	164/160	166/160
Ratios	1.14E+00	5.11E-01	0.348	7.22E-01	2.42E-01	2.50E-01
%StdErr	6.18E-04	5.44E-04	0	3.96E-14	8.79E-04	1.14E-03

for %StdErr: input %StdErr from online normalized values, or from offline PrSm correction sheet

for comparison only	**142/144**	**143/144**	**145/144**	**146/144**	**148/144**	**150/144**
DePaolo 88, p.14, ln. B':	1.141854	na	0.348416	0.721882	0.241572	na

FINAL Interference subtracted grand mean ratios: **146/144 set to 0.7219**

	142/144	**143/144**	**145/144**	**146/144**	**148/144**	**150/144**	**150t/144s**
Ratios	1.141896	0.512016	0.347585	0.721900	0.241586	0.236471	71.295671
2 S.E.	0.000014	0.000006	0.000000	0.000000	0.000004	0.000005	0.001624

Epsilon143= -12.13 using (143/144)chur= 0.512638
± 0.11 (Hamilton et al. 1983)

linked from Sm sheet

[Sm147]= 6.262273 nm/g
± 0.000302
[Sm]= 6.278601 ppm
± 0.000303
TOT ng Sm= 123.186146

[Nd144]= 27.73799 nm/g
± 0.00063
[Nd]= 16.82239 ppm
± 0.00038
TOT ng Nd= 330.0552976

Sm147/Nd144= 0.225765
± 0.000012

Sample:	**Gt C2-1 matrix1**		
Date:	7/18/2015	Position #:	10
Approx Nd load (ng):	-		

Rspike Values Nd {SmNd 0.15 A spike, 6-12-08 calib}

142/144	143/144	145/144	146/144	148/144	150/144	[Nd150]
0.830433	0.494001	0.436936	0.885201	0.740574	198.371260	0.125778

nm/g

Wt Sample (g)=	0.002938	g
Wt Spike (g)=	0.26348	g

Mass Spectrometer Information:

Number of cycles measured:	160			
Number of cycles used:	149			
Amplifier rotation:	yes			
	start	average (from sheet)	ending	
Filament Current range: from	3649.99161	3649.991608	3649.991608	mAmps
Beam intensity range: from	1.74526979	2.34419603	2.300813837	volts 142Nd.16O
Temperature range: from	1520.7326	1557.451631	1590.47619	°C

Final Ratio Data:

Interference Values

Ce140-O16/Nd144-O16	NO Ce	Ce interference is NOT corrected in this sheet
Pr141-O16/Nd144-O16	3.30E-03	
Sm152-O16/Nd144-O16	3.08E-03	(Measured-Includes Nd150-O18)
Sm154-O16/Nd144-O16	1.71E-03	
Sm152-O16/Nd144-O16	*0.002045*	*(Oxygen isotope interference subtracted)*

for Ratios: Non-interference subtracted grand mean ratios (input RAW values w/o normalization)

	158/160	159/160	161/160	162/160	164/160	166/160
Ratios	1.14E+00	5.11E-01	0.348	7.22E-01	2.44E-01	5.08E-01
%StdErr	1.60E-03	8.23E-04	0	2.85E-14	1.66E-03	1.82E-03

for %StdErr: input %StdErr from online normalized values, or from offline PrSm correction sheet

for comparison only	142/144	143/144	145/144	146/144	148/144	150/144
DePaolo 88, p.14:	1.141854	na	0.348416	0.721882	0.241572	na

FINAL Interference subtracted grand mean ratios: 146/144 set to 0.7219

	142/144	143/144	145/144	146/144	148/144	150/144	150t/144s
Ratios	1.142179	0.511967	0.347382	0.721900	0.241604	0.236471	3.673395
2 S.E.	0.000037	0.000008	0.000000	0.000000	0.000008	0.000009	0.000134

Epsilon143= -13.09 using (143/144)chur= 0.512638

± 0.16 (Hamilton et al. 1983)

linked from Sm sheet

[Sm147]=	4.835204	nm/g		[Nd144]=	41.43510	nm/g
±	0.000263			±	0.00151	
[Sm]=	4.847811	ppm		[Nd]=	25.12934	ppm
±	0.000263			±	0.00091	
TOT ng Sm=	14.2428682			TOT ng Nd=	73.83000005	
		Sm147/Nd144=	0.116693	Tot pg Nd=	**73830.00005**	
		±	0.000008	pg Nd/mL	25129339.7	

Sample:	**this is really c2-1 wr2 despite file name**		
Date:	7/18/2015	Position #:	11
Approx Nd load (ng):	-		

Rspike Values Nd {SmNd 0.15 A spike, 6-12-08 calib}

142/144	143/144	145/144	146/144	148/144	150/144	[Nd150]
0.830433	0.494001	0.436936	0.885201	0.740574	198.371260	0.125778

nm/g

Wt Sample (g)=	0.0058	g
Wt Spike (g)=	0.31427	g

Mass Spectrometer Information:

Number of cycles measured:	200			
Number of cycles used:	199			
Amplifier rotation:	yes			
	start	average (from sheet)	ending	
Filament Current range: from	3499.96796	3499.967956	3499.967956	mAmps
Beam intensity range: from	1.42269262	3.42473438	1.832400178	volts 142Nd.16O
Temperature range: from	1474.23687	1534.891405	1585.494505	°C

Final Ratio Data:

Interference Values

Ce140-O16/Nd144-O16	NO Ce	Ce interference is NOT corrected in this sheet
Pr141-O16/Nd144-O16	2.33E-03	
Sm152-O16/Nd144-O16	1.37E-03	(Measured-Includes Nd150-O18)
Sm154-O16/Nd144-O16	5.03E-04	
Sm152-O16/Nd144-O16	*0.000612*	*(Oxygen isotope interference subtracted)*

for Ratios: Non-interference subtracted grand mean ratios (input RAW values w/o normalization)

	158/160	159/160	161/160	162/160	164/160	166/160
Ratios	1.14E+00	5.11E-01	0.348	7.23E-01	2.44E-01	3.70E-01
%StdErr	7.98E-04	5.87E-04	0	2.63E-14	1.14E-03	1.36E-03

for %StdErr: input %StdErr from online normalized values, or from offline PrSm correction sheet

for comparison only	142/144	143/144	145/144	146/144	148/144	150/144
DePaolo 88, p.14:	1.141854	na	0.348416	0.721882	0.241572	na

FINAL Interference subtracted grand mean ratios: 146/144 set to 0.7219

	142/144	143/144	145/144	146/144	148/144	150/144	150t/144s
Ratios	1.141912	0.511975	0.347238	0.721900	0.241600	0.236471	7.534131
2 S.E.	0.000018	0.000006	0.000000	0.000000	0.000006	0.000006	0.000204

Epsilon143= -12.94 using (143/144)chur= 0.512638
± 0.12 (Hamilton et al. 1983)

linked from Sm sheet

[Sm147]=	6.037285	nm/g	[Nd144]=	51.34676	nm/g
±	0.000270		±	0.00139	
[Sm]=	6.053026	ppm	[Nd]=	31.14051	ppm
±	0.000271		±	0.00084	
TOT ng Sm=	35.1075523		TOT ng Nd=	180.6149397	
	Sm147/Nd144=	0.117579	Tot pg Nd=	**180614.9397**	
	±	0.000006	pg Nd/mL	31140506.85	

Sample:	**Gt C2-1 wr3**		
Date:	7/18/2015	Position #:	12
Approx Nd load (ng):	-		

Rspike Values Nd {SmNd 0.15 A spike, 6-12-08 calib}

142/144	143/144	145/144	146/144	148/144	150/144	[Nd150]
0.830433	0.494001	0.436936	0.885201	0.740574	198.371260	0.125778

nm/g

Wt Sample (g)=	0.0058	g
Wt Spike (g)=	0.31427	g

Mass Spectrometer Information:

Number of cycles measured:	500			
Number of cycles used:	500			
Amplifier rotation:	yes			
	start	average (from sheet)	ending	
Filament Current range: from	3649.99161	3690.031281	3700.041199	mAmps
Beam intensity range: from	1.13979007	1.77612257	2.09037101	volts 142Nd.16O
Temperature range: from	1452.64957	1509.884151	1563.076923	°C

Final Ratio Data:

Interference Values

Ce140-O16/Nd144-O16	NO Ce	Ce interference is NOT corrected in this sheet
Pr141-O16/Nd144-O16	1.55E-02	
Sm152-O16/Nd144-O16	1.25E-03	(Measured-Includes Nd150-O18)
Sm154-O16/Nd144-O16	4.45E-04	
Sm152-O16/Nd144-O16	*0.000539*	*(Oxygen isotope interference subtracted)*

for Ratios: Non-interference subtracted grand mean ratios (input RAW values w/o normalization)

	158/160	159/160	161/160	162/160	164/160	166/160
Ratios	1.14E+00	5.11E-01	0.348	7.22E-01	2.43E-01	3.50E-01
%StdErr	5.92E-04	4.90E-04	0	3.72E-14	7.92E-04	1.05E-03

for %StdErr: input %StdErr from online normalized values, or from offline PrSm correction sheet

for comparison only	142/144	143/144	145/144	146/144	148/144	150/144
DePaolo 88, p.14:	1.141854	na	0.348416	0.721882	0.241572	na

FINAL Interference subtracted grand mean ratios: 146/144 set to 0.7219

	142/144	143/144	145/144	146/144	148/144	150/144	150t/144s
Ratios	1.141909	0.511984	0.347444	0.721900	0.241597	0.236471	8.784305
2 S.E.	0.000014	0.000005	0.000000	0.000000	0.000004	0.000005	0.000185

Epsilon143= -12.77 using (143/144)chur= 0.512638
± 0.10 (Hamilton et al. 1983)

linked from Sm sheet

[Sm147]=	6.962841	nm/g	[Nd144]=	59.86696	nm/g
±	0.018907		±	0.00126	
[Sm]=	6.980996	ppm	[Nd]=	36.30780	ppm
±	0.018957		±	0.00077	
TOT ng Sm=	40.4897776		TOT ng Nd=	210.5852253	
	Sm147/Nd144=	0.116305	Tot pg Nd=	**210585.2253**	
	±	0.000316	pg Nd/mL	36307797.47	

Sample: c2-1 zone 1
Date:
Approx Nd load (ng):
Position #:

Rspike Values Nd {SmNd 1.0 A spike, 6-12-08 calib}

142/144	143/144	145/144	146/144	148/144	150/144	[Nd150]
0.830433	0.494001	0.436936	0.885201	0.740574	198.371260	0.049114
						nm/g

Wt Sample (g)= 0.001 g
Wt Spike (g)= 0.02573 g

Mass Spectrometer Information:

Number of cycles measured:
Number of cycles used:
Amplifier rotation: yes

	start	average (from sheet)	ending	
Filament Current range: from		0.000000		mAmps
Beam intensity range: from		0.00469309		Volts 142Nd.16O
Temperature range: from		0.000000		° C

Final Ratio Data:

Interference Values

Ce140-O16/Nd144-O16	NO Ce	Ce interference is NOT corrected in this sheet
Pr141-O16/Nd144-O16	6.47E-01	
Sm152-O16/Nd144-O16	2.36E-02	(Measured-Includes Nd150-O18)
Sm154-O16/Nd144-O16	5.89E-03	
Sm152-O16/Nd144-O16	*0.009091*	*(Oxygen isotope interference subtracted)*

for Ratios: Non-interference subtracted grand mean ratios (input RAW values w/o normalization)

	158/160	159/160	161/160	162/160	164/160	166/160
Ratios	1.24E+00	5.10E-01	0.348	7.29E-01	2.65E-01	7.09E+00
%StdErr	3.08E-01	1.41E-01	0	1.70E-14	2.55E-01	2.47E-01

for %StdErr: input %StdErr from online normalized values, or from offline PrSm correction sheet

for comparison only	**142/144**	**143/144**	**145/144**	**146/144**	**148/144**	**150/144**
DePaolo 88, p.14, ln. B':	1.141854	na	0.348416	0.721882	0.241572	na

FINAL Interference subtracted grand mean ratios: **146/144 set to 0.7219**

	142/144	**143/144**	**145/144**	**146/144**	**148/144**	**150/144**	**150t/144s**
Ratios	1.265634	0.511370	0.344258	0.721900	0.242726	0.236471	0.141390
2 S.E.	0.007803	0.001439	0.000000	0.000000	0.001238	0.001168	0.000698

Epsilon143= -24.74 **using (143/144)chur= 0.512638**
± 28.15 **(Hamilton et al. 1983)**

linked from Sm sheet

[Sm147]= 0.115178 nm/g
± 0.000237
[Sm]= 0.115478 ppm
± 0.000237
TOT ng Sm= 0.11547849

[Nd144]= **0.17867** nm/g
± **0.00088**
[Nd]= **0.10836** ppm
± **0.00054**
TOT ng Nd= **0.108361407**

Sm147/Nd144= **0.644627**
± **0.003449**

Sample:	gt C2-1 zone2		
Date:	7/17/2015	Position #:	5
Approx Nd load (ng):	-		

Rspike Values Nd {SmNd 1.0 A spike, 6-12-08 calib}

142/144	143/144	145/144	146/144	148/144	150/144	[Nd150]
0.830433	0.494001	0.436936	0.885201	0.740574	198.371260	0.049114 nm/g

Wt Sample (g)=	0.003	g
Wt Spike (g)=	0.07737	g

Mass Spectrometer Information:

Number of cycles measured:	281			
Number of cycles used:	160			
Amplifier rotation:	yes			
	start	average (from sheet)	ending	
Filament Current range: from	3599.94202	3603.618315	3643.234913	mAmps
Beam intensity range: from	0.03620871	0.0508987	0.040200835	Volts 142Nd.16O
Temperature range: from	1502.46642	1526.451160	1555.189255	° C

Final Ratio Data:

Interference Values

Ce140-O16/Nd144-O16	NO Ce	Ce interference is NOT corrected in this sheet
Pr141-O16/Nd144-O16	6.98E-02	
Sm152-O16/Nd144-O16	1.29E-02	(Measured-Includes Nd150-O18)
Sm154-O16/Nd144-O16	6.05E-03	
Sm152-O16/Nd144-O16	*0.007195*	*(Oxygen isotope interference subtracted)*

for Ratios: Non-interference subtracted grand mean ratios (input RAW values w/o normalization)

	158/160	159/160	161/160	162/160	164/160	166/160
Ratios	1.14E+00	5.10E-01	0.348	7.25E-01	2.53E-01	2.77E+00
%StdErr	2.80E-02	9.71E-03	0	2.80E-14	2.11E-02	1.86E-02

for %StdErr: input %StdErr from online normalized values, or from offline PrSm correction sheet

for comparison only	**142/144**	**143/144**	**145/144**	**146/144**	**148/144**	**150/144**
DePaolo 88, p.14, ln. B':	1.141854	na	0.348416	0.721882	0.241572	na

FINAL Interference subtracted grand mean ratios: **146/144 set to 0.7219**

	142/144	**143/144**	**145/144**	**146/144**	**148/144**	**150/144**	**150t/144s**
Ratios	1.149160	0.512252	0.346287	0.721900	0.241721	0.236471	0.390732
2 S.E.	0.000644	0.000099	0.000000	0.000000	0.000102	0.000088	0.000146

Epsilon143= -7.53 using (143/144)chur= 0.512638
± 1.94 (Hamilton et al. 1983)

linked from Sm sheet

[Sm147]=	1.256303	nm/g	**[Nd144]=**	**0.49492**	nm/g
±	0.000317		**±**	**0.00018**	
[Sm]=	1.259579	ppm	**[Nd]=**	**0.30016**	ppm
±	0.000318		**±**	**0.00011**	
TOT ng Sm=	3.77873592		**TOT ng Nd=**	**0.900467746**	
	Sm147/Nd144=	**2.538401**			
	±	**0.001142**			

Sample:	gt C2-1 zone 3		
Date:	7/17/2015	Position #:	4
Approx Nd load (ng):	-		

Rspike Values Nd {SmNd 1.0 A spike, 6-12-08 calib}

142/144	143/144	145/144	146/144	148/144	150/144	[Nd150]
0.830433	0.494001	0.436936	0.885201	0.740574	198.371260	0.049114 nm/g

Wt Sample (g)=	0.001	g
Wt Spike (g)=	0.05202	g

Mass Spectrometer Information:

Number of cycles measured:	137			
Number of cycles used:	60			
Amplifier rotation:	yes			
	start	average (from sheet)	ending	
Filament Current range: from	3649.99161	3649.991608	3649.991608	mAmps
Beam intensity range: from	0.02279742	0.02360623	0.021400547	Volts 142Nd.16O
Temperature range: from	1535.26252	1561.136142	1573.040293	° C

Final Ratio Data:

Interference Values

Ce140-O16/Nd144-O16	NO Ce	Ce interference is NOT corrected in this sheet
Pr141-O16/Nd144-O16	2.89E-01	
Sm152-O16/Nd144-O16	1.71E-02	(Measured-Includes Nd150-O18)
Sm154-O16/Nd144-O16	7.22E-03	
Sm152-O16/Nd144-O16	*0.008456*	*(Oxygen isotope interference subtracted)*

for Ratios: Non-interference subtracted grand mean ratios (input RAW values w/o normalization)

	158/160	159/160	161/160	162/160	164/160	166/160
Ratios	1.19E+00	5.11E-01	0.348	7.26E-01	2.56E-01	4.21E+00
%StdErr	5.49E-02	3.18E-02	0	2.42E-14	6.16E-02	6.33E-02

for %StdErr: input %StdErr from online normalized values, or from offline PrSm correction sheet

for comparison only	**142/144**	**143/144**	**145/144**	**146/144**	**148/144**	**150/144**
DePaolo 88, p.14, ln. B':	1.141854	na	0.348416	0.721882	0.241572	na

FINAL Interference subtracted grand mean ratios: **146/144 set to 0.7219**

	142/144	**143/144**	**145/144**	**146/144**	**148/144**	**150/144**	**150t/144s**
Ratios	1.206234	0.512233	0.345757	0.721900	0.241518	0.236471	0.246749
2 S.E.	0.001325	0.000326	0.000000	0.000000	0.000297	0.000299	0.000312

Epsilon143= -7.90 using (143/144)chur= 0.512638
± 6.36 (Hamilton et al. 1983)

linked from Sm sheet

[Sm147]=	1.273577	nm/g	**[Nd144]=**	**0.63042**	nm/g
±	0.000805		**±**	**0.00080**	
[Sm]=	1.276898	ppm	**[Nd]=**	**0.38233**	ppm
±	0.000807		**±**	**0.00048**	
TOT ng Sm=	1.27689817		**TOT ng Nd=**	**0.382333422**	
		Sm147/Nd144=	**2.020207**		
		±	**0.002858**		

Sample:	gt C2-1 zone4		
Date:	7/17/2015	Position #:	3
Approx Nd load (ng):	-		

Rspike Values Nd {SmNd 1.0 A spike, 6-12-08 calib}

142/144	143/144	145/144	146/144	148/144	150/144	[Nd150]
0.830433	0.494001	0.436936	0.885201	0.740574	198.371260	0.049114 nm/g

Wt Sample (g)=	0.005	g
Wt Spike (g)=	0.09864	g

Mass Spectrometer Information:

Number of cycles measured:	1420			
Number of cycles used:	1319			
Amplifier rotation:	yes			
	start	average (from sheet)	ending	
Filament Current range: from	3774.99046	3895.737284	4100.062562	mAmps
Beam intensity range: from	0.10611913	0.21659631	0.172609513	Volts 142Nd.16O
Temperature range: from	1512.01465	1544.884023	1590.47619	° C

Final Ratio Data:

Interference Values

Ce140-O16/Nd144-O16	NO Ce	Ce interference is NOT corrected in this sheet
Pr141-O16/Nd144-O16	9.67E-03	
Sm152-O16/Nd144-O16	1.61E-03	(Measured-Includes Nd150-O18)
Sm154-O16/Nd144-O16	5.75E-04	
Sm152-O16/Nd144-O16	*0.000667*	*(Oxygen isotope interference subtracted)*

for Ratios: Non-interference subtracted grand mean ratios (input RAW values w/o normalization)

	158/160	159/160	161/160	162/160	164/160	166/160
Ratios	1.14E+00	5.11E-01	0.348	7.23E-01	2.44E-01	4.59E-01
%StdErr	1.49E-03	1.11E-03	0	3.42E-14	2.09E-03	2.26E-03

for %StdErr: input %StdErr from online normalized values, or from offline PrSm correction sheet

for comparison only	**142/144**	**143/144**	**145/144**	**146/144**	**148/144**	**150/144**
DePaolo 88, p.14, ln. B':	1.141854	na	0.348416	0.721882	0.241572	na

FINAL Interference subtracted grand mean ratios: **146/144 set to 0.7219**

	142/144	**143/144**	**145/144**	**146/144**	**148/144**	**150/144**	**150t/144s**
Ratios	1.143064	0.511998	0.347139	0.721900	0.241596	0.236471	4.518182
2 S.E.	0.000034	0.000011	0.000000	0.000000	0.000010	0.000011	0.000204

Epsilon143= -12.48 using (143/144)chur= 0.512638
± 0.22 (Hamilton et al. 1983)

linked from Sm sheet

[Sm147]=	0.938955	nm/g	**[Nd144]=**	**4.37775**	nm/g
±	0.000077		**±**	**0.00020**	
[Sm]=	0.941403	ppm	**[Nd]=**	**2.65499**	ppm
±	0.000077		**±**	**0.00012**	
TOT ng Sm=	4.70701679		**TOT ng Nd=**	**13.27496539**	
	Sm147/Nd144=	**0.214484**			
	±	**0.000020**			

Sample:	**C2-1 zone 4 powder**
Date:	Position #:
Approx Nd load (ng):	

Rspike Values Nd {SmNd 0.15 A spike, 6-12-08 calib}

142/144	143/144	145/144	146/144	148/144	150/144	[Nd150]
0.830433	0.494001	0.436936	0.885201	0.740574	198.371260	0.125778

nm/g

Wt Sample (g)=	0.001	g
Wt Spike (g)=	0.04768	g

Mass Spectrometer Information:

Number of cycles measured:	100			
Number of cycles used:	80			
Amplifier rotation:	yes			
	start	average (from sheet)	ending	
Filament Current range: from	3700.0412	3700.041199	3700.041199	mAmps
Beam intensity range: from	1.53424142	1.80753855	1.312584873	volts 142Nd.16O
Temperature range: from	1521.56288	1556.491758	1587.155067	°C

Final Ratio Data:

Interference Values

Ce140-O16/Nd144-O16	NO Ce	Ce interference is NOT corrected in this sheet
Pr141-O16/Nd144-O16	3.29E-03	
Sm152-O16/Nd144-O16	2.40E-03	(Measured-Includes Nd150-O18)
Sm154-O16/Nd144-O16	1.47E-03	
Sm152-O16/Nd144-O16	*0.001742*	*(Oxygen isotope interference subtracted)*

for Ratios: Non-interference subtracted grand mean ratios (input RAW values w/o normalization)

	158/160	159/160	161/160	162/160	164/160	166/160
Ratios	1.14E+00	5.11E-01	0.348	7.23E-01	2.44E-01	3.23E-01
%StdErr	2.02E-03	1.21E-03	0	2.41E-14	2.17E-03	2.54E-03

for %StdErr: input %StdErr from online normalized values, or from offline PrSm correction sheet

for comparison only	142/144	143/144	145/144	146/144	148/144	150/144
DePaolo 88, p.14:	1.141854	na	0.348416	0.721882	0.241572	na

FINAL Interference subtracted grand mean ratios: 146/144 set to 0.7219

	142/144	143/144	145/144	146/144	148/144	150/144	150t/144s
Ratios	1.142398	0.511976	0.347315	0.721900	0.241606	0.236471	11.663239
2 S.E.	0.000046	0.000012	0.000000	0.000000	0.000010	0.000012	0.000593

Epsilon143= -12.92 using (143/144)chur= 0.512638

± 0.24 (Hamilton et al. 1983)

linked from Sm sheet

[Sm147]=	10.913235	nm/g		[Nd144]=	69.94559	nm/g
±	0.000406			±	0.00355	
[Sm]=	10.941690	ppm		[Nd]=	42.42023	ppm
±	0.000407			±	0.00216	
TOT ng Sm=	10.9416901			TOT ng Nd=	42.42022693	
		Sm147/Nd144=	0.156025	Tot pg Nd=	**42420.22693**	
		±	0.000010	pg Nd/mL	42420226.93	

Sample:	**Gt B6 wr2**		
Date:	7/18/2015	Position #:	13
Approx Nd load (ng):	-		

Rspike Values Nd {SmNd 0.15 A spike, 6-12-08 calib}

142/144	143/144	145/144	146/144	148/144	150/144	[Nd150]
0.830433	0.494001	0.436936	0.885201	0.740574	198.371260	0.125778

nm/g

Wt Sample (g)=	0.00698	g
Wt Spike (g)=	0.31365	g

Mass Spectrometer Information:

Number of cycles measured:	340			
Number of cycles used:	340			
Amplifier rotation:	yes			
	start	average (from sheet)	ending	
Filament Current range: from	3499.96796	3499.967956	3499.967956	mAmps
Beam intensity range: from	1.14372908	2.38557085	2.175934614	volts 142Nd.16O
Temperature range: from	1456.38584	1511.866911	1576.776557	°C

Final Ratio Data:

Interference Values

Ce140-O16/Nd144-O16	NO Ce	Ce interference is NOT corrected in this sheet
Pr141-O16/Nd144-O16	1.53E-02	
Sm152-O16/Nd144-O16	8.66E-04	(Measured-Includes Nd150-O18)
Sm154-O16/Nd144-O16	1.28E-04	
Sm152-O16/Nd144-O16	*0.000169*	*(Oxygen isotope interference subtracted)*

for Ratios: Non-interference subtracted grand mean ratios (input RAW values w/o normalization)

	158/160	159/160	161/160	162/160	164/160	166/160
Ratios	1.14E+00	5.11E-01	0.348	7.23E-01	2.43E-01	3.40E-01
%StdErr	6.36E-04	5.33E-04	0	1.59E-14	8.99E-04	1.13E-03

for %StdErr: input %StdErr from online normalized values, or from offline PrSm correction sheet

for comparison only	142/144	143/144	145/144	146/144	148/144	150/144
DePaolo 88, p.14:	1.141854	na	0.348416	0.721882	0.241572	na

FINAL Interference subtracted grand mean ratios: 146/144 set to 0.7219

	142/144	143/144	145/144	146/144	148/144	150/144	150t/144s
Ratios	1.141914	0.511988	0.347226	0.721900	0.241598	0.236471	9.692471
2 S.E.	0.000015	0.000005	0.000000	0.000000	0.000004	0.000005	0.000219

Epsilon143= -12.67 using (143/144)chur= 0.512638
± 0.11 (Hamilton et al. 1983)

linked from Sm sheet

[Sm147]=	6.428769	nm/g	[Nd144]=	54.78091	nm/g
±	0.000839		±	0.00124	
[Sm]=	6.445531	ppm	[Nd]=	33.22324	ppm
±	0.000841		±	0.00075	
TOT ng Sm=	44.9898056		TOT ng Nd=	231.8981885	
		Sm147/Nd144= 0.117354	Tot pg Nd=	**231898.1885**	
		± 0.000016	pg Nd/mL	33223236.17	

Sample:	gt B6 Zone1+2		
Date:	7/17/2015	Position #:	7
Approx Nd load (ng):	-		

Rspike Values Nd {SmNd 1.0 A spike, 6-12-08 calib}

142/144	143/144	145/144	146/144	148/144	150/144	[Nd150]
0.830433	0.494001	0.436936	0.885201	0.740574	198.371260	0.049114 nm/g

Wt Sample (g)=	0.001	g
Wt Spike (g)=	0.02365	g

Mass Spectrometer Information:

Number of cycles measured:	157			
Number of cycles used:	118			
Amplifier rotation:	yes			
	start	average (from sheet)	ending	
Filament Current range: from	3599.94202	3607.234199	3649.991608	mAmps
Beam intensity range: from	0.01170367	0.01190137	0.006611796	Volts 142Nd.16O
Temperature range: from	1520.31746	1561.331926	1602.100122	° C

Final Ratio Data:

Interference Values

Ce140-O16/Nd144-O16	NO Ce	Ce interference is NOT corrected in this sheet
Pr141-O16/Nd144-O16	2.72E-01	
Sm152-O16/Nd144-O16	1.29E-02	(Measured-Includes Nd150-O18)
Sm154-O16/Nd144-O16	7.12E-03	
Sm152-O16/Nd144-O16	*0.008453*	*(Oxygen isotope interference subtracted)*

for Ratios: Non-interference subtracted grand mean ratios (input RAW values w/o normalization)

	158/160	159/160	161/160	162/160	164/160	166/160
Ratios	1.19E+00	5.11E-01	0.348	7.25E-01	2.52E-01	2.17E+00
%StdErr	8.51E-02	4.79E-02	0	2.82E-14	1.01E-01	1.02E-01

for %StdErr: input %StdErr from online normalized values, or from offline PrSm correction sheet

for comparison only	**142/144**	**143/144**	**145/144**	**146/144**	**148/144**	**150/144**
DePaolo 88, p.14, ln. B':	1.141854	na	0.348416	0.721882	0.241572	na

FINAL Interference subtracted grand mean ratios: **146/144 set to 0.7219**

	142/144	**143/144**	**145/144**	**146/144**	**148/144**	**150/144**	**150t/144s**
Ratios	1.201924	0.513145	0.346431	0.721900	0.241510	0.236471	0.515894
2 S.E.	0.002046	0.000491	0.000000	0.000000	0.000488	0.000480	0.001048

Epsilon143= **9.89** **using (143/144)chur=** **0.512638**
± **9.57** **(Hamilton et al. 1983)**

linked from Sm sheet

[Sm147]=	0.403001	nm/g	**[Nd144]=**	**0.59923**	nm/g
±	0.000664		**±**	**0.00122**	
[Sm]=	0.404052	ppm	**[Nd]=**	**0.36342**	ppm
±	0.000666		**±**	**0.00074**	
TOT ng Sm=	0.40405218		**TOT ng Nd=**	**0.363419505**	
	Sm147/Nd144=	**0.672529**			
	±	**0.001759**			

APPENDIX C: Field data

The samples for this thesis were collected from two broad field areas: The Ballentrae ophiolite complex in northern Scotland and The Betic Cordillera in southwest Spain. The only Scottish sample, 11ESC-18A was collected by Katie Eccles, Claire Ostwald and Ethan Baxter in the summer of 2011. The suite of Spanish samples was collected over the course of several years. Samples B13c, B2b, B3b, and B17a were provided by Domingo Aerden and are described in detail in Aerden *et al*. 2013. Sample 27.1.2 was collected by Emily Stewart and Domingo Aerden in the summer of 2014. This section includes maps of all sample locations and available field data.

Table C.1 Lists each sample and gives the date collected, a brief petrologic description and available GPS coordinates in decimal degrees according to WGS84.

Sample	Collected by	Latitude (N)	Longitude (E)	description
11ESC-18A	EFB, KAE, CO	55.185967	-4.87941667	gt amphibolite
27.1.2	EMS, DGA	37.293690	-2.82786267	micaschist
B13c	DGA	37.174862	-3.05335021	micaschist
B17a	DGA	37.331223	-2.76918049	micaschist
B2b	DGA	37.105297	-3.41757528	micaschist
B3b	DGA	37.108652	-3.41714350	micaschist

Table C.1
Sample List and Field Data

Figure C.1 Geologic map of Ballentrae Ophiolite near Knocklaugh showing the approximate location of sample 11ESC-18A. Map taken from Stephenson, D. *et al.,* 1999.

Figure C.2 Geologic map of the Betic Cordillera showing the location of samples 27.2.1, B13c, B17a, B2b, and B3b. Map is from Cartografía Geológica MILLON provided by the Instituto Geológica y Minero de España's "Sistema de consulta y difusión web de cartografía geológica continua" (SIGECO). Sample locations applied using Google Earth. Note that the respective locations of samples B2b and B3b are unresolvable at this scale.

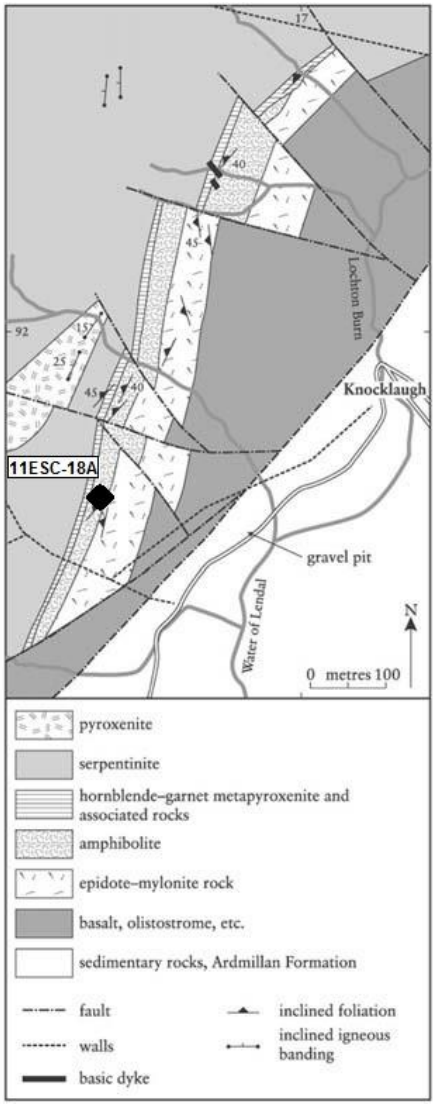

Figure C.1
Geologic Map of the Ballentrae Ophiolite near Knocklaugh

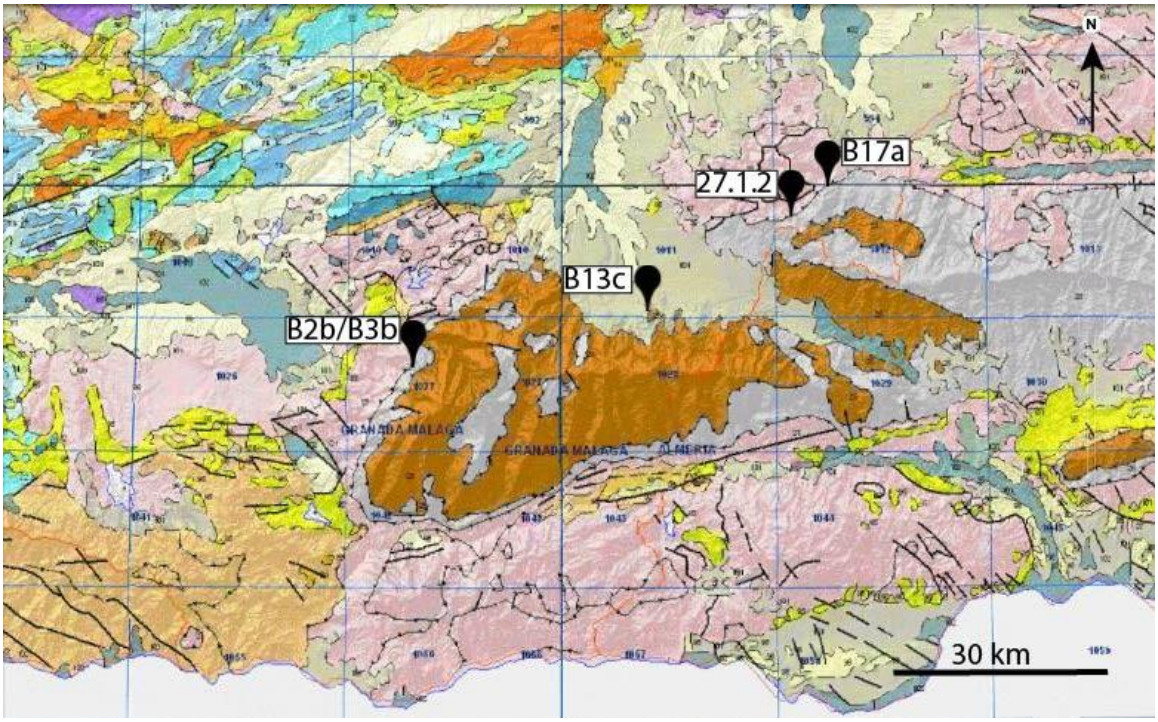

Figure C.2
Geologic Map of Betic Cordillera

APPENDIX D: Blank Correction for Individual Garnet Zones

This appendix addresses the effect of our full procedural Sm and Nd blanks on the small zones of garnets B6 and C2-1. Using the MatLab script in Appendix E, a blank-subtraction un-mixing calculation was performed on each sample. While we find that there is a significant effect on measured isotopic values, we do not find a significant effect (within error) on the resultant age calculation. Table D.1 summarizes these results.

Table D.1 lists isotopic data for all individual zones studied in chapter 2 before and after blank correction. All errors are 2 sigma absolute errors.

Sample	$^{143}Nd/^{144}Nd$ before corr.	$^{143}Nd/^{144}Nd$ after corr.	$^{147}Sm/^{144}Nd$ before corr.	$^{147}Sm/^{144}Nd$ after corr.	Age before corr.	Age after corr.
C2-1 Zone B	0.512252 ± 0.000099	0.512237 ± 0.000105	2.5384 ± 0.0011	2.5933 ± 0.0199	17.6 ± 6.2 Ma	16.2 ± 6.4 Ma
C2-1 Zone C	0.512233 ± 0.000326	0.512194 ± 0.000347	2.0202 ± 0.00286	2.1257 ± 0.0397	21 ± 26 Ma	17 ± 26 Ma
C2- 1 Zone D	0.511998 ± 0.000011	0.511997 ± 0.000011	0.2145 ± 0.00005	0.2147 ± 0.00011	36 ± 19 Ma	34 ± 19 Ma
B6 Zone A+B	0.513145 ± 0.000491	0.513154 ± 0.000517	0.67253 ± 0.00176	0.70778 ± 0.01365	318 ± 130 Ma	302 ± 130 Ma

Table D.1
Blank Corrected Isotope Data for Ch. 2

APPENDIX E: MatLab Script for Blank Correction

The following is a MatLab script written for blank correction calculations. Anyone's data can be plugged into the sheet to blank-correct his/her data.

```
%%%%%%%%%%%%%%%%%%%%%%%%%%%%%%%%%%%%%%%%%%%%%%%%%%%%%%%%%%%%%%%%%%%%%%%
%%%%
% blankprop
%%%%%%%%%%%%%%%%%%%%%%%%%%%%%%%%%%%%%%%%%%%%%%%%%%%%%%%%%%%%%%%%%%%%%%%
%%%%
% Written by: Emily Stewart
% Date: 6/12/14
%%%%%%%%%%%%%%%%%%%%%%%%%%%%%%%%%%%%%%%%%%%%%%%%%%%%%%%%%%%%%%%%%%%%%%%
%%%%
%
% 1. Program uses a Monte Carlo simulation to generate a random
%distribution
% of blank-corrected sample values of 143/144Nd and 147Sm/144Nd.
% 2. Monte Carlo values are used to recalculate a mean and standard
% deviation for "blank corrected" values.
% 3. A correlation coefficient (r) is calculated.
%
%%%%%%%%%%%%%%%%%%%%%%%%%%%%%%%%%%%%%%%%%%%%%%%%%%%%%%%%%%%%%%%%%%%%%%%
%%%%

%%%%%%%%%%%%%%%%%%%%%%%
Sample=input('Enter mixture data [pg
mix,143/144Nd,2sig,147Sm/144Nd,2sig] ');
Mmass=Sample(1);
Sa=Sample(2);
Sau=0.5*Sample(3);
Sb=Sample(4);
Sbu=0.5*Sample(5);
Blank=[pg blank,2sig,143/144 blank,2sig,147/144 blank,2sig];%<--your
data here%
Bmass=Blank(1);
Bmassu=0.5*Blank(2);
Ba=Blank(3);
Bau=0.5*Blank(4);
Bb=Blank(5);
Bbu=0.5*Blank(6);


%%%%%%%%%%%%%%%%%%%%%%%
%Monte Carlo
%%%%%%%%%%%%%%%%%%%%%%%
Sam=zeros(10000,1);
Sbm=zeros(10000,1);
Bam=zeros(10000,1);
```

```
Bbm=zeros(10000,1);
Bmassm=zeros(10000,1);
Sam=Sa+Sau*randn(10000,1);
Sbm=Sb+Sbu*randn(10000,1);
Bam=Ba+Bau*randn(10000,1);
Bbm=Bb+Bbu*randn(10000,1);
Bmassm=Bmass+Bmassu*randn(10000,1);

%%%%%%%%%%%%%%%%%%%%%%%
%Blank Subtraction
%%%%%%%%%%%%%%%%%%%%%%%
newA=zeros(10000,1);
newB=zeros(10000,1);
for i=1:10000
    newA(i,1)=((Mmass)*Sam(i,1)-(Bmassm(i,1)*Bam(i,1)))/(Mmass-
Bmassm(i,1));
end

for i=1:10000
    newB(i,1)=((Mmass)*Sbm(i,1)-(Bmassm(i,1)*Bbm(i,1)))/(Mmass-
Bmassm(i,1));
end

%%%%%%%%%%%%%%%%%%%%%%%
%r value
%%%%%%%%%%%%%%%%%%%%%%%
x=zeros(10000,1);
y=zeros(10000,1);
xy=zeros(10000,1);
for i=1:10000
    x(i,1)=newA(i,1)-mean(newA);
    y(i,1)=newB(i,1)-mean(newB);
    x2(i,1)=(newA(i,1)-mean(newA))^2;
    y2(i,1)=(newB(i,1)-mean(newB))^2;
end
xy=x.*y;
num=sum(xy);
denom=sqrt(sum(x2)*sum(y2));

%%%%%%%%%%%%%%%%%%%%%%%
%Generating Outputs
%%%%%%%%%%%%%%%%%%%%%%%
format shortEng
Nd_value=mean(newA)
Nd_2sig=2*std(newA)
Sm_value=mean(newB)
Sm_2sig=2*std(newB)
r=num/denom
plot(newB,newA,'k*');
% Output to files
```

BIBLIOGRAPHY

Aerden, D.G. (2003). Preferred orientation of planar microstructures determined via statistical best-fit of measured intersection-lines: the 'FitPitch'computer program. *Journal of structural geology*, *25*(6), 923-934.

Aerden, D. G., Sayab, M., & Bouybaouene, M. L. (2010). Conjugate-shear folding: A model for the relationships between foliations, folds and shear zones. Journal of Structural Geology, 32(8), 1030-1045.

Aerden, D. G. A. M., Bell, T. H., Puga, E., Sayab, M., Lozano, J. A., & de Federico, A. D. (2013). Multi-stage mountain building vs. relative plate motions in the Betic Cordillera deduced from integrated microstructural and petrological analysis of porphyroblast inclusion trails. *Tectonophysics*.

Aerden, D., & Sayab, M. (2008). From Adria-to Africa-driven orogenesis: Evidence from porphyroblasts in the Betic Cordillera, Spain. *Journal of Structural Geology*, *30*(10), 1272-1287..

Ague, J. J., & Baxter, E. F. (2007). Brief thermal pulses during mountain building recorded by Sr diffusion in apatite and multicomponent diffusion in garnet. Earth and Planetary Science Letters, 261(3), 500-516.

Amelin, Y., & Rotenberg, E. (2004). Sm–Nd systematics of chondrites. Earth and Planetary Science Letters, 223(3), 267-282.

Anderson, J. G. C. (1936). Age of the Girvan-Ballantrae serpentine. Geological Magazine, 73(12), 535-545.

Augier, R., Agard, P., Monié, P., Jolivet, L., Robin, C., & Booth-Rea, G. (2005). Exhumation, doming and slab retreat in the Betic Cordillera (SE Spain): in situ40Ar/39Ar ages and P–T–d–t paths for the Nevado-Filabride complex. Journal of Metamorphic Geology, 23(5), 357-381.

Bakker, H. E., Jong, K., Helmers, H., & Biermann, C. (1989). The geodynamic evolution of the Internal Zone of the Betic Cordilleras (south-east Spain): a model based on structural analysis and geothermobarometry. *Journal of Metamorphic Geology*, *7*(3), 359-381.

Barrow, G. (1893). On an intrusion of muscovite-biotite gneiss in the south-eastern Highlands of Scotland, and its accompanying metamorphism. Quarterly Journal of the Geological Society, 49(1-4), 330-358.

Baxter, E. F., Ague, J. J., & Depaolo, D. J. (2002). Prograde temperature–time evolution in the Barrovian type–locality constrained by Sm/Nd garnet ages from Glen Clova, Scotland. Journal of the Geological Society, 159(1), 71-82.

Baxter, E. F., & Scherer, E. E. (2013). Garnet geochronology: timekeeper of tectonometamorphic processes. Elements, 9(6), 433-438.

Bell, T. H., & Johnson, S. E. (1989). Porphyroblast inclusion trails: the key to orogenesis. *Journal of Metamorphic Geology*, *7*(3), 279-310.

Bell, T. H., Forde, A., & Hayward, N. (1992). Do smoothly curving, spiral-shaped inclusion trails signify porphyroblast rotation?. *Geology*, *20*(1), 59-62.

Bluck, B. J., Halliday, A. N., Aftalion, M., & Macintyre, R. M. (1980). Age arid origin of Ballantrae ophiolite and its significance to the Caledonian orogeny and Ordovician time scale. Geology, 8(10), 492-495.

Bouvier, A., Vervoort, J. D., & Patchett, P. J. (2008). The Lu–Hf and Sm–Nd isotopic composition of CHUR: constraints from unequilibrated chondrites and implications for the bulk composition of terrestrial planets. Earth and Planetary Science Letters, 273(1), 48-57.

Carlson, W. D. (2006). Dana Lecture. Rates of Fe, Mg, Mn, and Ca diffusion in garnet. American Mineralogist, 91(1), 1-11.

Carlson, W. D. (2012). Rates and mechanism of Y, REE, and Cr diffusion in garnet. American Mineralogist, 97(10), 1598-1618.

Church, W. R., & Gayer, R. A. (1973). The Ballantrae ophiolite. Geological Magazine, 110(06), 497-510.

Cobbold, P. R., & Gapais, D. (1987). Shear criteria in rocks: an introductory review. Journal of structural geology, 9(5), 521-IN2.

Dallmeyer, R. D., & Williams, H. (1975). 40Ar/39Ar ages from the Bay of Islands metamorphic aureole: their bearing on the timing of Ordovician ophiolite obduction. Canadian Journal of Earth Sciences, 12(9), 1685-1690.

DePaolo, D. J., & Wasserburg, G. J. (1976). Inferences about magma sources and mantle structure from variations of^(143) Nd/^(144) Nd. Geophysical Research Letters, 3(12), 743-746.

Dragovic, B., Samanta, L. M., Baxter, E. F., & Selverstone, J. (2012). Using garnet to constrain the duration and rate of water-releasing metamorphic reactions during subduction: An example from Sifnos, Greece. *Chemical Geology*, *314*, 9-22.

Fay, C., Bell, T. H., & Hobbs, B. E. (2008). Porphyroblast rotation versus nonrotation: Conflict resolution!. *Geology*, *36*(4), 307-310.

Galdeano, D., & Sanz, C. (1990). Geologic evolution of the Betic Cordilleras in the Western Mediterranean, Miocene to the present. *Tectonophysics*, *172*(1), 107-119.

Goldstein, A. G. (1988). Factors affecting the kinematic interpretation of asymmetric boudinage in shear zones. Journal of Structural Geology, 10(7), 707-715.

Graham, C. M., & Powell, R. (1984). A garnet–hornblende geothermometer: calibration, testing, and application to the Pelona Schist, Southern California. Journal of metamorphic Geology, 2(1), 13-31

Hamilton, P. J., Bluck, B. J., & Halliday, A. N. (1984). Sm—Nd ages from the Ballantrae complex, SW Scotland. Transactions of the Royal Society of Edinburgh: Earth Sciences, 75(02), 183-187.

Handy, M. R., Schmid, S. M., Bousquet, R., Kissling, E., & Bernoulli, D. (2010). Reconciling plate-tectonic reconstructions of Alpine Tethys with the geological–geophysical record of spreading and subduction in the Alps. Earth-Science Reviews, 102(3), 121-158.

Hanmer, S., & Passchier, C. W. (1991). Shear sense indicators: a review.

Harrison, T. M. (1982). Diffusion of 40Ar in hornblende. Contributions to Mineralogy and Petrology, 78(3), 324-331.

Harvey, J., & Baxter, E. F. (2009). An improved method for TIMS high precision neodymium isotope analysis of very small aliquots (1–10 ng). *Chemical Geology*, *258*(3), 251-257.

Hayward, N. (1990). Determination of early fold axis orientations in multiply deformed rocks using porphyroblast inclusion trails. *Tectonophysics*, *179*(3), 353-369.

Jiang, S. Y., Yu, J. M., & Lu, J. J. (2004). Trace and rare-earth element geochemistry in tourmaline and cassiterite from the Yunlong tin deposit, Yunnan, China: implication for migmatitic–hydrothermal fluid evolution and ore genesis. Chemical Geology, 209(3), 193-213.

Ludwig, K. R. (2003). User's manual for Isoplot 3.00: a geochronological toolkit for Microsoft Excel (No. 4). Kenneth R. Ludwig.

Marks, M. A., Marschall, H. R., Schühle, P., Guth, A., Wenzel, T., Jacob, D. E., ... & Markl, G. (2013). Trace element systematics of tourmaline in pegmatitic and hydrothermal systems from the Variscan Schwarzwald (Germany): the importance of major element composition, sector zoning, and fluid or melt composition. Chemical Geology, 344, 73-90.

Matheron, G. (1963). Principles of geostatistics. Economic geology, 58(8), 1246-1266.

Meijninger, B. M. L., & Vissers, R. L. M. (2006). Miocene extensional basin development in the Betic Cordillera, SE Spain revealed through analysis of the Alhama de Murcia and Crevillente Faults. Basin Research, 18(4), 547-571.

Michard, A., Chalouan, A., Feinberg, H., Goffé, B., & Montigny, R. (2002). How does the Alpine belt end between Spain and Morocco?. *Bulletin de la Société géologique de France*, *173*(1), 3-15.

Oliver, G. J. (2001). Reconstruction of the Grampian episode in Scotland: its place in the Caledonian Orogeny. Tectonophysics, 332(1), 23-49.

Oliver, G. J. H., Chen, F., Buchwaldt, R., & Hegner, E. (2000). Fast tectonometamorphism and exhumation in the type area of the Barrovian and Buchan zones. Geology, 28(5), 459-462.

Passchier, C. W., Trouw, R. A. J., Zwart, H. J., & Vissers, R. L. M. (1992). Porphyroblast rotation: eppur si muove*?. *Journal of Metamorphic Geology*,*10*(3), 283-294.

Platt, J. P., Anczkiewicz, R., Soto, J. I., Kelley, S. P., & Thirlwall, M. (2006). Early Miocene continental subduction and rapid exhumation in the western Mediterranean. *Geology*, *34*(11), 981-984.

Platt, J. P., & Vissers, R. L. M. (1980). Extensional structures in anisotropic rocks. Journal of Structural Geology, 2(4), 397-410.

Pollington, A. D., & Baxter, E. F. (2011). High precision microsampling and preparation of zoned garnet porphyroblasts for Sm–Nd geochronology. *Chemical Geology*, *281*(3), 270-282..

Puga, E., De Federico, A. D., & Nieto, J. M. (2002). Tectonostratigraphic subdivision and petrological characterisation of the deepest complexes of the Betic zone: a review. *Geodinamica Acta*, *15*(1), 23-43.

Rosenbaum, G., Lister, G. S., & Duboz, C. (2002). Relative motions of Africa, Iberia and Europe during Alpine orogeny. *Tectonophysics*, *359*(1), 117-129

Rosenfeld, J. L. (1968). Garnet rotations due to the major Paleozoic deformations in southeast Vermont. *Studies of Appalachian Geology*, 185-202.

Sawaki, Y., Shibuya, T., Kawai, T., Komiya, T., Omori, S., Iizuka, T., ... & Maruyama, S. (2010). Imbricated ocean-plate stratigraphy and U-Pb zircon ages from tuff beds in cherts in the Ballantrae complex, SW Scotland. Geological Society of America Bulletin, 122(3-4), 454-464.

Spray, J. G., & Williams, G. D. (1980). The sub-ophiolite metamorphic rocks of the Ballantrae Igneous Complex, SW Scotland. Journal of the Geological Society, 137(3), 359-368.

Treloar, P. J., Bluck, B. J., Bowes, D. R., & Dudek, A. (1980). Hornblende-garnet metapyroxenite beneath serpentinite in the Ballantrae complex of SW Scotland and its bearing on the depth provenance of obducted oceanic lithosphere. Transactions of the Royal Society of Edinburgh: Earth Sciences, 71(04), 201-212.

Tucker, R. D., & McKerrow, W. S. (1995). Early Paleozoic chronology: a review in light of new U-Pb zircon ages from Newfoundland and Britain. Canadian Journal of Earth Sciences, 32(4), 368-379.

Viete, D. R., Forster, M. A., & Lister, G. S. (2011). The nature and origin of the Barrovian metamorphism, Scotland: 40Ar/39Ar apparent age patterns and the duration of metamorphism in the biotite zone. Journal of the Geological Society, 168(1), 133-146.

Viete, D. R., Oliver, G. J., Fraser, G. L., Forster, M. A., & Lister, G. S. (2013). Timing and heat sources for the Barrovian metamorphism, Scotland. Lithos, 177, 148-163.

Vissers, R. L. M., & Meijer, P. T. (2012). Iberian plate kinematics and Alpine collision in the Pyrenees. *Earth-Science Reviews*, *114*(1), 61-83.

Vorhies, S. H., & Ague, J. J. (2011). Pressure–temperature evolution and thermal regimes in the Barrovian zones, Scotland. Journal of the Geological Society, 168(5), 1147-1166.

Wendt, I., & Carl, C. (1991). The statistical distribution of the mean squared weighted deviation. Chemical Geology: Isotope Geoscience Section, 86(4), 275-285.

CURRICULUM VITAE